Appendix B

EFDC Hydrodynamic and Water Quality Model

Draft

Lake Fort Gibson TMDL Report

Prepared for

Oklahoma Department of Environmental Quality

Water Quality Division

May 2015

By

Dynamic Solutions, LLC

Appendix B – EFDC Hydrodynamic and Water Quality Model

Table of Contents

B-1 INTRODUCTION 7
B-2 MODEL DEVELOPMENT 10
B-2.1 Overview of the EFDC Model 10
B-2.2 Model Simulation Period 10
B-2.3 Model Constituents 10
B-2.4 Grid Development 11
B-2.5 Meteorological Data 13
B-2.6 Point Source Discharge 15
B-2.7 Boundary Conditions 17
B-2.8 HSPF-EFDC Linkage 24
B-3 WATER QUALITY AND SEDIMENT FLUX MODEL 27
B-3.1 Water Quality Model 27
B-3.2 Sediment Flux Model 36
B-4 CALIBRATION AND VALIDATION STATIONS 42
B-4.1 Stage Calibration and Validation Stations 42
B-4.2 Water Quality Calibration and Validation Stations 42
B-5 MODEL PERFORMANCE AND STATISTICS 44
B-6 HYDRODYNAMIC MODEL CALIBRATION AND VALIDATION 46
B-6.1 Lake Stage Calibration 46
B-6.2 Lake Stage Validation 47
B-7 WATER QUALITY MODEL CALIBRATION AND VALIDATION 48
B-7.1 Introduction 48
B-7.2 Water Temperature Calibration and Validation 48
B-7.3 Total Suspended Solids Calibration and Validation 58
B-7.4 Dissolved Oxygen 63
B-7.5 Algae Calibration and Validation 77
B-7.6 Trophic State Index Calibration and Validation 80
B-7.7 Organic Carbon Calibration and Validation 83
B-7.8 Nitrogen 88
B-7.9 Phosphorus Calibration and Validation 102
B-7.10 SOD and Sediment Flux 111
B-8 SUMMARY, CONCLUSIONS AND RECOMMENDATIONS 118
B-8.1 Summary 118
B-8.2 Conclusions 118
B-8.3 Recommendations 119
B-9 REFERENCES 120

List of Figures

Figure B-1 Location of Fort Gibson Lake 9
Figure B-2 Modeling Domain of the Fort Gibson Lake EFDC 12
Figure B-3 Fort Gibson Lake Stage and Storage Volume. 13
Figure B-4 Location of the MESONET Stations 14
Figure B-5 Location of the NPDES Facilities Discharging to the Fort Gibson Lake EFDC Model 16
Figure B-6 HSPF Tributary and Catchment Locations. 19
Figure B-7 Location of USGS Gage Station 07191500. 20
Figure B-8 Location of OWRB Water Quality Observation Station for Upstream Boundary 21
Figure B-9 Location of GRDA Water Quality Observation Station for Upstream Boundary 22
Figure B-10 Location of USACE Station GIBO2 and 1GIBOKN0008 23
Figure B-11 Spatial Water Quality Kinetic Zones Defined for Fort Gibson Lake 31
Figure B-12 Location of the Atmospheric Deposition Monitoring Stations 35
Figure B-13 Location of the USACE Monitoring Stations 43
Figure B-14 Comparison of Simulated and Observed Water Level during Jan 2005 to Dec 2005 46
Figure B-15 Comparison of Simulated and Observed Water Level during Jan 2006 to Dec 2006 47
Figure B-16 Surface Layer Water Temperature Calibration Plot at Station 1GIBOKN0003 50
Figure B-17 Bottom Layer Water Temperature Calibration Plot at Station 1GIBOKN0003 50
Figure B-18 Surface Layer Water Temperature Calibration Plot at Station 1GIBOKN0005 51
Figure B-19 Bottom Layer Water Temperature Calibration Plot at Station 1GIBOKN0005 51
Figure B-20 Surface Layer Water Temperature Validation Plot at Station 1GIBOKN0003 52
Figure B-21 Bottom Layer Water Temperature Validation Plot at Station 1GIBOKN0003 52
Figure B-22 Surface Layer Water Temperature Validation Plot at Station 1GIBOKN0005 53
Figure B-23 Bottom Layer Water Temperature Validation Plot at Station 1GIBOKN0005 53
Figure B-24 Water Temperature Vertical Profile Comparison Plot at Station 1GIBOKN0003 (page 1-2) .. 54
Figure B-25 Water Temperature Vertical Profile Comparison Plot at Station 1GIBOKN0005 (page 1-2) .. 56
Figure B-26 Surface Layer TSS Calibration Plot at Station 1GIBOKN0003 59
Figure B-27 Bottom Layer TSS Calibration Plot at Station 1GIBOKN0003 59
Figure B-28 Surface Layer TSS Calibration Plot at Station 1GIBOKN0005 60
Figure B-29 Bottom Layer TSS Calibration Plot at Station 1GIBOKN0005 60
Figure B-30 Surface Layer TSS Validation Plot at Station 1GIBOKN0003 61
Figure B-31 Bottom Layer TSS Validation Plot at Station 1GIBOKN0003 61
Figure B-32 Surface Layer TSS Validation Plot at Station 1GIBOKN0005 62
Figure B-33 Bottom Layer TSS Validation Plot at Station 1GIBOKN0005 62
Figure B-34 Surface Layer Dissolved Oxygen Calibration Plot at Station 1GIBOKN0003 66
Figure B-35 Bottom Layer Dissolved Oxygen Calibration Plot at Station 1GIBOKN0003 66
Figure B-36 Surface Layer Dissolved Oxygen Calibration Plot at Station 1GIBOKN0005 67
Figure B-37 Bottom Layer Dissolved Oxygen Calibration Plot at Station 1GIBOKN0005 67
Figure B-38 Surface Layer Dissolved Oxygen Validation Plot at Station 1GIBOKN0003 68
Figure B-39 Bottom Layer Dissolved Oxygen Validation Plot at Station 1GIBOKN0003 68
Figure B-40 Surface Layer Dissolved Oxygen Validation Plot at Station 1GIBOKN0005 69
Figure B-41 Bottom Layer Dissolved Oxygen Validation Plot at Station 1GIBOKN0005 69
Figure B-42 Dissolved Oxygen Vertical Profile Comparison Plot at Station 1GIBOKN0003 (page 1-2) 70
Figure B-43 Dissolved Oxygen Vertical Profile Comparison Plot at Station 1GIBOKN0005 (page 1-2) 72
Figure B-44 Anoxic Volume at Stations 1GIBOKN0003 (red line) and 1GIBOKN0305 (blue line) 74
Figure B-45 Anoxic Volume at Stations 1GIBOKN0355 (red line) and 1GIBOKN0386 (blue line) 74
Figure B-46 Anoxic Volume of Fort Gibson Lake on July 25, 2006 00:00 75

Figure B-47 Box-Whisker plots of the Fort Gibson Lake Observed Surface Layer DO 75
Figure B-48 Box-Whisker plots of the Fort Gibson Lake Model Validation Results 76
Figure B-49 Box-Whisker plots of the Fort Gibson Lake Observed Bottom Layer DO 76
Figure B-50 Box-Whisker plots of the Fort Gibson Lake Model Validation Results 77
Figure B-51 Surface Layer Chlorophyll a Calibration Plot at Station 1GIBOKN0003 78
Figure B-52 Bottom Layer Chlorophyll a Calibration Plot at Station 1GIBOKN0004 79
Figure B-53 Surface Layer Chlorophyll a Calibration Plot at Station 1GIBOKN0005 79
Figure B-54 Surface TSI Calibration Plot at Station 1GIBOKN0003 81
Figure B-55 Bottom TSI Calibration Plot at Station 1GIBOKN0004 82
Figure B-56 Surface TSI Calibration Plot at Station 1GIBOKN0005 82
Figure B-57 Box-Whisker plots of the Fort Gibson Lake Observed Surface Layer TSI 82
Figure B-58 Box-Whisker plots of the Fort Gibson Lake EFDC Calibration Results 83
Figure B-59 Surface Layer TOC Calibration Plots at Station 1GIBOKN0003 84
Figure B-60 Bottom Layer TOC Calibration Plots at Station 1GIBOKN0003 85
Figure B-61 Surface Layer TOC Calibration Plots at Station 1GIBOKN0005 85
Figure B-62 Bottom Layer TOC Calibration Plots at Station 1GIBOKN0005 86
Figure B-63 Surface Layer TOC Validation Plots at Station 1GIBOKN0003 86
Figure B-64 Bottom Layer TOC Validation Plots at Station 1GIBOKN0003 87
Figure B-65 Surface Layer TOC Validation Plots at Station 1GIBOKN0005 87
Figure B-66 Bottom Layer TOC Validation Plots at Station 1GIBOKN0005 88
Figure B-67 Surface Layer NH4 Calibration Plots at Station 1GIBOKN0003 90
Figure B-68 Bottom Layer NH4 Calibration Plots at Station 1GIBOKN0003 91
Figure B-69 Surface Layer NH4 Calibration Plots at Station 1GIBOKN0005 91
Figure B-70 Bottom Layer NH4 Calibration Plots at Station 1GIBOKN0005 92
Figure B-71 Surface Layer NH4 Validation Plots at Station 1GIBOKN0003 92
Figure B-72 Bottom Layer NH4 Validation Plots at Station 1GIBOKN0003 93
Figure B-73 Surface Layer NH4 Validation Plots at Station 1GIBOKN0005 93
Figure B-74 Bottom Layer NH4 Validation Plots at Station 1GIBOKN0005 94
Figure B-75 Surface Layer NO3 Calibration Plots at Station 1GIBOKN0003 94
Figure B-76 Bottom Layer NO3 Calibration Plots at Station 1GIBOKN0003 95
Figure B-77 Surface Layer NO3 Calibration Plots at Station 1GIBOKN0005 95
Figure B-78 Bottom Layer NO3 Calibration Plots at Station 1GIBOKN0005 96
Figure B-79 Surface Layer NO3 Validation Plots at Station 1GIBOKN0003 96
Figure B-80 Bottom Layer NO3 Validation Plots at Station 1GIBOKN0003 97
Figure B-81 Surface Layer NO3 Validation Plots at Station 1GIBOKN0005 97
Figure B-82 Bottom Layer NO3 Validation Plots at Station 1GIBOKN0005 98
Figure B-83 Surface Layer TKN Calibration Plots at Station 1GIBOKN0003 98
Figure B-84 Bottom Layer TKN Calibration Plots at Station 1GIBOKN0003 99
Figure B-85 Surface Layer TKN Calibration Plots at Station 1GIBOKN0005 99
Figure B-86 Bottom Layer TKN Calibration Plots at Station 1GIBOKN0005 100
Figure B-87 Surface Layer TKN Validation Plots at Station 1GIBOKN0003 100
Figure B-88 Bottom Layer TKN Validation Plots at Station 1GIBOKN0003 101
Figure B-89 Surface Layer TKN Validation Plots at Station 1GIBOKN0005 101
Figure B-90 Bottom Layer TKN Validation Plots at Station 1GIBOKN0005 102
Figure B-91 Surface Layer TPO4 Calibration Plots at Station 1GIBOKN0003 104
Figure B-92 Bottom Layer TPO4 Calibration Plots at Station 1GIBOKN0003 104
Figure B-93 Surface Layer TPO4 Calibration Plots at Station 1GIBOKN0005 105
Figure B-94 Bottom Layer TPO4 Calibration Plots at Station 1GIBOKN0005 105

Figure B-95 Surface Layer TPO4 Validation Plots at Station 1GIBOKN0003 106
Figure B-96 Bottom Layer TPO4 Validation Plots at Station 1GIBOKN0003 106
Figure B-97 Surface Layer TPO4 Validation Plots at Station 1GIBOKN0005 107
Figure B-98 Bottom Layer TPO4 Validation Plots at Station 1GIBOKN0005 107
Figure B-99 Surface Layer TP Calibration Plots at Station 1GIBOKN0003 108
Figure B-100 Bottom Layer TP Calibration Plots at Station 1GIBOKN0003 108
Figure B-101 Surface Layer TP Calibration Plots at Station 1GIBOKN0005 109
Figure B-102 Bottom Layer TP Calibration Plots at Station 1GIBOKN0005 109
Figure B-103 Surface Layer TP Validation Plots at Station 1GIBOKN0003..... 110
Figure B-104 Bottom Layer TP Validation Plots at Station 1GIBOKN0003 110
Figure B-105 Surface Layer TP Validation Plots at Station 1GIBOKN0005..... 111
Figure B-106 Bottom Layer TP Validation Plots at Station 1GIBOKN0005 111
Figure B-107 – Sediment Flux of Phosphate (PO4) (as g/m2-day) Calibration Results at 1GIBOKN0003 and 1GIBOKN0305 113
Figure B-108 – Sediment Flux of Phosphate (PO4) (as g/m2-day) Calibration Results at 1GIBOKN0355 and 1GIBOKN0386 113
Figure B-109 SOD (as g/m^2-day) Calibration Results at 1GIBOKN0003 and 1GIBOKN0305 114
Figure B-110 SOD (as g/m2-day) Calibration Results at 1GIBOKN0355 and 1GIBOKN0386..... 114
Figure B-111 – Sediment Flux of Phosphate (PO4) (as g/m2-day) Model Calibration Results 115
Figure B-112 SOD (as g/m2-day) Model Calibration Results in Fort Gibson Lake (May 15-Oct 1)..... 116
Figure B-113 – Comparisons of anoxic release rates of phosphorus (as mg/m2-day)..... 116

List of Tables

Table B-1 Information for the NPDES Wastewater Treatment Facilities..... 15
Table B-2 Fort Gibson Lake EFDC Model Flow Boundaries and Data Source..... 18
Table B-3 HSPF State Variables and Units for the Fort Gibson Lake Model 24
Table B-4 HSPF-EFDC Linkage..... 25
Table B-5 Refractory, Labile and Dissolved Splits for Organic Matter..... 26
Table B-6 EFDC State Variables 28
Table B-7 EFDC model parameter values for cohesive solids 29
Table B-8 Dry and Wet Atmospheric Deposition for Nutrients..... 34
Table B-9 EFDC Sediment Diagenesis Model State Variables 37
Table B-10 Calibration and Validation Stations for the Fort Gibson Lake EFDC Model..... 42
Table B-11 Summary Model Performance Statistics for Hydrodynamic Model of Fort Gibson Lake 46
Table B-12 Summary Statistics of Water Temperature (°C)..... 49
Table B-13 Summary Statistics of TSS (mg/l) 58
Table B-14 Summary Statistics of DO (mg/l)..... 64
Table B-15 Summary Statistics of Chlorophyll a (µg/l) 78
Table B-16 Summary Statistics of Trophic State Index (TSI) 80
Table B-17 Summary Statistics of TOC (mg/l) 84
Table B-18 Summary Statistics of NH4 (mg/l)..... 89
Table B-19 Summary Statistics of NO3 (mg/l)..... 89
Table B-20 Summary Statistics of TKN (mg/l) 90
Table B-21 Summary Statistics of TPO4 (mg/l) 103
Table B-22 Summary Statistics of TP (mg/l)..... 103
Table B-23 Comparison of Measured Sediment Flux Rates for Oxygen and Phosphate in Central Plains. 117

List of Acronyms and Abbreviations

BUMP	Beneficial Uses Monitoring Program
CASTNET	Clean Air Status and Trends Network
Chl-a	Chlorophyll-a
COD	Chemical Oxygen Demand
USACE	United States Army Corps of Engineers
ODEQ	Oklahoma Department of Environmental Quality
DO	Dissolved Oxygen
DOC	Dissolved Organic Carbon
DOM	Dissolved Organic Matter
DON	Dissolved Organic Nitrogen
DOP	Dissolved Organic Phosphorus
DSLLC	Dynamic Solutions, LLC
EFDC	Environmental Fluid Dynamics Code
EPA	Environmental Protection Agency
HSPF	Hydrologic Simulation FORTRAN Program
HUC	Hydrologic Unit Code
LPOC	Labile particulate organic carbon
LPON	Labile particulate organic nitrogen
LPOP	Labile particulate organic phosphorus
MGD	Mega Gallon per Day
NADP	National Atmospheric Deposition Program
NGVD29	National Geodetic Vertical Datum of 1929
NLW	Nutrient Limited Waterbody
NPS	Nonpoint Source
OWRB	Oklahoma Water Resources Board
POC	Particulate Organic Carbon
POM	Particulate Organic Matter
PON	Particulate Organic Nitrogen
POP	Particulate Organic Phosphorus
RMS	Root Mean Square
RMSE	Root Mean Square Error
RPOC	Refractory particulate organic carbon
RPON	Refractory particulate organic nitrogen
RPOP	Refractory particulate organic phosphorus
SOD	Sediment Oxygen Demand
TKN	Total Kjedhal Nitrogen (Total Organic Nitrogen + Ammonia-N)
TMDL	Total Maximum Daily Load
TN	Total Nitrogen
TOC	Total Organic Carbon
TON	Total Organic Nitrogen
TOP	Total Organic Phosphorus
TP	Total Phosphorus
TPO4	Total Phosphate
TSI	Trophic State Index
TSS	Total Suspended Solids
USGS	United States Geological Survey
WWAC	Warm Water Aquatic Community

B-1 INTRODUCTION

Fort Gibson Lake, located at the downstream end of the Lower Neosho watershed (HUC 11070209) about 5 miles northwest of Fort Gibson, OK, was formed as a 19,900 acre reservoir in 1953 by impounding the Lower Neosho River for hydropower and flood control. The reservoir, owned and operated by the USACE, Tulsa District, is located about 7.7 miles upstream of the confluence of the Neosho River with the Arkansas River. In addition to the Lower Neosho River, tributary inflows to the reservoir are contributed by Snake Creek, Clear Creek and Fourteen Mile Creek on the eastern shore of the lake. Lake Hudson, Spavinaw Lake and Lake Eucha are other impoundments in the Lower Neosho watershed that are upstream of Fort Gibson Lake. Grand Lake, a large reservoir in the Lake of the Cherokees Catalog Unit (11070206), is located upstream of Fort Gibson Lake. Figure B-1 shows the location of Fort Gibson Lake at the downstream end of the Lower Neosho watershed.

In the 2009 OWRB BUMP report on the lakes of Oklahoma, Fort Gibson Lake is identified as impaired for beneficial uses related to (a) Fish & Wildlife Propagation (FWP) because of low dissolved oxygen and (b) Aesthetic (AES) uses because of its status as a Nutrient Limited Watershed (NLW). Using monitoring data collected for the BUMP surveys, Fort Gibson Lake is one of 21 lakes in Oklahoma that have been designated as Nutrient Limited Watersheds in Oklahoma Water Quality Standards because of Carlson's Trophic Status Index (TSI) (Carlson, 1977). Sources of nutrient loading to Fort Gibson Lake that are related to nutrient enrichment and eutrophication in the lake include loading from the Headwaters-Upper-Middle Neosho basins, Elk and Spring basins and Lake of the Cherokees watersheds via outflows from Grand Lake and loading from the Lower Neosho basin via outflows from Lake Hudson, Lake Eucha, Spavinaw Lake and local loading downstream of Lake Hudson to Fort Gibson Lake from tributaries and nonpoint sources.

Since Fort Gibson Lake is listed as a Nutrient Limited Watershed, a Nutrient Impairment Study is needed to definitively determine the presence or absence of nutrient impairment in the lake. In addition to its status as a NLW by ODEQ, Fort Gibson Lake was also identified in the 2010 EPA 303(d) report as impaired for Fish and Wildlife Propagation in a warm water aquatic community because of low dissolved oxygen and high turbidity. A TMDL assessment for Fort Gibson Lake is required by EPA to determine appropriate load reductions that could be implemented to achieve compliance with water quality standards for the lake. The objective of this modeling work is to develop and calibrate a watershed runoff model using HSPF and a 3-dimensional hydrodynamic and water quality model using the Environmental Fluid Dynamic Code (EFDC) to address the water quality issues and facilitate the development of TMDLs.

The setup, calibration, and validation of the lake EFDC hydrodynamic and water quality model that uses the most current data are summarized in this report. The scope of the project included the following elements:

- Develop the EFDC model grid based on shoreline boundary and lake bathymetry;

- Setup and develop data linkages between HSPF watershed runoff model and the EFDC lake model of hydrodynamics and water quality. The HSPF model results are used to provide streamflow, water temperature, suspended solids (TSS), organic carbon, nutrients (N,P), algae biomass, and dissolved oxygen as input data for the EFDC lake model;

- Analyze, process and format lake surface elevation, storage volume and release flow measured at the dam at Station GIBO2 by the USACE, Tulsa District;

- Analyze, process and format wind and meteorological input data from Oklahoma Mesonet at stations INOL, PORT, and TAHL;

- Analyze, process, and format available OWRB and USACE station data to describe time series and vertical profiles of water temperature and dissolved oxygen;

- Analyze, process, and format available OWRB and USACE station data to describe time series of water elevation, total suspended solids (TSS), turbidity, nutrients (N,P), algae biomass as chlorophyll a, and organic carbon;

- Process all data in formats required for input to the EFDC model for setup of the hydrodynamic, sediment transport, water quality and sediment diagenesis model;

- Calibrate the hydrodynamic and water quality model for the 365 day period from 1 January 2005 through 31 December 2005 to records for water level elevation, water temperature, suspended solids, dissolved oxygen, organic carbon, nutrients (N,P) and algae biomass as chlorophyll-a at four (4) station locations in Ft. Gibson Lake;

- Validate the hydrodynamic and water quality model for the 365 day period from 1 January 2006 through 31 December 2006 to records for water level elevation, water temperature, suspended solids, dissolved oxygen, organic carbon, nutrients (N,P) and algae biomass as chlorophyll-a at four (4) station locations in Ft. Gibson Lake;

- Analyze, process and present calibrated water quality model results to show comparisons to water quality targets for dissolved oxygen, chlorophyll-a, and Carlson's Trophic State Index (TSI) for chlorophyll-a;

- Based on calibrated HSPF and EFDC models, compile mass balance budgets to compare external watershed loading of inorganic solids, organic carbon and nutrients from the HSPF model and internal loading of nutrients across the sediment-water interface from the EFDC sediment diagenesis model;

- Prepare and submit draft and final technical reports documenting the development, calibration and application of the Ft. Gibson Lake EFDC hydrodynamic and water quality model; and

- Using the calibrated HSPF watershed and EFDC lake models simulate the in-lake response to load allocation scenarios.

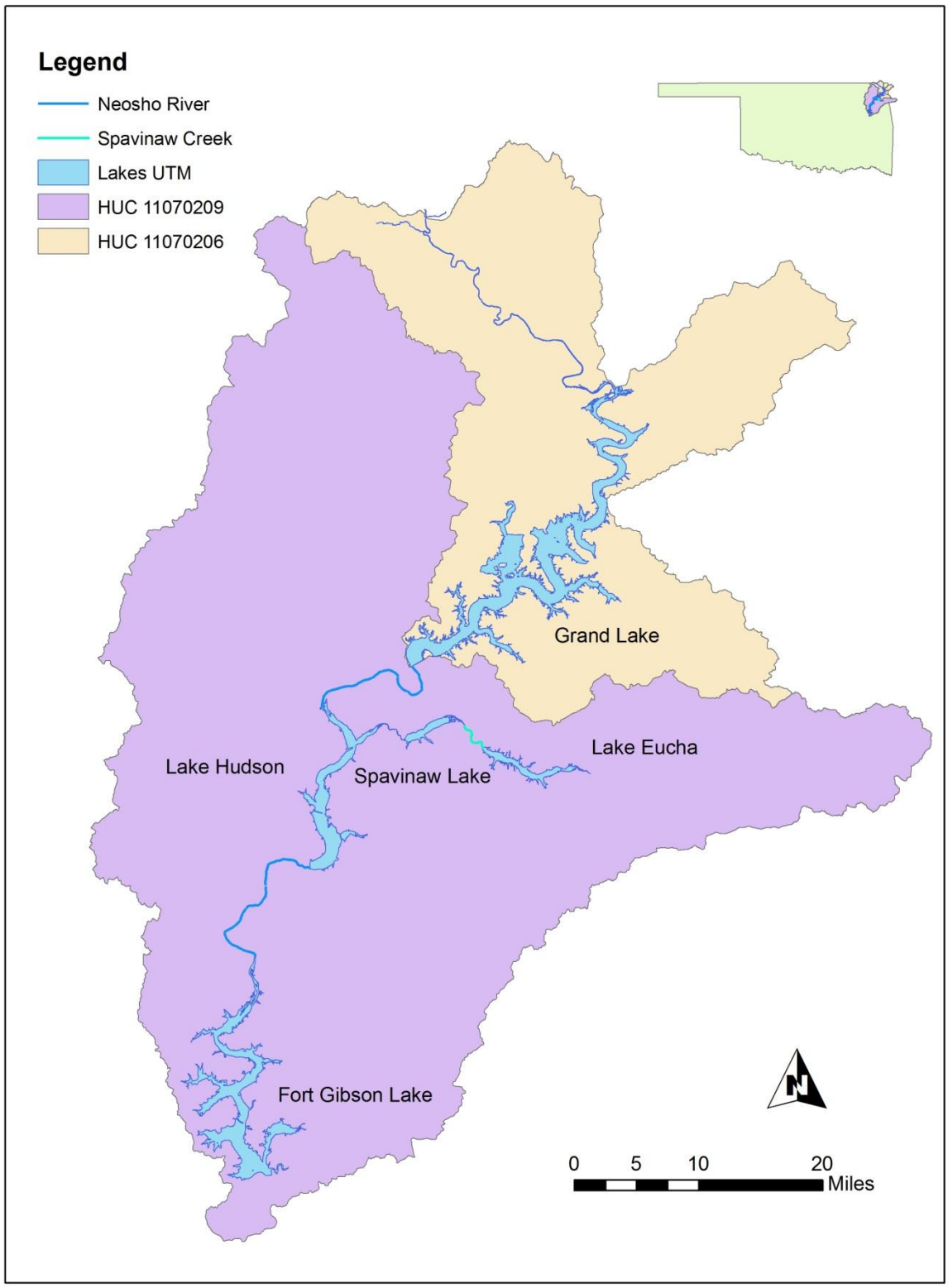

Figure B-1 Location of Fort Gibson Lake

B-2 MODEL DEVELOPMENT

B-2.1 Overview of the EFDC Model

The Environmental Fluid Dynamics Code (EFDC) is a general-purpose surface water modeling package for simulating three-dimensional (3-D) circulation, mass transport, sediments and biogeochemical processes in surface waters including rivers, lakes, estuaries, reservoirs, nearshore and continental shelf-scale coastal systems. The EFDC model was originally developed at the Virginia Institute of Marine Science for estuarine and coastal applications (Hamrick, 1992; 1996). Over the past decade, the US Environmental Protection Agency (EPA) has continued to support its development, and EFDC is now part of a family of public domain surface water models recommended by EPA to support water quality investigations. In addition to state of the art hydrodynamics with salinity, water temperature and dye tracer simulation capabilities, EFDC can also simulate cohesive and non-cohesive sediment transport, the transport and fate of toxic contaminants in the water and sediment bed, and water quality interactions that include dissolved oxygen, nutrients, organic carbon, algae and bacteria. A state of the art sediment diagenesis model (Di Toro, 2001) is coupled with the water quality model (Park et al., 2000). Special enhancements to the hydrodynamic code, such as vegetation resistance, drying and wetting, hydraulic structure representation, wave-current boundary layer interaction, and wave-induced currents, allow refined modeling of tidal systems, wetland and marsh systems, controlled-flow systems, and near-shore wave-induced currents and sediment transport. The EFDC code has been extensively tested, documented and used in more than 100 surface water modeling studies (Ji, 2008). The EFDC model is currently used by university, government, engineering and environmental consulting organizations worldwide.

Dynamic Solutions, LLC (DSLLC), has developed a version of the EFDC code that streamlines the modeling process and provides links to DSLLC's pre- and post-processing software tool EFDC_Explorer7 (Craig, 2012). The DSLLC version of the EFDC code is open source and DSLLC coordinates with EPA to provide ongoing updates and enhancements to both DSLLC's version of EFDC as well as the version of the EFDC code provided by EPA.

B-2.2 Model Simulation Period

The EFDC model simulation period is 1 January 2005 through 31 December 2006. The Fort Gibson Lake EFDC model is calibrated for the period of 1 January 2005 through 31 December 2005 and validated for the period of 1 January 2006 through 31 December 2006.

B-2.3 Model Constituents

The modeled constituents in the Fort Gibson Lake EFDC model are given below.

- Stage
- Water temperature
- Total suspended solids (TSS)
- Nitrogen (TN, organic N, TKN, NO2+NO3, NH3/NH4)
- Phosphorus (TP, organic P, Ortho-Phosphate)

- Total organic carbon (TOC)
- Phytoplankton (as Chl-a)
- Dissolved oxygen (DO)

B-2.4 Grid Development

The EFDC grid of Fort Gibson Lake was developed based on the shoreline downloaded from the National Hydrography Dataset (NHD) of USGS. Grid generation software from Delft Hydraulics was used to create the EFDC modeling grid (Delft Hydraulics, 2007). Figure B-2 shows a plan view map of the 483 horizontal cells that has been developed for the Fort Gibson EFDC model. Eight (8) vertical layers were used to simulate stratification and vertical mixing of water and water quality constituents.

Bathymetry data, collected by OWRB, were obtained from the ODEQ with the highest bathymetric elevation of 168.73 m (as NGVD 29). The comparison of the stage-volume relationship derived from the USACE observed data and the EFDC computational grid is shown in Figure B-3. For a given lake stage, the EFDC model has a relatively smaller volume than the observed data because the observed relationship is calculated from pre-impoundment topography and the discrepancy might be caused by sedimentation that has occurred over the decades since the Fort Gibson Dam was completed in 1953 (http://www.swt.usace.army.mil/Locations/TulsaDistrictLakes/Oklahoma/FortGibsonLake/History.aspx).

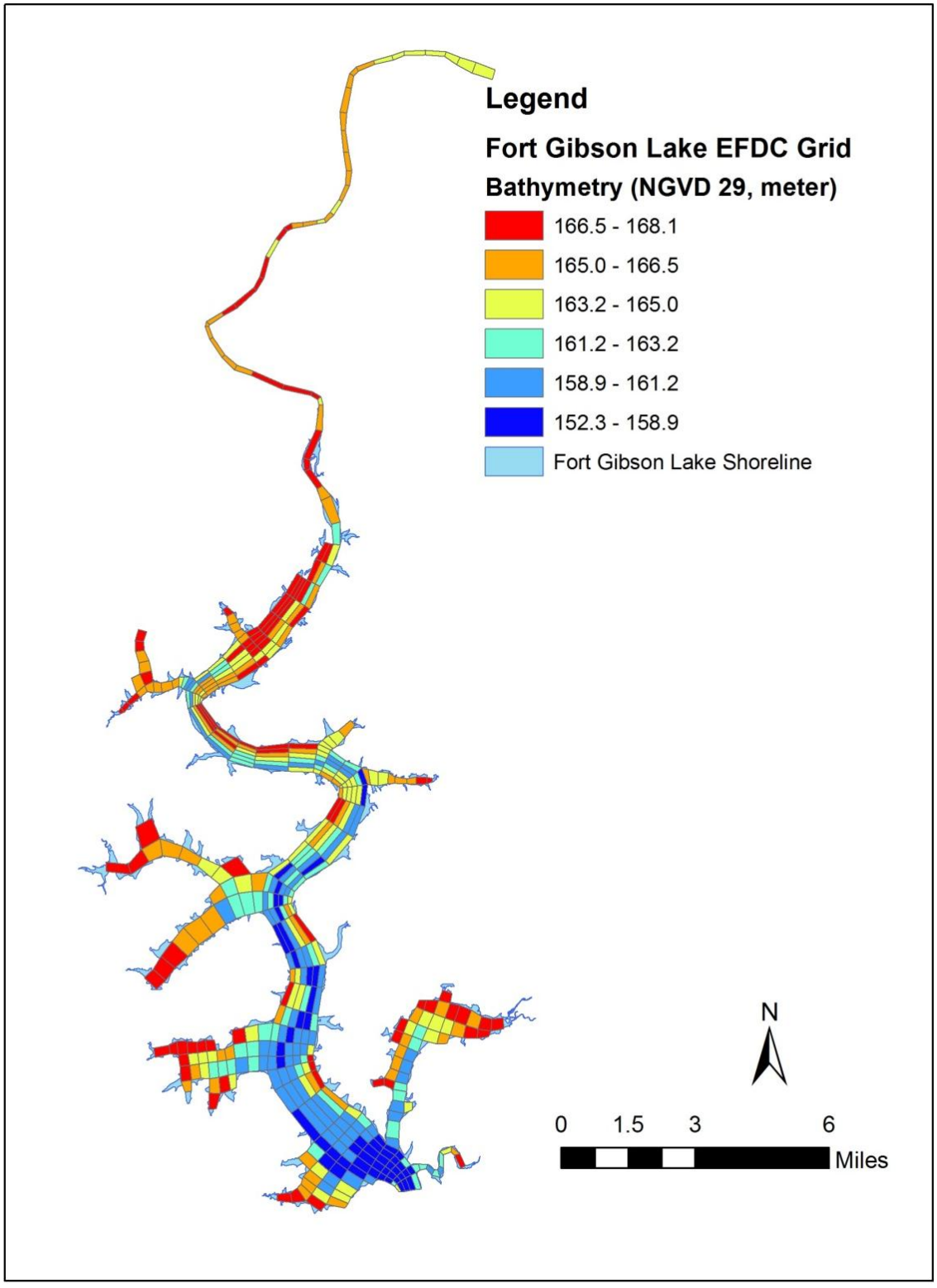

Figure B-2 Modeling Domain of the Fort Gibson Lake EFDC

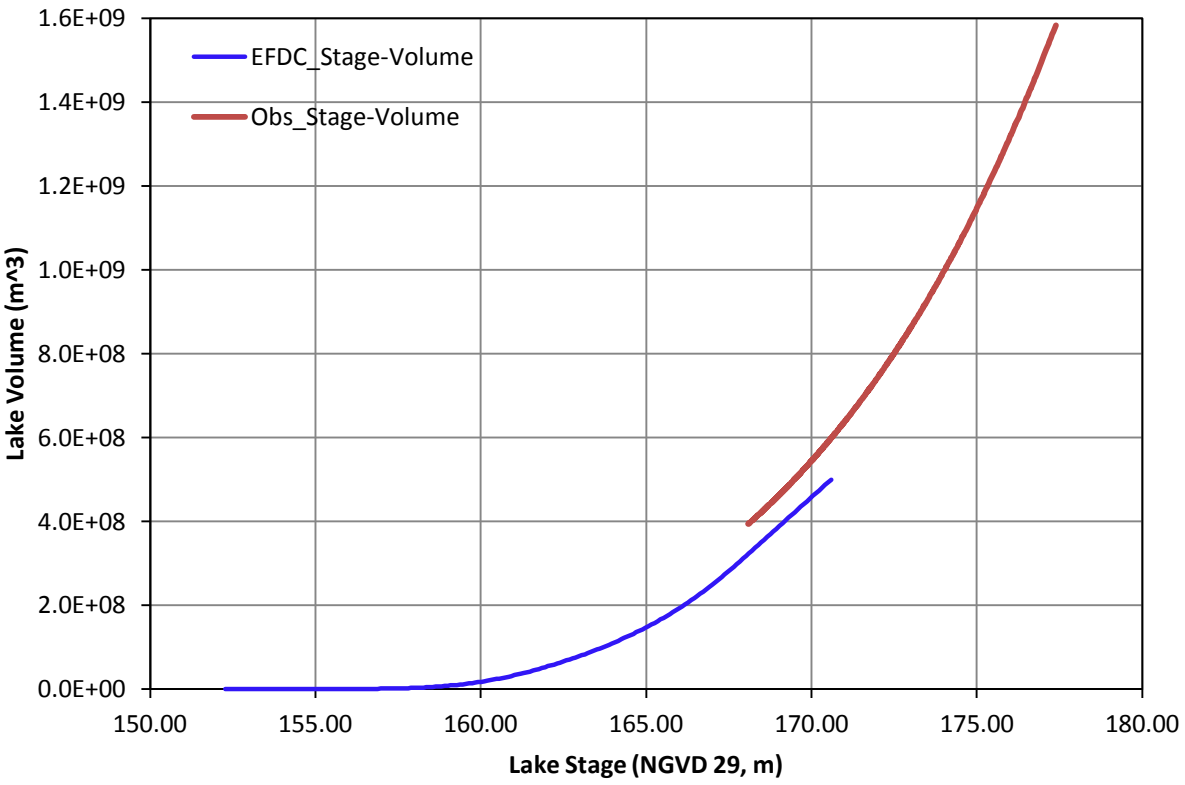

Figure B-3 Fort Gibson Lake Stage and Storage Volume.
Comparison of Observed Data and EFDC Model

B-2.5 Meteorological Data

Meteorological data used in EFDC includes rainfall, wind speed and direction, relative humidity, atmospheric pressure, cloud cover, solar radiation, and air temperature. These data are used to calculate the atmospheric impact on water temperature and circulation in the system. The data are also used to calculate evapotranspiration within the model domain. The three MESONET stations used in the EFDC model (PORT, INOL, and TAHL) are shown in Figure B-4.

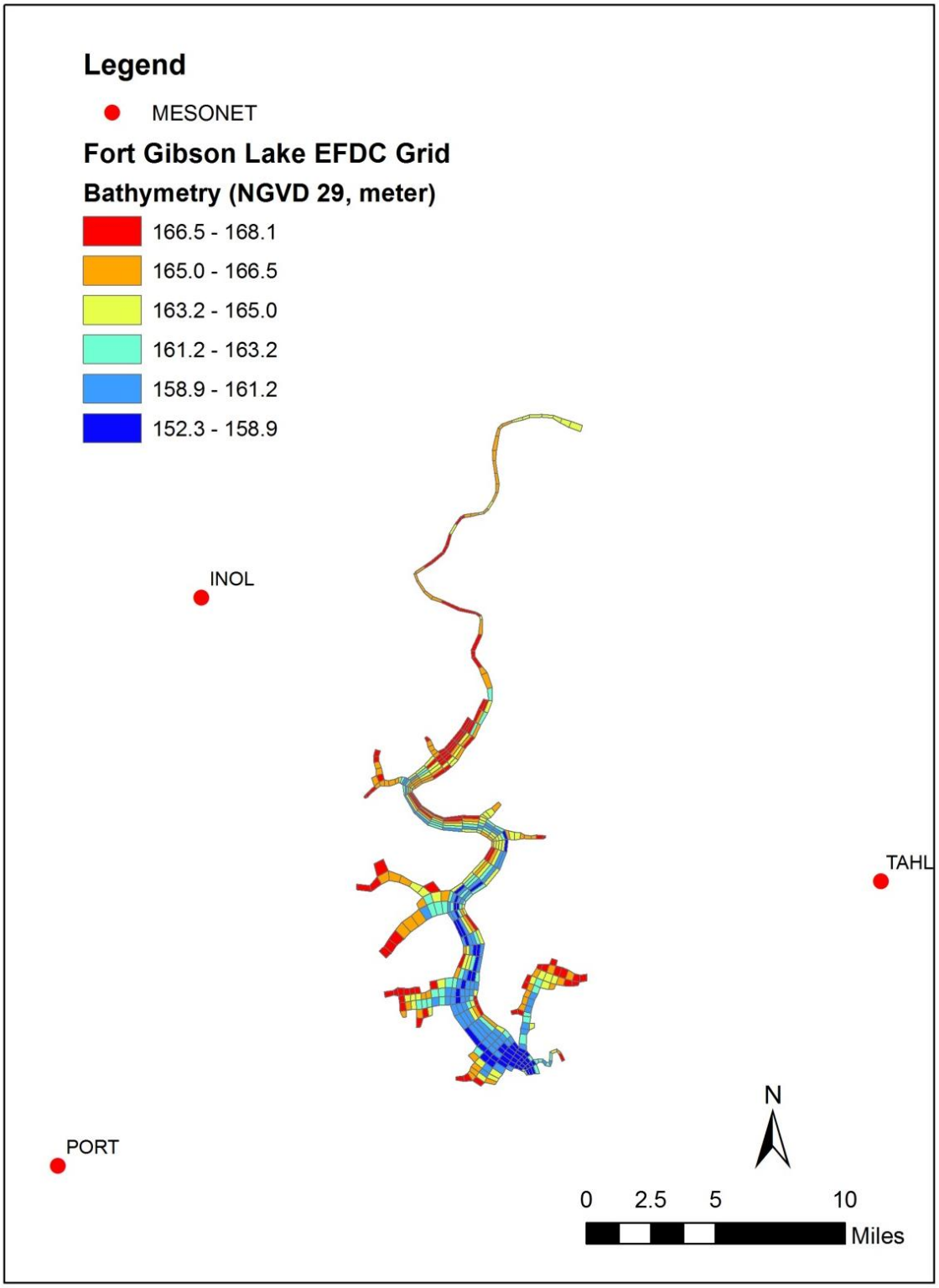

Figure B-4 Location of the MESONET Stations

B-2.6 Point Source Discharge

The EPA National Pollutant Discharge Elimination System (NPDES) reports 6 wastewater facilities (point sources) that discharge into either the Neosho River or Fort Gibson Lake. Detailed information for these six facilities is given in Figure B-5 and Table B-1. The waterbody (Neosho River or Ft. Gibson Lake) receiving the effluent from each point source was identified using either the EPA's Permit Compliance System (PCS) data or their geographic locations using GIS.

Table B-1 Information for the NPDES Wastewater Treatment Facilities

Permit #	Facility Name	Receiving water	Latitude	Longitude	Design flow (MGD)
OK0000272	PRYOR IND CONSERVE PICC	Neosho River	36.19	-95.25	3.7
OK0033791	WAGONER CNTY RWD NUMBER 2	Ft Gibson Lake	35.956	-95.28	Report, water treatment plant, no BOD limits
OK0034568	OKLA ORDNANCE WORKS ATHRTY OOWA PRYOR	Neosho River	36.21	-95.25	4.6
OK0035149	GRAND RIVER DAM ATHRTY CHOUTEAU COAL FIRED COMPLEX	Grand Neosho River	36.18	-95.28	Report, steam electric power plant, no BOD limits
OK0040479	PRYOR CREEK WWTP	MidAmericaCk/ Pryor Ck/Neosho R	36.27	-95.34	1.67
OKG380001 (changed to OK0046035 in 2012)	WAGONER WTP	Ft Gibson Lake	36.02	-95.30	Report, water treatment plant, no BOD limits

Effluent data for these NPDES facilities are required for model inputs for flow, water temperature, Total Suspended Solids (TSS), Total Organic Carbon (TOC), Nitrogen (TN, TKN, TON, NH3, NO3), Phosphorus (TP, TOP, PO4), and Inorganic Suspended Solids (InorgSS). Discharge Monitoring Report (DMR) data were obtained from the EPA website. Monthly data were available for these six NPDES facilities for the period from January 2005 to December 2006.

If a required water quality parameter is not available from the DMR data then stoichiometric ratios of typical effluent concentrations were used to estimate the missing parameter from available observations according to the level of treatment for the facility type and literature values (Metcalf & Eddy, Inc., 1991; Rozzi et al., 1999; Stoddard et al., 2002; Hyder and Bari, 2011). Based on the BOD5 and TSS effluent data available from the DMR files, the Wagoner County RWD Number 2 (OK0033791) and Wagoner WTP (OKG380001) are categorized as tertiary or advanced waste treatment (AWT) facilities. Oklahoma Ordance Works Authority (OOWA) Pryor (IK0034568), Grand River Dam Authority (GRDA) Chouteau Coal Fired Complex (OK0035149), and Associated Electric Coop (AECI) Chouteau Power Plant (OK0043907) are described as secondary treatment (SEC). Pryor Industrial Conservation (PICC) (OK0000272) is classified as a pulp and paper facility. Daily time series of flow and all effluent water quality parameters were assigned from either observed data or estimated data that was based on linear interpolation of effluent data from 1 January 2005 through 31 December 2006

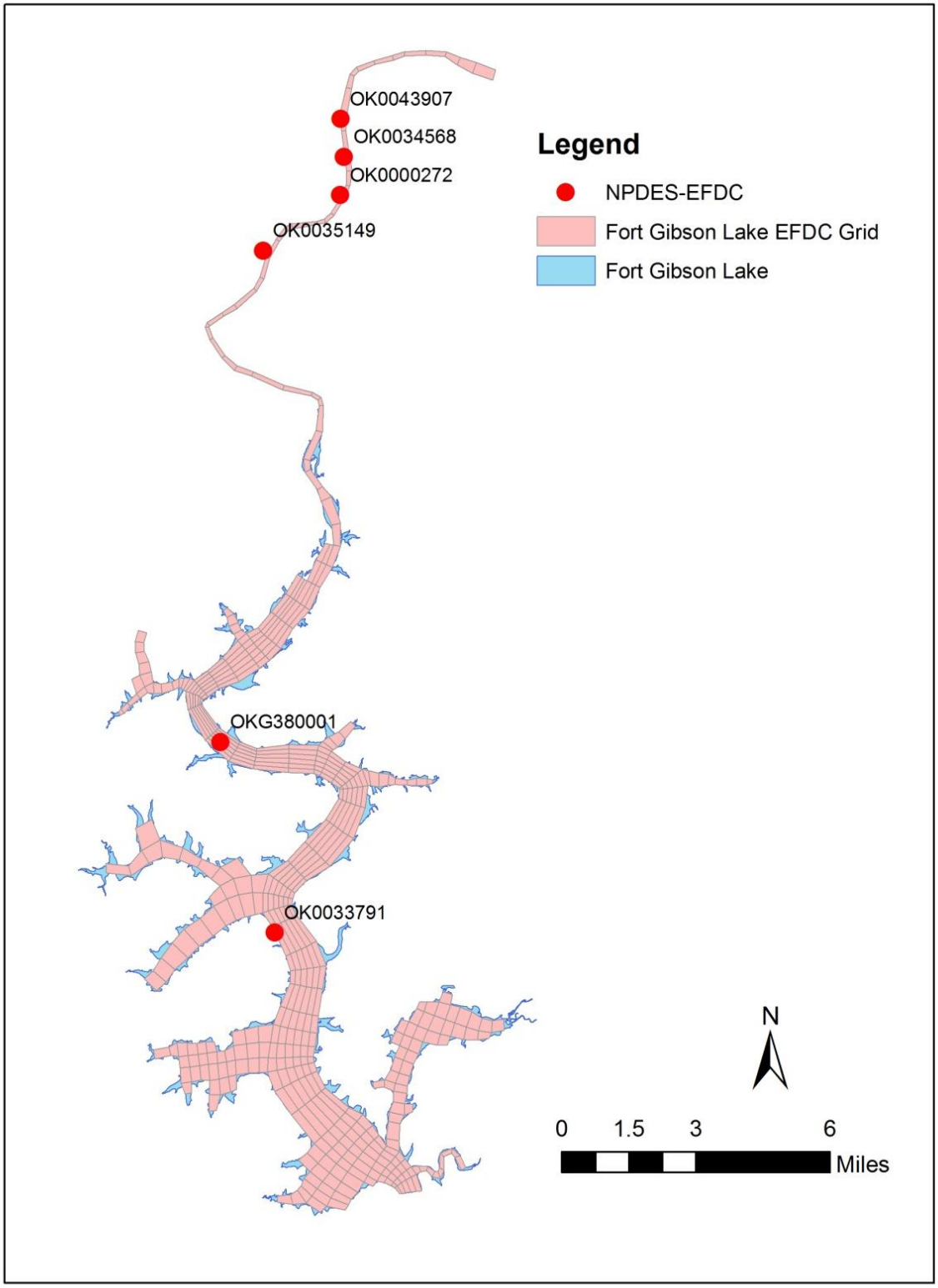

Figure B-5 Location of the NPDES Facilities Discharging to the Fort Gibson Lake EFDC Model

B-2.7 Boundary Conditions

Boundary conditions for EFDC must be specified for flow boundary conditions to define external inflows and withdrawals of water and mass loading into the EFDC model domain. Flow boundary datasets required for input to EFDC include time series of flow, water temperature, suspended solids and water quality constituents to define mass loading inputs to a waterbody. Data sources for flow boundary condition time series datasets can include (a) USGS streamflow and water quality monitoring station locations; (b) simulated streamflow and water quality from watershed models; and (c) NPDES program discharge monitoring records (DMR) for effluent flow and pollutants for wastewater facilities and stormwater outflows.

The Fort Gibson Lake model was developed with eight (8) flow boundaries to define water coming into the lake from the HSPF watershed model, six (6) flow boundaries to define water coming into the lake from the NPDES wastewater point source facilities, one (1) flow boundary to define the discharge from Hudson Lake to the Neosho River, and two (2) flow boundaries to account for releases of water at the dam and a flow balance. The flow balance was computed to account for water removed from the lake by water supply withdrawals and other unaccounted flows. Table B-2 lists the eighteen (18) model flow boundary indexes with the number of the EFDC grid cells assigned for the flow boundary and the HSPF_ID corresponding to that location.

External flow boundary conditions from the HSPF model were assigned to grid cells based on physical location and the specific boundary condition represented in the lake model (Figure B-6). Simulated streamflow and runoff, water temperature, suspended solids, organic carbon, nutrients, dissolved oxygen and algae biomass records provided by the HSPF model were used to assign flow boundaries for six (6) tributaries and two (2) NPS catchments for input to the lake model. Figure B-6 shows the HSPF watershed model locations that provided the flow and water quality data for input to the lake model. The effluent flow and effluent water quality boundary time series from the NPDES facilities were defined as described in Section 2.6.

The upstream flow boundary of the Neosho River was obtained from the USGS gage station 07191500 (Figure B-7). The upstream water quality boundary at the Neosho River was obtained from the two stations: OWRB 121600020020-01 and Grand River Dam Authority (GRDA) Kerr dam as shown in Figures B-8 and B-9. These two stations are located in the forebay area of Lake Hudson. Monthly time series for water quality constituents were developed as the boundary condition for the simulation period of 2005 to 2006. If the data were not available for a particular month during 2005 to 2006, the multiple-year (1999-2013) average value for that month was used to fill in the missing data. EFDC model uses a linear interpolation scheme to interpolate water quality values using the defined monthly data at the boundary for each time step. Reliability of the upstream water quality boundary conditions were further confirmed with the downstream water quality station OWRB 1GIBOKN0008 shown in Figure B-10. Detailed discussions are presented in Appendix H.

Daily flow release records at the dam (designated by the USACE as Station GIBO2 shown in Figure B-10) are maintained by the USACE Tulsa District. The water supply withdrawals from multiple water intakes in Fort Gibson Lake were not available. Water withdrawals were represented in the computation of a flow

balance derived from all water inflows including all HSPF simulated watershed flows, rainfall, point source flows, and flow from upstream Lake Hudson and all water outflows including evaporation and flow releases at the dam. Using these data sets, a flow balance that incorporated unknown water supply withdrawals was computed to ensure that the simulated lake stage was in agreement with the observed lake stage. Sections 6.1 and 6.2 present a comparison of model results and observed data for lake stage for model calibration and validation.

Table B-2 Fort Gibson Lake EFDC Model Flow Boundaries and Data Source.

BC	Boundary Group Name	Data	Cells
1	Dam Release	Outflow	1
2	Inflow	USGS 07191500	1
3	Pryor Creek	HSPF	1
4	Choteau Creek	HSPF	1
5	Spring Creek	HSPF	1
6	Clear Creek	HSPF	1
7	Fourteen Mile Creek	HSPF	1
8	Upper Fort Gibson	HSPF	3
9	Lower Fort Gibson	HSPF	4
10	Crutch Field Branch	HSPF	1
11	OK0043907	NPDES	1
12	OK0034568	NPDES	1
13	OK0000272	NPDES	1
14	OK0035149	NPDES	1
15	OKG380001	NPDES	1
16	OK0033791	NPDES	1
17	Balance Flow	Estimated	4

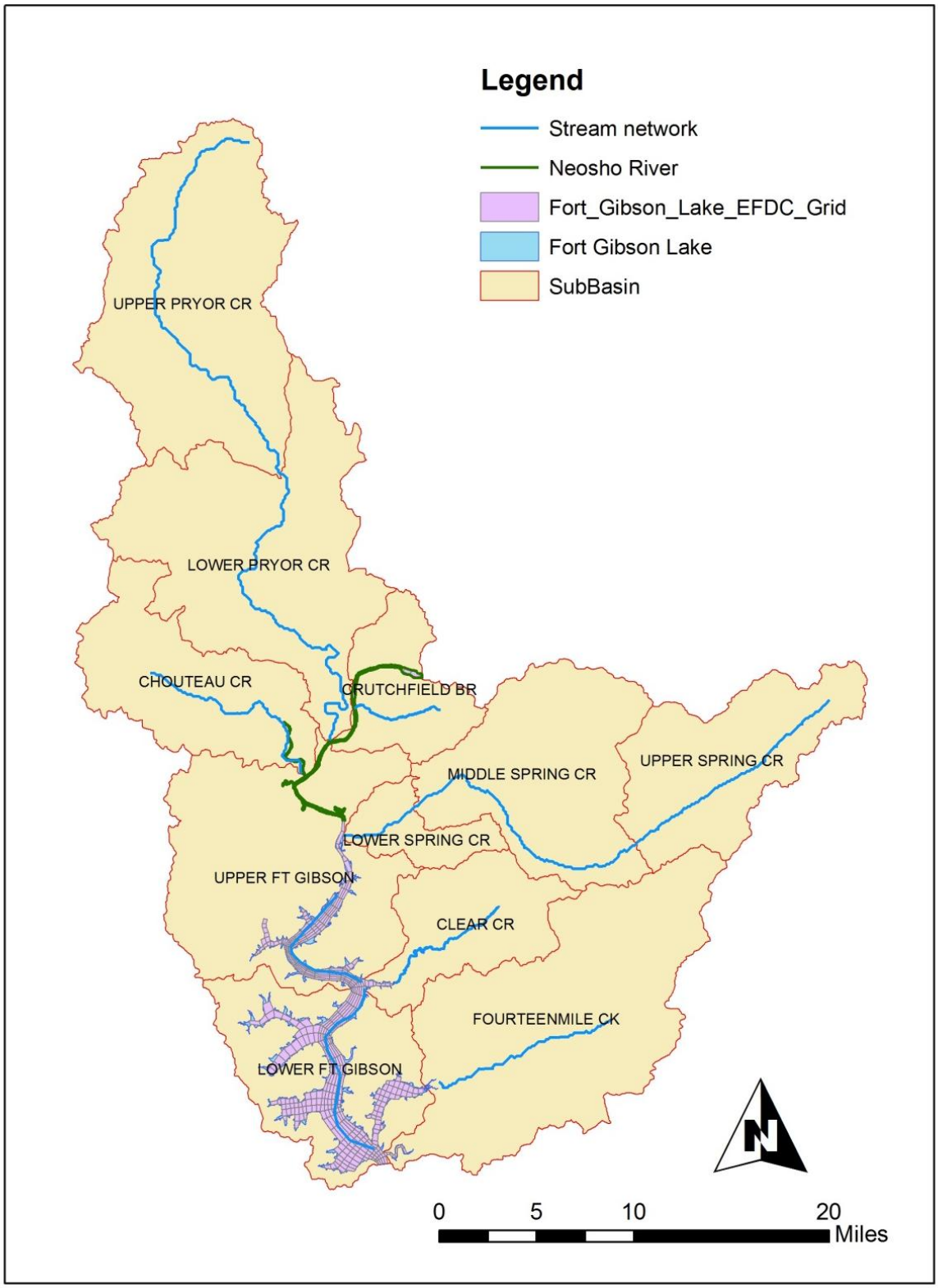

Figure B-6 HSPF Tributary and Catchment Locations.

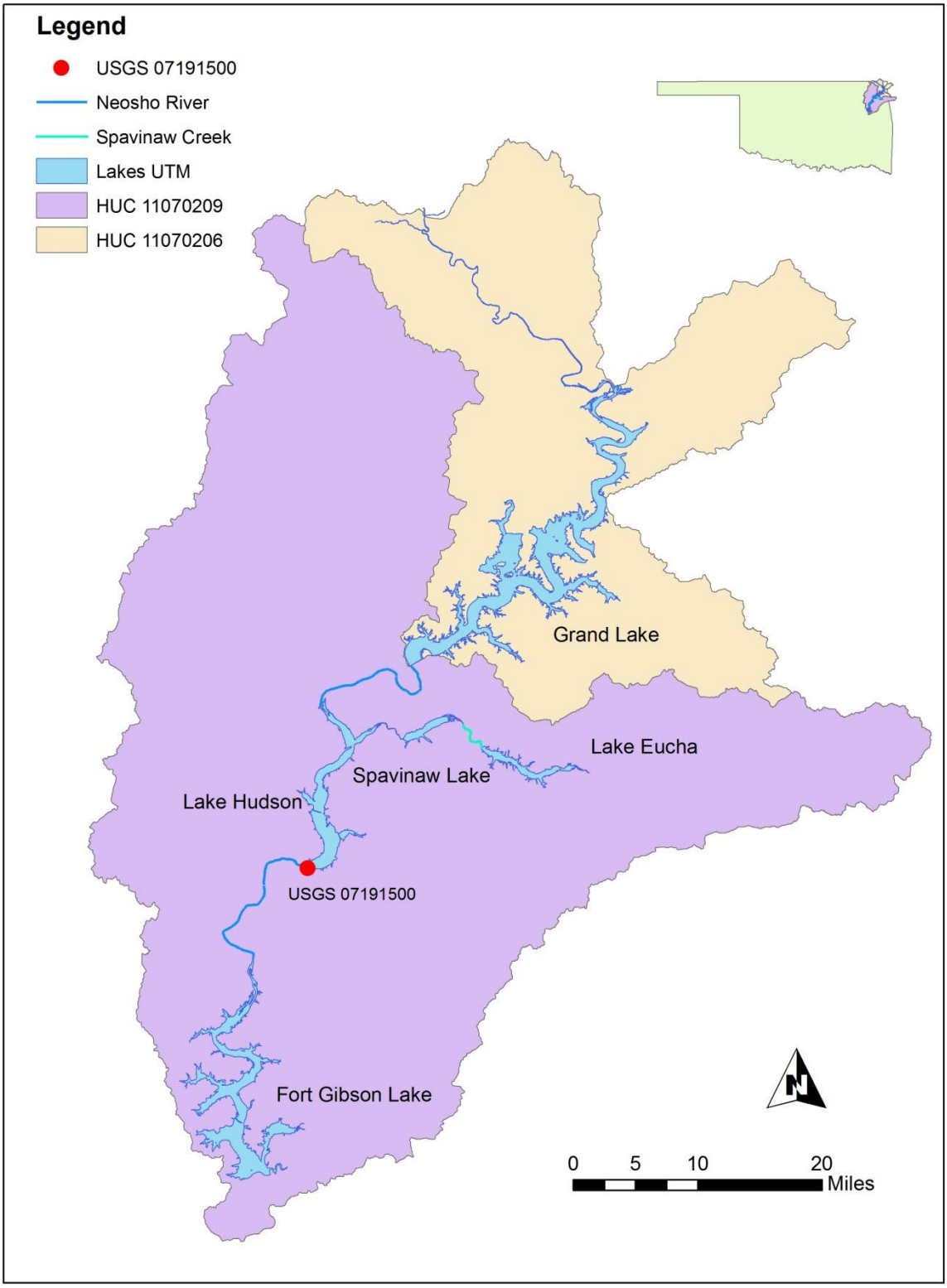

Figure B-7 Location of USGS Gage Station 07191500.

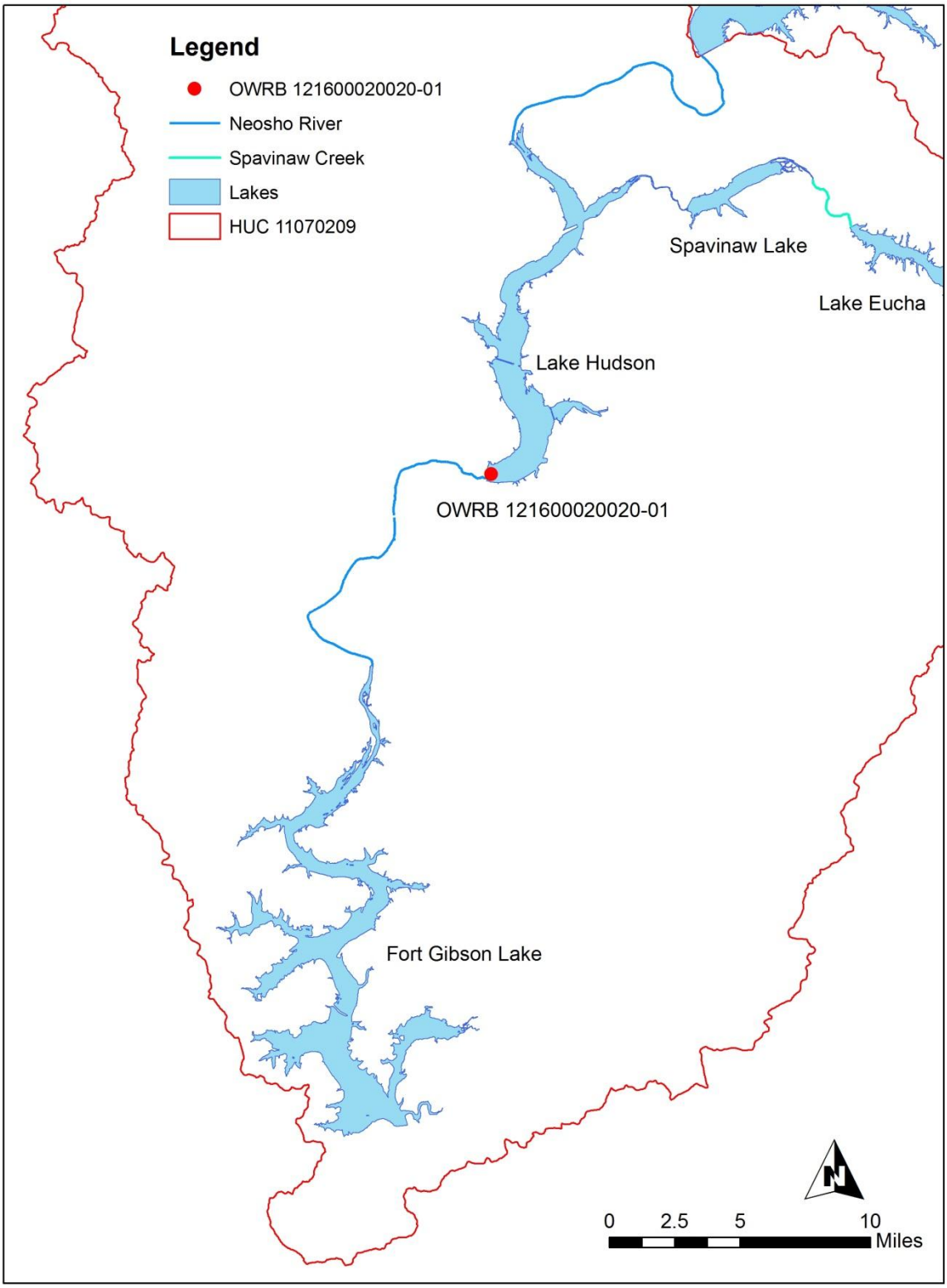

Figure B-8 Location of OWRB Water Quality Observation Station for Upstream Boundary

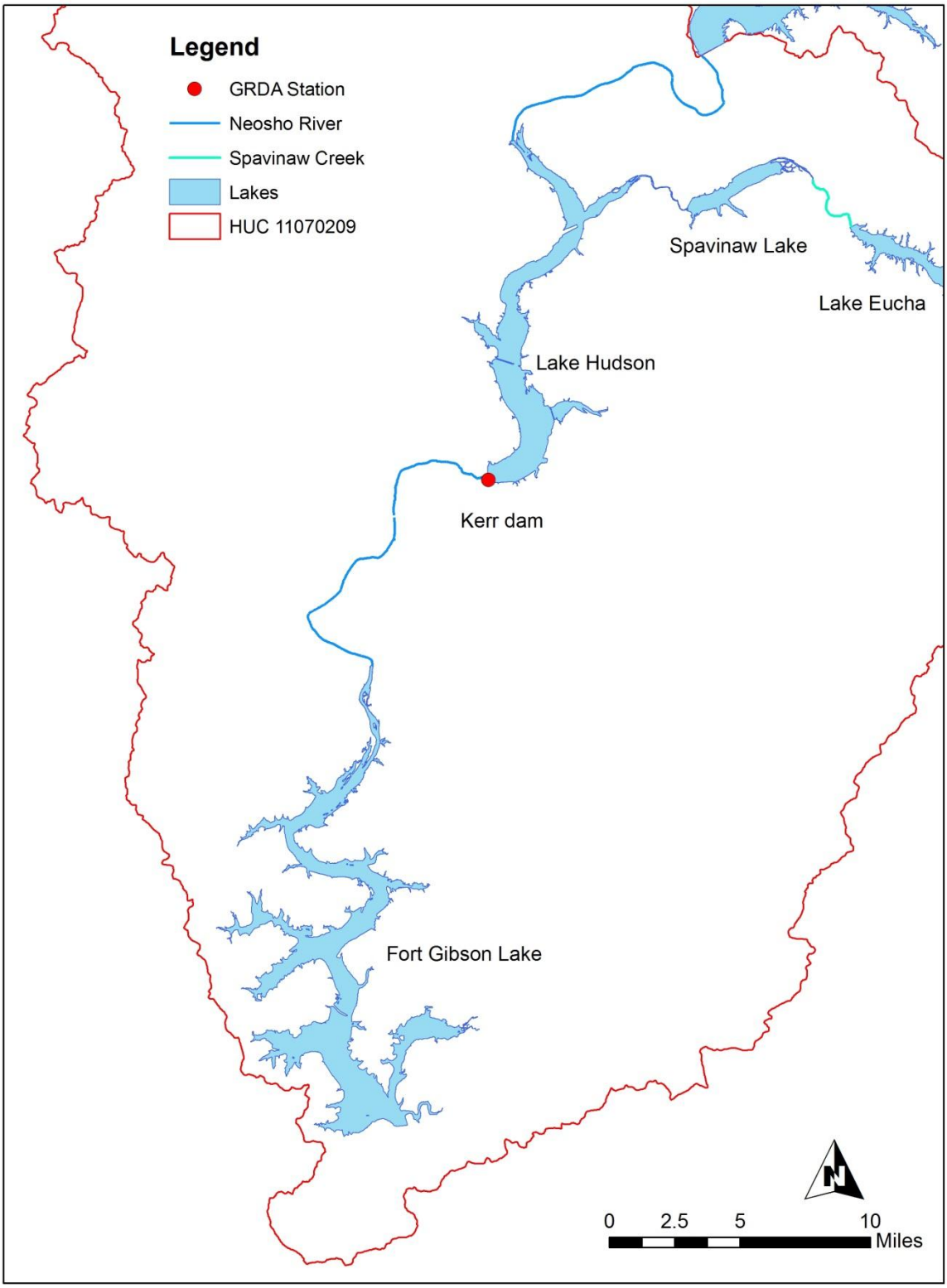

Figure B-9 Location of GRDA Water Quality Observation Station for Upstream Boundary

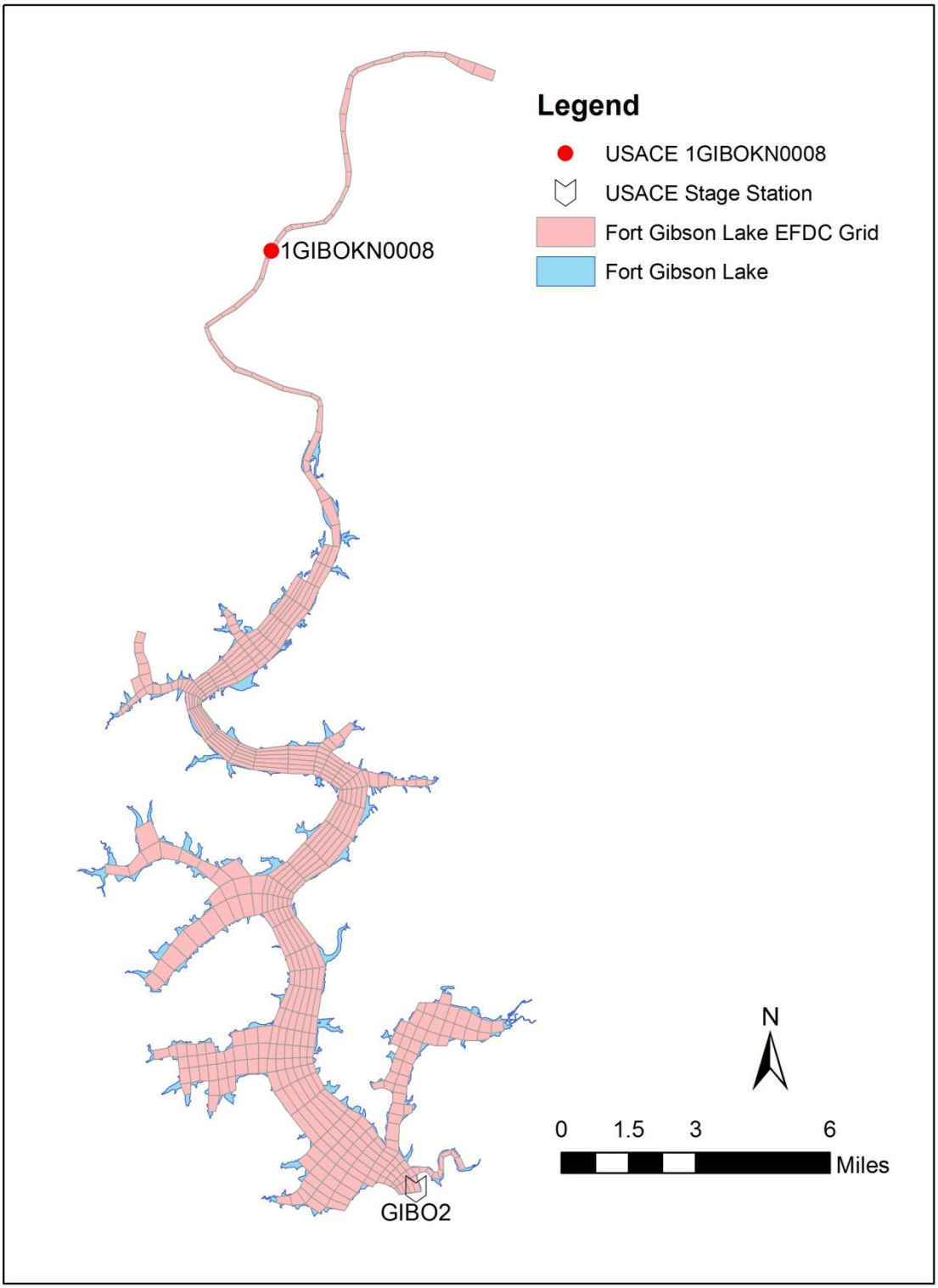

Figure B-10 Location of USACE Station GIBO2 and 1GIBOKN0008

B-2.8 HSPF-EFDC Linkage

For the Fort Gibson Lake model, streamflow and pollutant loading data obtained from the HSPF model are developed to represent watershed runoff over the drainage area to the reservoir. Sub-watersheds of the HSPF model, defined by reaches where flow and pollutant loads are routed through a one-dimensional reach network, simulate flow and water quality concentrations at fixed downstream outlet locations. Sub-watersheds that are not defined by an in-stream reach simulate water volume and constituent loads as distributed NPS runoff over the drainage area of the sub-watershed. The HSPF sub-watersheds defined as in-stream reaches (TRIB) and distributed catchments (NPS) that provide external flow and loads to the lake are listed in Table B-2.

State variables of the HSPF watershed model developed for the Fort Gibson Lake project are listed in Table B-3 with the **s**tate variable units identified for in-stream reaches (TRIB) and distributed catchments (NPS).

Table B-3 HSPF State Variables and Units for the Fort Gibson Lake Model

HSPF State Variable	Name	Units	Units
HYDROLOGY		TRIB	NPS
Streamflow; NPS Runoff	FLOW	cfs	cf/hr
Water Temperature	WTEM	Deg-F	Deg-F
SEDIMENT TRANSPORT			
Inorganic Total Suspended Solids	TSS	mg/L	tons/hr
WATER QUALITY			
Algae biomass (as Chl-a)	PHYT	mg/L	lbs/hr
CBOD	CBOD	mg/L	lbs/hr
Refractory Organic Carbon	TORC	mg/L	lbs/hr
Refractory Organic Phosphorus	TORP	mg/L	lbs/hr
Total Phosphate	PO4	mg/L	lbs/hr
Total Phosphorus	TP	mg/L	lbs/hr
Refractory Organic Nitrogen	TORN	mg/L	lbs/hr
Ammonia+Ammonium-Nitrogen	NH3+NH4	mg/L	lbs/hr
Nitrate+Nitrite-Nitrogen	NO2+NO3	mg/L	lbs/hr
Total Nitrogen	TN	mg/L	lbs/hr
Dissolved Oxygen	DOX	mg/L	lbs/hr

The functional relationships used to link the HSPF results for input to the EFDC model are listed in Table B-4. The HSPF-EFDC linkage of flow, water temperature, suspended solids, phosphate, ammonia, nitrate and dissolved oxygen is straightforward and only requires conversion of some of the HSPF units to EFDC units. HSPF-EFDC linkage of algae and organic matter however requires transformations as shown in Table B- 4 and described below.

Table B-4 HSPF-EFDC Linkage

EFDC HYDRODYNAMICS & SEDIMENT TRANSPORT	Units	HSPF-EFDC Linkage
Flow	cms	HSPF Streamflow; Runoff
Water Temperature	C	HSPF Water Temperature (WTEM)
Inorganic Cohesive Solids	mg/L	HSPF TSS
EFDC WATER QUALITY		
Bluegreen Algae	mg/L	HSPF PHYT Biomass * C/Chl * F_BG
Diatoms Algae	mg/L	HSPF PHYT Biomass * C/Chl * F_D
Green Algae	mg/L	HSPF PHYT Biomass * C/Chl * F_G
Refractory Particulate Org Carbon	mg/L	HSPF (CBOD/(CVBO/CDW) + ORC)* F_R
Labile Particulate Org Carbon	mg/L	HSPF (CBOD/(CVBO/CDW) + ORC)* F_L
Diss Org Carbon	mg/L	HSPF (CBOD/(CVBO/CDW) + ORC)* F_D
Refractory Particulate Org Phosphorus	mg/L	HSPF (CBOD/(CVBO/CDW) *P/C + ORP)* F_R
Labile Particulate Org Phosphorus	mg/L	HSPF (CBOD/(CVBO/CDW) *P/C + ORP)* F_L
Diss Org Phosphorus	mg/L	HSPF (CBOD/(CVBO/CDW)*P/C + ORP)* F_D
Total Phosphate	mg/L	HSPF PO4
Refractory Particulate Org Nitrogen	mg/L	HSPF (CBOD/(CVBO/CDW)*N/C + ORN)* F_R
Labile Particulate Org Nitrogen	mg/L	HSPF (CBOD/(CVBO/CDW)*N/C + ORN)* F_L
Diss Org Nitrogen	mg/L	HSPF (CBOD/(CVBO/CDW)*N/C + ORN)* F_D
Ammonium Nitrogen	mg/L	HSPF NH3+NH4
Nitrate+Nitrite Nitrogen	mg/L	HSPF NO2+NO3
Chemical Oxygen Demand	mg/L	HSPF n/a COD=0
Dissolved Oxygen	mg/L	HSPF DOX

HSPF represents algae as a single assemblage of phytoplankton with output units as mg Chl/L for the Fort Gibson Lake project. The fraction assigned to diatoms (F_D) and blue green (F_BG) algae for input to the EFDC model is zero since observed diatom and blue green algae data are not available and is not

represented in the lake model. A C/Chl ratio of 0.05 mg C/ug Chl is assigned to convert the HSPF results for chlorophyll biomass to organic carbon for input to EFDC.

Labile HSPF CBOD and refractory HSPF organic carbon (ORC), organic phosphorus (ORP), and organic nitrogen (ORN) are added as shown in the HSPF-EFDC linkage in Table B-4 to derive non-living TOC, TOP and TON for input to the EFDC model. HSPF derived TOC, TOP and TON is then split for input to EFDC as refractory, labile and dissolved components of total organic matter using the fractions given in Table B-5. CBOD is represented as ultimate CBOD in the HSPF model. The stoichiometric ratio for oxygen: dry weight of biomass (CVBO) has a value of CVBO=1.98 mg O2/mg-DW and the ratio of carbon: dry weight (CDW) is 0.49 mg C/mg-DW. The parameter values used to convert CBOD to an equivalent organic carbon basis for input to the EFDC model are taken from the parameter values assigned for the HSPF model.

The stoichiometric ratios for Phosphorus to Carbon and Nitrogen to Carbon are based on Redfield ratios where C/P = 41.1 mg C/mg-P and C/N = 5.7 mg C/mg-N (Di Toro 2001). Parameter values for assignment of the splits of TOC, TOP and TON (Table B-5) are taken from the CE-QUAL-W2 modeling study of the Tenkiller Ferry Lake (Wells et al., 2008).

Table B-5 Refractory, Labile and Dissolved Splits for Organic Matter

	Refractory F_R	Labile F_L	Dissolved F_D
	RPOM	LPOM	DOM
TOC	0.25	0.25	0.5
TOP	0.25	0.25	0.5
TON	0.25	0.25	0.5

B-3 WATER QUALITY AND SEDIMENT FLUX MODEL

B-3.1 Water Quality Model

For the Fort Gibson Lake EFDC model, the water quality model is internally coupled with the hydrodynamic model, a sediment transport model, and a sediment diagenesis model. The hydrodynamic model describes circulation and physical transport processes including turbulent mixing and water column stratification during the summer months. The sediment transport model describes the water column distribution of inorganic cohesive particles resulting from deposition and resuspension processes. The sediment diagenesis model describes the coupling of particulate organic matter deposition from the water column to the sediment bed, decomposition of organic matter in the bed, and the exchange of nutrients and dissolved oxygen across the sediment-water interface.

State variables of the EFDC hydrodynamic model (water temperature) and sediment transport model (inorganic suspended solids) are internally coupled with the EFDC water quality model. State variables of the EFDC water quality model include algae; organic carbon, inorganic phosphorus (orthophosphate), organic phosphorus; inorganic nitrogen (ammonium and nitrite + nitrate), organic nitrogen; chemical oxygen demand (COD) and dissolved oxygen. The state variables represented in the Fort Gibson Lake hydrodynamic and water quality model are listed in Table B-6. The EFDC water quality model is based on the kinetic processes developed for the Chesapeake Bay model (Cerco and Cole, 1995; Cerco et al., 2002). An overview of the source and sink terms for each state variable is presented in this section. The details of the state variable equations and kinetic terms for each state variable are presented in Park et al. (1995), Hamrick (2007) and Ji (2008). Tables listing the calibrated values of selected water quality model parameters and coefficients are presented in **Appendix A**.

Table B-6 EFDC State Variables

	EFDC State Variable		EFDC UNITS	Used in Model
	Flow	FLOW	cms	Yes
	Water_Temperature	TEM	Deg-C	Yes
	Salinity	SAL	ppt	No
	Cohesive Suspended Solids	COH	mg/L	Yes
	Nocohesive Suspended Solids	NONCOH	mg/L	No
1	BlueGreen_Algae	CHC	mgC/L	No
2	Diatoms_Algae	CHD	mgC/L	No
3	Green_Algae	CHG	mgC/L	Yes
4	Refractory_Particulate_Org_C	RPOC	mgC/L	Yes
5	Labile_Particulate_Org_C	LPOC	mgC/L	Yes
6	Diss_Org_C	DOC	mgC/L	Yes
7	Refractory_Particulate_Org_P	RPOP	mgP/L	Yes
8	Labile_Particulate_Org_P	LPOP	mgP/L	Yes
9	Diss_Org_P	DOP	mgP/L	Yes
10	Total_PhosphatePO4	TPO4	mgP/L	Yes
11	Refractory_Particulate_Org_N	RPON	mgN/L	Yes
12	Labile_Particulate_Org_N	LPON	mgN/L	Yes
13	Diss_Org_N	DON	mgN/L	Yes
14	Ammonium_N	NH4	mgN/L	Yes
15	Nitrate+Nitrite_N	NO3	mgN/L	Yes
16	Particulate-Biogenic_Silica	PBSI	mgSi/L	No
17	Available_Silica	SI	mgSi/L	No
18	Chemical_Oxy_Demand	COD	mg/L	Yes
19	Dissolved_Oxygen	OXY	mgO2/L	Yes
20	Total_Active_Metal	TAM	mg/L	No
21	Fecal_Coliform_Bacteria	FCB	# /100mL	No

Suspended Solids

Suspended solids in the EFDC model can be differentiated by size classes of cohesive and non-cohesive solids. For the Fort Gibson Lake model, suspended solids are represented as a single size class of cohesive particles. Cohesive suspended solids are included in the model to account for the inorganic solids component of light attenuation in the water column. Since cohesive particles derived from silts and clays are characterized by a small particle diameter (< 62 microns) and a low settling velocity, cohesive particles can remain suspended in the water column for long periods of time and contribute to light attenuation that can influence algae production. Non-cohesive particles, consisting of fine to coarse size sands, by contrast, are characterized by much larger particles (> 62 microns) with rapid settling velocities that quickly remove any resuspended non-cohesive particles from the water column.

The key processes that control the distribution of cohesive particles are transport in the water column, flocculation and settling, deposition to the sediment bed, consolidation within the bed, and resuspension or erosion of the sediment bed. In the EFDC model for Fort Gibson Lake, cohesive settling is defined by a constant settling velocity that is determined by model calibration. Deposition and erosion are controlled by the assignment of critical stresses for deposition and erosion and the bottom layer velocity and shear stress computed by the hydrodynamic model. The critical stress for erosion is typically defined with a factor of 1.2 times the critical deposition stress (Ji, 2008). Initial critical stresses for deposition and erosion of cohesive particles are taken from parameter values defined by Ji (2008) for a sediment transport model of Lake Okeechobee and then adjusted during model calibration. Parameter values for deposition and erosion assigned for the calibration of cohesive solids are summarized in Table B-7**.**

Table B-7 EFDC model parameter values for cohesive solids

Variable	Value	Description	Units
SDEN	3.84615E-07	Sediment Specific Volume	m^3/g
SSG	2.6	Sediment Specific Gravity	--
WSEDO	1.0E-08	Constant Sediment Settling Velocity	m/s
TAUD	0.001	Critical Stress for Deposition	$(m/s)^2$
WRSPO	2.0E-05	Reference Surface Erosion Rate	$g/m^2/s$
TAUR	0.0012	Critical Stress for Erosion	$(m/s)^2$

The units of $(m/s)^2$ shown for critical shear stress for deposition and erosion are not typical units in the sediment transport literature. The units assigned for the EFDC model are derived by normalizing the units typically measured for shear stress (e.g., dynes/cm^2) by a water density of 1000 kg/m^3. A critical shear stress for erosion of 0.16 dynes/cm^2 is thus assigned for input to EFDC with a value of 1.6e-05 $(m/s)^2$ by multiplying the shear stress of 0.16 dynes/cm^2 by a factor of 1.0e-04 since 1 dyne is defined as 1 g-cm/sec^2.

Algae

Phytoplankton in the EFDC model can be represented by three different functional groups of algae as (1) blue-green cyanobacteria; (2) diatoms and (3) green chlorophytes. For Fort Gibson Lake, there is no observed data available to identify the species of the algae. Hence, it is assumed that all the algae are in the form of green algae as a generic species group.

Kinetic processes represented for algae include photosynthetic production, basal metabolism (respiration and excretion), settling and predation. Photosynthetic production is described by a growth rate that is functionally dependent on a maximum growth rate, water temperature, the availability of sunlight at the surface, light extinction in the water column, the optimum light level for growth, and half-saturation dependent nutrient limitation by either nitrogen or phosphorus. Growth and basal metabolism are temperature dependent processes while settling and predation losses are assigned as constant parameter values.

Initial values of key parameters for kinetic coefficients for the algae model were obtained from the Thunderbird Lake EFDC model (Dynamic Solutions, 2012). For the Fort Gibson Lake EFDC model, four zones were used to represent the spatial variations in algae kinetics (Figure B-11). Other kinetic coefficients determined for calibration of the algae model are presented in **Appendix A**.

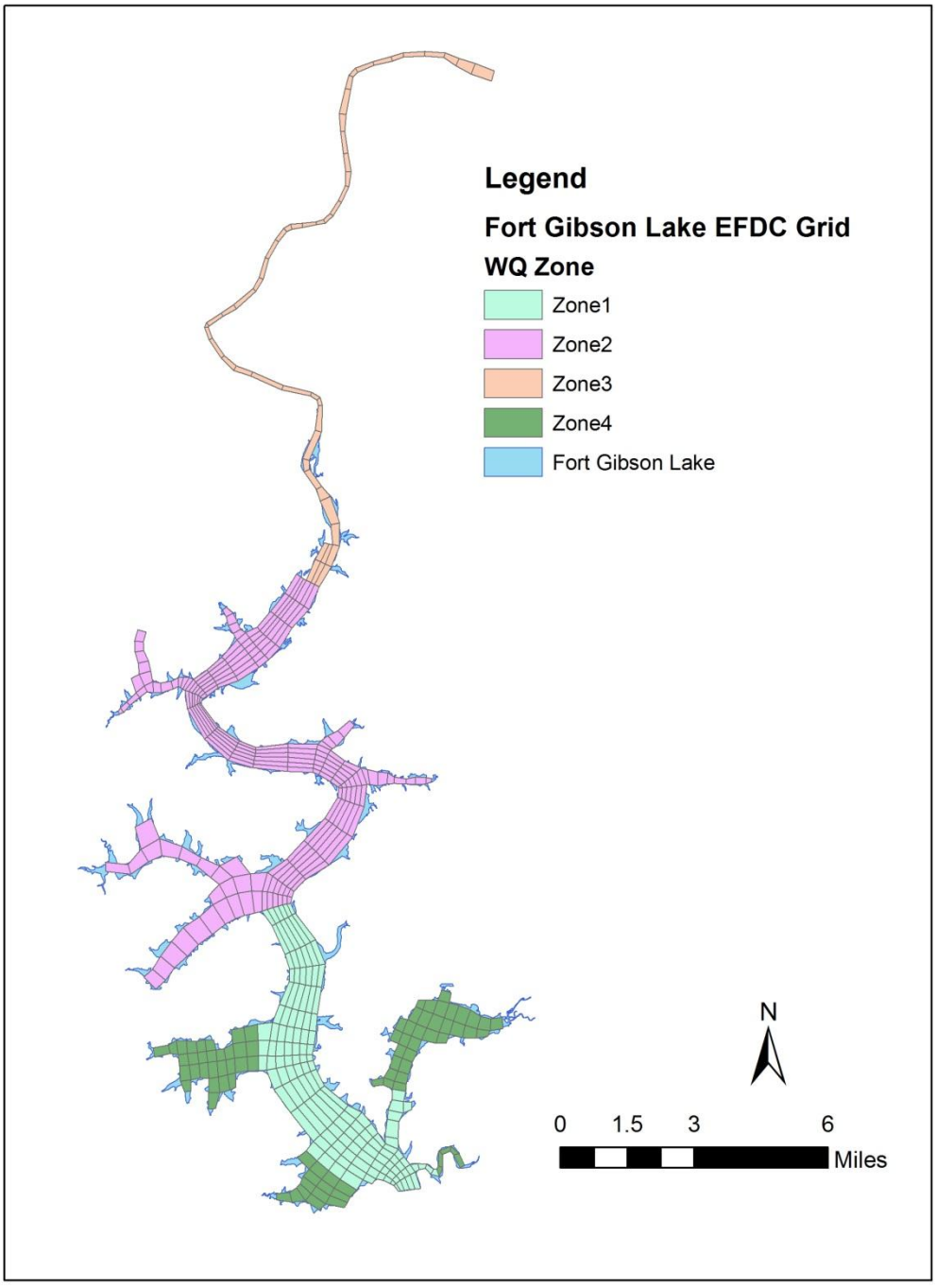

Figure B-11 Spatial Water Quality Kinetic Zones Defined for Fort Gibson Lake

Organic Carbon

Total organic carbon is represented in the model with three state variables as dissolved organic carbon (DOC) and refractory and labile particulate organic carbon (RPOC and LPOC). The time scale for decomposition of particulate organic matter (POM) is used to differentiate refractory and labile POM with labile matter decomposing rapidly (weeks to months) while decay of refractory POM takes much longer (years). Although DOC is not termed "labile", DOC is considered to react with a rapid time scale for decomposition (weeks to months).

Kinetic processes represented in the model for particulate organic carbon (POC) include algal predation, dissolution of RPOC and LPOC to DOC, and settling. Kinetic processes for DOC include sources from algal excretion and predation and dissolution of POC and losses from decomposition and denitrification. With the exception of settling of POC, all the kinetic reaction processes are temperature dependent.

Phosphorus

Total organic phosphorus is represented in the model with three state variables as dissolved organic phosphorus (DOP) and refractory and labile particulate organic phosphorus (RPOP and LPOP). As with organic carbon, the time scale for decomposition of particulate organic matter (POM) is used to differentiate refractory and labile POP. Kinetic processes represented in the model for POP include algal metabolism, predation, dissolution of RPOP and LPOP to DOP, and settling. Kinetic processes for DOP include sources from algal metabolism and predation and dissolution of POP to DOP with losses of DOP from mineralization to phosphate. With the exception of settling of POP, the kinetic reaction processes are temperature dependent.

Inorganic phosphorus is represented as single state variable for total phosphate which accounts for both the dissolved and sorbed forms of phosphate. Adsorption and desorption of phosphate is defined on the basis of equilibrium partitioning using an assigned phosphate partition coefficient for suspended solids. Kinetic terms for total phosphate include sources from algal metabolism and predation and mineralization from DOP. Losses for phosphate include settling of the sorbed fraction of total phosphate and uptake by phytoplankton growth. Depending on the concentration gradient between the bottom water column and sediment bed porewater phosphate, the sediment-water interface can serve as either a source or a loss term for phosphate in the water column. With the exception of the partition coefficient and the settling of sorbed phosphate, the kinetic reaction processes for phosphate are temperature dependent.

Nitrogen

Total organic nitrogen is represented in the model with three state variables as dissolved organic nitrogen (DON) and refractory and labile particulate organic nitrogen (RPON and LPON). As with organic carbon, the time scale for decomposition of particulate organic matter (POM) is used to differentiate refractory and labile PON. Kinetic processes represented in the model for PON include algal metabolism, predation, dissolution of RPON and LPON to DON, and settling. Kinetic processes for DON include

sources from algal metabolism and predation, dissolution of PON to DON and losses of DON from mineralization of PON to ammonium. With the exception of settling of PON, the kinetic reaction processes are temperature dependent.

Inorganic nitrogen (ammonia, nitrite and nitrate) is represented by two state variables as (1) ammonia and (2) nitrite+nitrate. Kinetic terms for ammonia include sources from algal metabolism and predation and mineralization from DON. Losses for ammonia include bacterially mediated transformation to nitrite and nitrate by nitrification and uptake by phytoplankton growth. Depending on the concentration gradient between the bottom water column and sediment bed porewater ammonia, the sediment-water interface can serve as either a source or a loss term for ammonia in the water column. The kinetic reaction processes for ammonia are temperature dependent. Since the time scale for conversion of nitrite to nitrate is very rapid, nitrite and nitrate are combined as a single state variable representing the sum of these two forms of nitrogen. Kinetic terms for nitrite/nitrate include sources from nitrification from ammonia to nitrite and nitrate. Losses include uptake by phytoplankton growth and denitrification to nitrogen gas. Depending on the concentration gradient between the bottom water column and sediment bed porewater nitrite/nitrate, the sediment-water interface can serve as either a source or a loss term for nitrite/nitrate in the water column. The kinetic reaction processes for nitrite/nitrate are temperature dependent.

Chemical Oxygen Demand (COD)

In the EFDC water quality model, chemical oxygen demand (COD) represents the concentration of reduced substances that can be oxidized through inorganic processes. The principal source of COD in freshwater is methane released from oxidation of organic carbon in the sediment bed across the sediment-water interface. Since sediment bed decomposition is accounted for in the coupled sediment diagenesis model, the only source of COD to the water column is the flux of methane across the sediment-water interface. Sources from the open water boundaries and upstream flow boundaries are set to zero for COD. The loss term in the water column is defined by a temperature dependent first order oxidation rate.

Dissolved Oxygen

Dissolved oxygen is a key state variable in the water quality model since several kinetic processes interact with, and can be controlled by, dissolved oxygen. Kinetic processes represented in the oxygen model include sources from atmospheric reaeration in the surface layer and algal photosynthetic production. Kinetic loss terms include algal respiration, nitrification, decomposition of DOC, oxidation of COD, and bottom layer consumption of oxygen from sediment oxygen demand. Sediment oxygen demand is coupled with particulate organic matter deposition from the water column and is computed internally in the sediment flux model. The kinetic reaction processes for dissolved oxygen are all temperature dependent.

Kinetic Coefficients

Most of the water quality parameters and coefficients needed by the EFDC water quality model were initialized with default values as indicated in the user's manual (Park, et.al., 1995 and Hamrick, 2007). These default values are, in general, the same as the parameter values determined for the Chesapeake Bay model (Cerco and Cole, 1995). Models developed for Lake Washington (Arhonditsis and Brett, 2005) and the tributaries of Chesapeake Bay (Cerco et al., 2002) also provided several of the kinetic coefficients needed for the EFDC water quality model. Kinetic coefficients and model parameters were adjusted, as needed, within ranges reported in the literature, during model calibration to obtain the most reasonable agreement between observed and simulated water quality concentrations such as suspended solids, algal biomass, organic carbon, dissolved oxygen and nutrients. A large body of literature is available from numerous advanced modeling studies developed over the past decade to provide information on reported ranges of parameter values that can be assigned for site-specific modeling projects (see Ji, 2008; Park et al, 1995; Hamrick, 2007). Kinetic coefficients and model parameters assigned for the water quality model as either global or spatial zone dependent parameters for the Fort Gibson Lake model are listed in **Appendix A**.

Atmospheric Deposition

Atmospheric deposition is represented in the EFDC model with separate source terms for dry deposition and wet deposition. Dry deposition is defined by a constant mass flux rate (as g/m^2-day) for a constituent that settles as dust or is deposited on a dry surface during a period of no precipitation. Wet deposition is defined by a constant concentration (as mg/L) of a constituent in rainfall and the time series of precipitation assigned for input to the hydrodynamic model. For Fort Gibson Lake, wet and dry deposition data **(**Table B-8) was assigned as the average of annual data from 2005-2006 for ammonia and nitrate from the National Atmospheric Deposition Program (NADP) for Station AR27 (Fayetteville, Lat 36.1011; Lon -94.1737) and the Clean Air Status and Trends Network (CASTNET) Station CHE185 (Cherokee Nation, Lat 35.7507, Lon -94.67) (Figure B-12). Since data was not available from the CASTNET and NADP sites for phosphate, dry deposition for phosphate was estimated using annual average ratios of N/P for atmospheric deposition of N and P reported for 6 sites located in Iowa (Anderson and Downing, 2006) and the ammonia and nitrate data obtained from the NADP and CASTNET data sources.

Table B-8 Dry and Wet Atmospheric Deposition for Nutrients

	Dry g/m^2-day	Wet mg/L	Data Source
TPO4	7.786E-06	0.001	Anderson & Downing (2006), Table VII
NH4	1.143E-04	0.274	Dry (CASTNET, CHE185); Wet (NADP, AR27); average 2005-2005
NO3	3.205E-05	0.19	Dry (CASTNET, CHE185); Wet (NADP, AR27); average 2005-2006

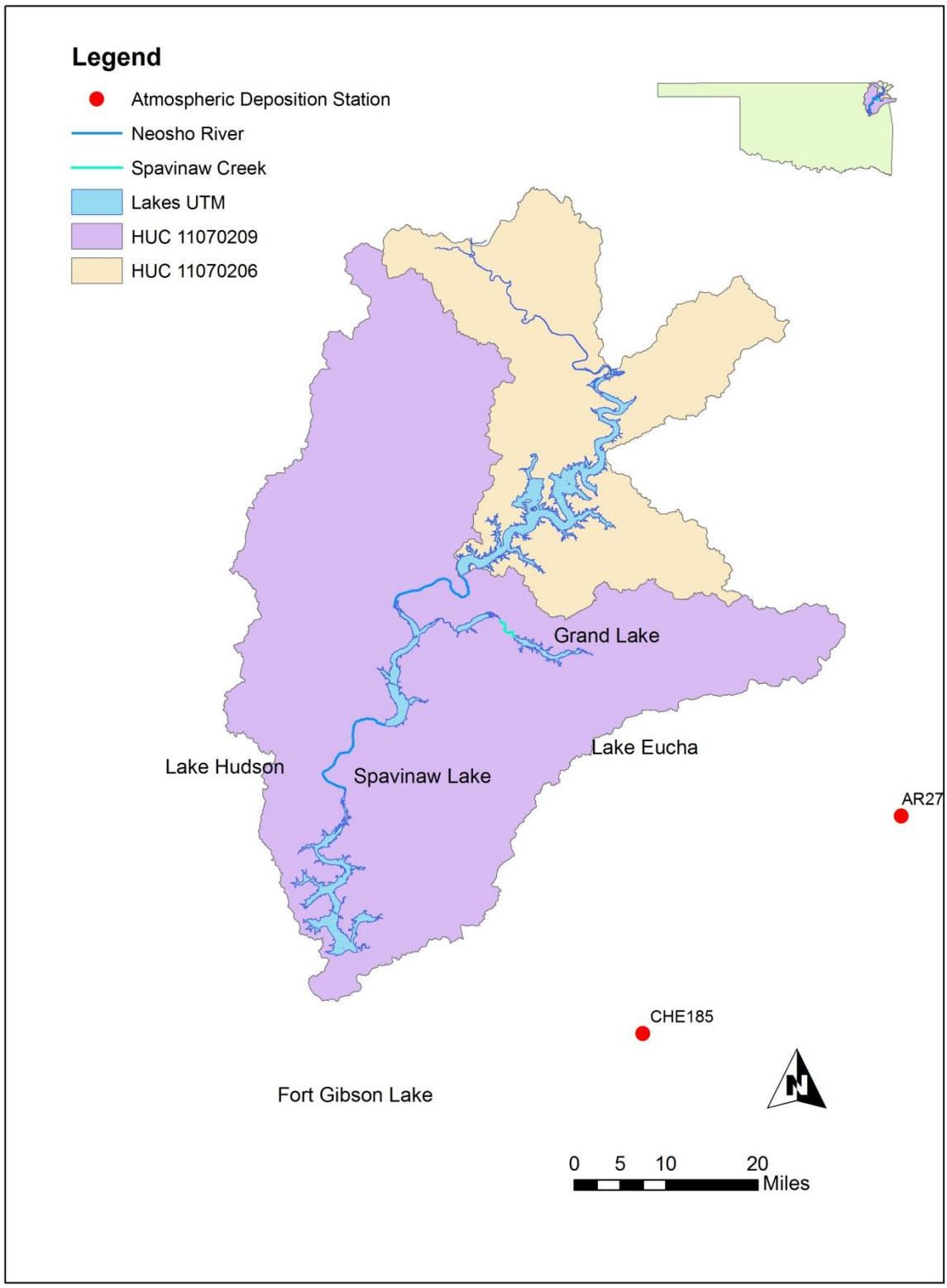

Figure B-12 Location of the Atmospheric Deposition Monitoring Stations

B-3.2 Sediment Flux Model

The EFDC water quality model provides three options for defining the sediment-water interface fluxes for nutrients and dissolved oxygen. The options are: (1) externally forced spatially and temporally constant fluxes; (2) externally forced spatially and temporally variable fluxes; and (3) internally coupled fluxes simulated with the sediment diagenesis model. The water quality state variables that are controlled by diffusive exchange across the sediment-water interface include phosphate, ammonia, nitrate, silica, chemical oxygen demand and dissolved oxygen. The first two options require that the sediment fluxes be assigned as spatial/temporal forcing functions based on either observed site-specific data from field surveys or best estimates based on the literature and sediment bed characteristics. The first two options, although acceptable for model calibration against historical data sets, do not provide the cause-effect predictive capability that is needed to evaluate future water quality conditions that might result from implementation of pollutant load reductions from watershed runoff. The third option, activation of the sediment diagenesis model developed by Di Toro (2001), does provide the cause-effect predictive capability to evaluate how water quality conditions might change with implementation of alternative load reduction or management scenarios. For the Fort Gibson Lake model, the third option was selected to implement the sediment diagenesis model so that load allocation scenarios could be evaluated to determine an appropriate load allocation for Fort Gibson Lake.

Living and non-living particulate organic carbon deposition, simulated in the EFDC water quality model, is internally coupled with the EFDC sediment diagenesis model. The sediment diagenesis model, based on the sediment flux model of Di Toro (2001), describes the decomposition of particulate organic matter in the sediment bed, the consumption of dissolved oxygen at the sediment-water interface (SOD) and the exchange of dissolved constituents (ammonia, nitrate, phosphate, silica, COD) across the sediment-water interface, State variables of the EFDC sediment flux model are sediment bed temperature, sediment bed particulate organic carbon (POC), particulate organic nitrogen (PON), particulate organic phosphorus (POP), porewater concentrations of phosphate, ammonia, nitrate, silica and sulfide/methane. The sediment diagenesis model computes sediment-water fluxes of chemical oxygen demand (COD), sediment oxygen demand (SOD), phosphate, ammonium, nitrate, and silica. The state variables modeled for the Fort Gibson Lake sediment flux model are listed in Table B-9**.** An overview of the source and sink terms is presented with a description of each state variable group in this section. The details of the state variable equations, kinetic terms and numerical solution methods for the sediment diagenesis model are presented in Di Toro (2001), Park et al. (1995) and Ji (2008).

Table B-9 EFDC Sediment Diagenesis Model State Variables

No.	Name	Bed Layer	Units	Activated
1	POC-G1	Layer-2	g/m^3	Yes
2	POC-G2	Layer-2	g/m^3	Yes
3	POC-G3	Layer-2	g/m^3	Yes
4	PON-G1	Layer-2	g/m^3	Yes
5	PON-G2	Layer-2	g/m^3	Yes
6	PON-G3	Layer-2	g/m^3	Yes
7	POP-G1	Layer-2	g/m^3	Yes
8	POP-G2	Layer-2	g/m^3	Yes
9	POP-G3	Layer-2	g/m^3	Yes
10	Partic-Biogenic-Silica	Layer-2	g/m^3	No
11	Sulfide/Methane	Layer-1	g/m^3	Yes
12	Sulfide/Methane	Layer-2	g/m^3	Yes
13	Ammonia-N	Layer-1	g/m^3	Yes
14	Ammonia-N	Layer-2	g/m^3	Yes
15	Nitrate-N	Layer-1	g/m^3	Yes
16	Nitrate-N	Layer-2	g/m^3	Yes
17	Phosphate-P	Layer-1	g/m^3	Yes
18	Phosphate-P	Layer-2	g/m^3	Yes
19	Available-Silica	Layer-1	g/m^3	No
20	Available-Silica	Layer-2	g/m^3	No
21	Ammonia-N-Flux		g/m^2-day	Yes
22	Nitrate-N-Flux		g/m^2-day	Yes
23	Phosphate-P-Flux		g/m^2-day	Yes
24	Silica Flux		g/m^2-day	Yes
25	SOD		g/m^2-day	Yes
26	COD Flux		g/m^2-day	Yes
27	Bed Temperature		Deg-C	Yes

Particulate Organic Matter

The sediment diagenesis model incorporates three key processes: (1) depositional flux of particulate organic matter (POM) from the water column to the sediment bed; (2) diagenesis or decomposition of POM in the sediment bed; and (3) the resulting fluxes of dissolved oxygen, chemical oxygen demand, sulfide and nutrients across the sediment-water interface. Particulate organic matter is represented as carbon (POC), nitrogen (PON), and phosphorus (POP) stoichiometric equivalents based on carbon-to-dry weight and Redfield ratios for C/N, and C/P. In the water quality model, POM deposition describes the settling flux from the water column to the bed of non-living refractory and labile detrital matter and living algal biomass. In the sediment flux model, POM is split into three classes of reactivity. The labile fraction (POM-G1) is defined by the fastest reaction rate with a half-life on the order of 20 days. The

refractory fraction (POM-G2) is defined by a slower reaction rate with a half-life of about 1 year. The inert fraction (POM-G3) is non-reactive with negligible decay before ultimate burial into the deep inactive layer of the sediment bed.

The sediment flux model represents the sediment bed as a two layer system. The first layer is a very thin aerobic layer. The second layer is a thicker anaerobic active layer. The thickness of the aerobic layer, which is on the order of only a millimeter, is internally computed in the sediment flux model as a function of bottom layer dissolved oxygen concentration, the sediment oxygen demand rate and the diffusivity coefficient for dissolved oxygen. The thickness of the anaerobic active layer is assigned as a parameter for model setup. The depth of the anaerobic active layer, defined by the depth to which benthic organisms mix particles within a homogeneous bed layer, can range from ~5 to 15 cm (Ji, 2008). An active anaerobic layer thickness of ~10 cm has been determined from both theoretical considerations and field observations in estuaries (Di Toro, 2001). Any particle mass transported out of the active layer is not recycled back into the active layer since these particles are lost to deep burial out of the sediment bed.

The thickness of the active anaerobic layer controls the volume of the anaerobic layer, the amount of mass stored in the anaerobic layer and the long-term response of the sediment bed to changes in organic matter deposition from the water column. A relatively thin active layer will respond quickly to changes in watershed loading and water column deposition of particulate matter. Conversely, a thick active layer will respond slowly to changes in watershed loading and deposition of particulate materials from the water column to the bed. The rate at which solutes stored in the anaerobic active layer are transported between the thin aerobic and thick anaerobic active layer, and potentially the overlying water column, is controlled by the mixing coefficients assigned as model parameters for particulate and dissolved substances. Anaerobic active layer thickness and diffusive mixing rates are considered to be adjustable parameters for model calibration to determine the most appropriate parameter values for each spatial zone. As documented in **Appendix B** an anaerobic layer thickness of 10 cm is assigned for each spatial zone of the sediment flux model

Since the surface aerobic sediment layer is very thin, the depositional flux from the overlying water column is assigned to the lower anaerobic active sediment layer where decomposition then occurs. The source term for the three “G” classes of POM is the depositional flux from the overlying water column to the sediment bed. The loss terms for POM are the temperature dependent decay (i.e., diagenesis) of POM and removal by burial from the aerobic (upper) to active anaerobic (lower) layers and from the anaerobic (lower) layer to deep burial out of the sediment bed model domain.

Dissolved Constituents

The decay or mineralization of POM results in the diagenetic production of dissolved constituents. The concentration gradients of ammonia, nitrate, phosphate, and sulfide/methane within the two porewater layers and between the surficial porewater layer 1 and the bottom layer of the water column control the sediment fluxes computed in the model. Mineralization of POP produces phosphate which is then subject to adsorption/desorption by linear partitioning with solids in the sediment bed. Diffusive

exchange is controlled by the concentration gradient of dissolved constituents, the diffusion velocity, and the bed layer thickness. Other processes that govern the mass balance of dissolved materials in the sediment bed include burial, particle mixing and removal by kinetic reactions.

Ammonia and Nitrate

Ammonia is produced in layer 2 by temperature dependent decomposition of the reactive G1 and G2 classes of PON. Ammonia is nitrified to nitrate with a temperature and oxygen dependent process. The only source term for nitrate is nitrification in the surficial layer. Nitrate is removed from both layers by temperature dependent denitrification with the carbon required for this process supplied by organic carbon diagenesis. Nitrogen is lost from the sediment bed by the denitrification flux out of the sediments as nitrogen gas (N2). The sediment-water fluxes of ammonia and nitrate to the overlying water column are then computed from the concentration gradients, the porewater diffusion coefficient and the thickness of the surficial bed layer.

Phosphate

Phosphate is produced by temperature dependent decomposition of the reactive G1 and G2 classes of POP in the lower layer 2 of the sediment bed. Since linear partitioning with solids is defined for phosphate, a fraction of total phosphate is computed as particulate phosphate and a fraction remains in the dissolved form. The partition coefficient for phosphate for the surficial layer 1 is functionally dependent on (a) the oxygen concentration in the overlying bottom layer of the water column based on the assignment of 2 mg/L as a critical concentration for oxygen that triggers the oxygen dependent process, (b) the magnitude of the partition coefficient assigned for the lower layer 2, and (c) an enhancement factor multiplier. There are no removal terms for phosphate in either of the two layers. The sediment-water flux of dissolved phosphate to the overlying water column is then computed from the concentration gradient, the porewater diffusion coefficient and the thickness of the surficial bed layer.

Methane/Sulfide

Sulfide is produced by temperature dependent decomposition of the reactive G1 and G2 classes of POC in the lower layer of the sediment bed. Sulfide is lost from the system by the organic carbon consumed by denitrification. Linear partitioning with solids is also defined for sulfide to account for the formation of iron sulfide. The sediment flux model accounts for three pathways for loss of sulfide from the sediment bed: (1) temperature dependent oxidation of sulfide; (2) aqueous flux of sulfide to the overlying water column; and (3) burial out of the model domain. If the overlying water column oxygen concentration is low then the sulfide that is not completely oxidized in the upper sediment layer can diffuse into the bottom layer of the water column. The aqueous flux of sulfide from the sediments is the source term for the flux of chemical oxygen demand (COD) from the sediment bed to the water column.

When sulfate is depleted, methane can be produced by carbon diagenesis and oxidation of methane then consumes oxygen. In saltwater systems, such as estuaries and coastal waters, sulfate is abundant

and methane production and oxidation are not represented in the sediment flux model. In freshwater systems, such as Fort Gibson Lake, sulfate is typically characterized by very low concentrations and methane production and oxidation are represented in the sediment diagenesis model instead of sulfide production and oxidation.

Sediment Oxygen Demand

The sulfide/methane oxidation reactions in the surficial layer result in an oxygen flux to the sediment bed from the overlying water column. Sediment oxygen demand (SOD) includes the carbonaceous oxygen demand (CSOD) from sulfide/methane oxidation and the nitrogenous oxygen demand (NSOD) from nitrification. The total SOD is computed as the sum of the carbonaceous and nitrogenous components of the oxygen flux.

Sediment Diagenesis Model Parameters and Kinetic Coefficients

The sediment diagenesis model requires the assignment of a large number of model parameters and kinetic coefficients. Based on the results of sediment flux models developed for estuaries, coastal systems and lakes, Di Toro (2001) has summarized parameter values used for diagenesis, sediment properties, mixing and kinetic coefficients for the different projects. The comparison of data assigned for several different projects shows the robustness of the sediment flux model since many of the parameter values and kinetic coefficients were essentially unchanged for model applications unless there was a site-specific reason that supported the use of a different value. The exception to this generality, however, is the extreme variation of the kinetic coefficients required to represent partitioning of phosphate in the upper and lower layers of the sediment bed and the benthic release of dissolved phosphate under anoxic conditions in the hypolimnion. Since the sediment flux model does not explicitly represent the chemical reactions and interactions that determine phosphate sorption, particularly under low oxygen conditions in the overlying water column when dissolved phosphate is released across the sediment-water interface, the sediment flux model coefficients that represent phosphate partitioning are parameters that were adjusted, as needed, to calibrate the model.

Ideally calibration of the sediment flux model would be supported by comparison of model results to site-specific measurements of sediment fluxes of oxygen, phosphate, ammonia and nitrate under aerobic and anoxic conditions. Since sediment flux measurements for oxygen and nutrients, however, are not available for Fort Gibson Lake, measurements of phosphate fluxes from Lake Wister (Haggard and Scott, 2011); Lake Frances (Haggard and Soerens, 2006); Eucha Lake (Haggard et al., 2005); Beaver Lake in Arkansas (Sen et al., 2007; Hamdan et al., 2010), Acton Lake in Ohio (Nowlin et al., 2005) and a set of 17 lakes/reservoirs in the Central Plains (Dzialowski and Carter, 2011) are used to provide a range of measured phosphate flux rates to support calibration of the sediment flux model for Fort Gibson Lake.

Kinetic coefficients and parameters of the sediment flux model were initially assigned based on the Chesapeake Bay Model (Cerco and Cole, 1995; Cerco et al., 2002) and the compilation of parameter values reported in Di Toro (2001). Selected coefficients, particularly the phosphate partitioning

parameters, were adjusted, as needed, to achieve calibration of the water quality and sediment flux model. Kinetic coefficients and model parameters assigned for calibration of the sediment diagenesis model as either global or spatial zone dependent parameters for the Fort Gibson Lake model are listed in **Appendix B**.

Initial Conditions for Sediment Diagenesis Model

The sediment diagenesis model requires specification of initial conditions for particulate organic matter content (as C, N, and P) and porewater concentrations of inorganic nutrients (as NH_4, NO_3, and PO_4). Sediment core data was not available for Fort Gibson Lake. Sediment core data from the Thunderbird Lake (Dynamic Solutions, 2012) was initially applied to the Fort Gibson Lake EFDC model. A one-year model spin-up was conducted to obtain dynamic steady-state sediment bed conditions prior to model calibration. Four diagenesis zones defined as water quality zones for the EFDC water quality model were applied to represent the spatial variations of the initial conditions of the sediment flux model in Figure B-11.

B-4 CALIBRATION AND VALIDATION STATIONS

B-4.1 Stage Calibration and Validation Stations

Observed stage data in Fort Gibson Lake is available at station GIBO2 by the USACE, Tulsa District. The location of station GIBO2 is shown in Figure B-10.

B-4.2 Water Quality Calibration and Validation Stations

The developed Fort Gibson Lake EFDC water quality model was calibrated and validated at seven (7) USACE stations listed in Table B-10 and shown in Figure B-13. These stations are spatially distributed throughout Fort Gibson Lake and have both surface and bottom observed water quality data to calibrate and validate the EFDC water quality model. These stations also have vertical profile data for water temperature and DO data for model calibration and validation.

Table B-10 Calibration and Validation Stations for the Fort Gibson Lake EFDC Model

Agency	Station_ID	Latitude	Longitude
USACE	1GIBOKN0003	35.87027778	-95.23027778
USACE	1GIBOKN0004	35.91527778	-95.22861111
USACE	1GIBOKN0005	35.96416667	-95.30055556
USACE	1GIBOKN0006	36.03666667	-95.31388889
USACE	1GIBOKN0305	35.91222222	-95.27888889
USACE	1GIBOKN0355	35.97666667	-95.26527778
USACE	1GIBOKN0386	36.04333333	-95.29444444

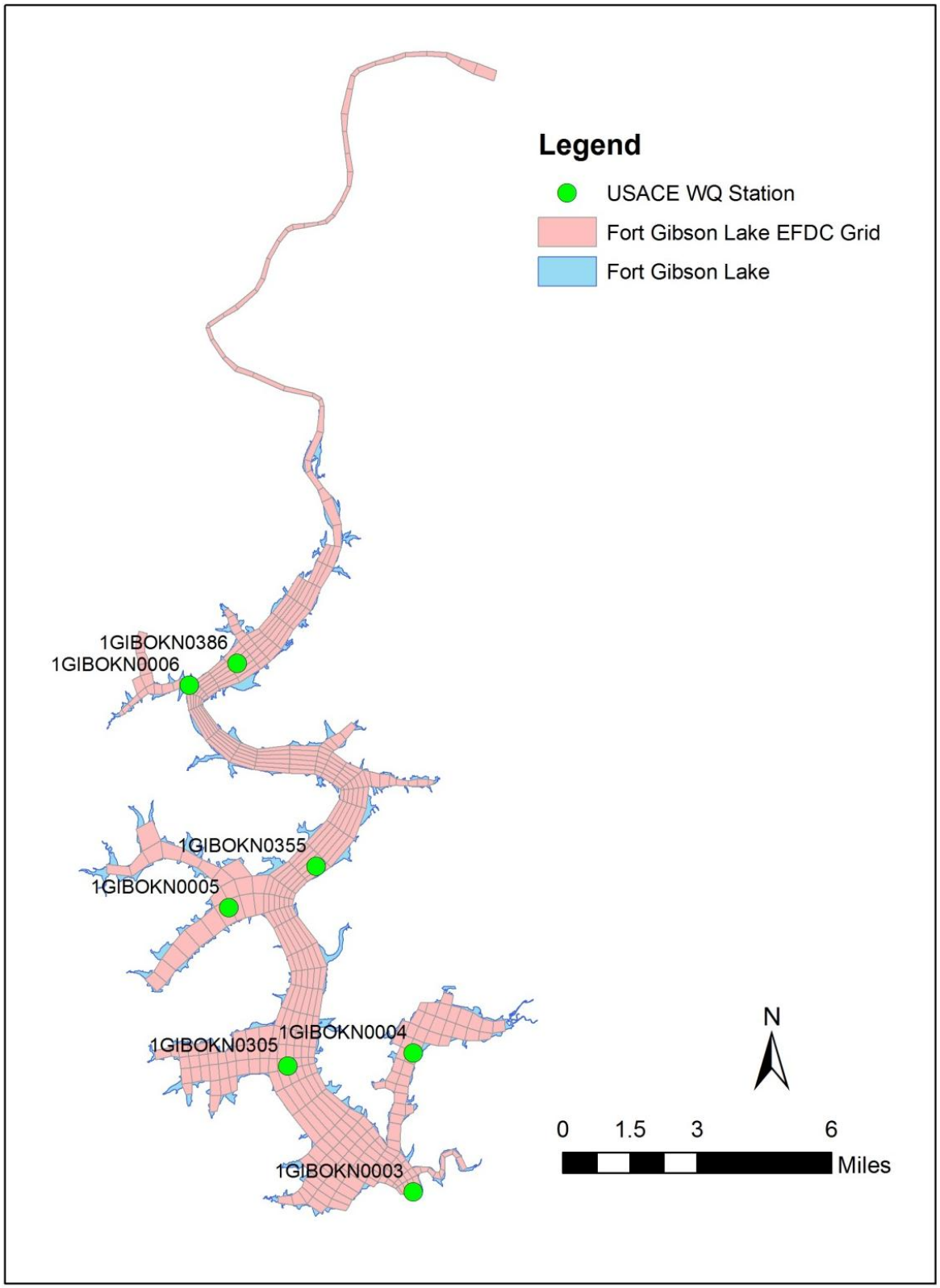

Figure B-13 Location of the USACE Monitoring Stations

B-5 MODEL PERFORMANCE AND STATISTICS

Model performance is evaluated to determine the endpoint for model calibration using a “weight of evidence” approach that has been adopted for many modeling studies. The “weight of evidence” approach includes the following steps: (a) visual inspection of plots of model results compared to observed datasets (e.g., station time series); and (b) analysis of model-data performance statistics as (a) Root Mean Square (RMS) Error and (b) Relative RMS Error as described below. The “weight of evidence” approach recognizes that, as an approximation of a waterbody, perfect agreement between observed data and model results is not expected and is not specified as a performance criterion for the success of model calibration. Model performance statistics are used, not as absolute criteria for acceptance of the model, but rather, as guidelines to supplement the visual evaluation of model-data time series plots to determine the endpoint for calibration of the model. The “weight of evidence” approach used for this study thus acknowledges the approximate nature of the model and the inherent uncertainty in both input data and observed data.

The model-data model performance statistic selected for the calibration of the hydrodynamic and water quality model are the (a) Root Mean Square Error (RMSE) and the (b) Relative RMS Error. The RMSE has units defined by the units of each state variable of the model. The Relative RMS error, computed as the ratio of the RMSE to the observed range of each water quality constituent and expressed as a percentage, is also used as a statistic to characterize model performance (Blumberg et al., 1999; Ji, 2008). Since the Relative RMS error is expressed as a percentage, this performance measure provides a straightforward statistic to evaluate the agreement between model results and observations.

The RMS Error, also known as the Standard Error of the mean, can be used to determine the width of the confidence interval around model predictions. The 95% confidence interval for the model is approximately equal to the model result at each point in time "+/- 2 x Standard Error". Since the RMS Error and the Standard Error of the mean represent the same statistic, the 95% confidence interval for the model is determined as +/- 2 x the root-mean-squared error.

Observed station data has been processed to define time series for each station location for the surface layer and bottom layer of the water column. Observed data is assigned to a vertical layer based on surface water elevation, station bottom elevation and the total depth of the water column estimated for the sampling date/time. Station locations are overlaid on the model grid to define a set of discrete grid cells that correspond to each monitoring site for extraction of model results. For time series of model results extracted for each grid cell (station) and surface and bottom depth layer, the match of the model simulation time with date/time of observations for comparison to the model is defined by a time tolerance parameter of +/- 1440 minutes. Model results are extracted for the set of model-data pairs if the model time is within the observed data date/time +/- time tolerance.

The equations for the RMSE and the Relative RMS Error are,

$$\mathrm{RMSE} = \sqrt{\frac{1}{N}\Sigma(O-P)^2} \qquad \text{Equation (1)}$$

$$\text{Relative RMS Error} = \frac{\mathrm{RMSE}}{(O_{range})} * 100 \qquad \text{Equation (2)}$$

Where

N is the number of paired records of observed measurements and EFDC model results,

O is the observed water quality measurement,

P is the predicted EFDC model result, and

O_{range} is the range of observed data computed from the maximum and minimum values.

In evaluating the results obtained with the EFDC model, a Relative RMS Error performance measure of $\pm 20\%$ is adopted for evaluation of the comparison of the model predicted results and observed measurements of water surface elevation of the lake. For the hydrographic state variables simulated with the EFDC hydrodynamic model, a Relative RMS Error performance measure of $\pm 50\%$ is adopted for evaluation of the comparison of the predicted results and observed measurements for water temperature. For the water quality state variables simulated with the EFDC water quality model, a Relative RMS Error performance measure of $\pm 20\%$ is adopted for dissolved oxygen; $\pm 50\%$ for nutrients and suspended solids; and $\pm 100\%$ for algal biomass for the evaluation of the comparison of the predicted results and observed water quality measurements for model calibration. These targets for hydrodynamic, sediment transport and water quality model performance, defined for the overall composite statistic computed from the set of station-specific statistics, are consistent with the range of model performance targets recommended for the HSPF watershed model (Donigian, 2000).

Given the lack of a general consensus for defining quantitative model performance criteria, the inherent errors in input and observed data, and the approximate nature of model formulations, absolute criteria for model acceptance or rejection are not appropriate for studies such as the development of the lake model for Fort Gibson Lake. The relative RMS errors presented above will be used as targets, but not as rigid criteria for rejection or acceptance of model results, for the performance evaluation of the calibration of the EFDC hydrodynamic and water quality model of Fort Gibson Lake.

B-6 HYDRODYNAMIC MODEL CALIBRATION AND VALIDATION

B-6.1 Lake Stage Calibration

In calibrating a hydrodynamic model of a water body, the first step is to obtain a satisfactory match between observed and modeled water surface elevation. The hydrodynamic model was calibrated for the time period of January 1, 2005 to December 31, 2005. Figure B-14 shows the comparison of observed lake elevation at the water intake location and simulated water surface elevation extracted from a grid cell at that location. Simulated lake elevation is in excellent agreement with the measured lake elevation for the entire calibration period from January 2005 through December 2005. The summary of calculated model performance statistics between observed and simulated water surface elevation for the calibration period is given in Table B-11.

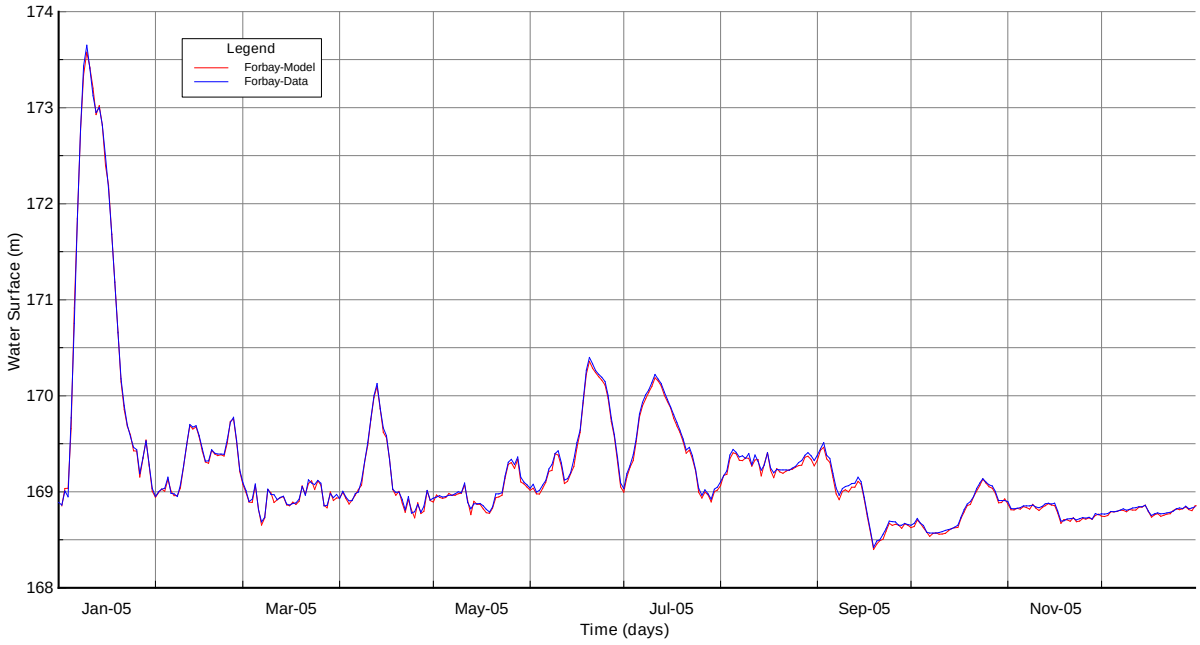

Figure B-14 Comparison of Simulated and Observed Water Level during Jan 2005 to Dec 2005

Table B-11 Summary Model Performance Statistics for Hydrodynamic Model of Fort Gibson Lake for Calibration and Validation Periods

Station ID	Parameter	Layer	Starting	Ending	# Pairs	RMS (m)	Rel RMS (%)	Data Average (m)	Model Average (m)
GIBO2	Stage (m)	Surface	1/2/2005 0:00	12/31/2005 0:00	364	0.033	0.6	169.25	169.23
GIBO2	Stage (m)	Surface	1/1/2006 0:00	12/31/2006 0:00	365	0.030	1.1	169.07	169.04

B-6.2 Lake Stage Validation

The Fort Gibson Lake EFDC model was validated for the time period of January 1, 2006 to December 31, 2006. The validation plot of surface water elevation at UASCE station GIBO2 is given in Figure B-15. The summary of calculated model performance statistics between observed and simulated water surface elevation for the validation period is given in Table B-11. The simulated average stage was 169.05 m which was very close to the average observed stage of 169.07 m. The calculated RMS error was 0.027 m and the relative RMS error was 1.0% (Table B-11).

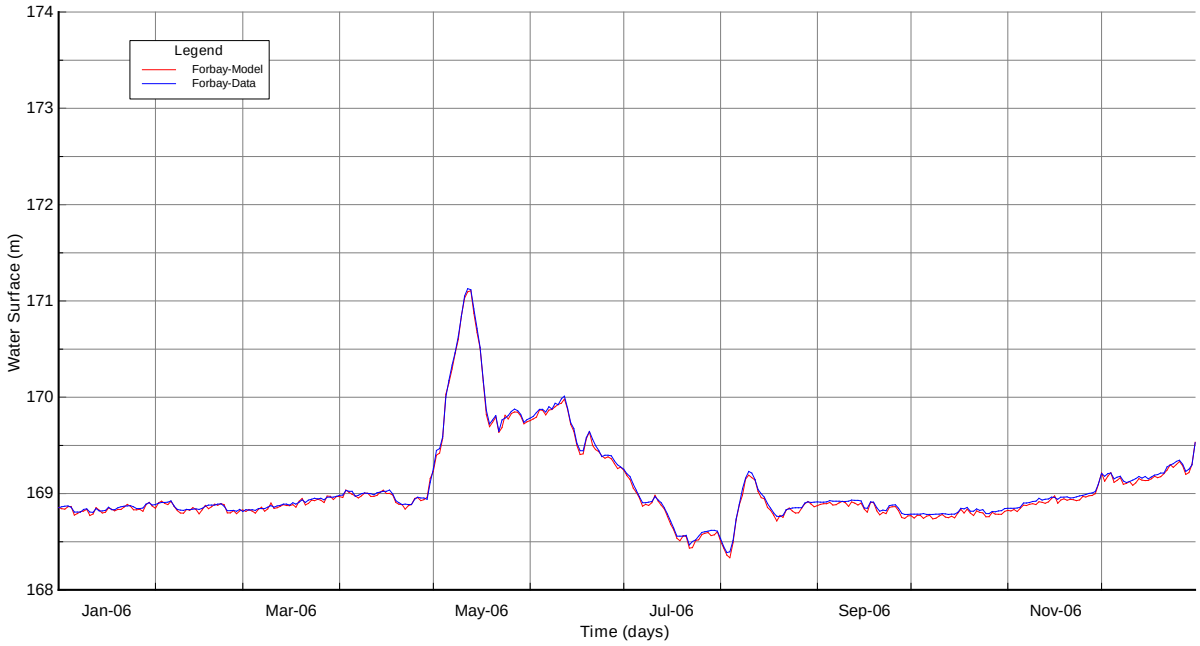

Figure B-15 Comparison of Simulated and Observed Water Level during Jan 2006 to Dec 2006

B-7 WATER QUALITY MODEL CALIBRATION AND VALIDATION

B-7.1 Introduction

Calibration of the lake water quality model is demonstrated with model-data comparisons for water temperature, suspended solids, dissolved oxygen, nutrients, organic carbon, and algae biomass as station time series. Vertical profiles are presented for water temperature and dissolved oxygen. Observed data collected near the surface is compared to model results for the surface layer (k=8) and data collected near the bottom is compared to model results for the bottom layer (k=1). Station results are presented in the main body of the report in this section to show model calibration for selected stations over Fort Gibson Lake as shown in Figure B-13. At stations 1GIBOKN0305, 1GIBOKN0355, and 1GIBOKN0386, only vertical profile data were available for one specific monitoring time; hence they cannot be used for time series comparison.

The observed water temperature, suspended solids, dissolved oxygen, nutrients, organic carbon, and chlorophyll at stations 1GIBOKN0003, 1GIBOKN0004, 1GIBOKN0005, and 1GIBOKN0006 were used for time series comparison with the For Gibson EFDC model for both surface and bottom layers except at station 1GIBOKN0006, where only surface data were available (Figure B-13). Over the calibration and validation periods (2005-2006), the observed data were very limited with the sample size for observed data for each year less than 10. In particular, there were no chlorophyll a data available for model validation. Hence, the comparison plots were provided separately for calibration and validation periods and the summary statistics for model performance were provided for the complete 2-year simulation.

B-7.2 Water Temperature Calibration and Validation

Modeled water temperature results are presented for comparison to the observed data for the surface layer (k=8) and bottom layer (k=1). Water temperature calibration plots at 1GIBOKN0003 and 1GIBOKN0005 are given in Figures B-16 through B-19. Water temperature validation plots at 1GIBOKN0003 and 1GIBOKN0005 are given in Figures B-20 through B- 23. The summary statistics for model performance for water temperature are given in Table B-12.

The comparisons of water temperature vertical profiles at 1GIBOKN0003 and 1GIBOKN0005 are given in Figures B-24 through B-25**.** The complete calibration and validation time series plots and vertical profiles for all monitoring stations developed for the lake model are given in APPENDIX C through APPENDIX F.

As can be seen in these model-data plots, the model results for the surface and bottom layer are in good agreement with measured water temperature for both calibration and validation periods. Model results for the bottom layer at Station 1GIBOKN0005 are somewhat cooler than the observed data collected during the summer months (Figure B-19 and Figure B-23).

The calculated RMS errors ranged from 0.54 ºC at the surface layer of station 1GIBOKN0004 to 1.98 ºC at the bottom layer of station 1GIBOKN0005 as shown in Table B-12. The calculated relative RMS errors

ranged from 2.72% at the surface layer (8) of station 1GIBOKN0004 and 10.73% at the bottom layer (1) of station 1GIBOKN0005. The model results are well within the defined model performance target of $\pm 50\%$ for water temperature.

Model results for vertical profiles are extracted as "snapshots' for a time interval of the simulation that matches the observed date/time records compiled for the hydrographic survey profiles**.** As can be seen in the model-data vertical profile plots, the model results are reasonably consistent with observed water temperature for both summer stratified conditions and well mixed winter conditions.

Table B-12 Summary Statistics of Water Temperature (°C)

Station ID	Layer	Starting	Ending	# Pairs	RMS (°C)	Rel RMS (%)	Data Average (°C)	Model Average (°C)
1GIBOKN0003	Layer 8	3/24/2005 10:20	9/6/2006 9:50	16	0.64	3.24	25.173	24.794
1GIBOKN0003	Layer 1	3/24/2005 10:20	9/6/2006 9:50	16	1.51	8.42	23.364	22.901
1GIBOKN0004	Layer 8	3/24/2005 10:50	9/6/2006 10:20	16	0.54	2.72	25.716	25.867
1GIBOKN0004	Layer 1	3/24/2005 10:50	9/21/2005 12:40	9	1.36	7.39	24.509	23.425
1GIBOKN0005	Layer 8	3/24/2005 12:50	9/6/2006 9:10	16	0.79	4.08	25.491	25.921
1GIBOKN0005	Layer 1	3/24/2005 12:50	9/6/2006 9:10	16	1.98	10.73	24.413	22.990
1GIBOKN0006	Layer 8	3/24/2005 9:25	9/6/2006 8:40	15	1.01	4.93	25.108	25.765

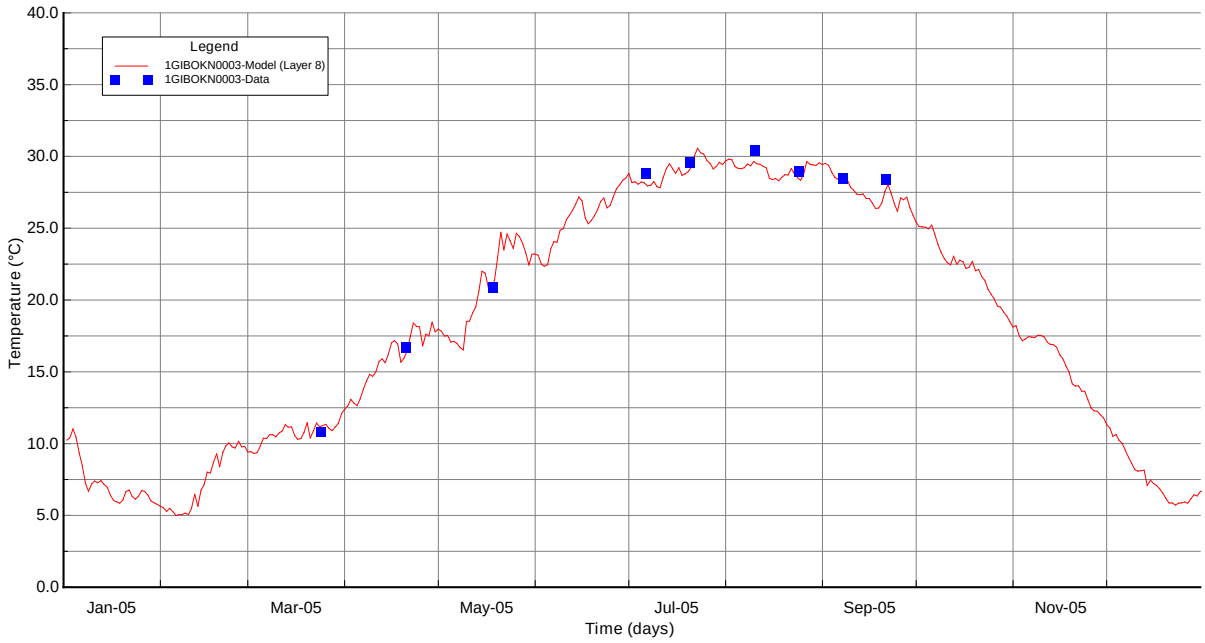

Figure B-16 Surface Layer Water Temperature Calibration Plot at Station 1GIBOKN0003

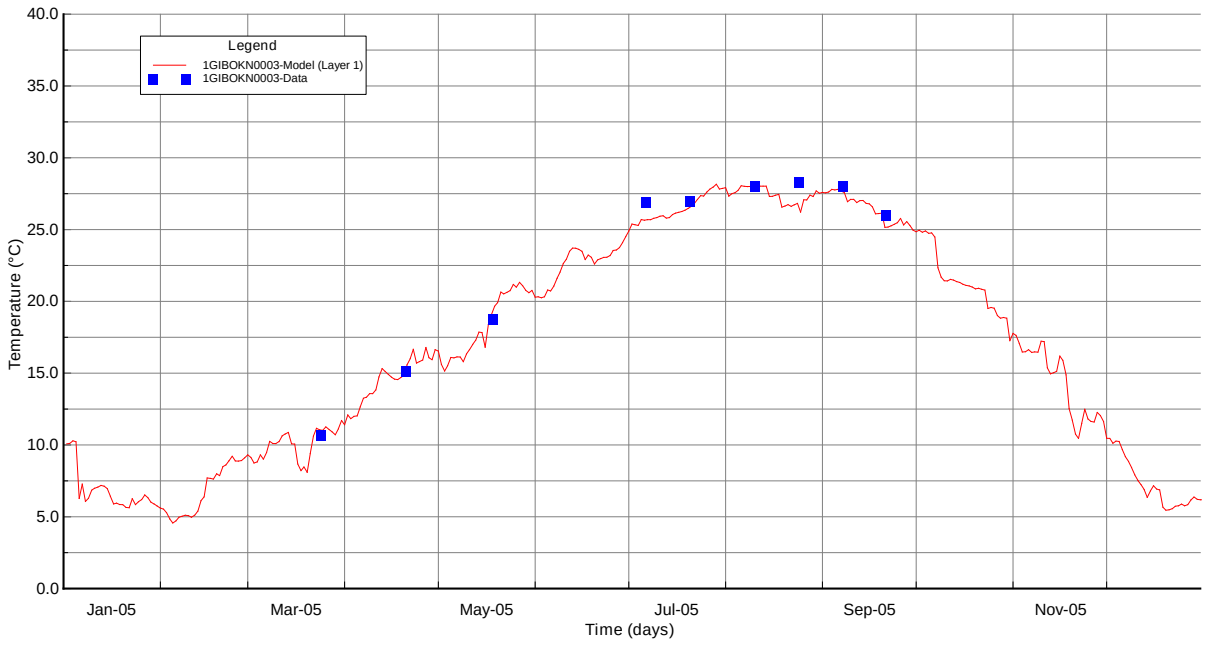

Figure B-17 Bottom Layer Water Temperature Calibration Plot at Station 1GIBOKN0003

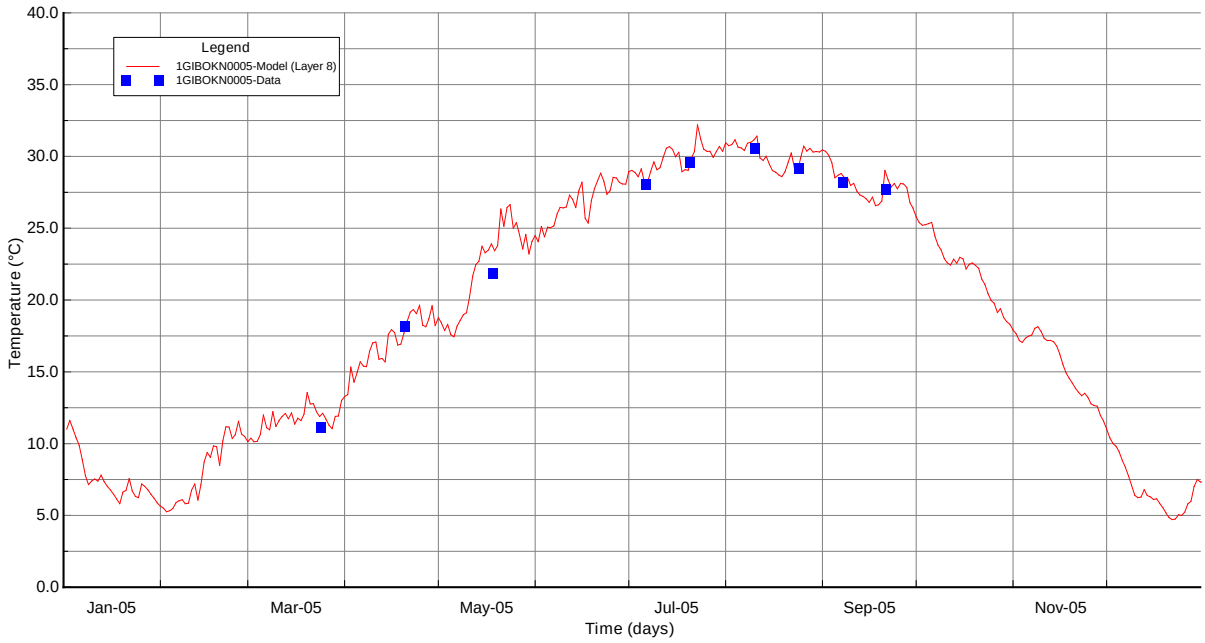

Figure B-18 Surface Layer Water Temperature Calibration Plot at Station 1GIBOKN0005

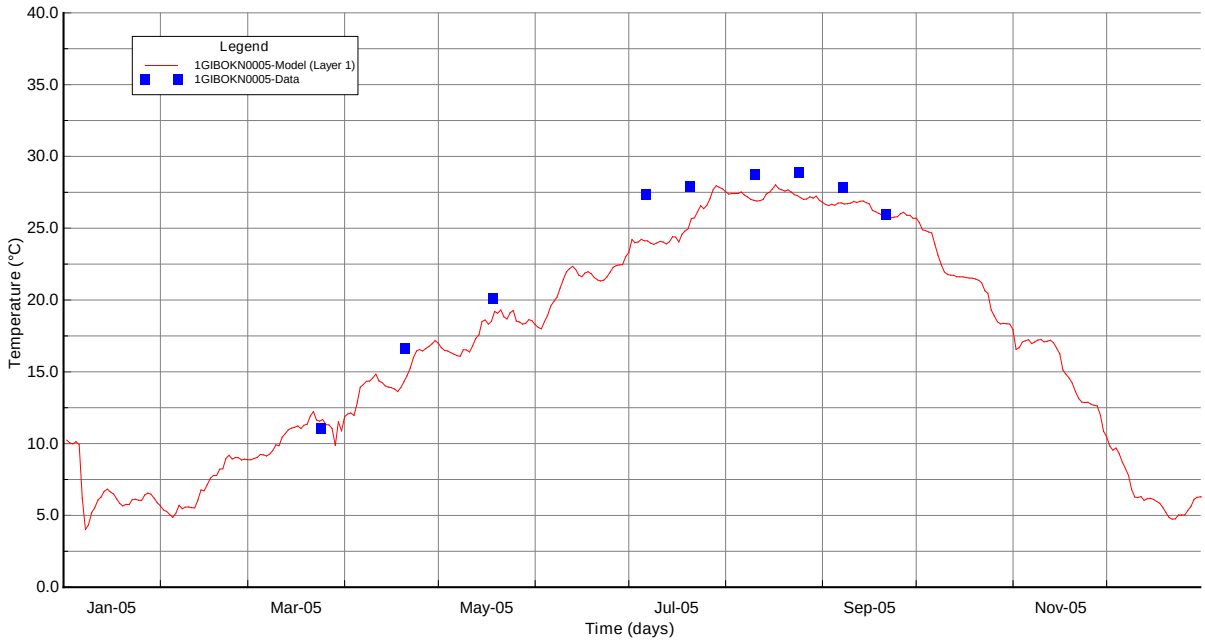

Figure B-19 Bottom Layer Water Temperature Calibration Plot at Station 1GIBOKN0005

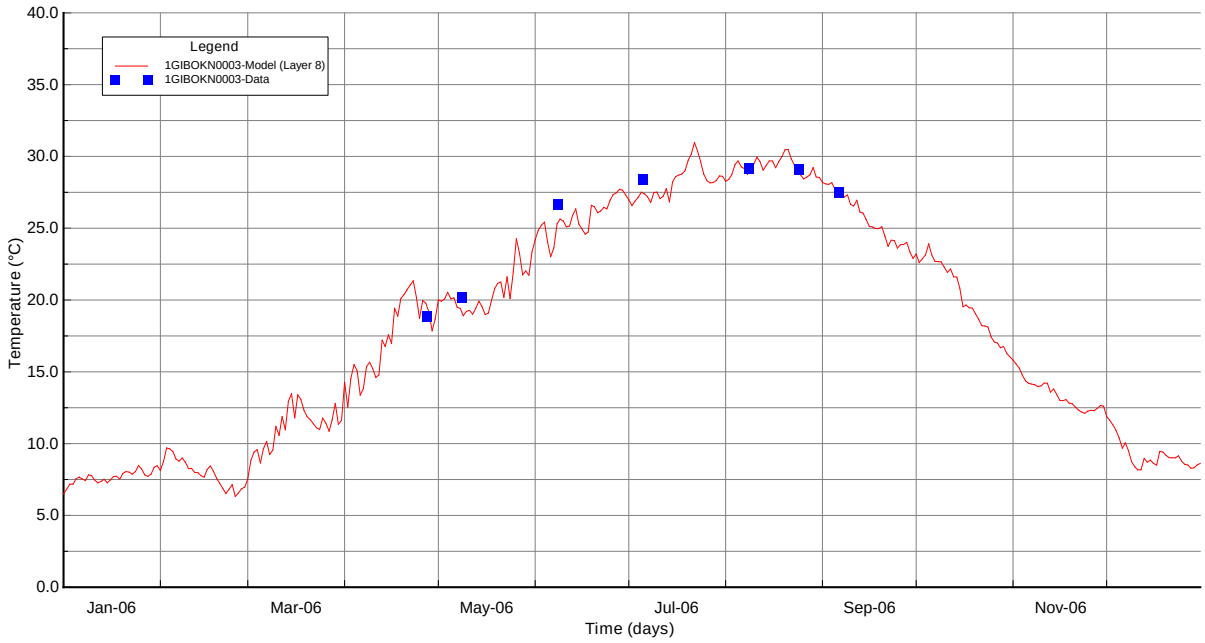

Figure B-20 Surface Layer Water Temperature Validation Plot at Station 1GIBOKN0003

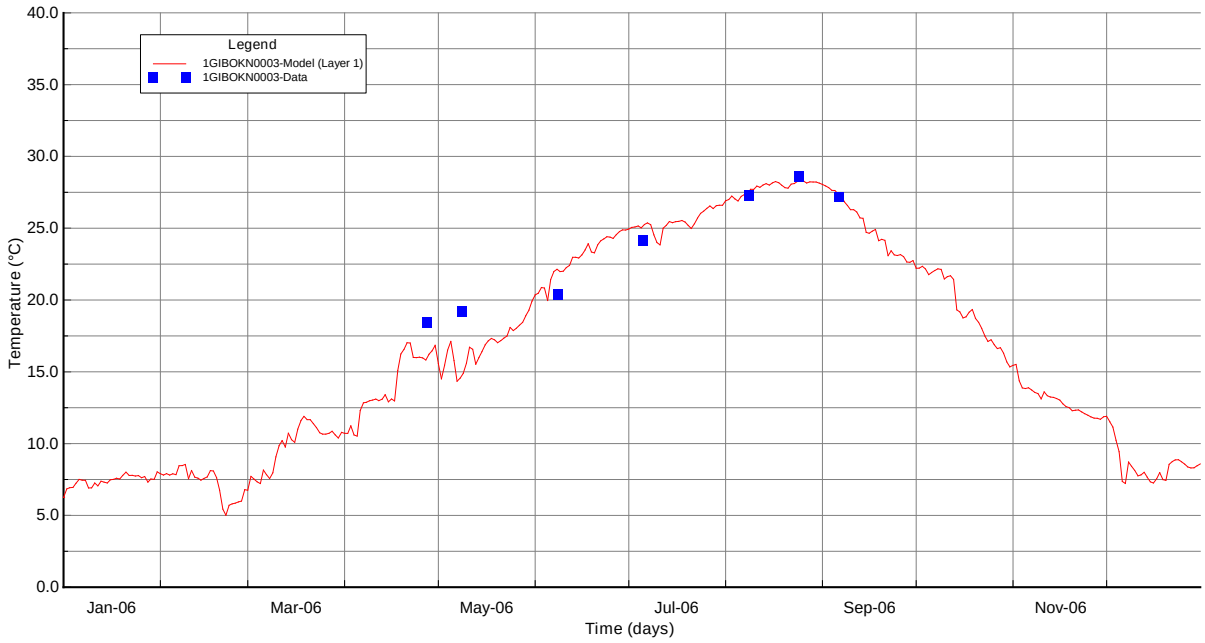

Figure B-21 Bottom Layer Water Temperature Validation Plot at Station 1GIBOKN0003

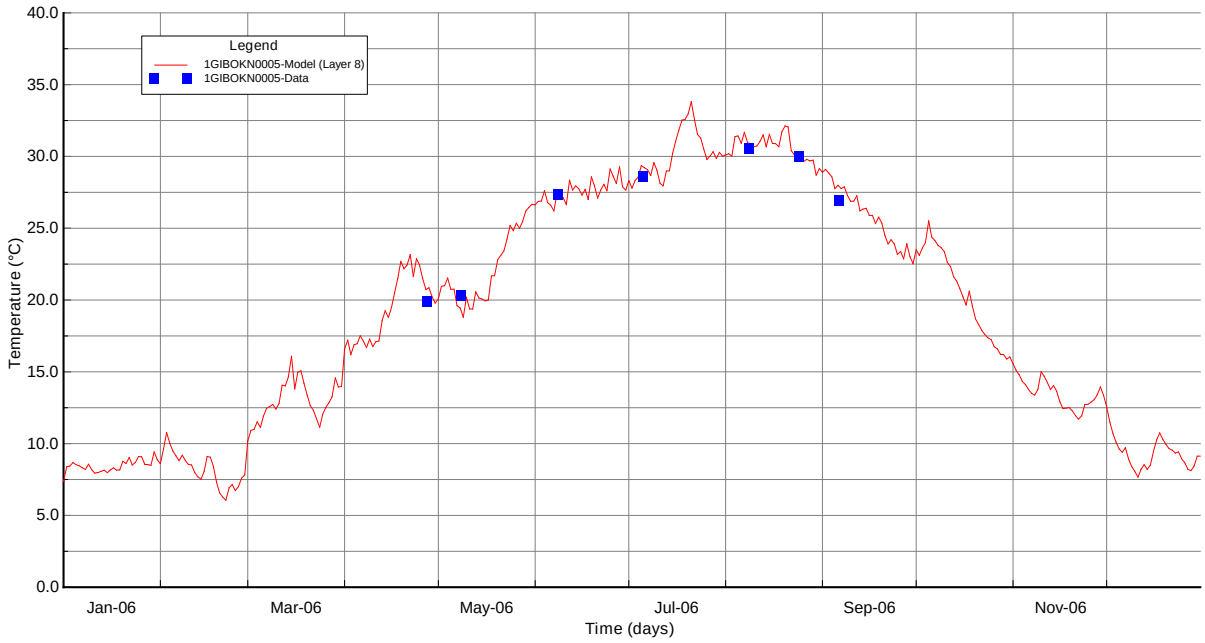

Figure B-22 Surface Layer Water Temperature Validation Plot at Station 1GIBOKN0005

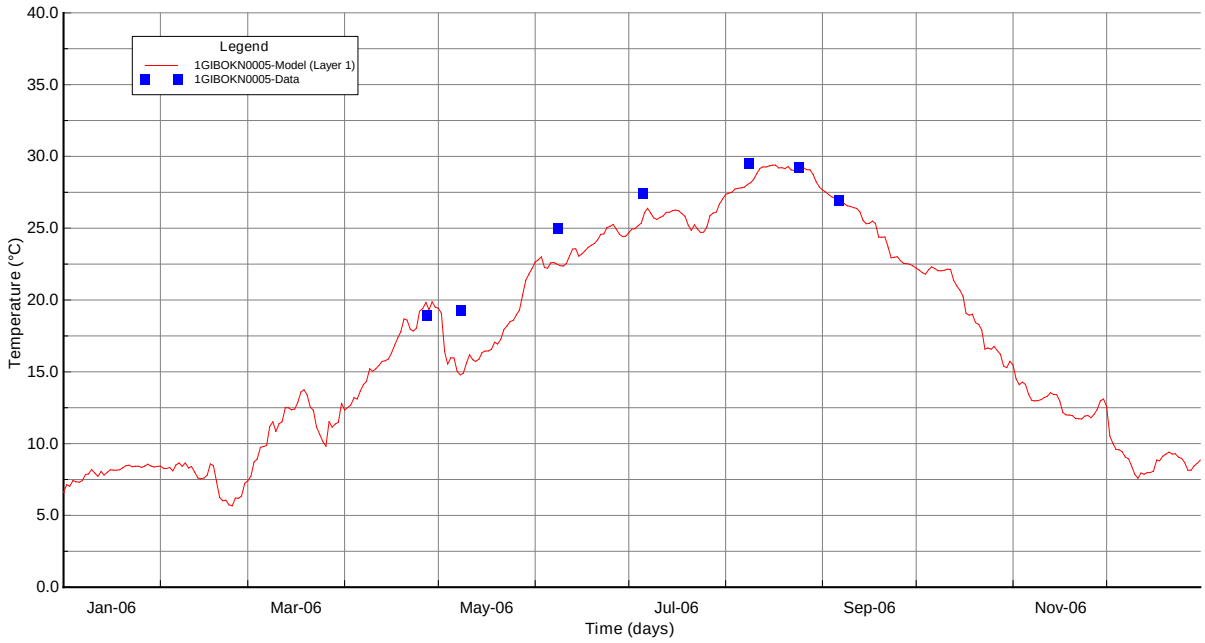

Figure B-23 Bottom Layer Water Temperature Validation Plot at Station 1GIBOKN0005

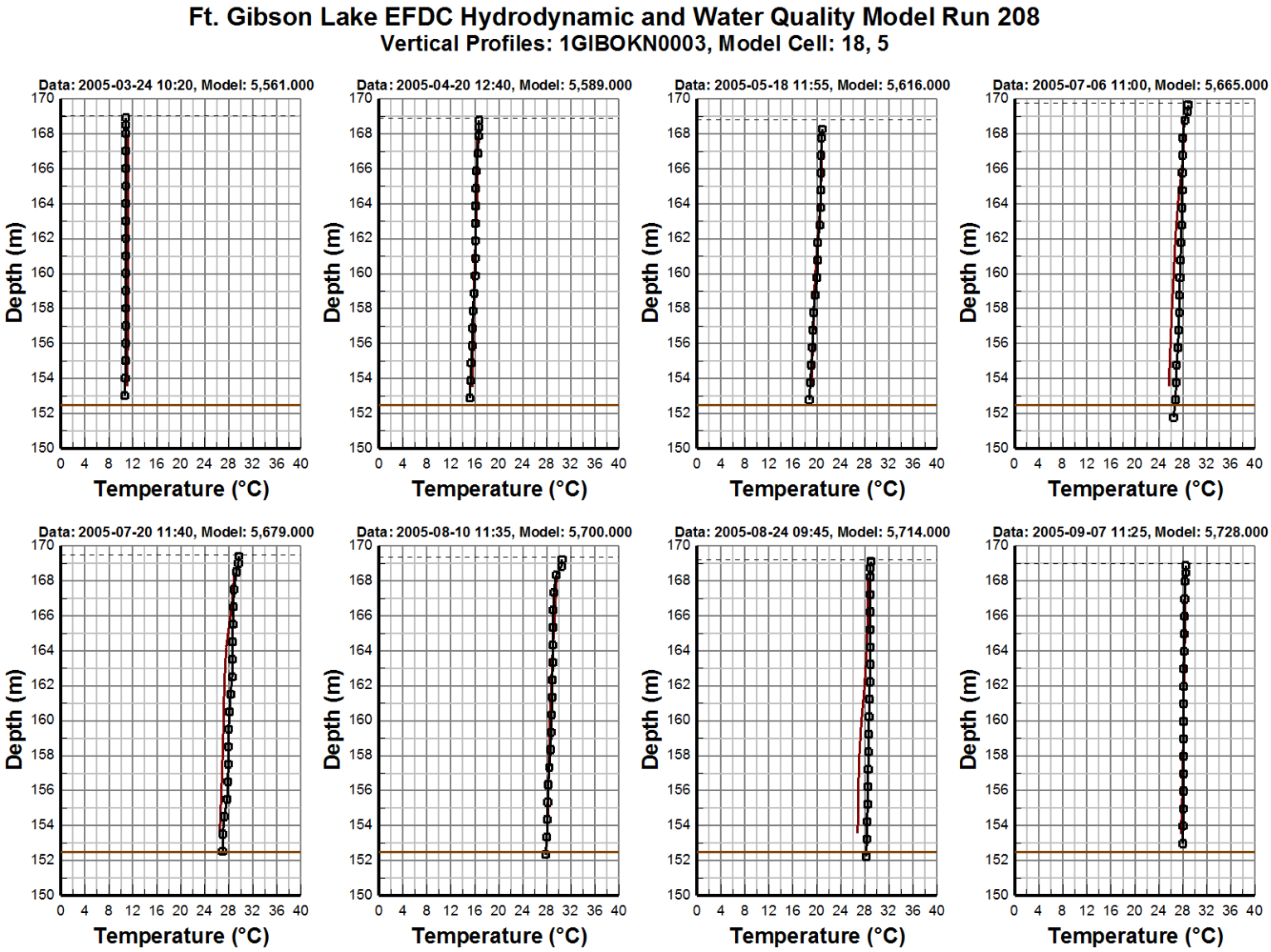

Figure B-24 Water Temperature Vertical Profile Comparison Plot at Station 1GIBOKN0003 (page 1-2)

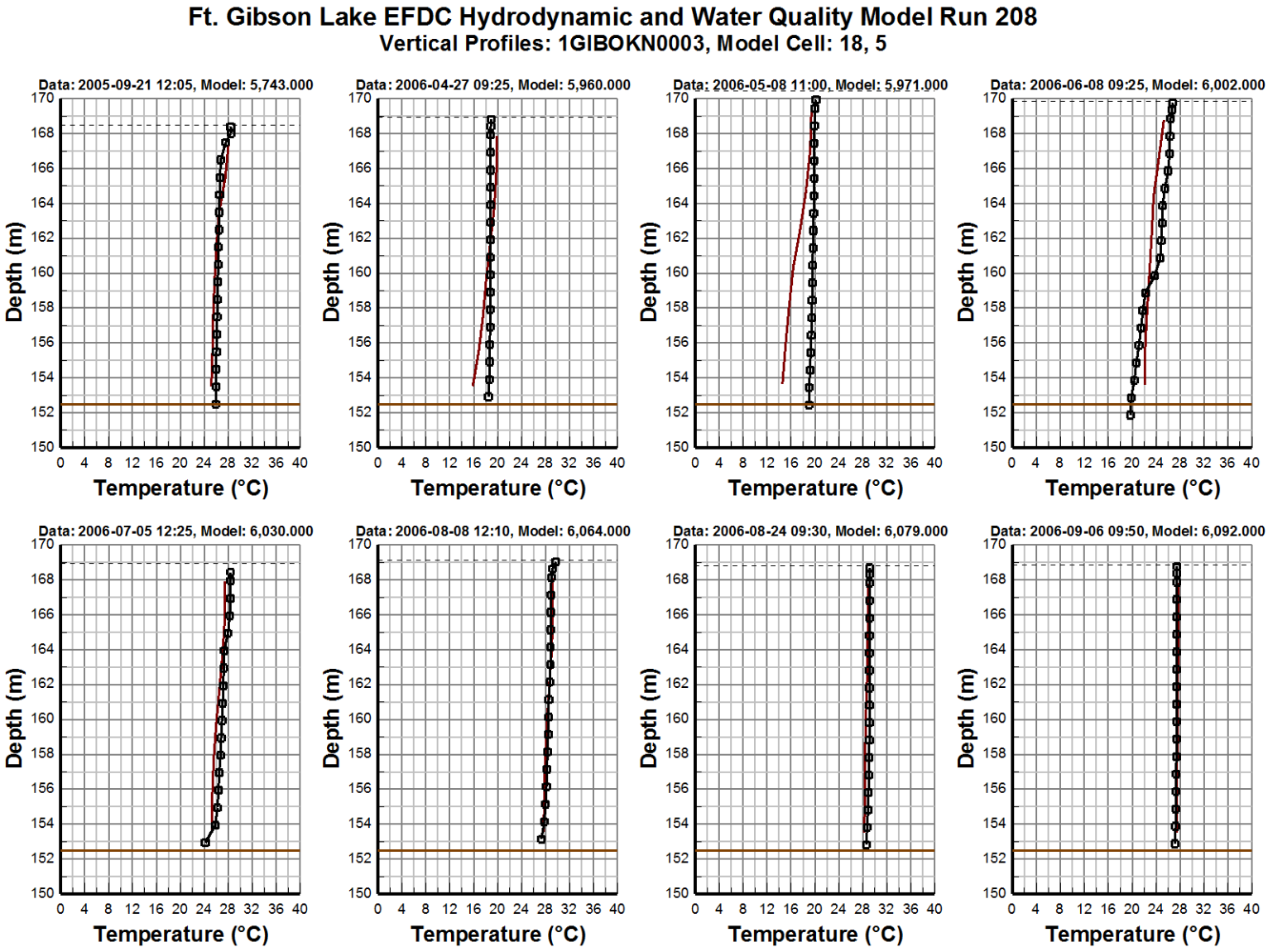

Figure B-24 Water Temperature Vertical Profile Comparison Plot at Station 1GIBOKN0003 (page 2-2)

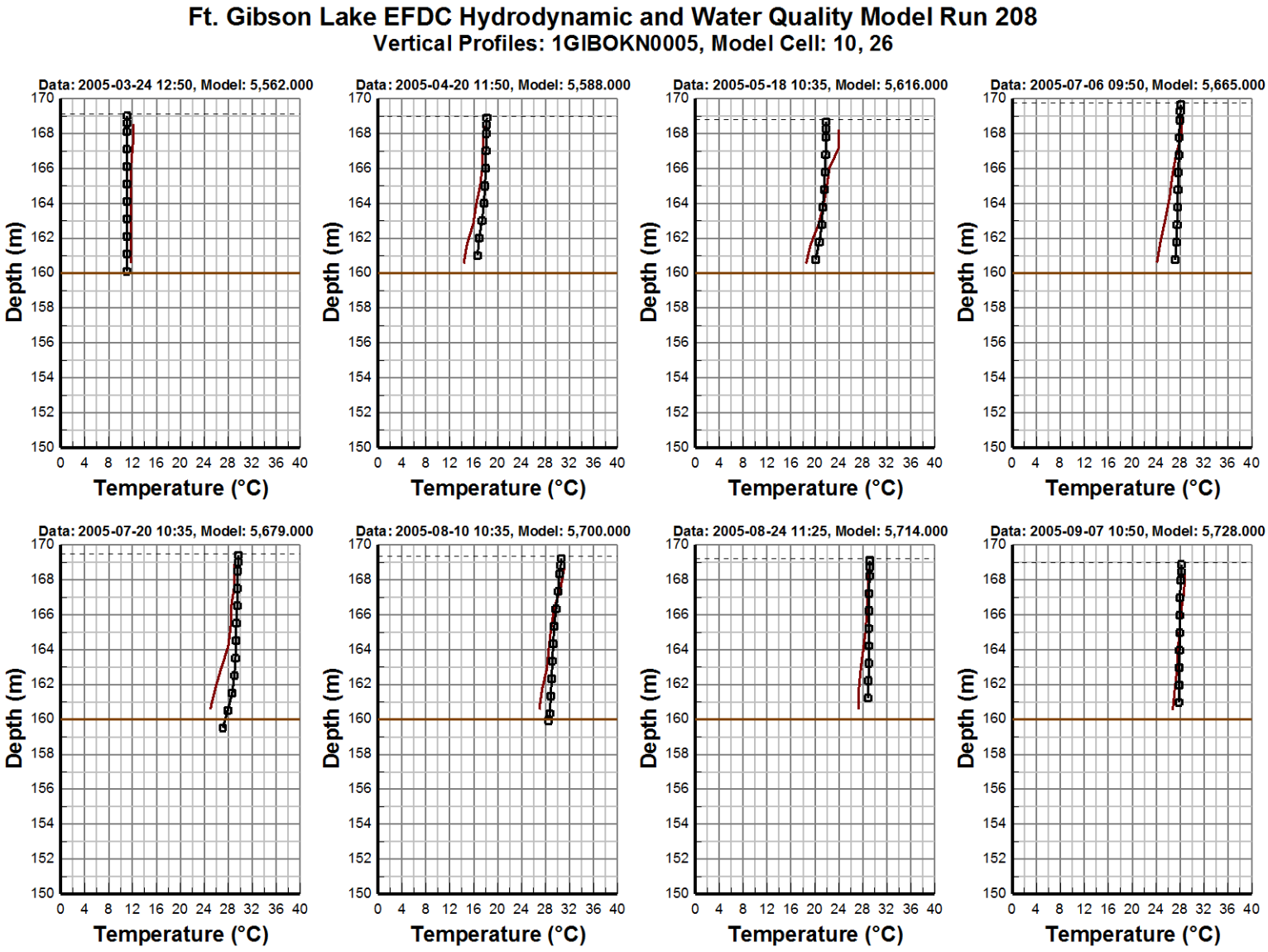

Figure B-25 Water Temperature Vertical Profile Comparison Plot at Station 1GIBOKN0005 (page 1-2)

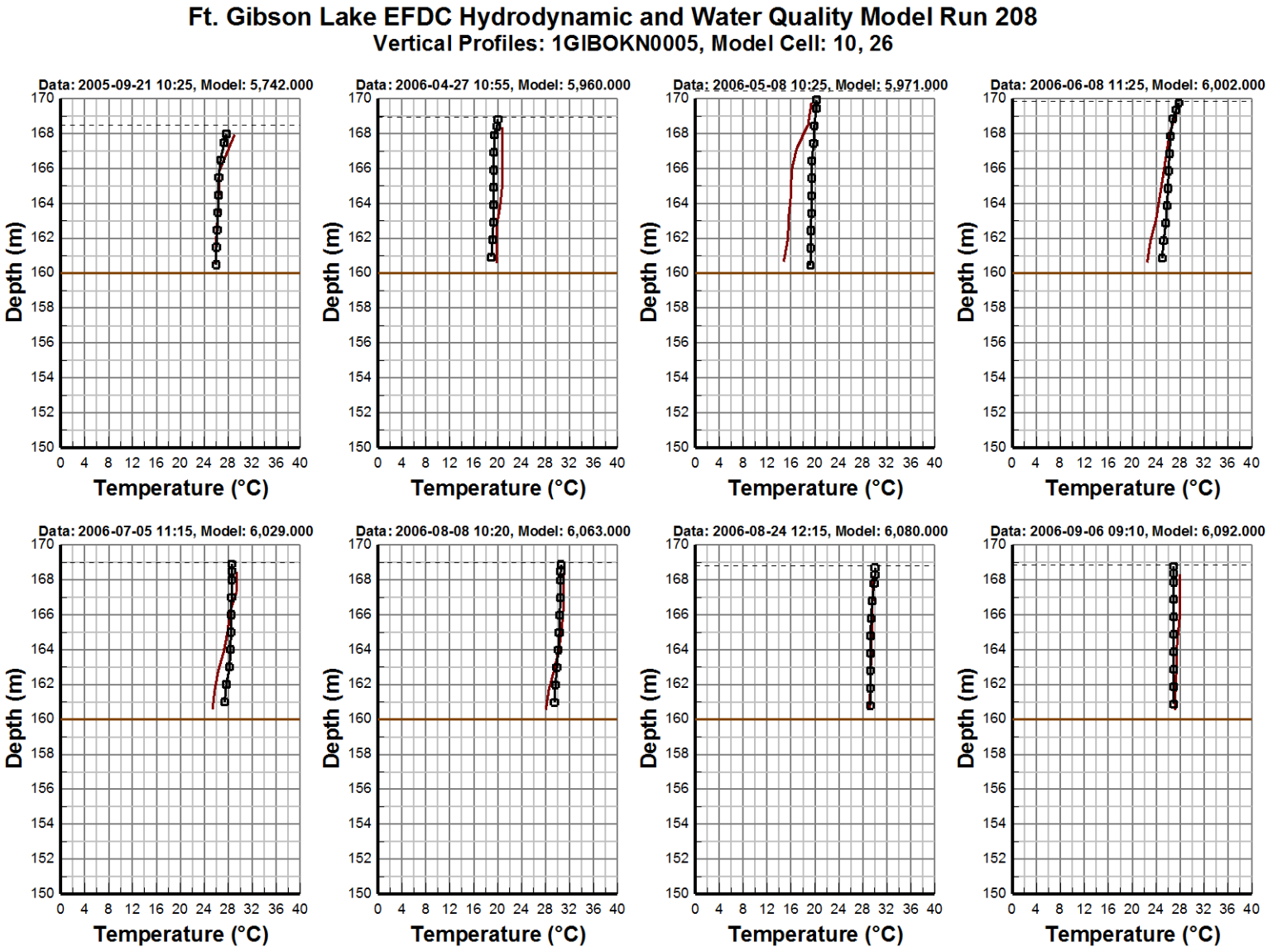

Figure B-25 Water Temperature Vertical Profile Comparison Plot at Station 1GIBOKN0005 (page 2-2)

B-7.3 Total Suspended Solids Calibration and Validation

Modeled TSS results are presented for comparison to the observed data for the surface layer (k=8) and bottom layer (k=1). Total suspended solids calibration plots at 1GIBOKN0003 and 1GIBOKN0005 are given in Figure B-26 through Figure B-30. Total suspended solids validation plots at 1GIBOKN0003 and 1GIBOKN0005 are given in Figure B-31 through B-33. The summary statistics for model performance of total suspended solids are given in Table B-13. The complete calibration and validation time series plots for all monitoring stations are given in APPENDIX C and APPENDIX D.

As can be seen in these model-data plots, the model results for the surface and bottom layer are in reasonable agreement with the measured TSS. The calculated RMS errors ranged from 5.21 mg/L at the surface layer of station 1GIBOKN0005 to 10.93 mg/L at the bottom layer of station 1GIBOKN0005 shown in Table B-13. The calculated relative RMS errors ranged from 26.10% at the surface layer of station 1GIBOKN0006 to 53.15% at the bottom layer of station 1GIBOKN0003. The model results are well within the defined model performance target of $\pm 50\%$ for TSS except for the bottom layer of station 1GIBOKN0003 where the relative RMS (53.15%) error is slightly higher than the target.

Table B-13 Summary Statistics of TSS (mg/l)

Station ID	Layer	Starting	Ending	# Pairs	RMS (mg/l)	Rel RMS (%)	Data Average (mg/l)	Model Average (mg/l)
1GIBOKN0003	Layer 8	3/24/2005 10:20	9/6/2006 9:50	17	5.22	37.24	5.694	7.301
1GIBOKN0003	Layer 1	3/24/2005 10:20	9/6/2006 9:50	13	5.32	53.15	10.246	5.891
1GIBOKN0004	Layer 8	3/24/2005 10:50	9/6/2006 10:21	17	6.87	31.22	7.824	7.935
1GIBOKN0004	Layer 1	3/24/2005 10:50	9/21/2005 12:40	9	9.36	36.01	10.333	8.478
1GIBOKN0005	Layer 8	3/24/2005 12:50	9/6/2006 9:10	16	5.21	43.40	5.975	7.903
1GIBOKN0005	Layer 1	3/24/2005 12:50	9/6/2006 9:10	16	10.93	35.26	11.488	9.409
1GIBOKN0006	Layer 8	3/24/2005 9:25	9/6/2006 8:40	17	5.74	26.10	8.329	6.82

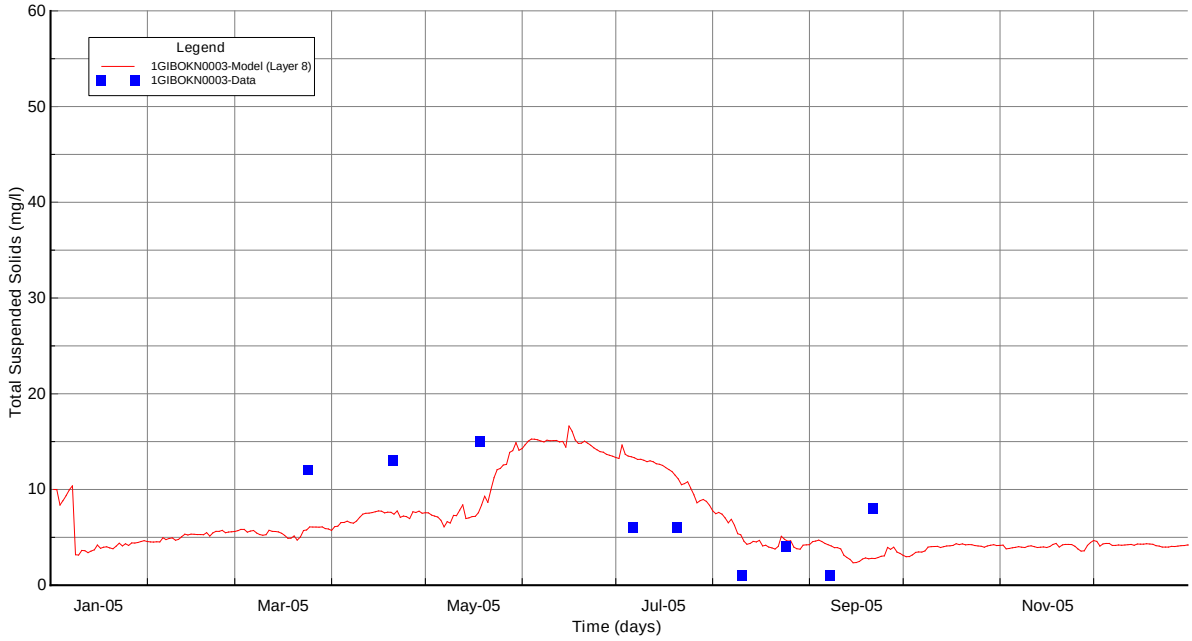

Figure B-26 Surface Layer TSS Calibration Plot at Station 1GIBOKN0003

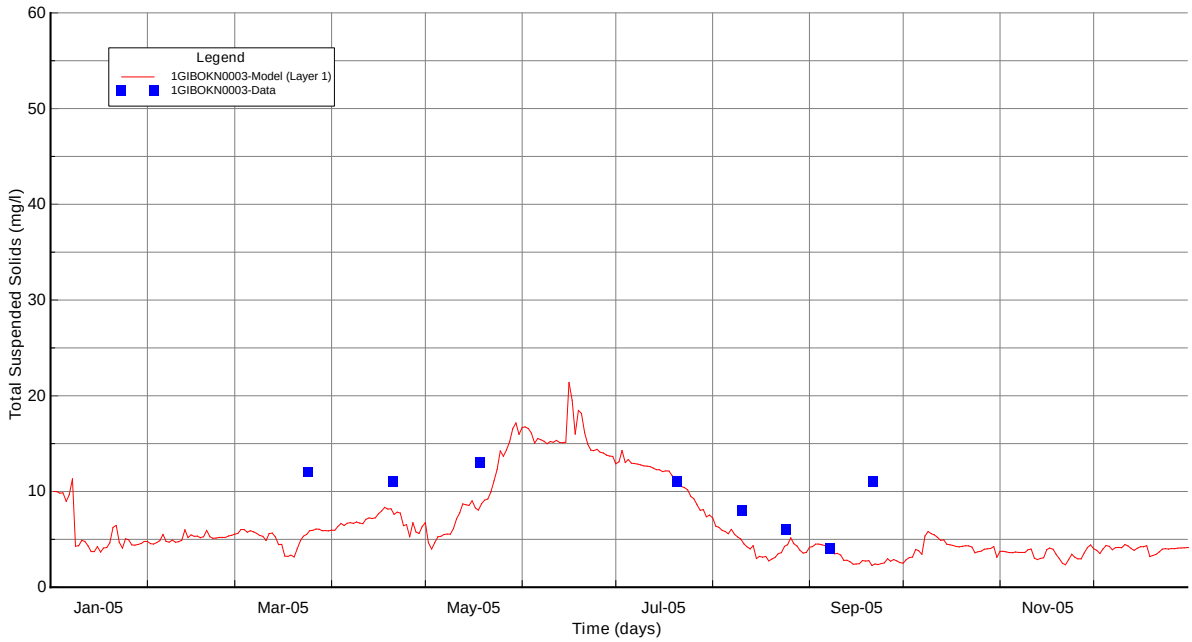

Figure B-27 Bottom Layer TSS Calibration Plot at Station 1GIBOKN0003

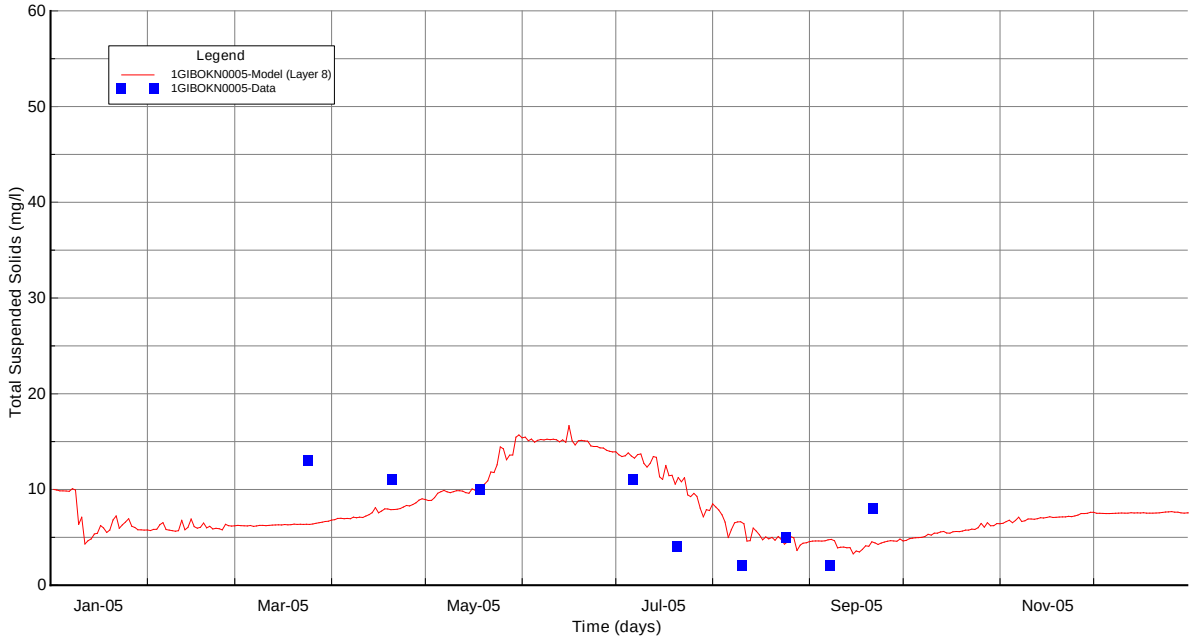

Figure B-28 Surface Layer TSS Calibration Plot at Station 1GIBOKN0005

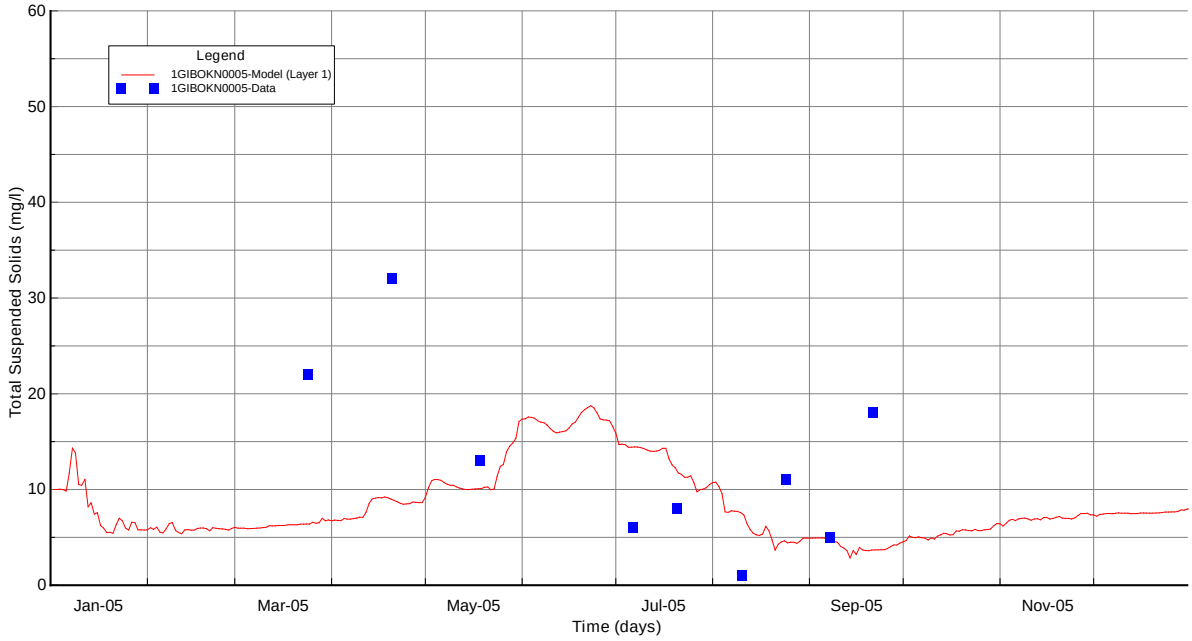

Figure B-29 Bottom Layer TSS Calibration Plot at Station 1GIBOKN0005

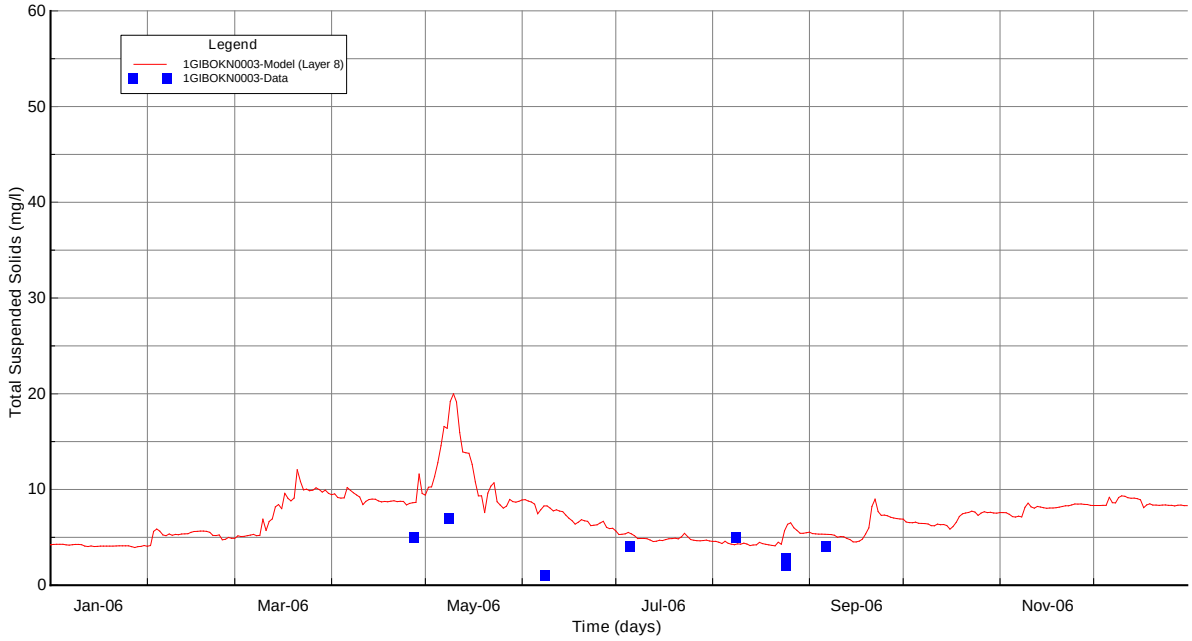

Figure B-30 Surface Layer TSS Validation Plot at Station 1GIBOKN0003

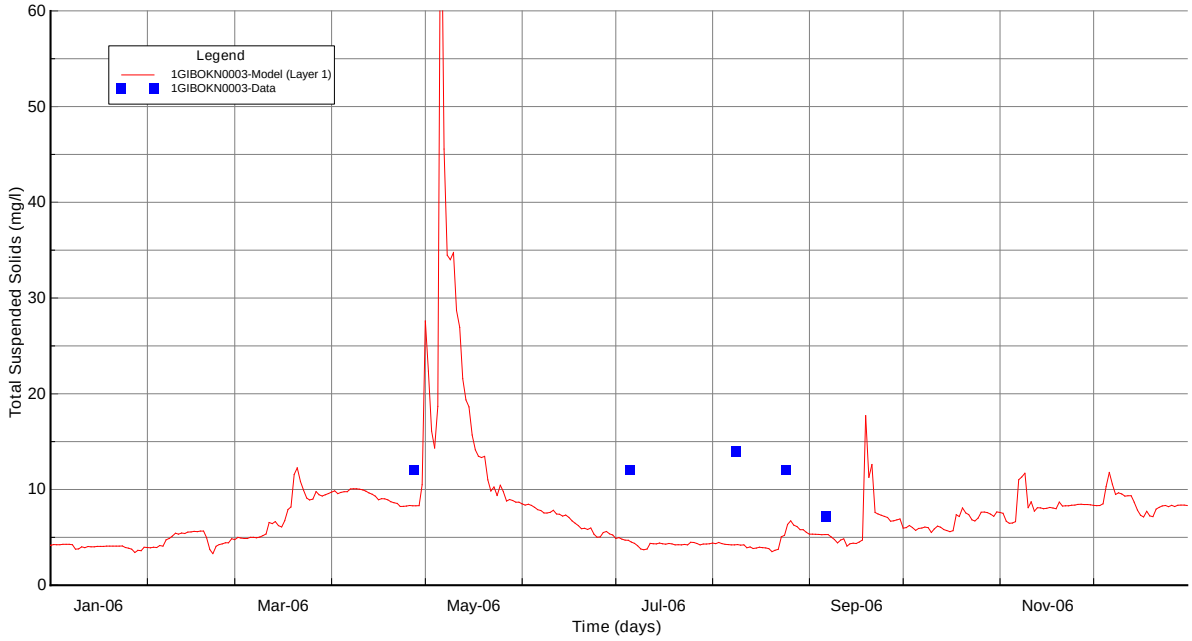

Figure B-31 Bottom Layer TSS Validation Plot at Station 1GIBOKN0003

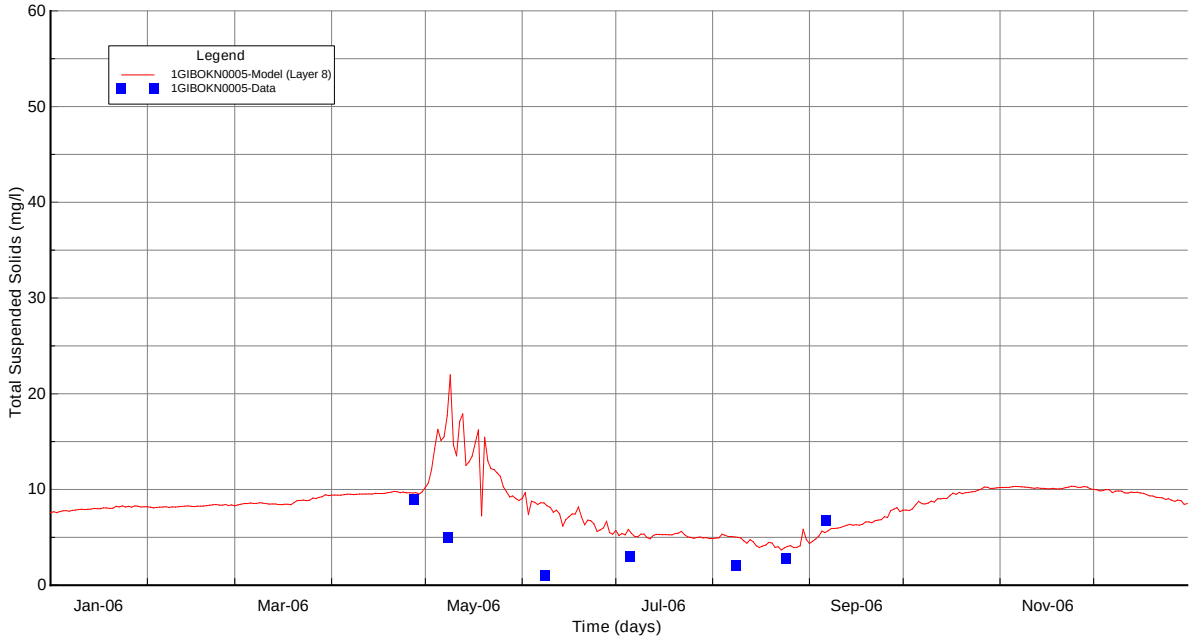

Figure B-32 Surface Layer TSS Validation Plot at Station 1GIBOKN0005

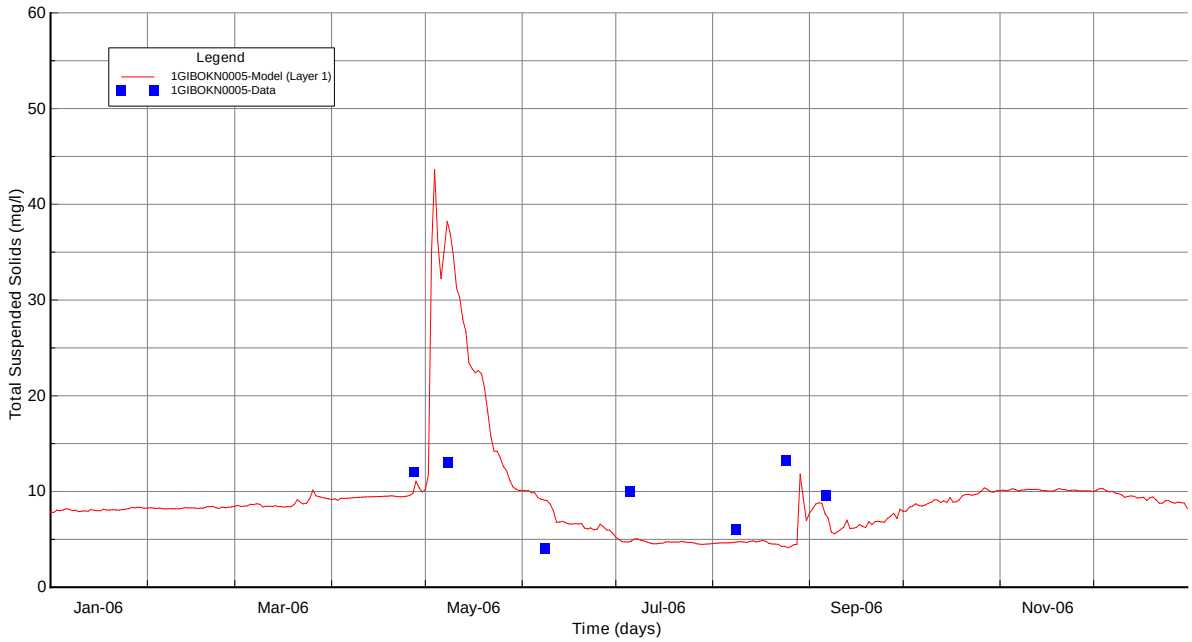

Figure B-33 Bottom Layer TSS Validation Plot at Station 1GIBOKN0005

B-7.4 Dissolved Oxygen

Modeled oxygen results are presented for comparison to the observed data for the surface layer (k=8) and bottom layer (k=1). Dissolved oxygen calibration plots at 1GIBOKN0003 and 1GIBOKN0005 are given in Figures B-34 through B-37. Dissolved oxygen validation plots at 1GIBOKN0003 and 1GIBOKN0005 are given in Figures B-38 through B-41. The summary statistics for model performance of dissolved oxygen are given in Table B-14.

The comparisons of dissolved oxygen vertical profiles at 1GIBOKN0003 and 1GIBOKN0005 are given in Figures B-42 through B-43**.** The complete calibration and validation time series plots and vertical profiles for all monitoring stations are given in APPENDIX C through APPENDIX F.

As can be seen in these model-data plots, the model results for both the surface and bottom layer are in good agreement with the measured oxygen. The exception is the period when super saturated oxygen conditions were observed in the surface layer during the summer months. Super saturated oxygen conditions are most likely caused by the photosynthetic oxygen production by algae which was not replicated by the model.

The calculated RMS errors ranged from 1.29 mg/L at the surface layer of station 1GIBOKN0006 to 2.27 mg/L at the surface layer of station 1GIBOKN0003 shown in Table B-14. The calculated relative RMS errors ranged from 12.94% at the bottom layer of station 1GIBOKN0003 to 30.28% at the surface layer of station 1GIBOKN0004. The model results are close to the defined model performance target of $\pm 20\%$ for dissolved oxygen.

For comparison at each station, lake model results are extracted as vertical “snapshots’ at different times when the observed data are available. As can be seen in these model-data vertical profile plots shown in Figure B-42 and B-43, the model results are reasonably consistent with the observed dissolved oxygen for both summer stratified conditions and well mixed winter conditions.

Full supporting compliance with Oklahoma water quality criteria for dissolved oxygen for lakes in the Warm Water Aquatic Community (WWAC) subcategory of Fish and Wildlife Propagation is achieved for the following conditions: (a) for lakes, no more than 50% of the water volume shall exhibit a DO concentration less than 2.0 mg/L. If no volumetric data is available, then no more than 70% of the water column at any given sample site shall exhibit a DO concentration less than 2.0 mg/L; (b) 10% or fewer of surface water oxygen are less than 6 mg/L at early life stages from April 1-June 15 and are less than 5 mg/L under summer conditions (June 16-October 15) and winter conditions (October 16-March 31) at other life stages (http://www.owrb.ok.gov/util/rules/pdf_rul/proposed/2015/Ch45.textforGovernor-CabinetSecretary.pdf).

Table B-14 Summary Statistics of DO (mg/l)

Station ID	Layer	Starting	Ending	# Pairs	RMS (mg/l)	Rel RMS (%)	Data Average (mg/l)	Model Average (mg/l)
1GIBOKN0003	Layer 8	3/24/2005 10:20	9/6/2006 9:50	16	2.27	21.94	7.906	7.179
1GIBOKN0003	Layer 1	3/24/2005 10:20	9/6/2006 9:50	16	1.32	12.94	2.604	2.16
1GIBOKN0004	Layer 8	3/24/2005 10:50	9/6/2006 10:20	16	1.80	30.28	8.674	8.132
1GIBOKN0004	Layer 1	3/24/2005 10:50	9/21/2005 12:40	9	1.94	18.96	5.759	4.544
1GIBOKN0005	Layer 8	3/24/2005 12:50	9/6/2006 9:10	16	1.48	29.39	8.562	8.271
1GIBOKN0005	Layer 1	3/24/2005 12:50	9/6/2006 9:10	16	1.50	14.32	3.778	3.921
1GIBOKN0006	Layer 8	3/24/2005 9:25	9/6/2006 8:40	15	1.29	23.17	8.33	8.514

Model calibration results for dissolved oxygen are processed using EFDC_Explorer to compute the volume of the lake that is defined as anoxic based on the criteria of 2 mg/L as a cutoff concentration. The anoxic volumes of the stations of 1GIBOKN0003, 1GIBOKN0355, and 1GIBOKN0386, are shown as percentages of the total volume as time series in Figure B-44 and Figure B-45. As can be seen in Figure B-44, the model results for the anoxic volume are in very good agreement with the observations at Station 1GIBOKN0003 near the dam. The anoxic volume is seen to gradually increase during summer stratified conditions and then decreases as stratification erodes and the water column becomes well mixed in late fall and winter.

The anoxic volume of the lake shown in Figure B-46 is a snapshot of model results on July 25, 2006 00:00. Figure B-46 shows the lake wide distribution of the anoxic volume at a date when the anoxic volume is seen to be the highest during the summer stratified season. The deeper area in the vicinity of the dam is characterized by the greatest anoxic volume of ~75%. For the complete calibration and validation periods, there are two days (July 25 and 28 in 2006) at station 1GIBOKN0003 with 75% of the water column exhibiting a DO concentration less than 2.0 mg/L, which is a violation of the criteria (a) described above. In addition, 20.5% of the modeled DO concentrations in the surface layers during June 16 – October 15 in 2006 are less than 5 mg/L at station 1GIBOKN0003, as shown in Figure B-48, which is a violation of the criteria (b) described above. Fort Gibson Lake is, therefore, impaired in terms of the DO criterion.

Observed data and model calibration results were processed for each site to compile summary statistics for data collected and simulated from June 16 through October 15. The statistics thus describe variability of observations and model results on a seasonal basis corresponding to summer conditions at other life stages. Summary statistics are shown as box-whisker plots for each monitoring site for

observed surface and bottom oxygen in Figure B-47 and Figure B-49 and simulated surface and bottom oxygen for model calibration in Figure B-48 and Figure B-50.

It must be pointed out that there are only 4 to 5 observations of surface or bottom DO data for a single calendar year. The summary statistics generated from these limited data sets might be biased or misleading for evaluation of the model results. The observed DO data at both calibration and validation periods, therefore, were pooled together and used to generate the box-whisker plots. The sample size of observed DO concentrations under summer conditions for both calibration and validation periods at the USACE sites varies from 6 to 10 observations with the smallest sample size of bottom DO at station 1GIBOKN0004. There are enough modeled DO data points with the sample size of 122 observations to generate the box-whisker plots for the validation period.

The lower and upper part of the box plot shows the 25th and 75th percentile with the 50th percentile shown as the line through the box. The mean is shown as a data point in the box and the lower and upper tails of the box show the 10th and 90th percentile. Minimum and maximum values are shown as data points plotted outside the tails of the box. The water quality target of 5 mg/L is shown as the horizontal green line on the box-whisker plots while the anoxic cutoff value of 2 mg/L is shown as the horizontal red line.

As shown in Figure B-48, at station 1GIBOKN0003 only, the 10^{th} percentile of the modeled surface DO concentration is lower than 5 mg/L. At stations 1GIBOKN0004, 1GIBOKN00045, and 1GIBOKN0006, the modeled lowest surface DO concentrations are all higher than 5 mg/L.

As shown in Figure B-50, the 75^{th} percentile of the modeled bottom DO concentration is lower than 2 mg/L and the 90^{th} percentile of the bottom DO concentration is lower than 4 mg/L at station 1GIBOKN0003. At stations 1GIBOKN0004 and 1GIBOKN0005, the 25^{th} percentile of the modeled DO concentration is higher than 2 mg/L.

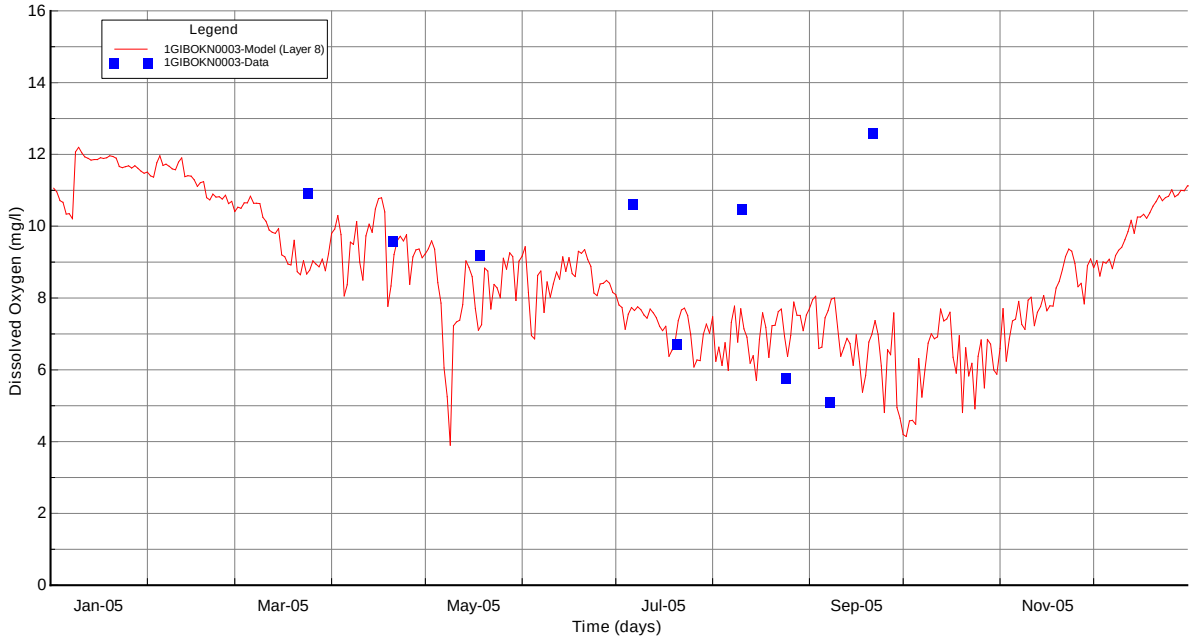

Figure B-34 Surface Layer Dissolved Oxygen Calibration Plot at Station 1GIBOKN0003

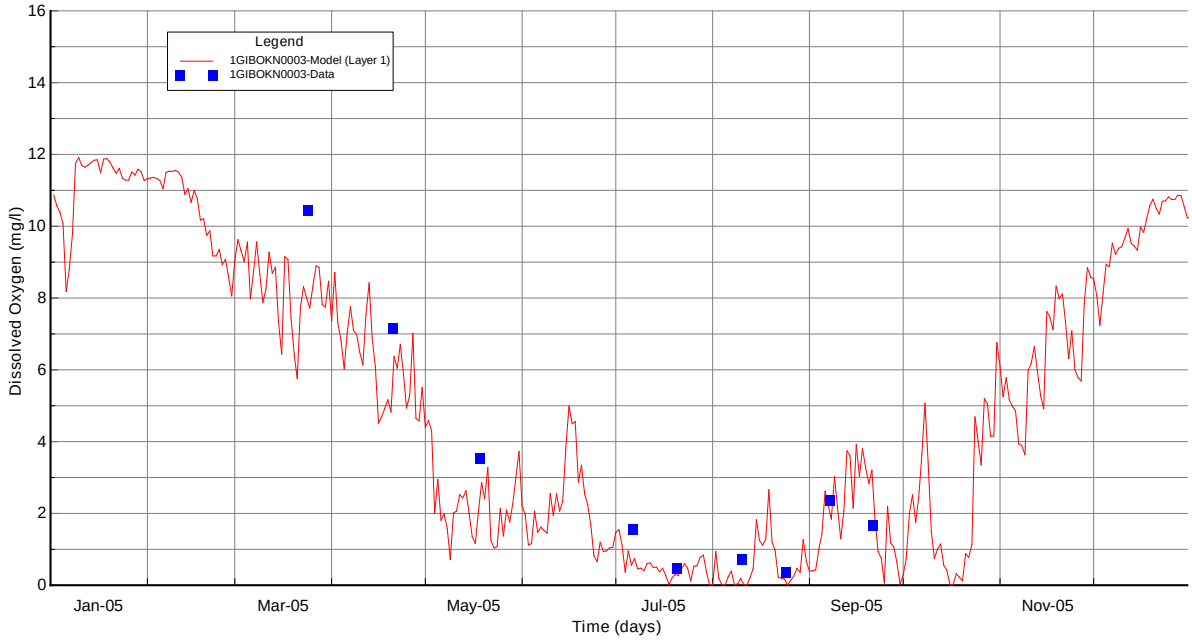

Figure B-35 Bottom Layer Dissolved Oxygen Calibration Plot at Station 1GIBOKN0003

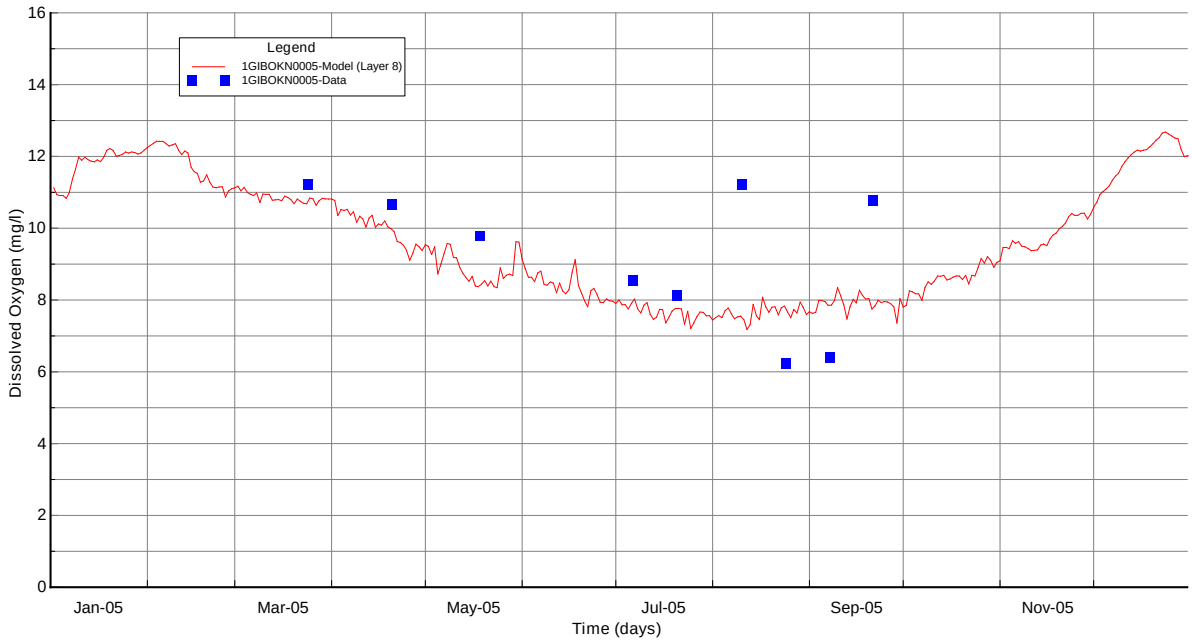

Figure B-36 Surface Layer Dissolved Oxygen Calibration Plot at Station 1GIBOKN0005

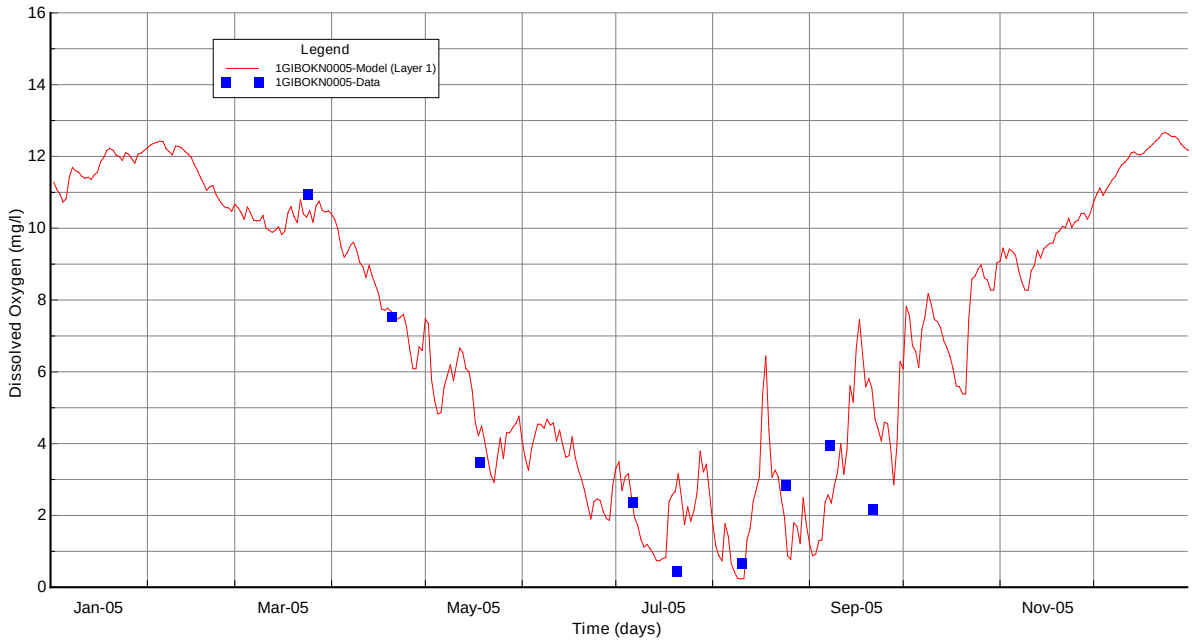

Figure B-37 Bottom Layer Dissolved Oxygen Calibration Plot at Station 1GIBOKN0005

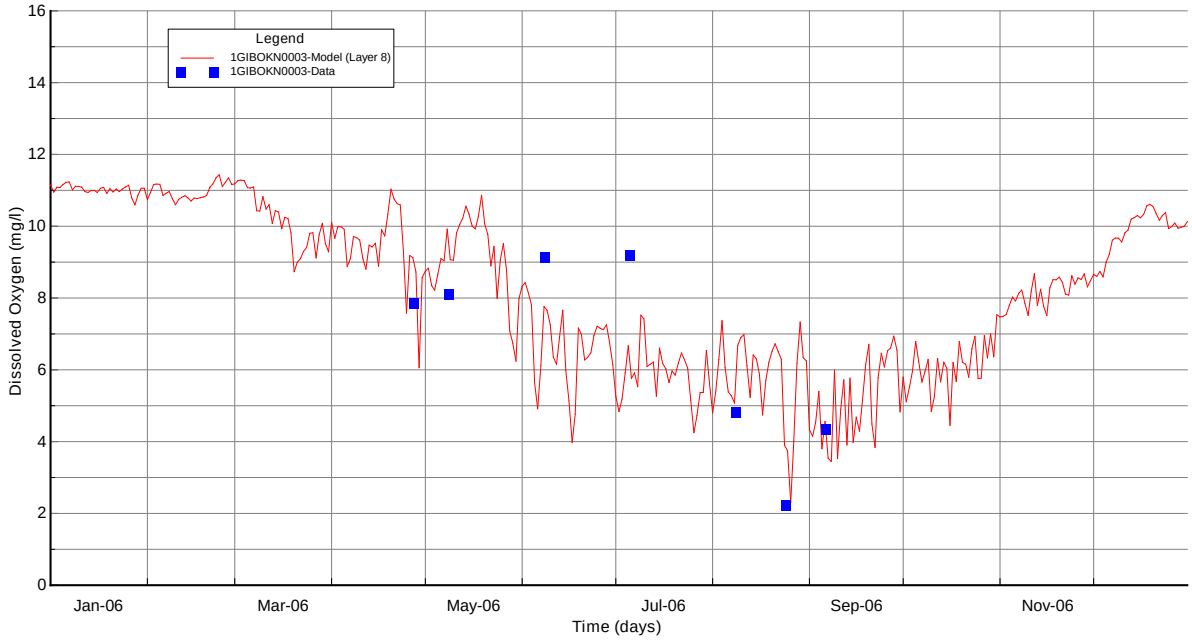

Figure B-38 Surface Layer Dissolved Oxygen Validation Plot at Station 1GIBOKN0003

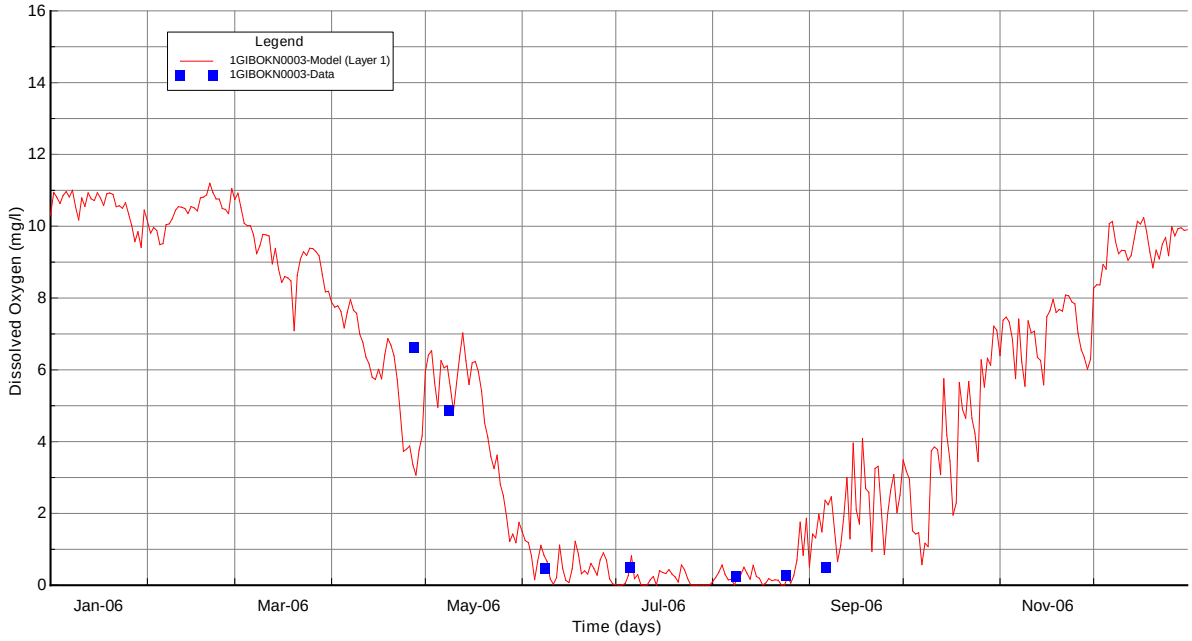

Figure B-39 Bottom Layer Dissolved Oxygen Validation Plot at Station 1GIBOKN0003

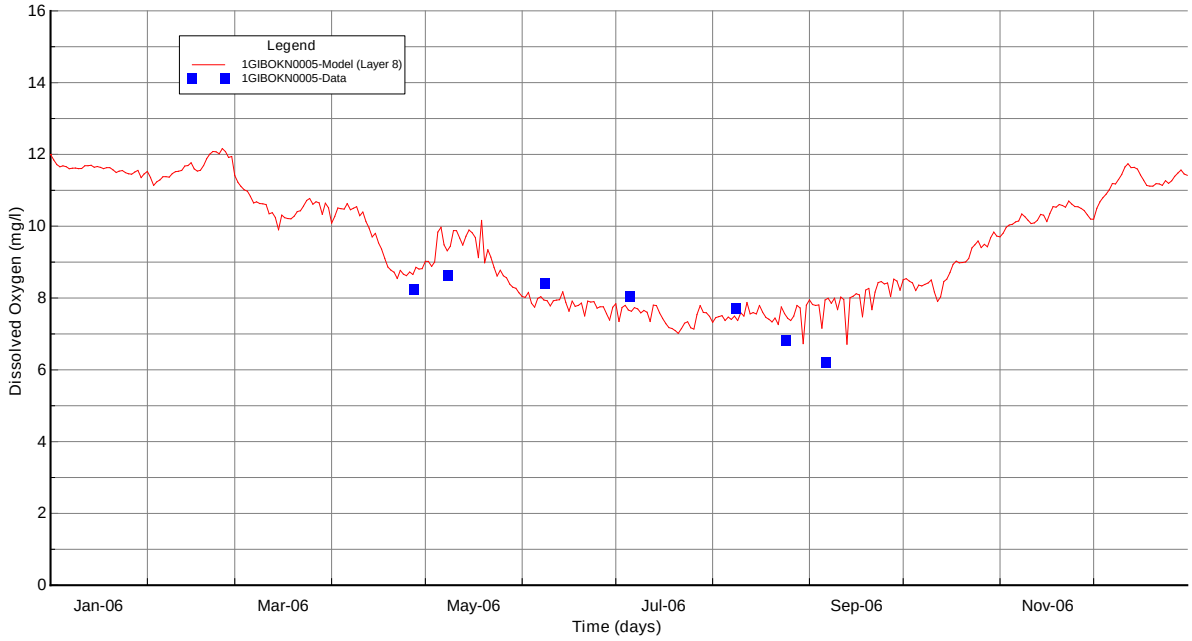

Figure B-40 Surface Layer Dissolved Oxygen Validation Plot at Station 1GIBOKN0005

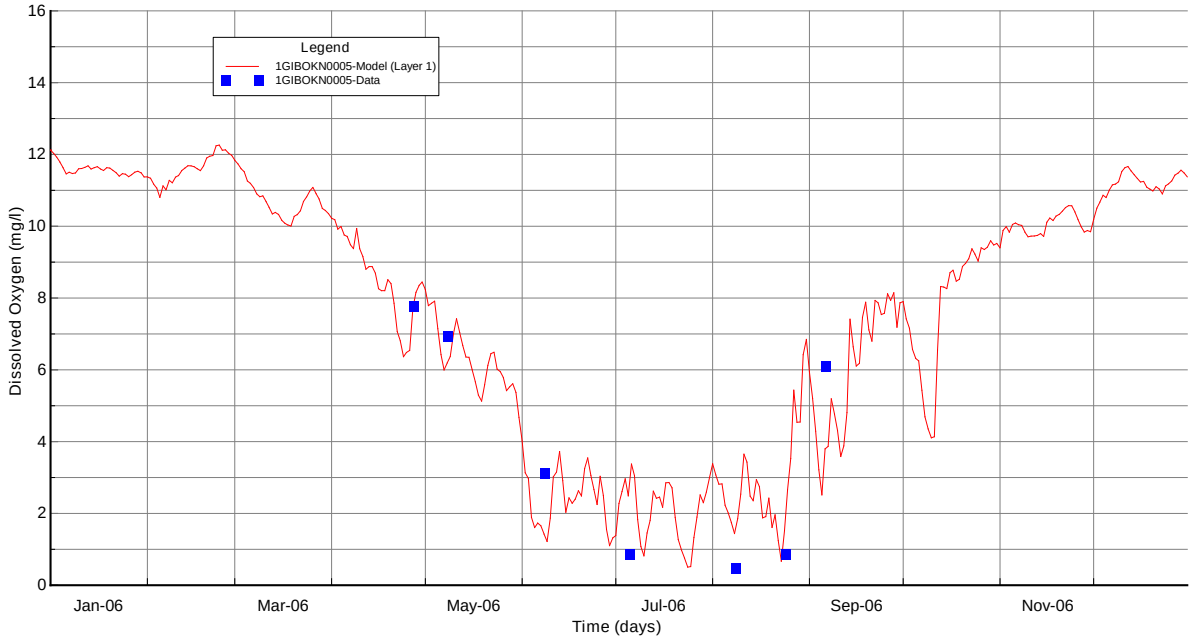

Figure B-41 Bottom Layer Dissolved Oxygen Validation Plot at Station 1GIBOKN0005

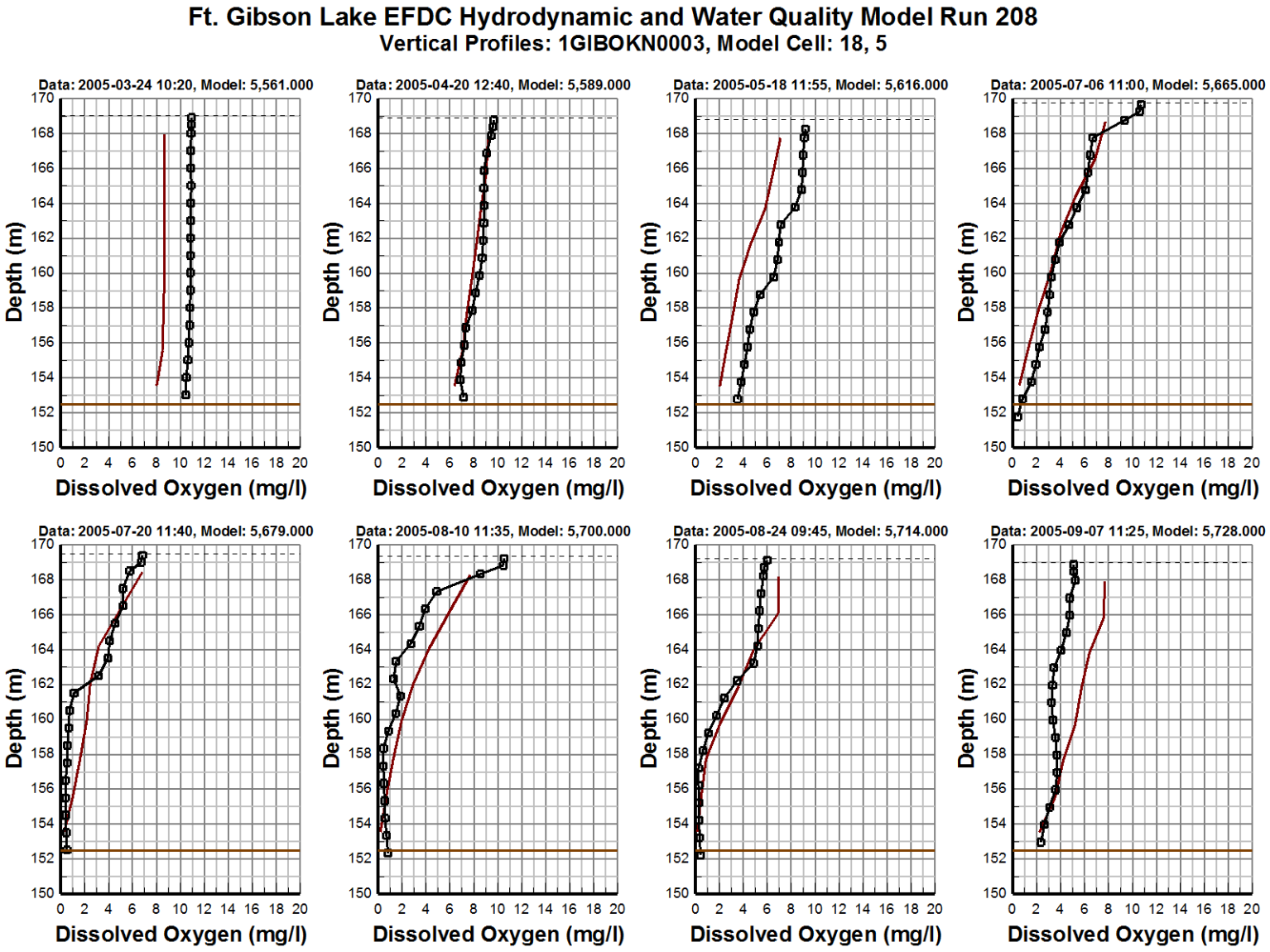

Figure B-42 Dissolved Oxygen Vertical Profile Comparison Plot at Station 1GIBOKN0003 (page 1-2)

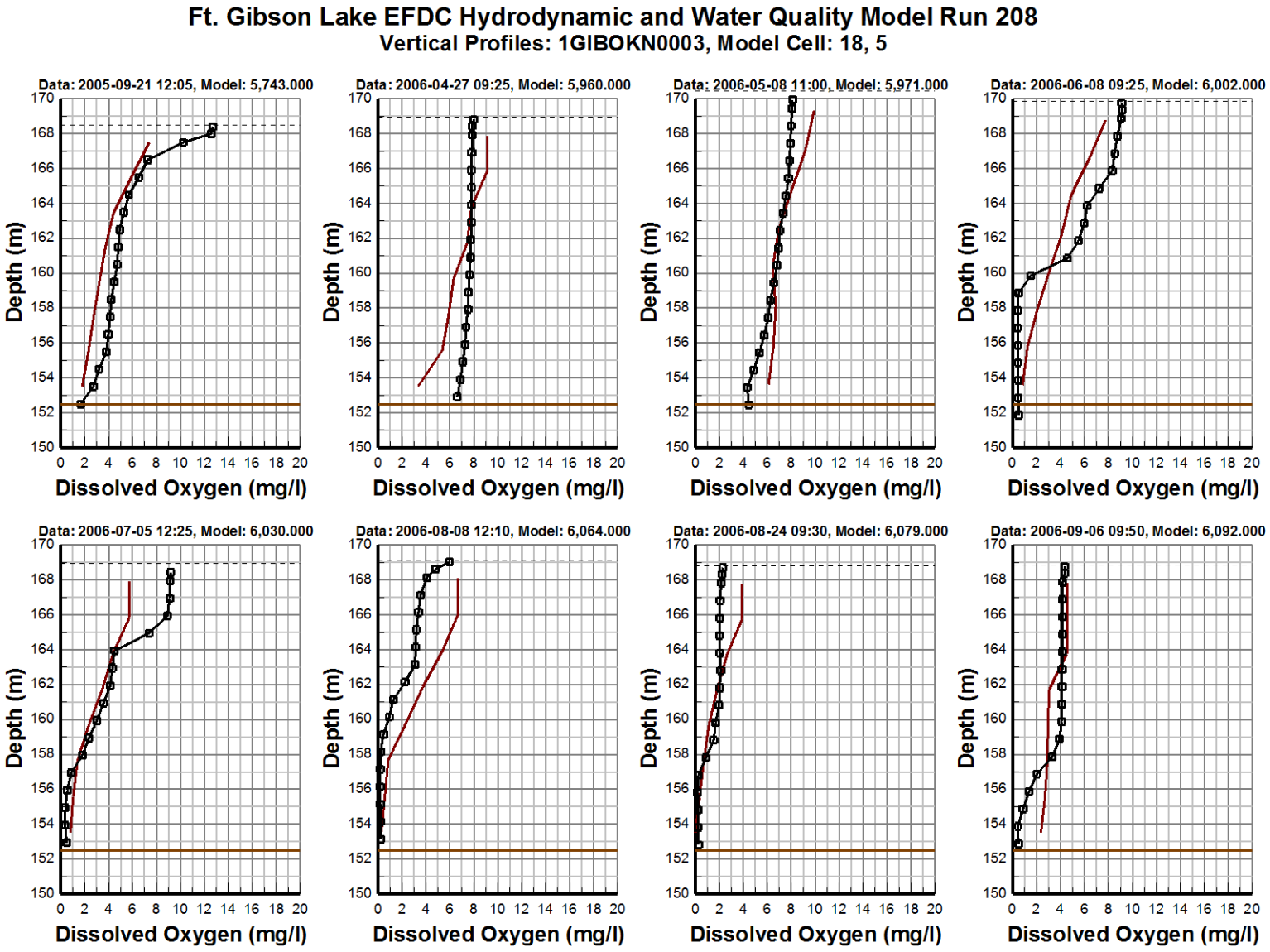

Figure B-42 Dissolved Oxygen Vertical Profile Comparison Plot at Station 1GIBOKN0003 (page 2-2)

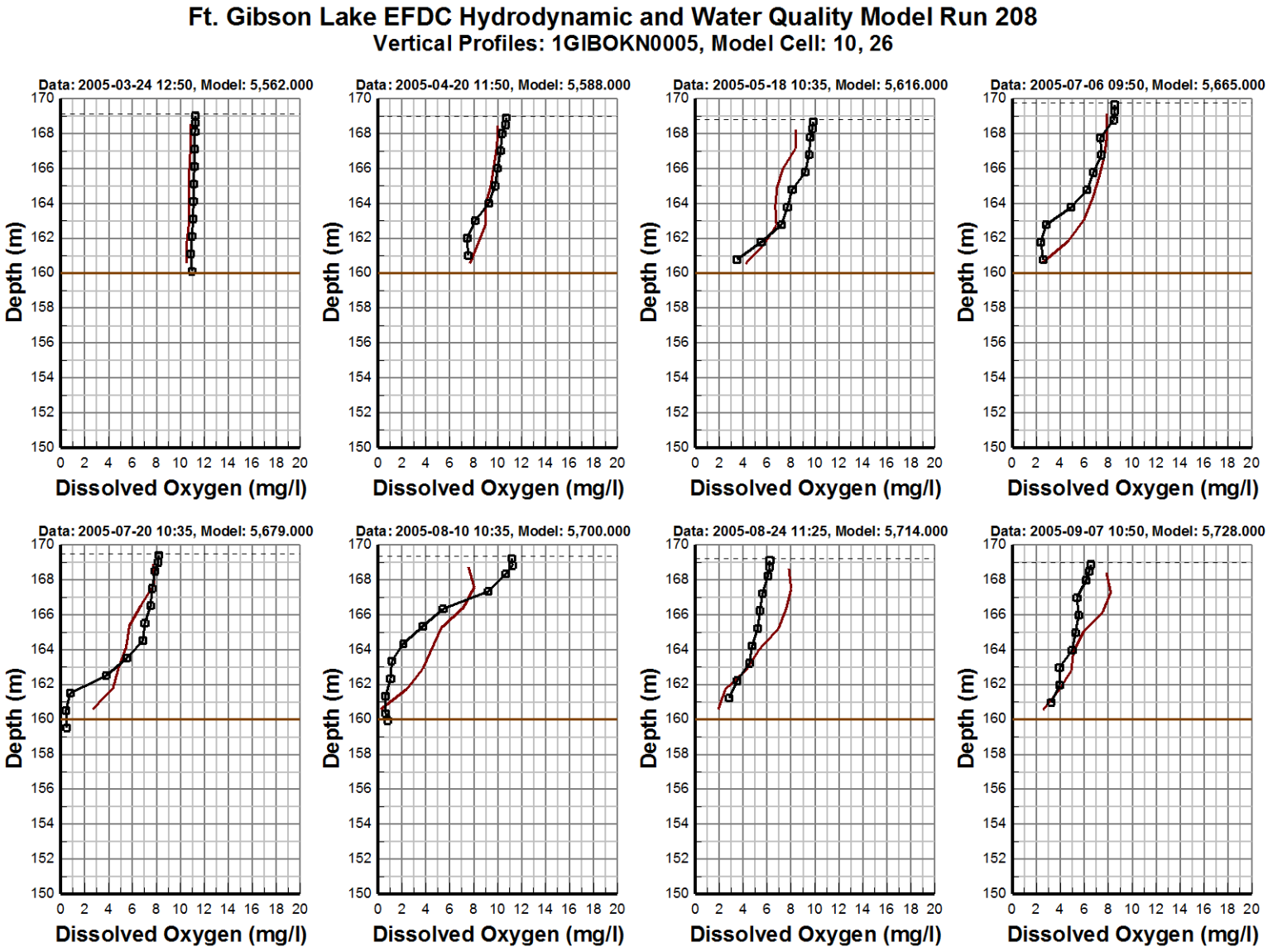

Figure B-43 Dissolved Oxygen Vertical Profile Comparison Plot at Station 1GIBOKN0005 (page 1-2)

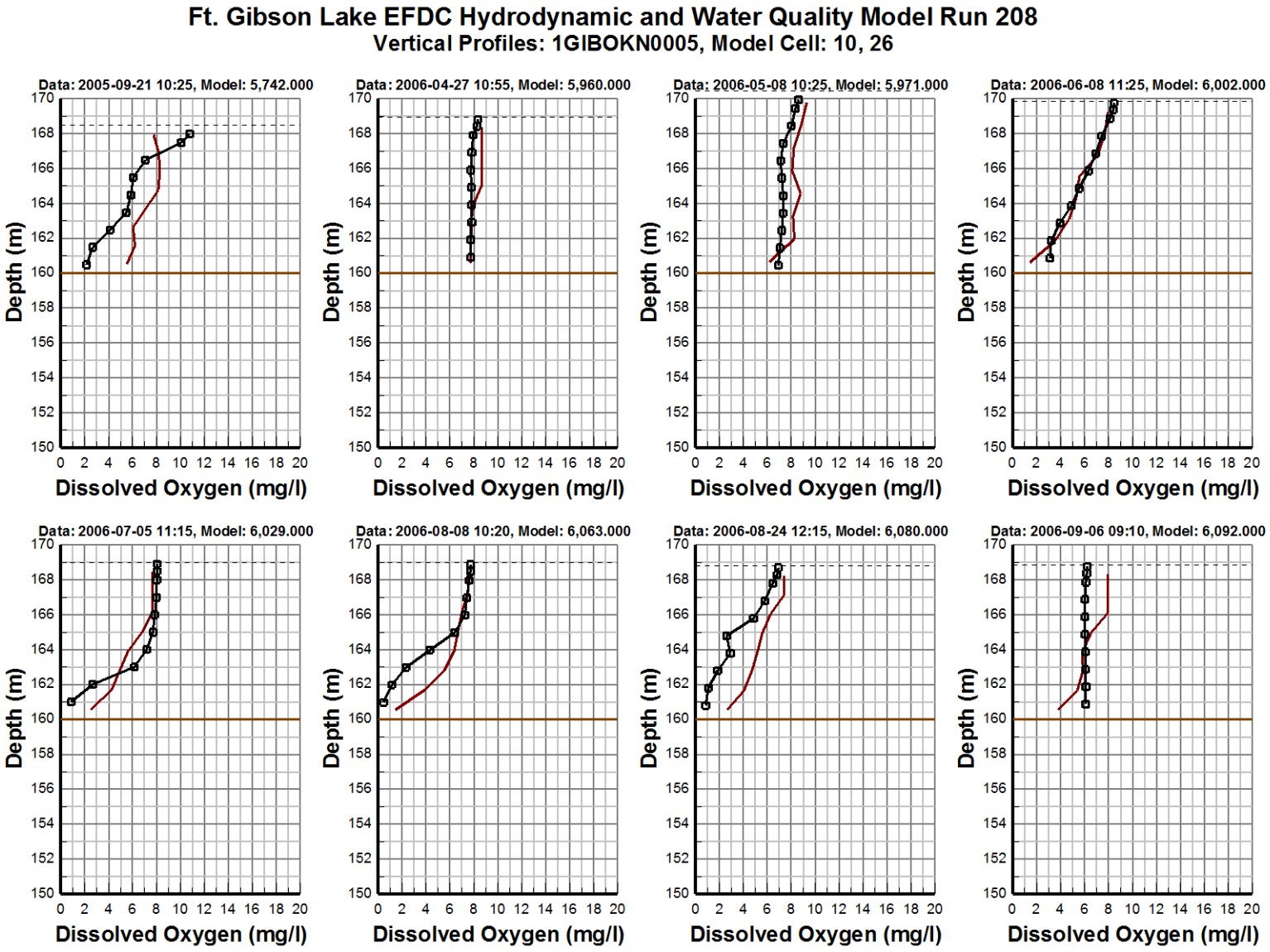

Figure B-43 Dissolved Oxygen Vertical Profile Comparison Plot at Station 1GIBOKN0005 (page 2-2)

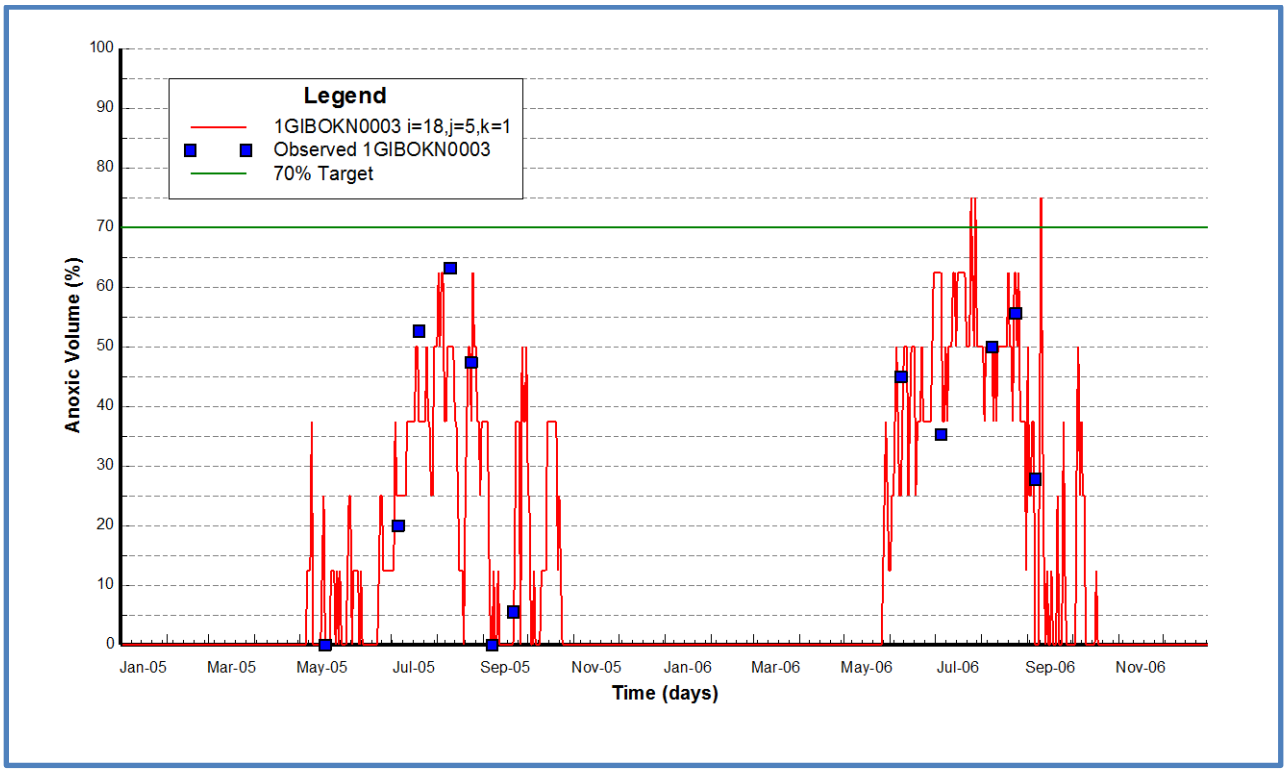

Figure B-44 Anoxic Volume at Station 1GIBOKN0003 (red line) and Observed Data

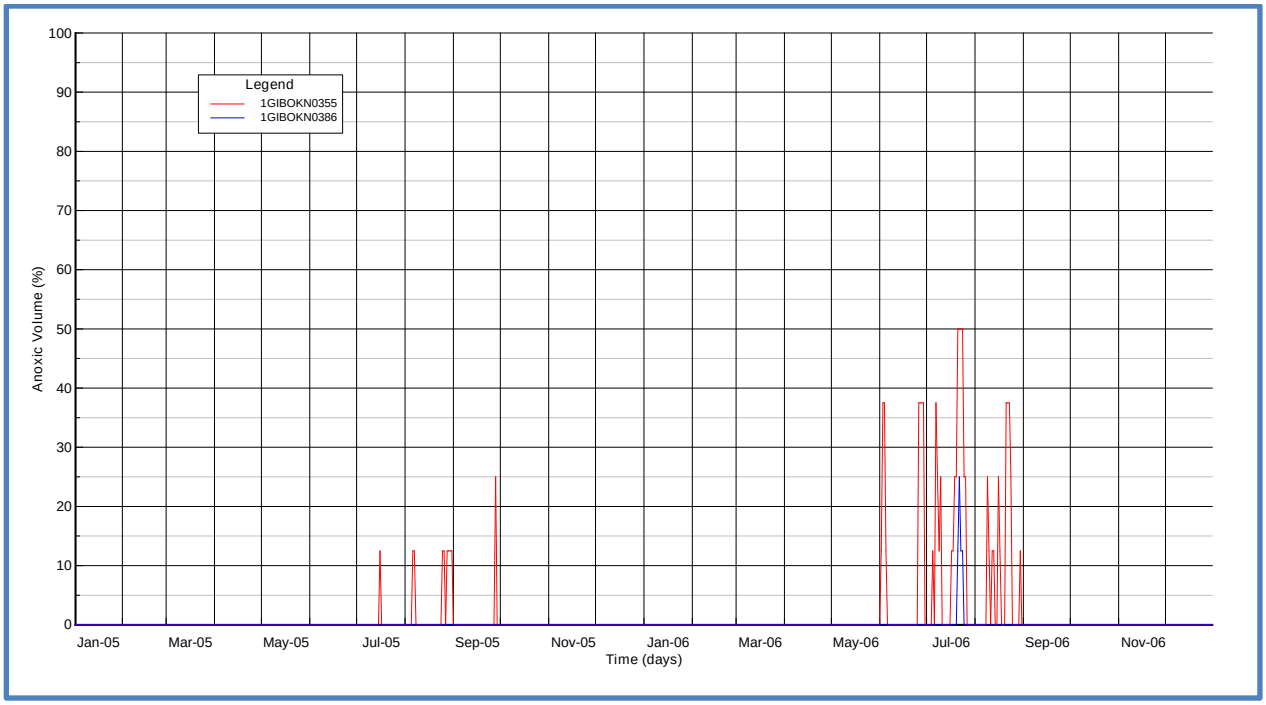

Figure B-45 Anoxic Volume at Stations 1GIBOKN0355 (red line) and 1GIBOKN0386 (blue line)

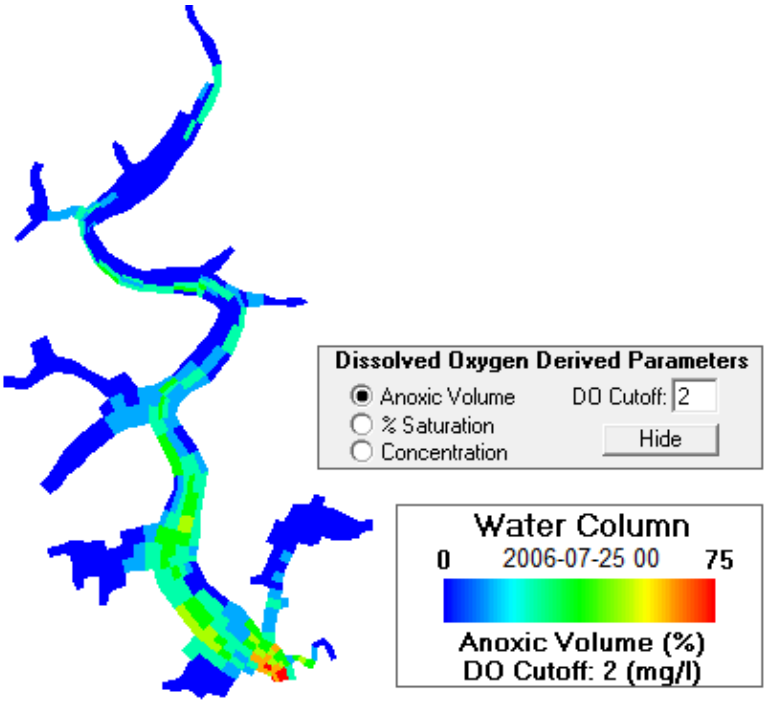

Figure B-46 Anoxic Volume of Fort Gibson Lake on July 25, 2006 00:00

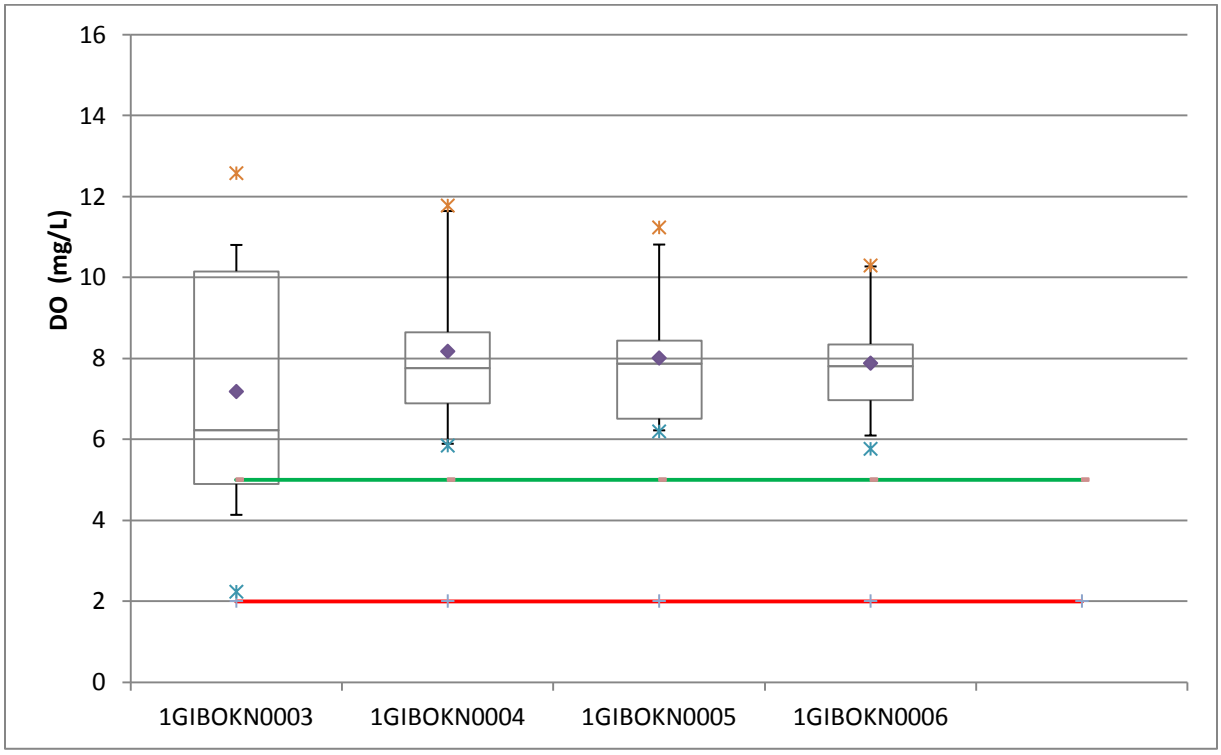

Figure B-47 Box-Whisker plots of the Fort Gibson Lake Observed Surface Layer DO for Summer Conditions by Monitoring Sites. Green line shows 5 mg/L water quality criteria for DO in the epilimnion and red line shows 2 mg/L anoxic cutoff value for DO.

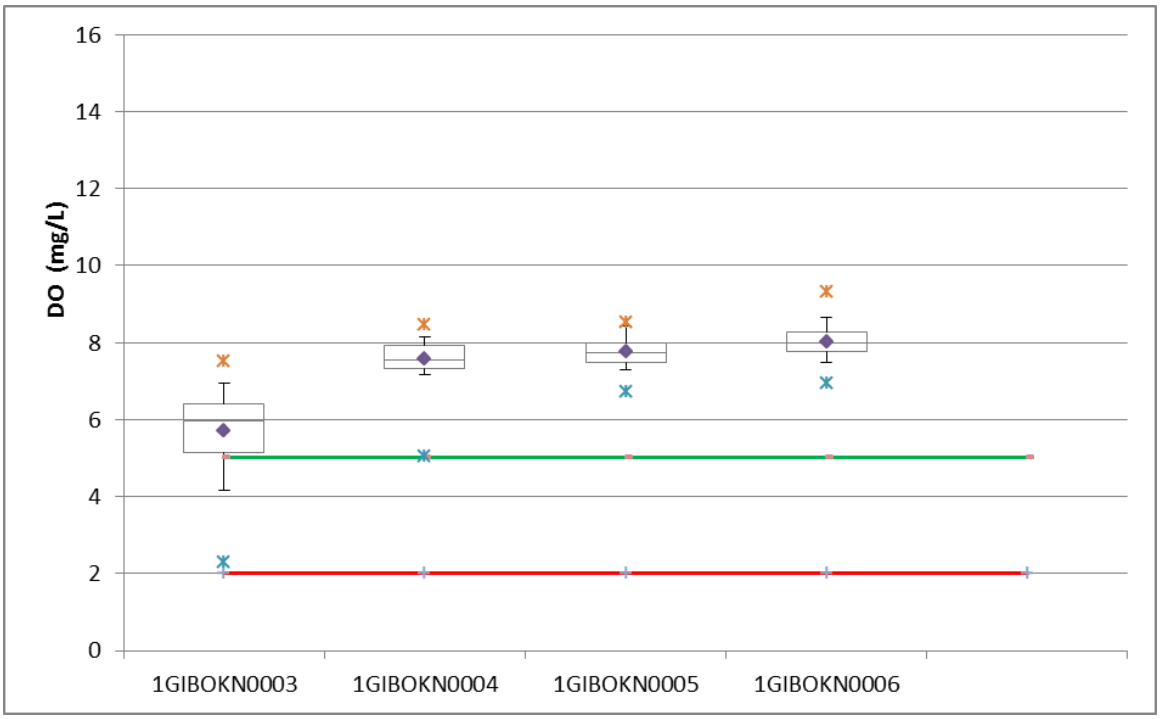

Figure B-48 Box-Whisker plots of the Fort Gibson Lake Model Validation Results for Surface Layer DO for Summer Conditions by Monitoring Sites. Green line shows 5 mg/L water quality criteria for DO in the epilimnion and red line shows 2 mg/L anoxic cutoff value for DO.

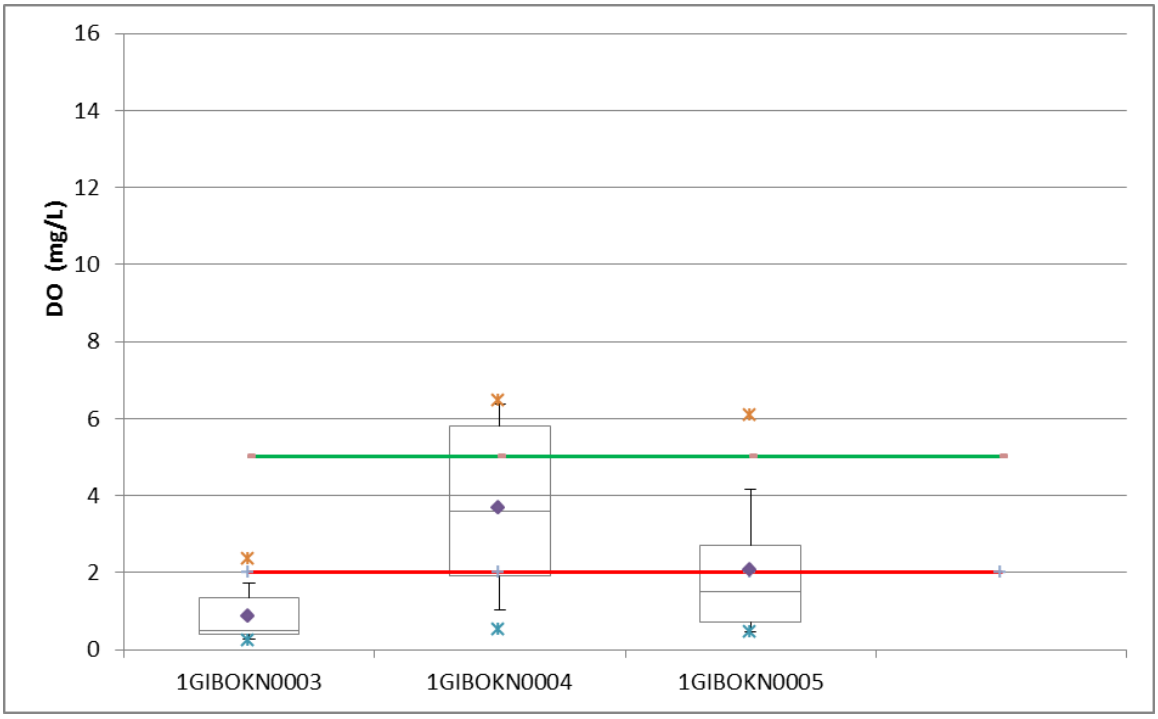

Figure B-49 Box-Whisker plots of the Fort Gibson Lake Observed Bottom Layer DO for Summer Conditions by Monitoring Sites. Green line shows 5 mg/L water quality criteria for DO in the epilimnion and red line shows 2 mg/L anoxic cutoff value for DO.

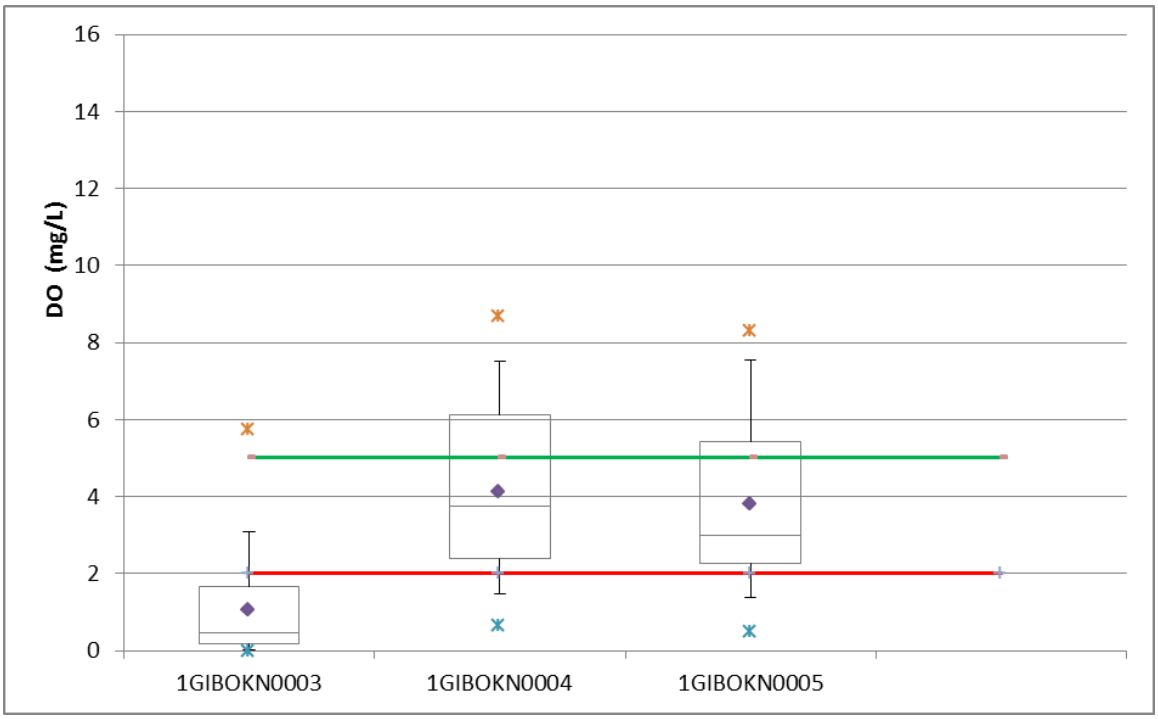

Figure B-50 Box-Whisker plots of the Fort Gibson Lake Model Validation Results

for Bottom Layer DO for Summer Conditions by Monitoring Sites. Green line shows 5 mg/L water quality criteria for DO in the epilimnion and red line shows 2 mg/L anoxic cutoff value for DO.

B-7.5 Algae Calibration and Validation

Modeled algae biomass results (as chlorophyll a) are presented for comparison to the observed data for the surface layer (k=8) and for the bottom layer (k=1). In the Fort Gibson Lake model, green algae were simulated to derive algae biomass for comparison to chlorophyll observations.

Chlorophyll a calibration plots at 1GIBOKN0003, 1GIBOKN0004, and 1GIBOKN0005 are given in Figure B-51 through Figure B-53. The summary statistics for model performance of chlorophyll a is given in Table B-15. As can be seen in these model-data plots, the model results are in good agreement with measured biomass for the calibration period. The EFDC simulated chlorophyll a concentrations follow the seasonal trend of observed chlorophyll a.

The calculated RMS errors ranged from 9.07 ug/L at the surface layer of station 1GIBOKN0003 to 13.95 ug/L at the surface layer of station 1GIBOKN0004 as shown in Table B-15. The calculated relative RMS errors ranged from 33.47% at the surface layer of station 1GIBOKN0006 to 58.88% at the surface layer of station 1GIBOKN0003. The model results are well within the defined model performance target of $\pm 100\%$ for algae.

The observed chlorophyll a data are only available for the calibration period. There was only one observation for chlorophyll a in the bottom layer which was located at station 1GIBOKN0004. The EFDC model replicated this observation well. The complete calibration and validation time series plots for all monitoring stations are given in APPENDIX C through APPENDIX D.

Table B-15 Summary Statistics of Chlorophyll a (µg/l)

Station ID	Layer	Starting	Ending	# Pairs	RMS (ug/l)	Rel RMS (%)	Data Average (ug/l)	Model Average (ug/l)
1GIBOKN0003	Layer 8	3/24/2005 10:20	9/21/2005 12:05	10	9.07	46.51	20.63	22.776
1GIBOKN0004	Layer 8	3/24/2005 10:50	9/21/2005 12:40	9	13.95	58.88	29.2	22.645
1GIBOKN0005	Layer 8	3/24/2005 12:25	9/21/2005 10:25	10	9.14	54.71	27.92	21.72
1GIBOKN0006	Layer 8	3/24/2005 9:25	9/21/2005 9:45	10	9.67	33.47	26.28	28.605

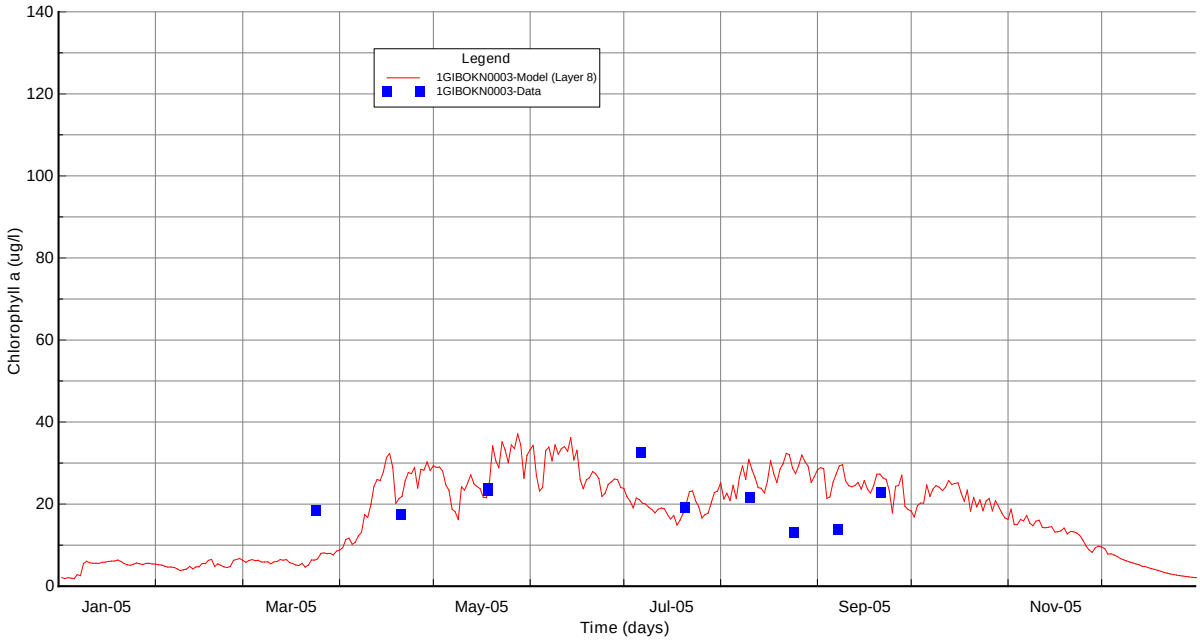

Figure B-51 Surface Layer Chlorophyll a Calibration Plot at Station 1GIBOKN0003

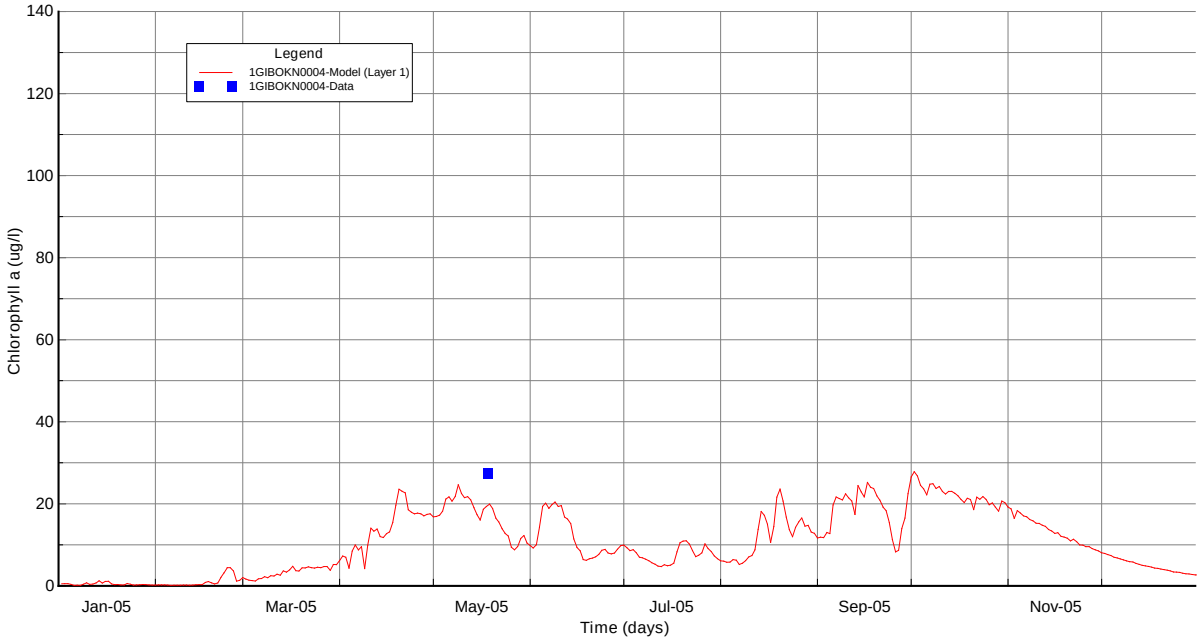

Figure B-52 Bottom Layer Chlorophyll a Calibration Plot at Station 1GIBOKN0004

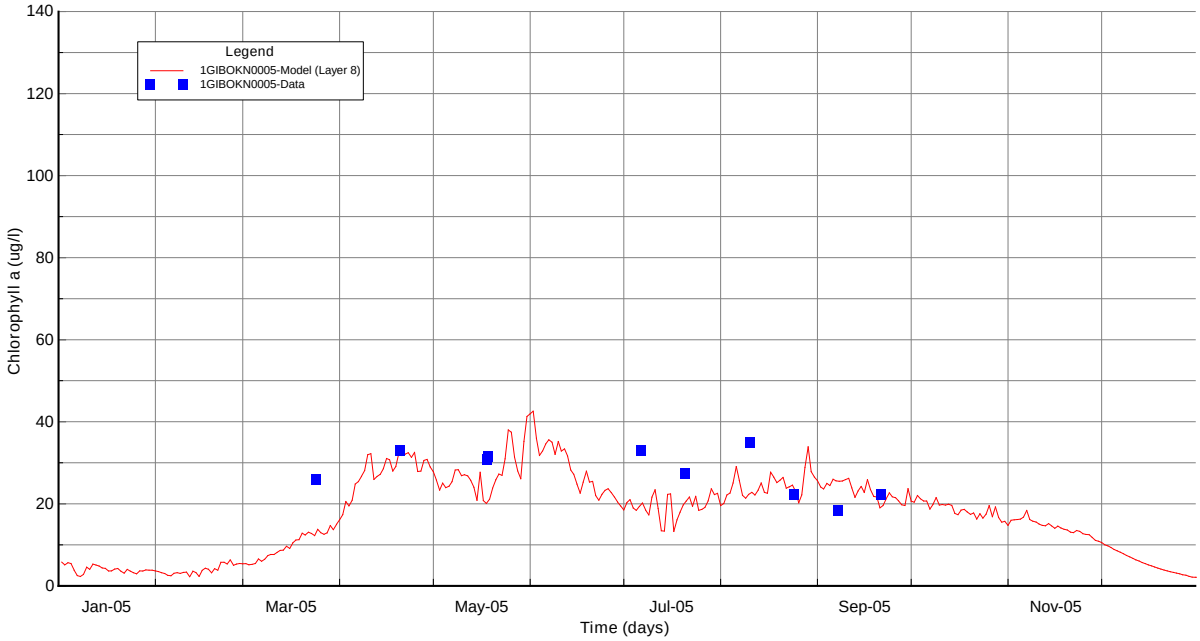

Figure B-53 Surface Layer Chlorophyll a Calibration Plot at Station 1GIBOKN0005

B-7.6 Trophic State Index Calibration and Validation

Lake Fort Gibson is classified as a Nutrient Limited Watershed (NLW) based on Carlson's (1977) Trophic State Index (TSI) because the chlorophyll-based TSI exceeds a numerical criteria value of 62. Carlson's equation for the chlorophyll-based TSI is given below for Chlorophyll-a as µg/L. Using this equation a chlorophyll-based TSI value of 62 is seen to correspond to 24 µg/L chlorophyll-a.

$$TSI = 9.81 * \ln(Chl) + 30.6 \qquad \text{Equation (3)}$$

Trophic state index results (as Chlorophyll a) are presented for comparison to the observed data for the surface layer (k=8) and for the bottom layer (k=1) (Carlson, 1977). Both the modeled and observed chlorophyll a data are processed to compute Carlson's TSI based on chlorophyll a.

TSI calibration plots at 1GIBOKN0003, 1GIBOKN0004, and 1GIBOKN0005 are given in Figure B-54 through Figure B-56. The summary statistics for model performance of TSI is given in Table B-16. As can be seen in these model-data plots, the model results are in good agreement with measured data for the calibration period.

The calculated RMS errors ranged from 3.7 at the surface layer of station 1GIBOKN0006 to 7.0 at the surface layer of station 1GIBOKN0004 shown in Table B-16. The calculated relative RMS errors ranged from 34.0% at the surface layer of station 1GIBOKN0006 to 90.5% at the surface layer of station 1GIBOKN0004 (Table B-16).

The observed chlorophyll a data are only available for the calibration period, so the TSI was compared only for the year of 2005. There was only one observation of chlorophyll a in the bottom layer, located at station 1GIBOKN0004. The modeled TSI value from EFDC was very close to the calculated TSI from the observed chlorophyll a concentration. The complete calibration and validation time series plots for all monitoring stations are given in APPENDIX C through APPENDIX D.

Table B-16 Summary Statistics of Trophic State Index (TSI)

Station ID	Layer	Starting	Ending	# Pairs	RMS	Rel RMS (%)	Data Average	Model Average
1GIBOKN0003	Layer 8	3/24/2005 10:20	9/21/2005 12:05	10	5.0	56.6	59.9	60.4
1GIBOKN0004	Layer 8	3/24/2005 10:50	9/21/2005 12:40	9	7.0	90.5	63.4	60.1
1GIBOKN0005	Layer 8	3/24/2005 12:25	9/21/2005 10:25	10	4.0	63.2	63.1	60.5
1GIBOKN0006	Layer 8	3/24/2005 9:25	9/21/2005 9:45	10	3.7	34.0	62.2	63.1

The summary statistics of the surface layer TSI for both observation and EFDC calibration results are also shown in the box-whisker plots (Figure B-57 and Figure B-58). Fort Gibson Lake is classified as a Nutrient Limited Watershed (NLW) based on Carlson's (1977) Trophic State Index (TSI) for chlorophyll exceeding a numerical value of 62.

As shown in Figure B-57, the 50th percentile of the surface layer TSI observations for all stations except 1GIBOKN0003 are greater than 62 and are thus are not in compliance with water quality criteria. At station 1GIBOKN0003, even the 90th percentile of the surface layer TSI is lower than 62. As shown in Figure B-58, the 90th percentile of the surface layer TSI of EFDC calibration results for all stations are greater than or equal to 62.

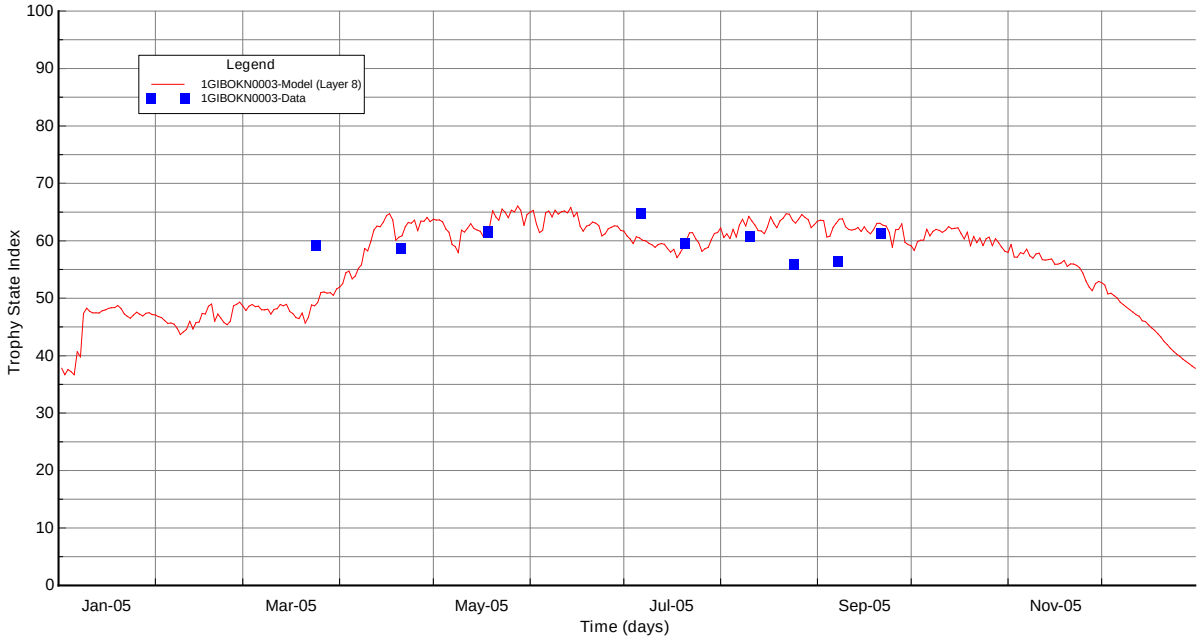

Figure B-54 Surface TSI Calibration Plot at Station 1GIBOKN0003

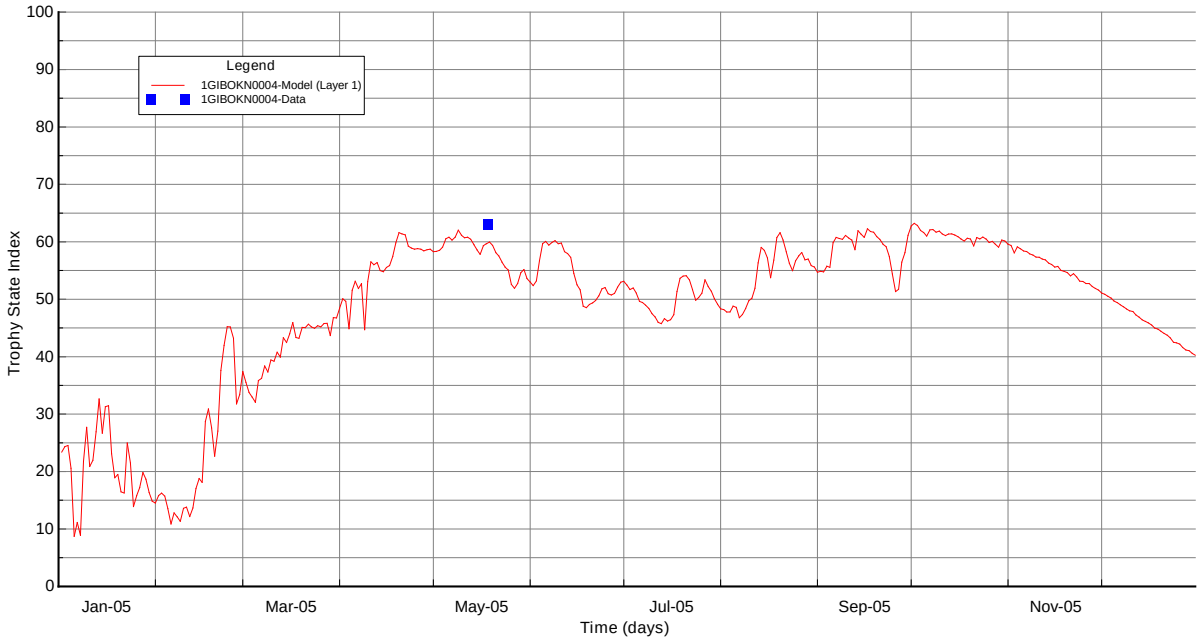

Figure B-55 Bottom TSI Calibration Plot at Station 1GIBOKN0004

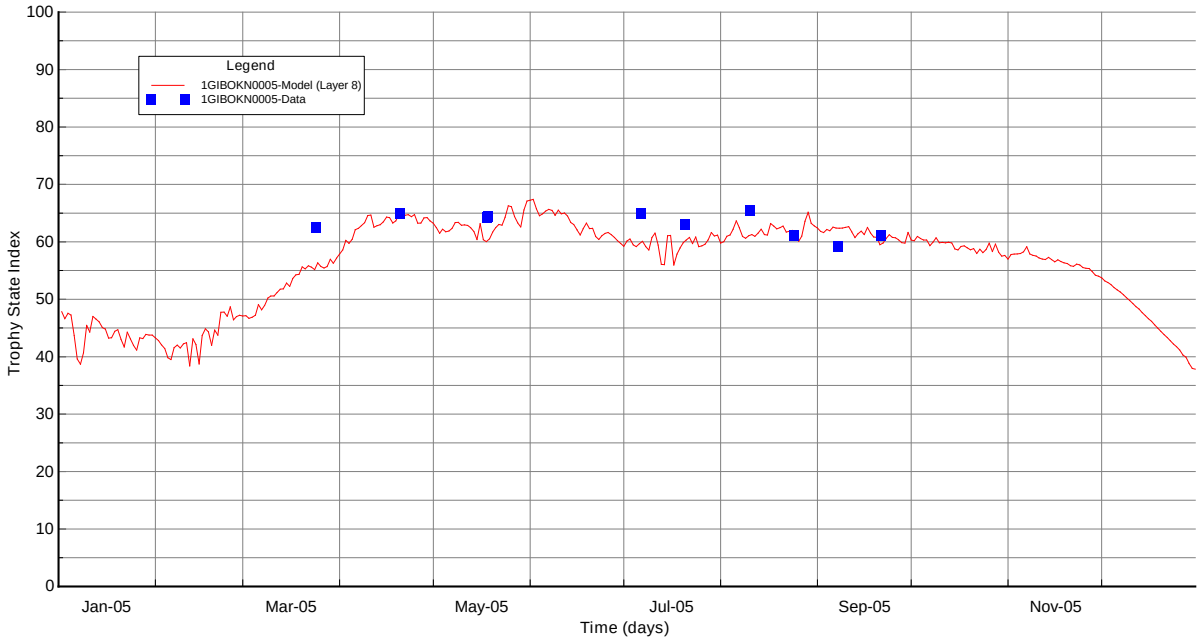

Figure B-56 Surface TSI Calibration Plot at Station 1GIBOKN0005

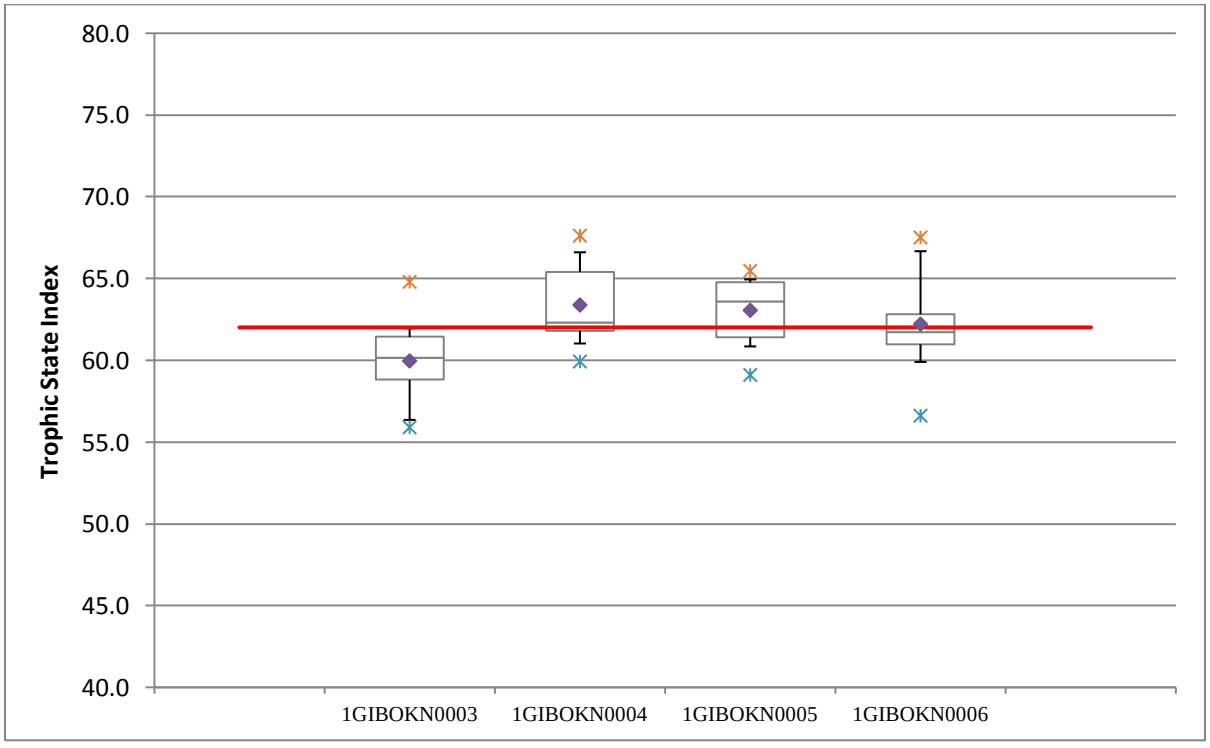

Figure B-57 Box-Whisker plots of the Fort Gibson Lake Observed Surface Layer TSI

by Monitoring Sites. Redline shows 62 water quality criteria for TSI.

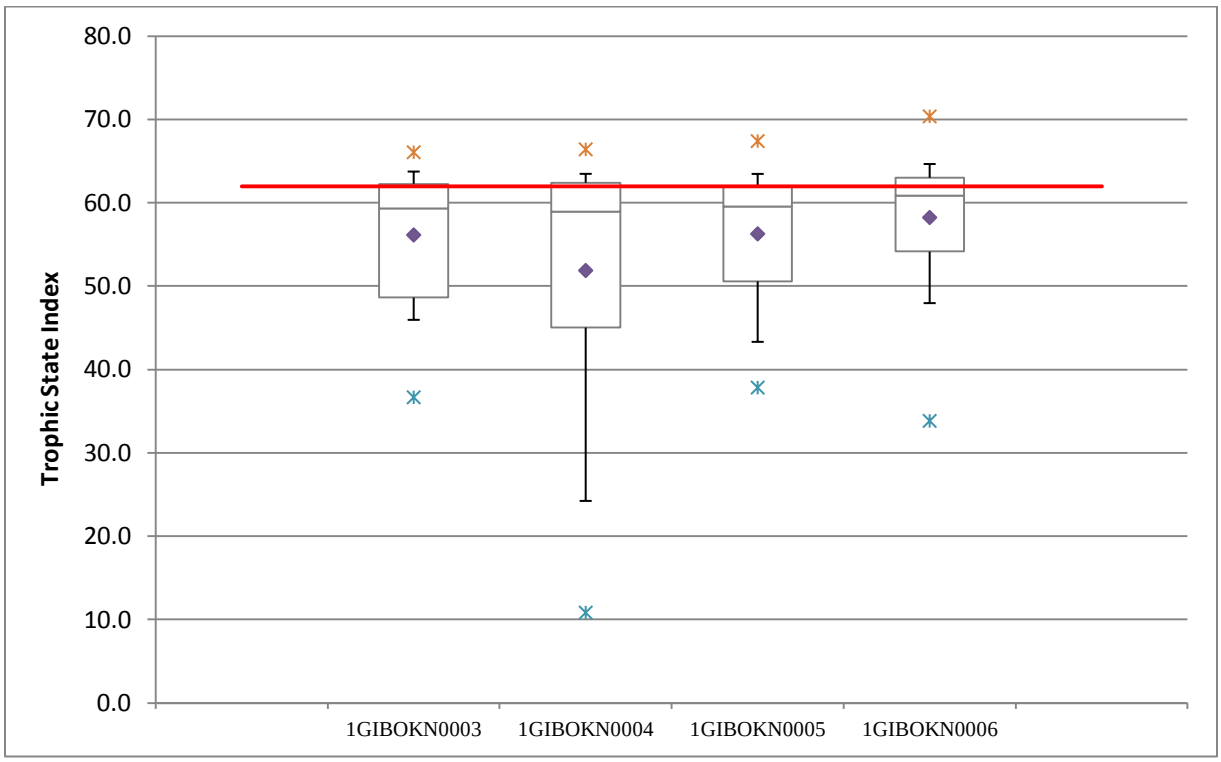

Figure B-58 Box-Whisker plots of the Fort Gibson Lake EFDC Calibration Results

of Surface Layer TSI by Monitoring Sites. Redline shows 62 water quality criteria for TSI.

B-7.7 Organic Carbon Calibration and Validation

Total organic carbon (TOC) model results are presented for comparison to the observed data for the surface layer (k=8) and bottom layer (k=1)**.** In the EFDC model**,** TOC is simulated by three forms: dissolved organic carbon, labile organic carbon, and refractory organic carbon. However, the observed data are only available in the form of TOC.

Total organic carbon calibration plots at 1GIBOKN0003 and 1GIBOKN0005 are given in Figure B-59 through Figure B-62. Total organic carbon validation plots at 1GIBOKN0003 and 1GIBOKN0005 are given in Figure B-63 through Figure B-66. The summary statistics for model performance of TOC are given in Table B-17. As can be seen in these model-data plots, the model results are in good agreement with the measured data for both calibration and validation periods.

The calculated RMS errors ranged from 0.72 mg/L at the bottom layer of station 1GIBOKN0004 to 1.16 mg/L at the surface layer of station 1GIBOKN0006 as shown in Table B-17, indicating very good model performance. The calculated relative RMS errors ranged from 78.66% at the surface layer of station 1GIBOKN0003 to 120.43% at the surface layer of station 1GIBOKN0006 (Table B-17). The complete calibration and validation time series plots for all monitoring stations are given in APPENDIX C through APPENDIX D.

The relatively higher values of the relative RMS error of TOC is caused by the small variations in the observed TOC data. For example, at the surface layer of station 1GIBOKN0004, the largest relative RMS

error of TOC is 120.43%. The observed TOC data at this station range only from 2.99 to 3.88 mg/L, which caused the relatively higher value of relative RMS error based on Equation (2). Model performance targets were not specifically identified for organic carbon in the QAPP for this project.

Table B-17 Summary Statistics of TOC (mg/l)

Station ID	Layer	Starting	Ending	# Pairs	RMS (mg/l)	Rel RMS	Data Average	Model Average
1GIBOKN0003	Layer 8	3/24/2005 10:20	8/24/2006 9:31	16	0.79	78.66	3.602	3.874
1GIBOKN0003	Layer 1	3/24/2005 10:20	8/24/2006 9:30	12	0.85	98.47	3.518	3.216
1GIBOKN0004	Layer 8	3/24/2005 10:50	8/24/2006 10:40	15	0.82	88.84	3.613	3.977
1GIBOKN0004	Layer 1	3/24/2005 10:50	9/21/2005 12:40	9	0.72	81.26	3.394	3.397
1GIBOKN0005	Layer 8	3/24/2005 12:50	8/24/2006 12:15	15	1.05	109.34	3.687	4.186
1GIBOKN0005	Layer 1	3/24/2005 12:50	8/24/2006 12:15	15	0.85	105.74	3.569	3.637
1GIBOKN0006	Layer 8	3/24/2005 9:25	8/24/2006 13:05	16	1.16	120.43	3.646	4.225

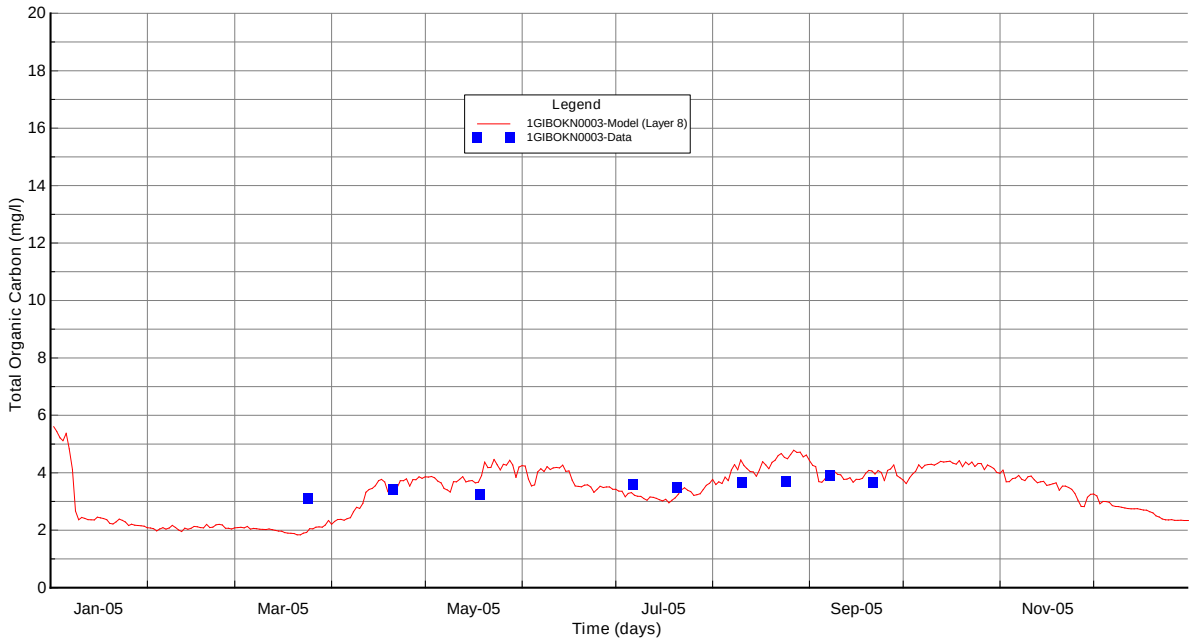

Figure B-59 Surface Layer TOC Calibration Plots at Station 1GIBOKN0003

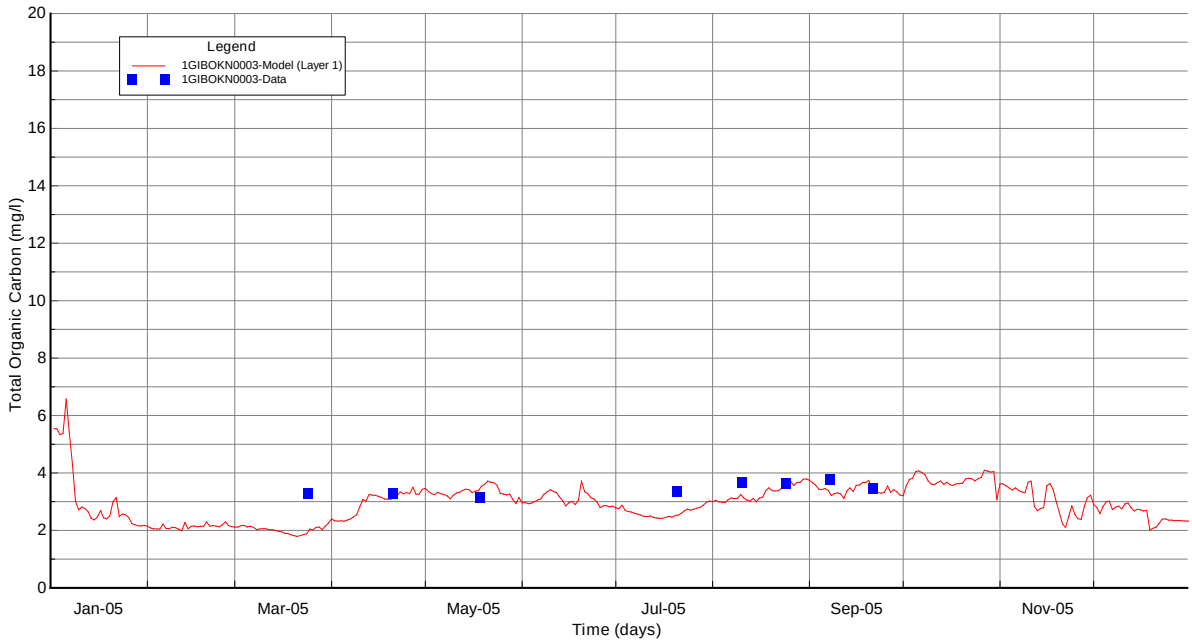

Figure B-60 Bottom Layer TOC Calibration Plots at Station 1GIBOKN0003

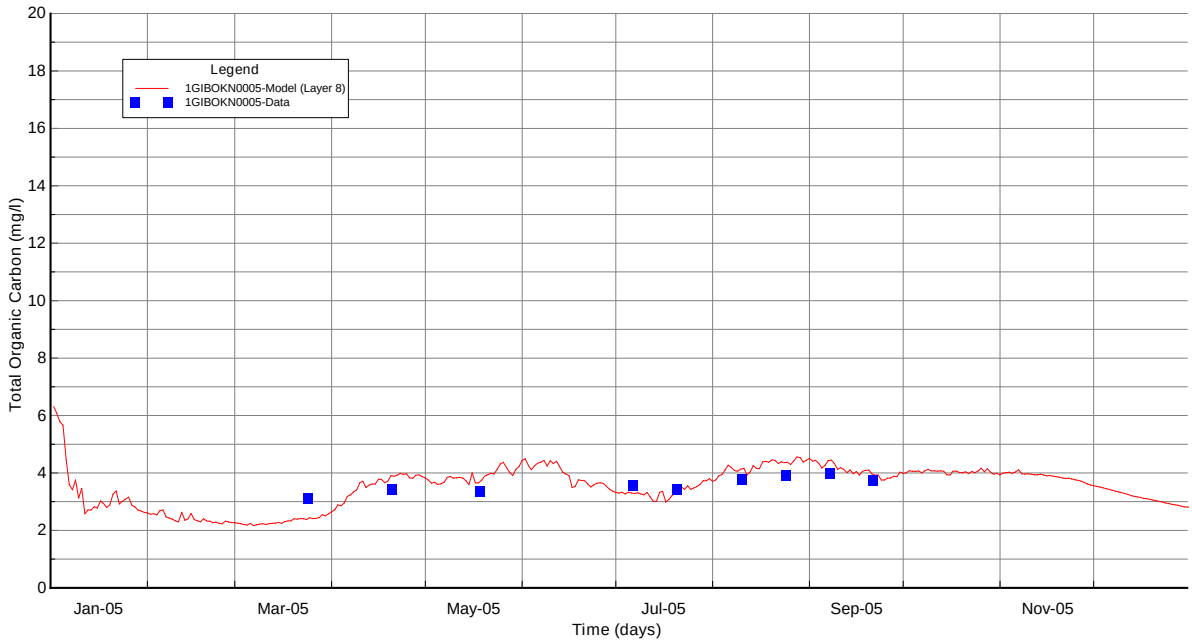

Figure B-61 Surface Layer TOC Calibration Plots at Station 1GIBOKN0005

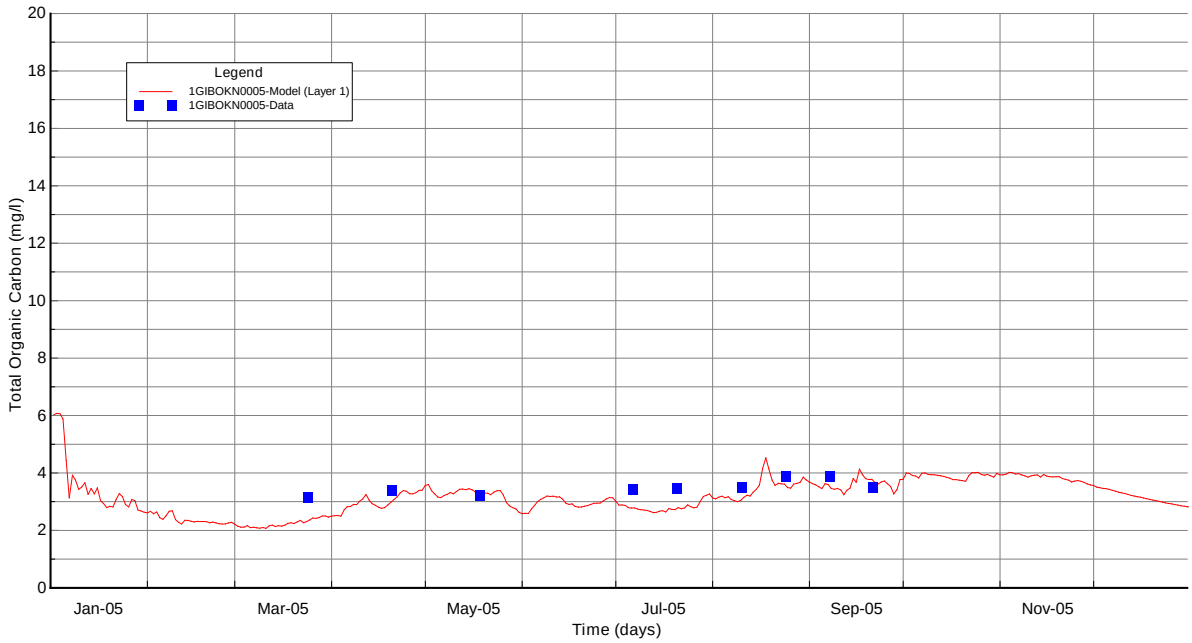

Figure B-62 Bottom Layer TOC Calibration Plots at Station 1GIBOKN0005

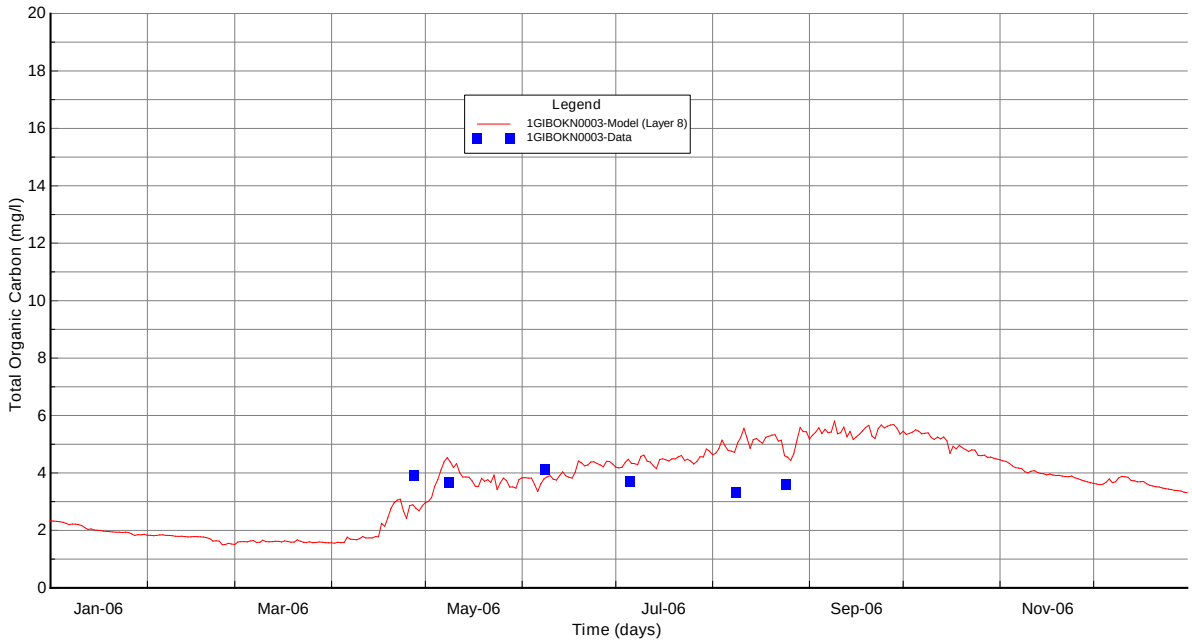

Figure B-63 Surface Layer TOC Validation Plots at Station 1GIBOKN0003

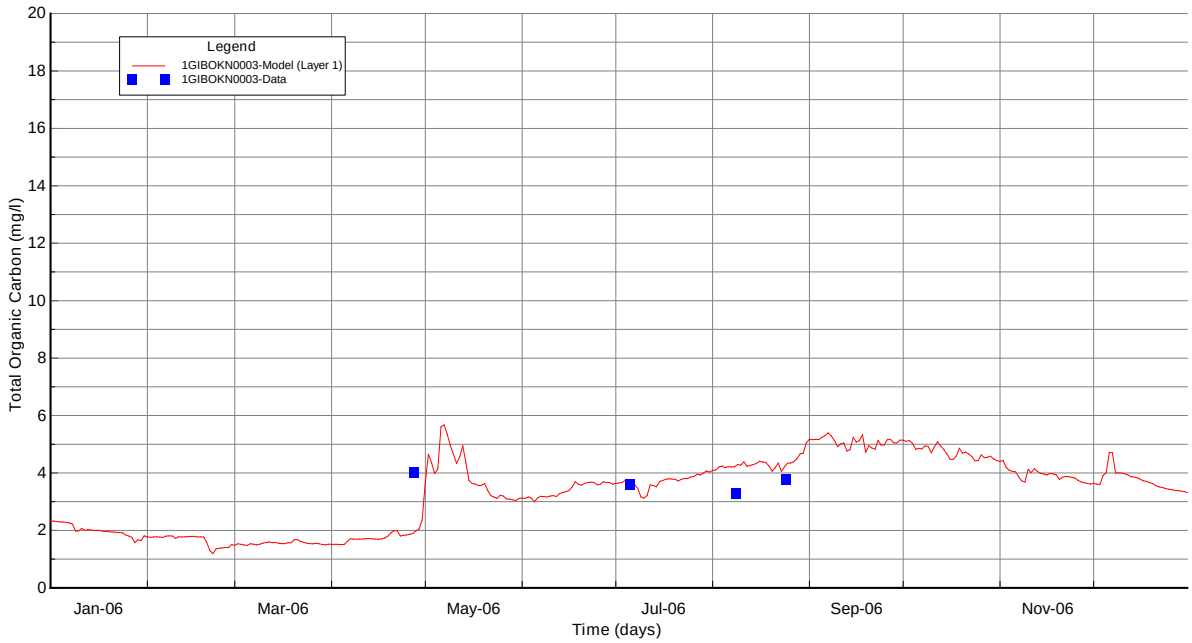

Figure B-64 Bottom Layer TOC Validation Plots at Station 1GIBOKN0003

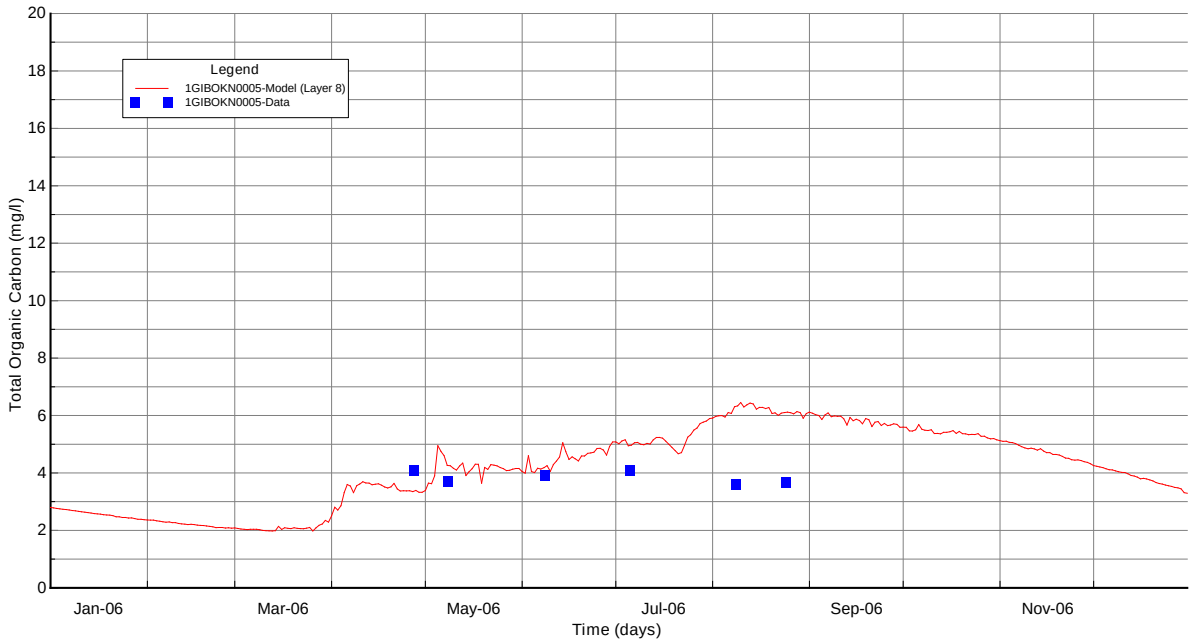

Figure B-65 Surface Layer TOC Validation Plots at Station 1GIBOKN0005

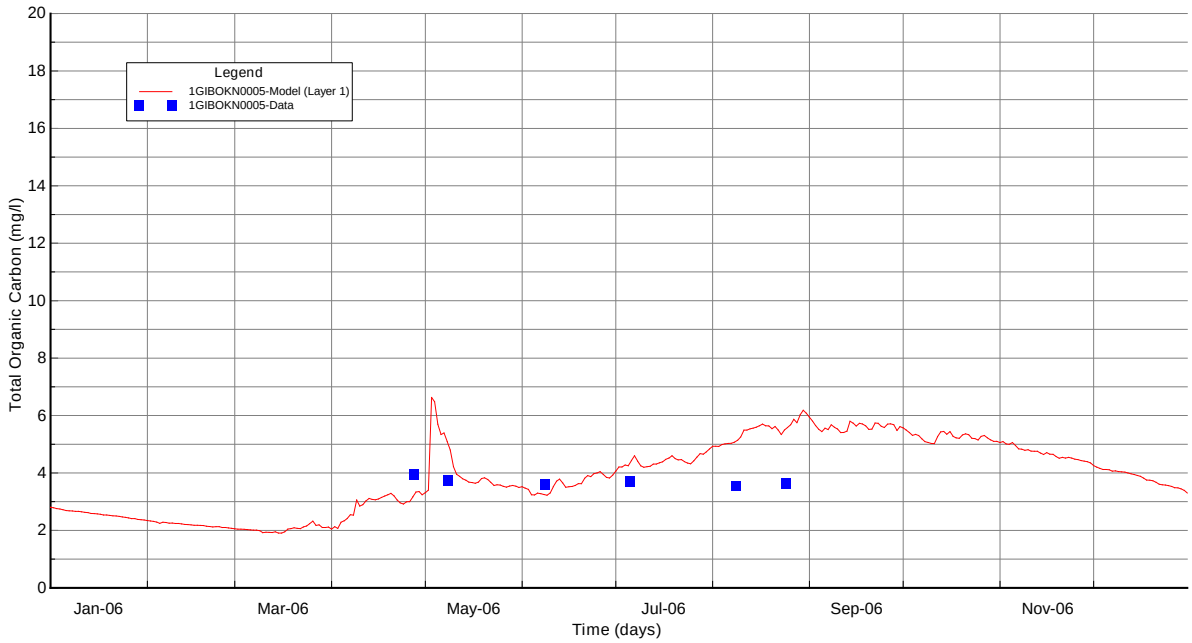

Figure B-66 Bottom Layer TOC Validation Plots at Station 1GIBOKN0005

B-7.8 Nitrogen

Ammonia-N (NH4), nitrite+nitrate-N (NO3), and total Kjeldahl nitrogen (TKN) model results are presented for comparison to the observed data for the surface layer (k=8) and bottom layer (k=1). The ammonium calibration and validation plots at 1GIBOKN0003 and 1GIBOKN0005 are given in Figure B-67 through Figure B-74. The nitrate calibration and validation plots at 1GIBOKN0003 and 1GIBOKN0005 are given in Figure B-75 through Figure B-82. The TKN calibration and validation plots at 1GIBOKN0003 and 1GIBOKN0005 are given in Figure B-83 through Figure B-90. As can be seen in the model-data plots, the model results are in reasonable agreement with measured NH4, NO3, and TKN for both calibration and validation periods.

The summary statistics for model performance for ammonium, nitrate, and TKN are given in Table B-18 through Table B-20. In most of the cases, the model results for NH4, NO3, and TKN are within or close to the defined model performance target of $\pm 50\%$ for nutrients. The complete calibration and validation time series plots for all monitoring stations are given in APPENDIX C through APPENDIX D.

The calculated RMS errors of NH4 ranged from 0.046 mg/L at the surface layer of station 1GIBOKN0006 to 0.146 mg/L at the bottom layer of station 1GIBOKN0003 (Table B-18). The calculated relative RMS errors of NH4 ranged from 25.60% at the bottom layer of station 1GIBOKN0005 to 95.28% at the surface layer of station 1GIBOKN0004 (Table B-18).

The calculated RMS errors of NO3 ranged from 0.124 mg/L at the surface layer of station 1GIBOKN0004 to 0.196 mg/L at the bottom layer of station 1GIBOKN0003 (Table B-19). The calculated relative RMS errors of NO3 ranged from 15.15% at the surface layer of station 1GIBOKN0006 to 31.41% at the bottom layer of station 1GIBOKN0004 (Table B-19).

The calculated RMS errors of TKN ranged from 0.157 mg/L at the bottom layer of station 1GIBOKN0005 to 0.355 mg/L at the bottom layer of station 1GIBOKN0003 (Table B-20). The calculated relative RMS errors of TKN ranged from 34.80% at the bottom layer of station 1GIBOKN0005 to 81.97% at the surface layer of station 1GIBOKN0006 (Table B-20).

Table B-18 Summary Statistics of NH4 (mg/l)

Station ID	Layer	Starting	Ending	# Pairs	RMS (mg/l)	Rel RMS	Data Average	Model Average
1GIBOKN0003	Layer 8	3/24/2005 10:20	9/6/2006 9:50	17	0.092	45.79	0.085	0.122
1GIBOKN0003	Layer 1	3/24/2005 10:20	9/6/2006 9:50	13	0.146	26.47	0.237	0.202
1GIBOKN0004	Layer 8	3/24/2005 10:50	9/6/2006 10:21	17	0.095	95.28	0.062	0.105
1GIBOKN0004	Layer 1	3/24/2005 10:50	9/21/2005 12:40	9	0.081	38.74	0.087	0.134
1GIBOKN0005	Layer 8	3/24/2005 12:50	9/6/2006 9:10	16	0.073	61.17	0.06	0.08
1GIBOKN0005	Layer 1	3/24/2005 12:50	9/6/2006 9:10	16	0.054	25.60	0.149	0.162
1GIBOKN0006	Layer 8	3/24/2005 9:25	9/6/2006 8:40	17	0.046	32.86	0.062	0.037

Table B-19 Summary Statistics of NO3 (mg/l)

Station ID	Layer	Starting	Ending	# Pairs	RMS (mg/l)	Rel RMS (%)	Data Average (mg/l)	Model Average (mg/l)
1GIBOKN0003	Layer 8	3/24/2005 10:20	9/6/2006 9:50	17	0.167	18.33	0.161	0.12
1GIBOKN0003	Layer 1	3/24/2005 10:20	9/6/2006 9:50	13	0.196	22.52	0.247	0.21
1GIBOKN0004	Layer 8	3/24/2005 10:50	9/6/2006 10:21	17	0.124	19.99	0.073	0.085
1GIBOKN0004	Layer 1	3/24/2005 10:50	9/21/2005 12:40	9	0.185	31.41	0.161	0.22
1GIBOKN0005	Layer 8	3/24/2005 12:50	9/6/2006 9:10	16	0.134	17.93	0.102	0.083
1GIBOKN0005	Layer 1	3/24/2005 12:50	9/6/2006 9:10	16	0.154	19.94	0.121	0.18
1GIBOKN0006	Layer 8	3/24/2005 9:25	9/6/2006 8:40	17	0.136	15.15	0.161	0.155

Table B-20 Summary Statistics of TKN (mg/l)

Station ID	Layer	Starting	Ending	# Pairs	RMS (mg/l)	Rel RMS (%)	Data Average (mg/l)	Model Average (mg/l)
1GIBOKN0003	Layer 8	3/24/2005 10:20	9/6/2006 9:50	17	0.162	38.66	0.628	0.635
1GIBOKN0003	Layer 1	3/24/2005 10:20	9/6/2006 9:50	13	0.355	37.00	0.788	0.593
1GIBOKN0004	Layer 8	3/24/2005 10:50	9/6/2006 10:21	17	0.233	62.99	0.741	0.567
1GIBOKN0004	Layer 1	3/24/2005 10:50	9/21/2005 12:40	9	0.252	68.09	0.68	0.505
1GIBOKN0005	Layer 8	3/24/2005 12:50	9/6/2006 9:10	16	0.186	41.43	0.727	0.676
1GIBOKN0005	Layer 1	3/24/2005 12:50	9/6/2006 9:10	16	0.157	34.80	0.739	0.627
1GIBOKN0006	Layer 8	3/24/2005 9:25	9/6/2006 8:40	17	0.246	81.97	0.674	0.819

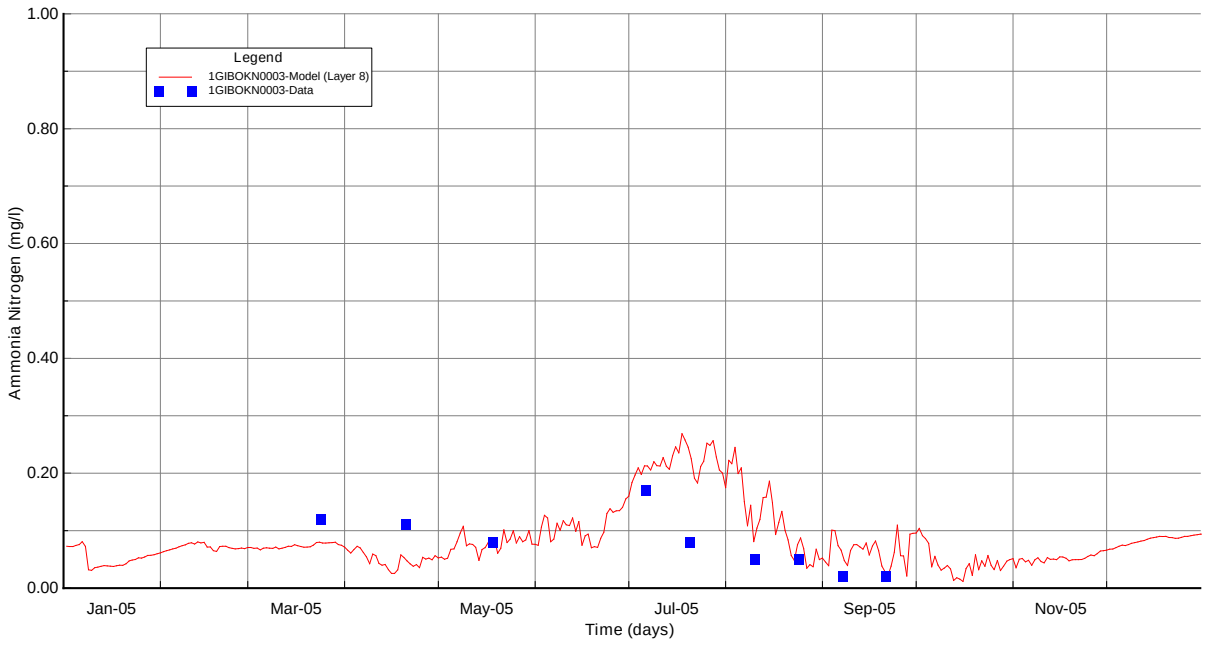

Figure B-67 Surface Layer NH4 Calibration Plots at Station 1GIBOKN0003

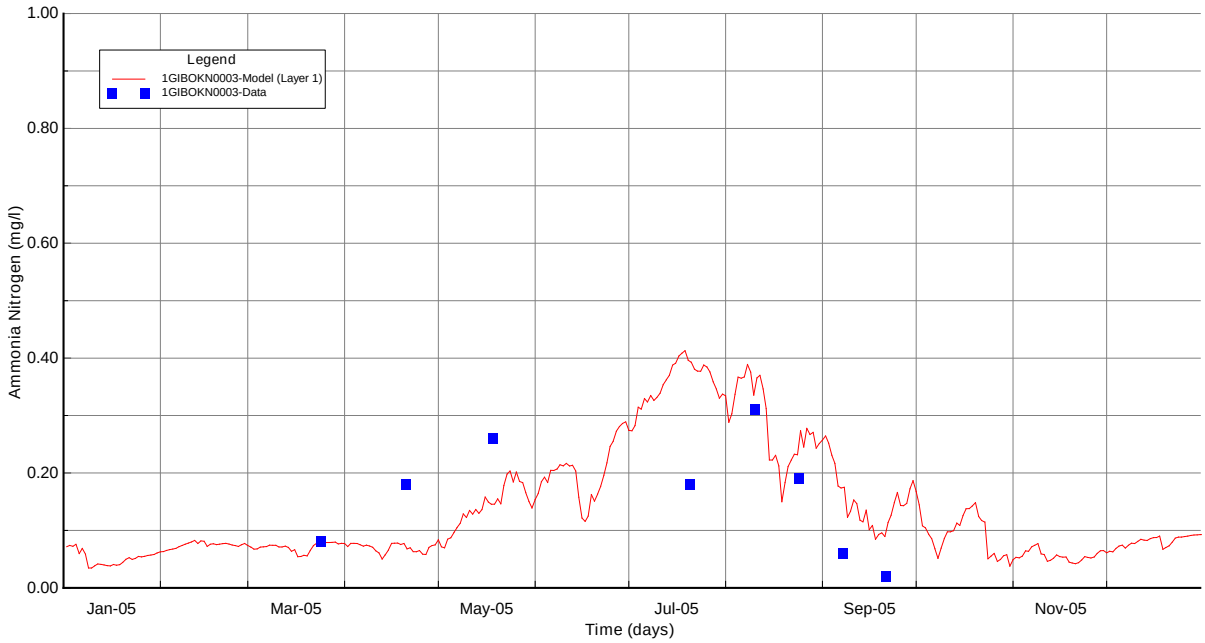

Figure B-68 Bottom Layer NH4 Calibration Plots at Station 1GIBOKN0003

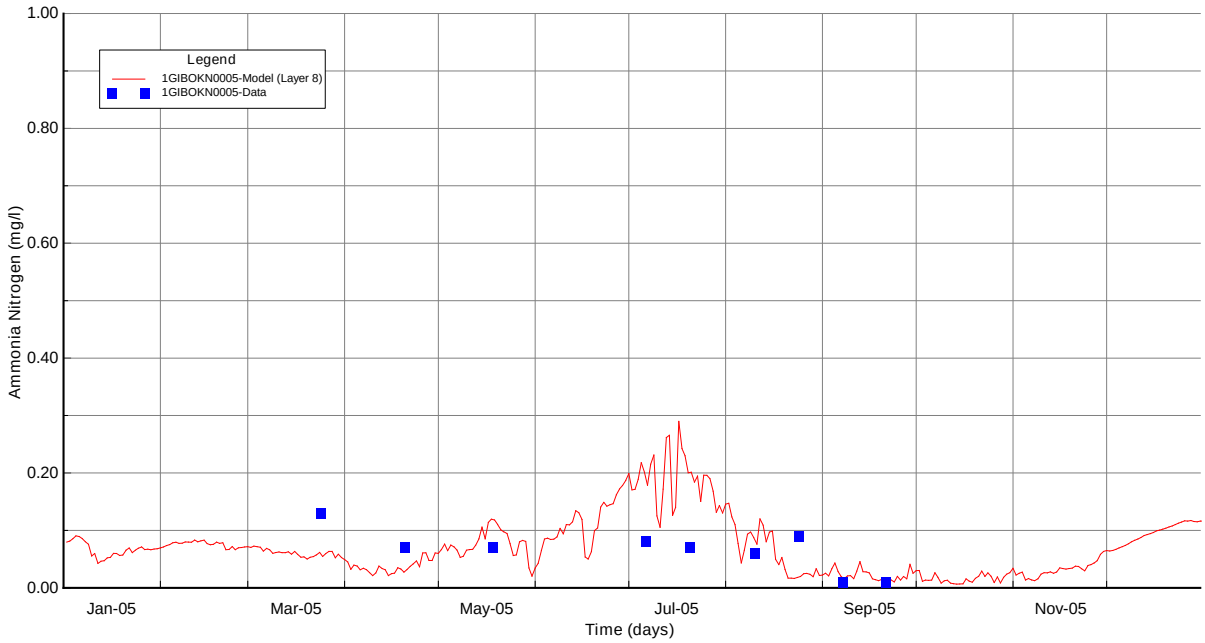

Figure B-69 Surface Layer NH4 Calibration Plots at Station 1GIBOKN0005

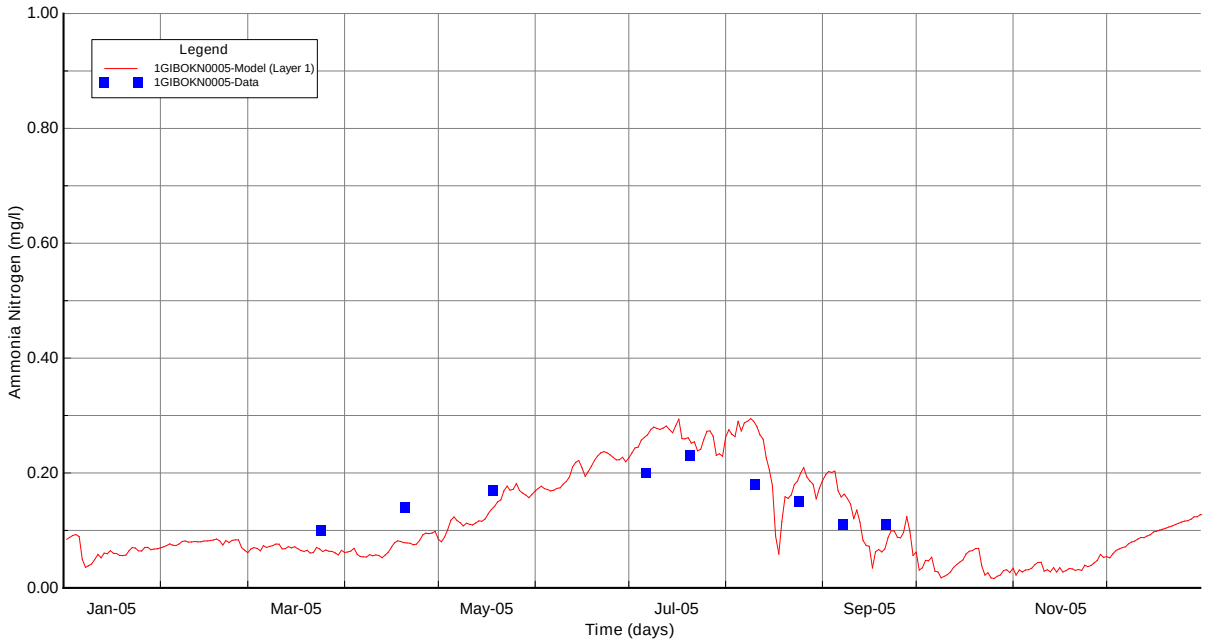

Figure B-70 Bottom Layer NH4 Calibration Plots at Station 1GIBOKN0005

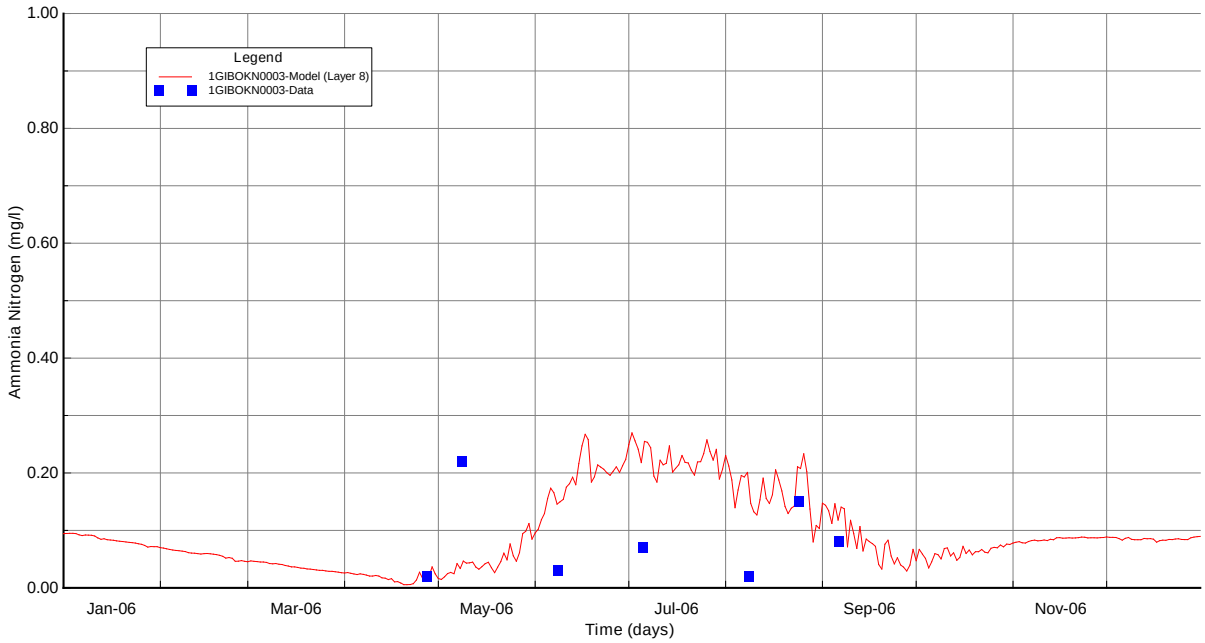

Figure B-71 Surface Layer NH4 Validation Plots at Station 1GIBOKN0003

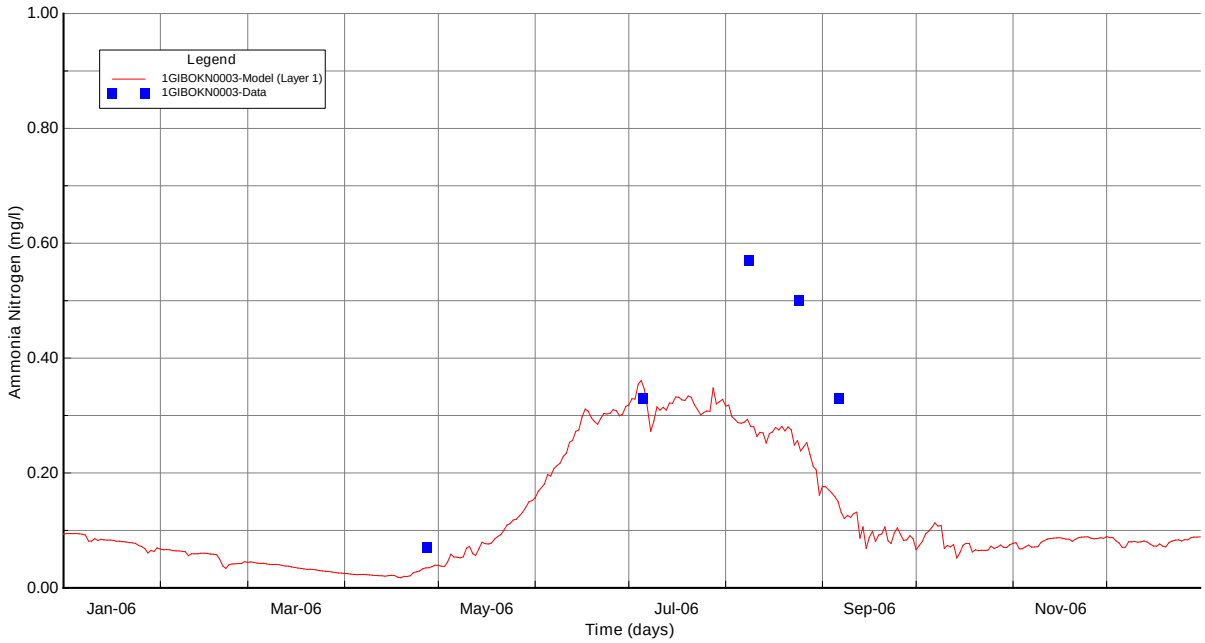

Figure B-72 Bottom Layer NH4 Validation Plots at Station 1GIBOKN0003

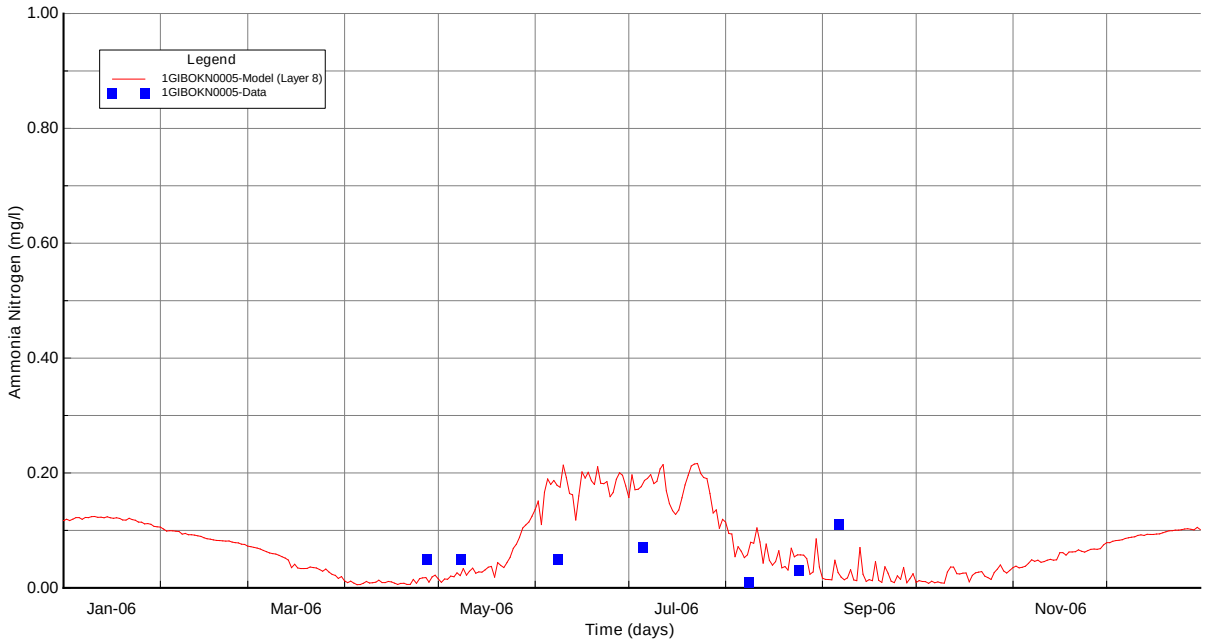

Figure B-73 Surface Layer NH4 Validation Plots at Station 1GIBOKN0005

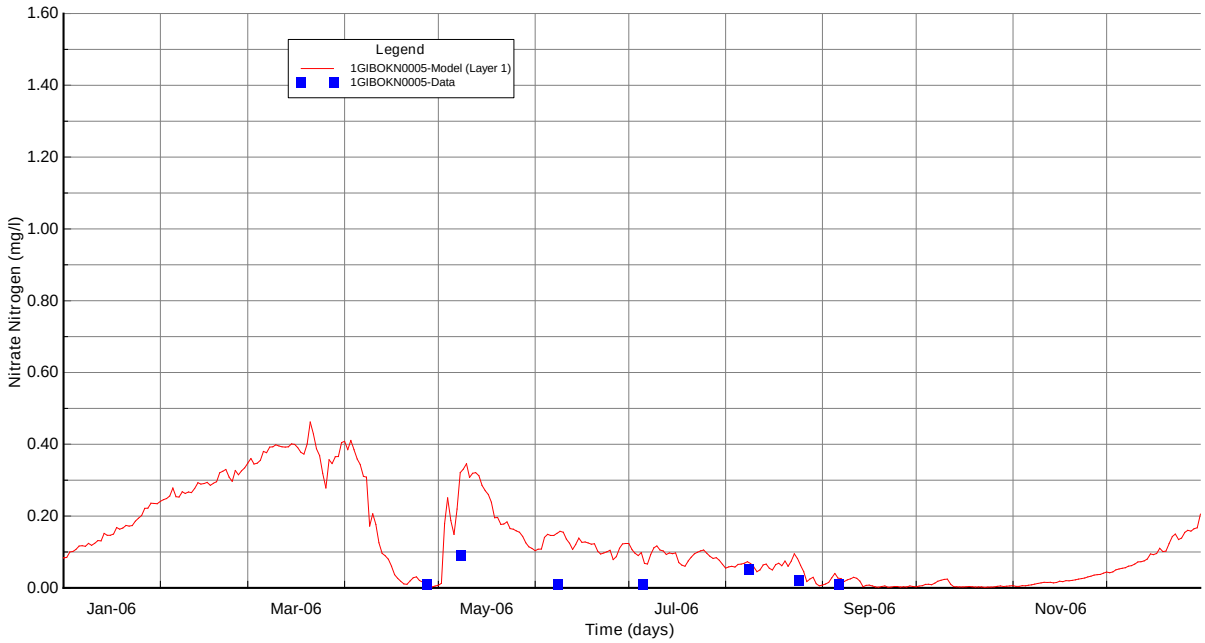

Figure B-74 Bottom Layer NH4 Validation Plots at Station 1GIBOKN0005

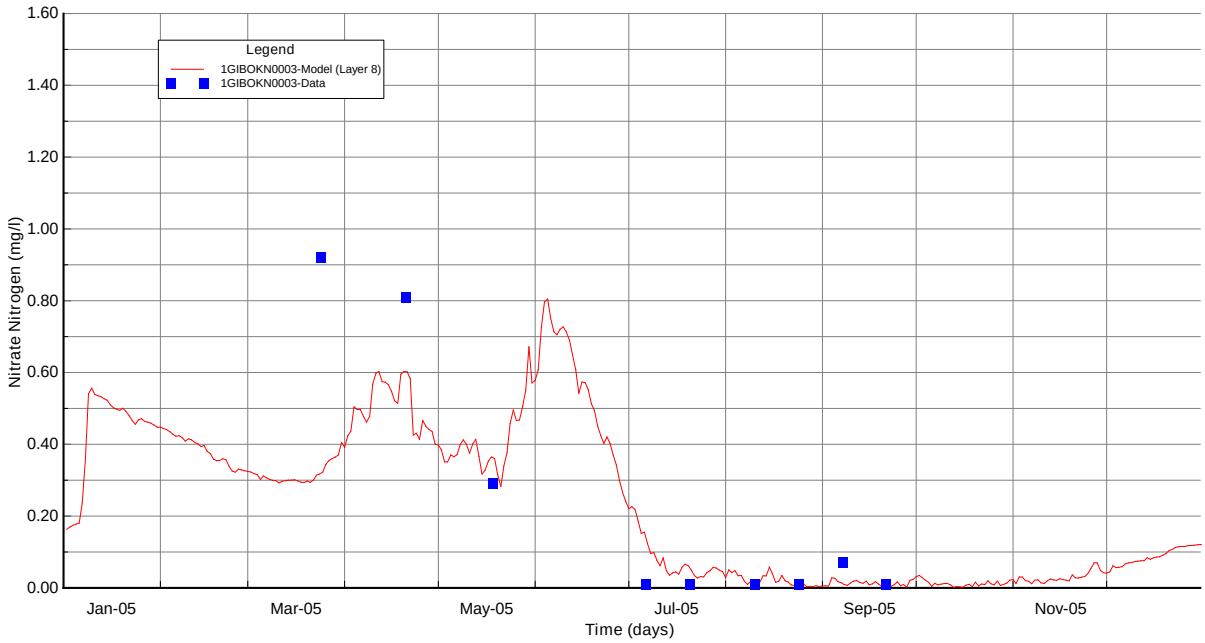

Figure B-75 Surface Layer NO3 Calibration Plots at Station 1GIBOKN0003

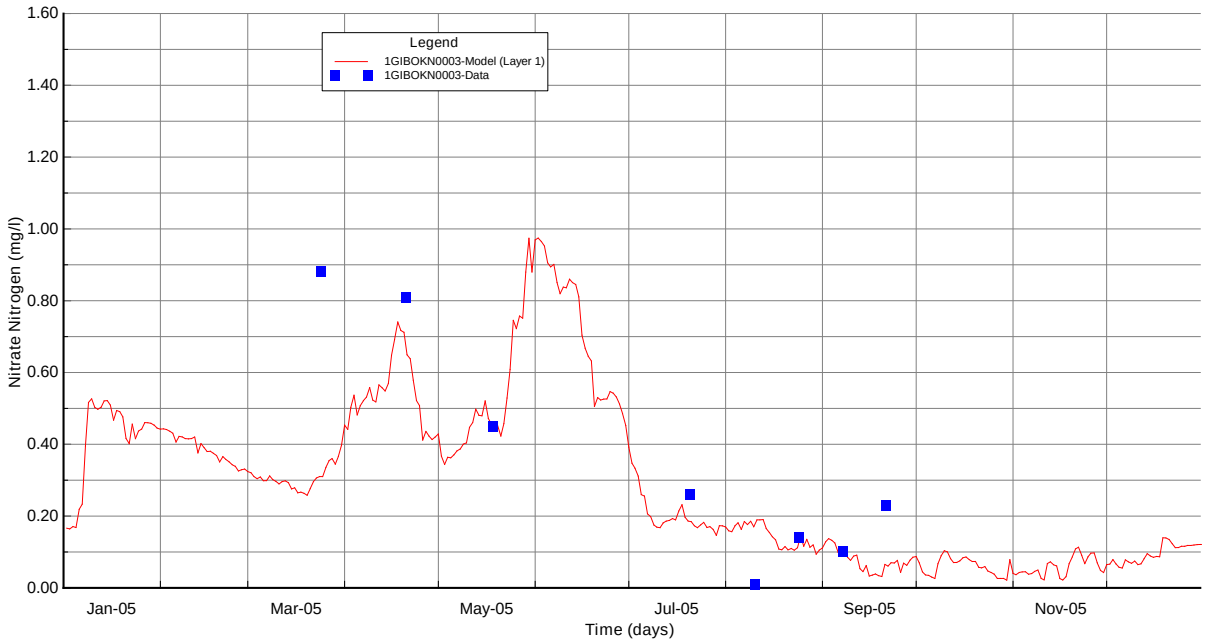

Figure B-76 Bottom Layer NO3 Calibration Plots at Station 1GIBOKN0003

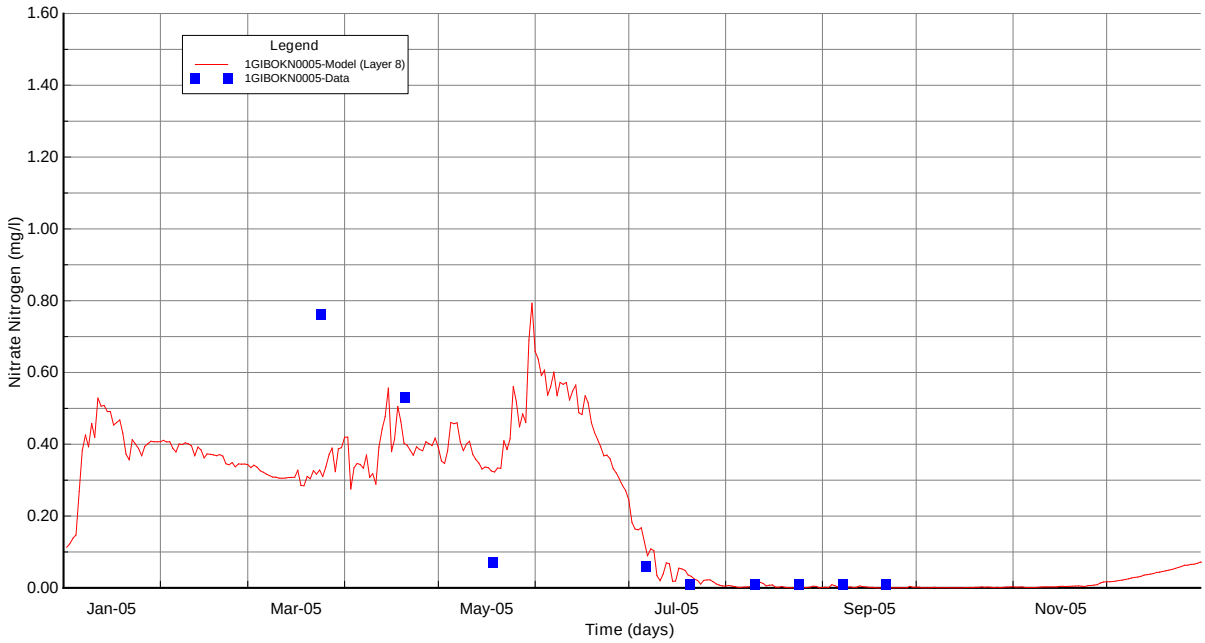

Figure B-77 Surface Layer NO3 Calibration Plots at Station 1GIBOKN0005

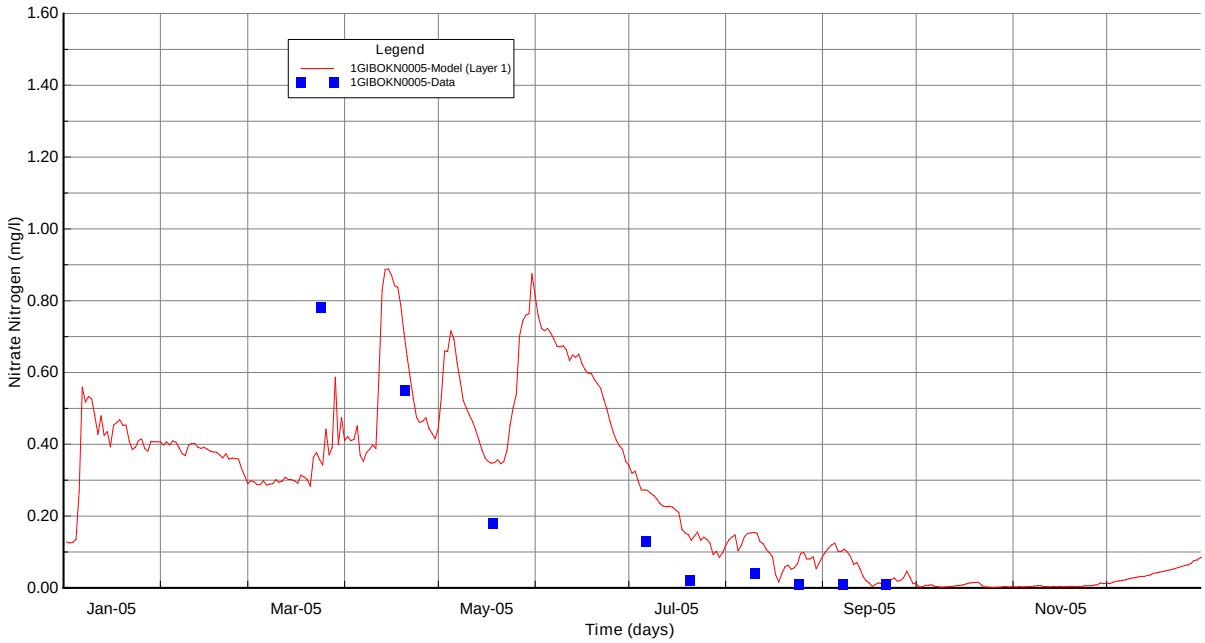

Figure B-78 Bottom Layer NO3 Calibration Plots at Station 1GIBOKN0005

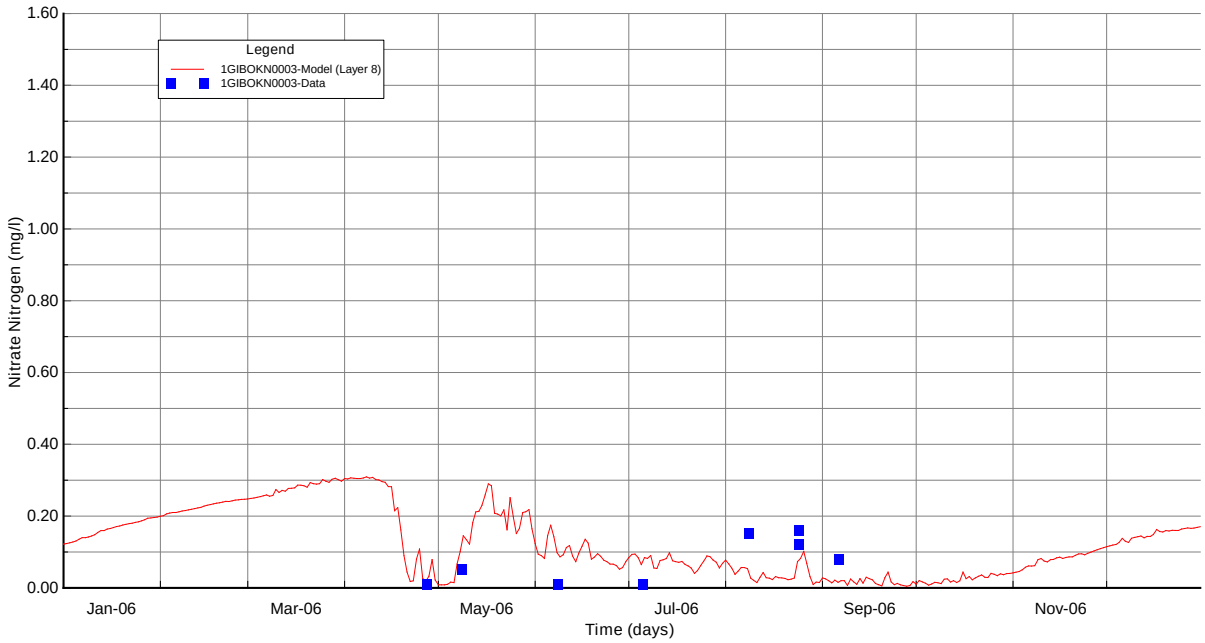

Figure B-79 Surface Layer NO3 Validation Plots at Station 1GIBOKN0003

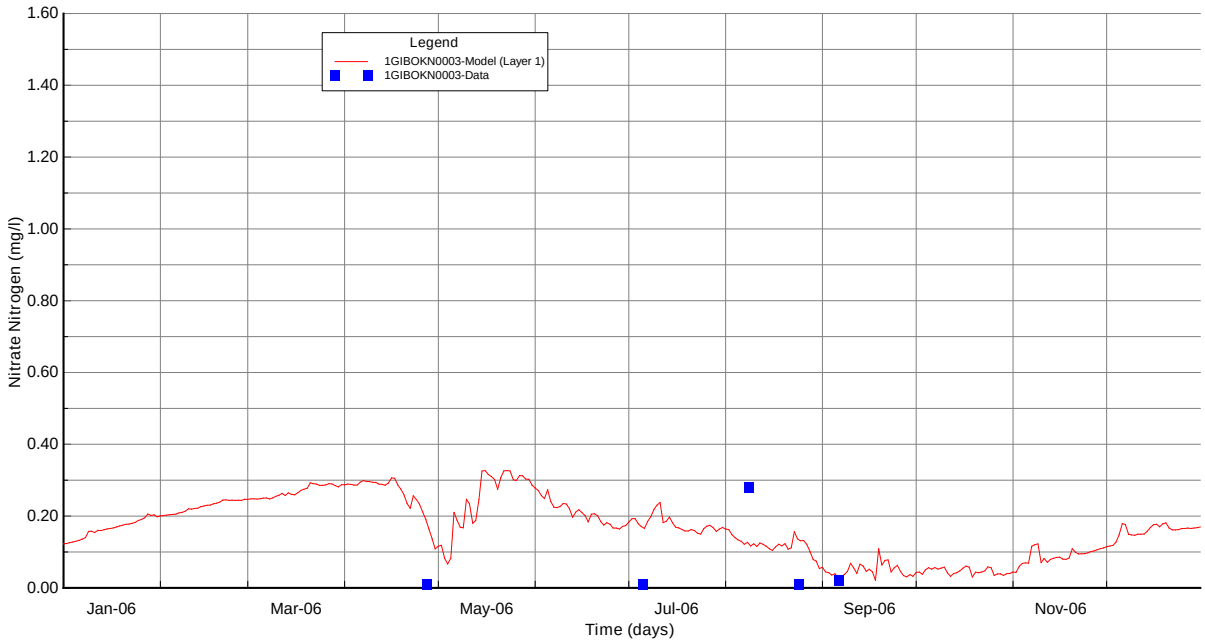

Figure B-80 Bottom Layer NO3 Validation Plots at Station 1GIBOKN0003

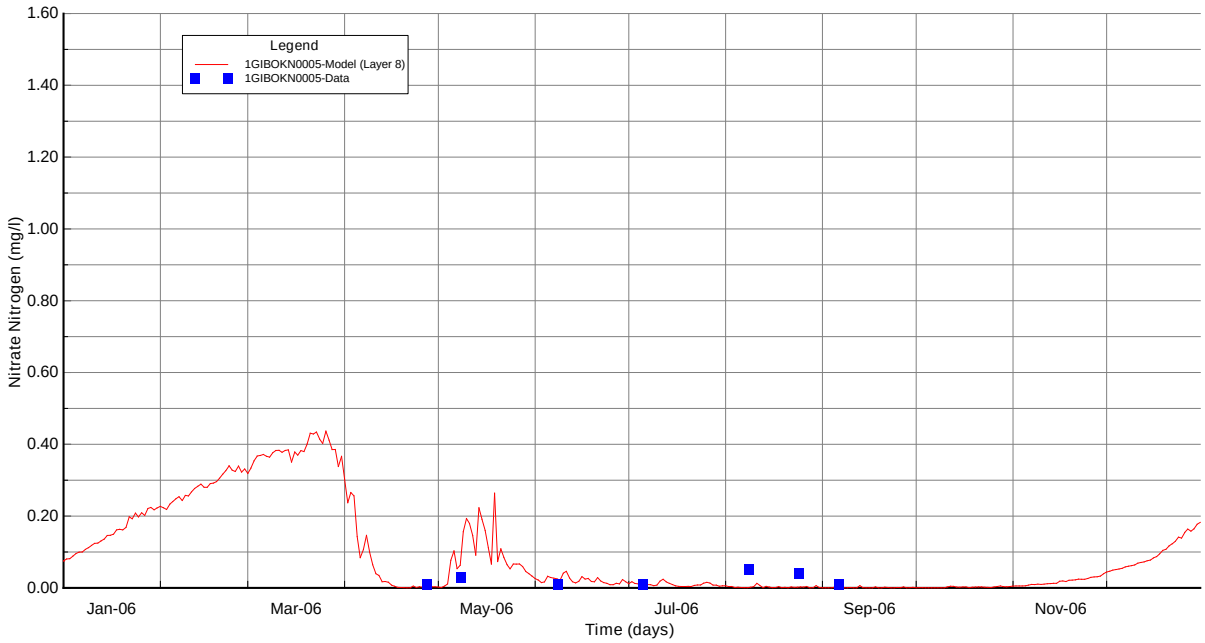

Figure B-81 Surface Layer NO3 Validation Plots at Station 1GIBOKN0005

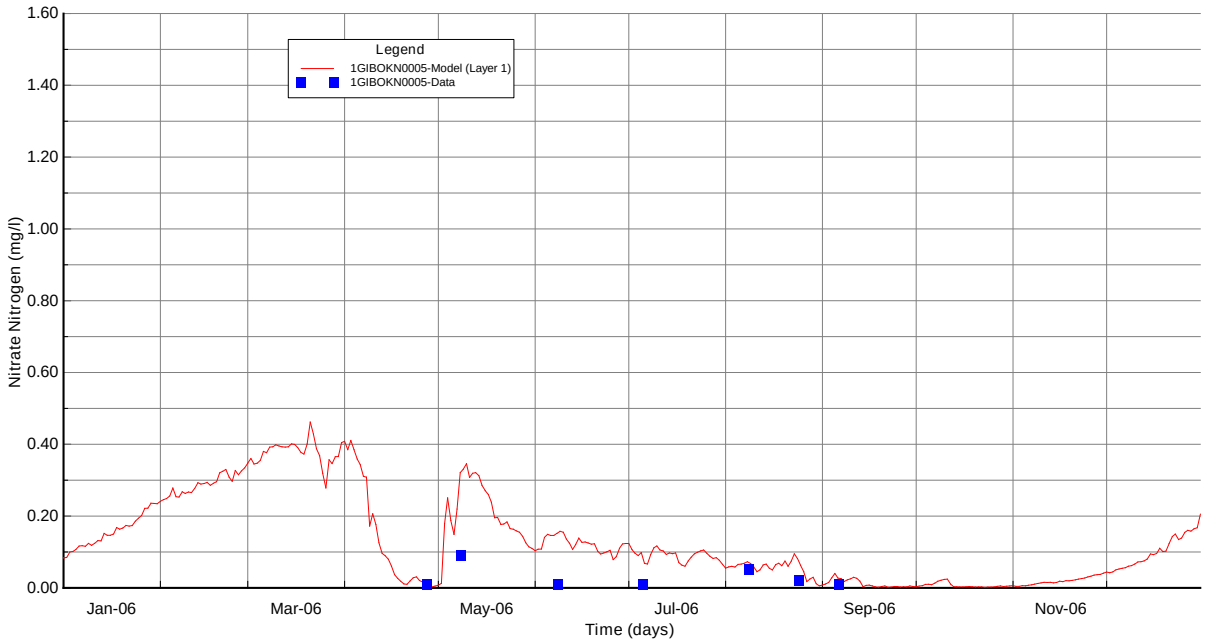

Figure B-82 Bottom Layer NO3 Validation Plots at Station 1GIBOKN0005

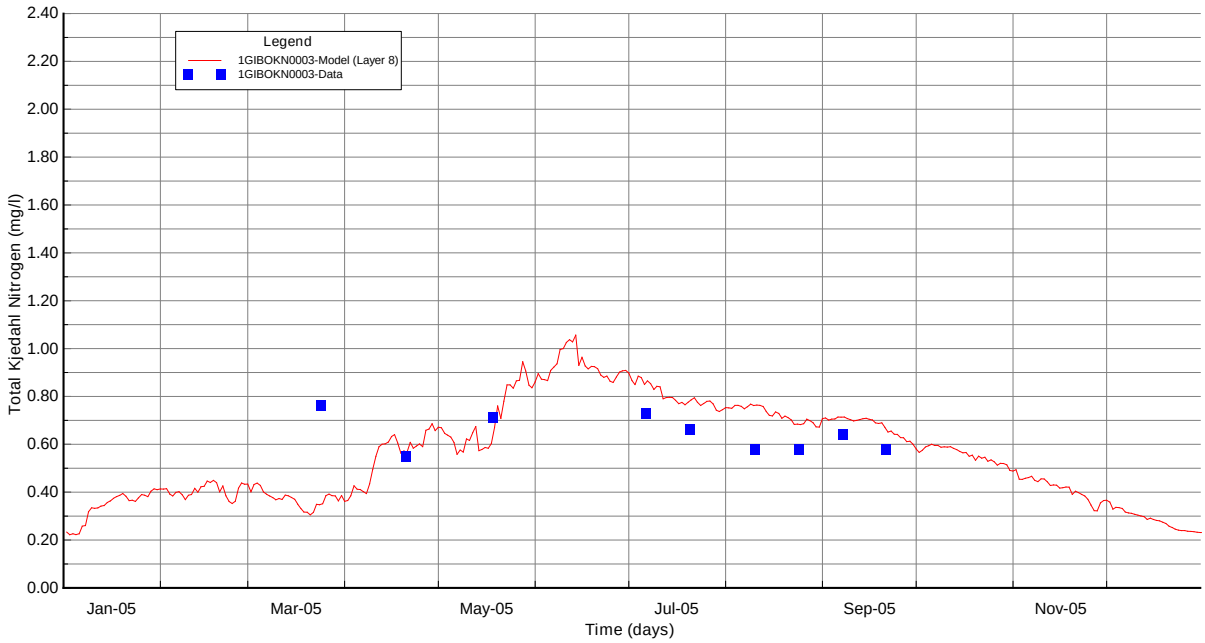

Figure B-83 Surface Layer TKN Calibration Plots at Station 1GIBOKN0003

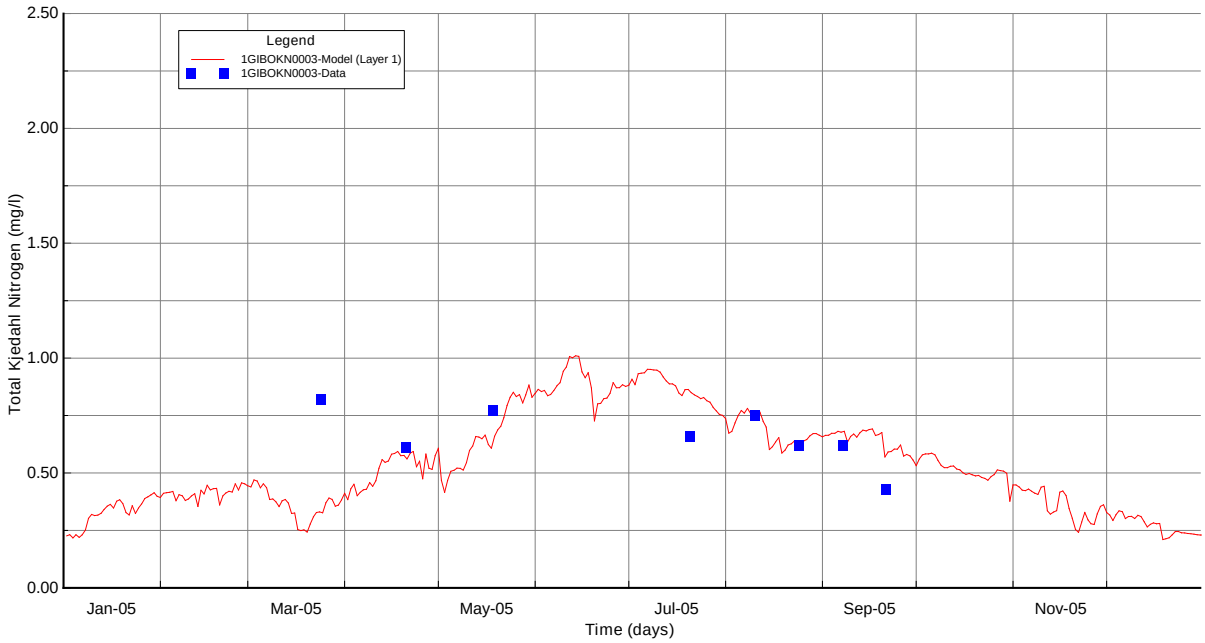

Figure B-84 Bottom Layer TKN Calibration Plots at Station 1GIBOKN0003

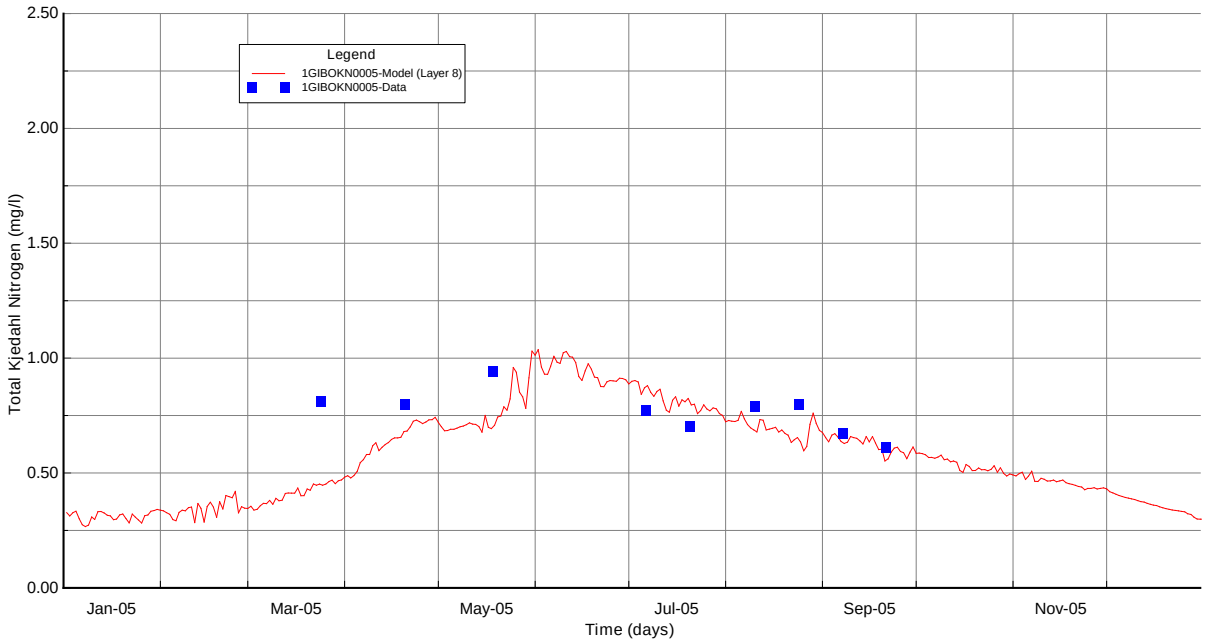

Figure B-85 Surface Layer TKN Calibration Plots at Station 1GIBOKN0005

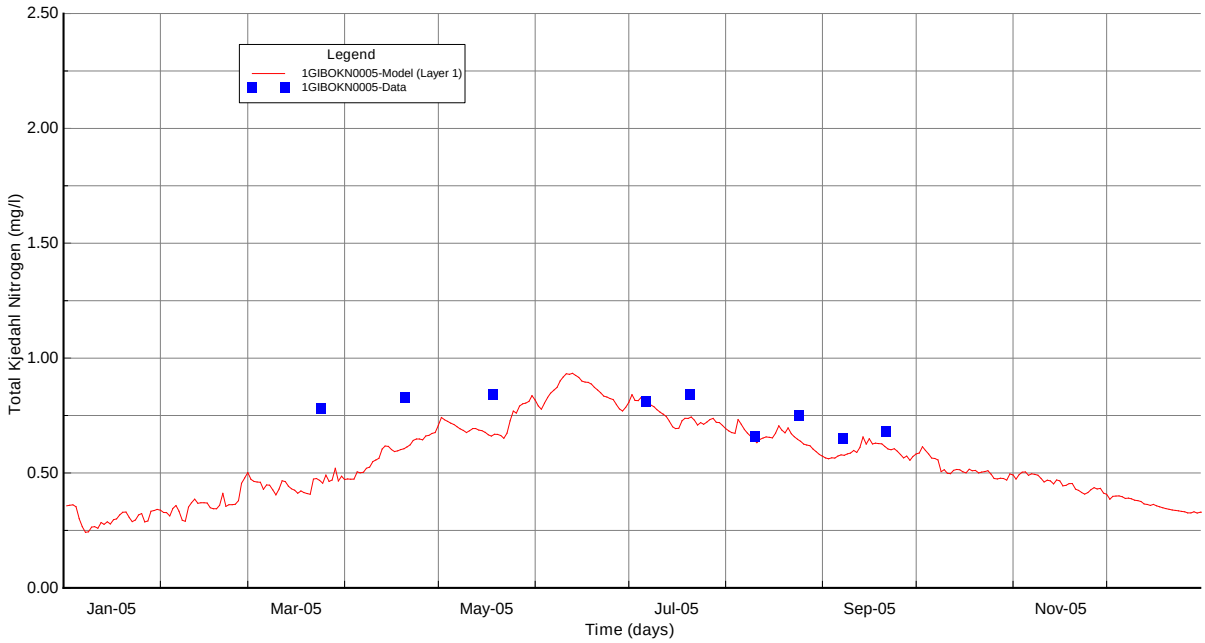

Figure B-86 Bottom Layer TKN Calibration Plots at Station 1GIBOKN0005

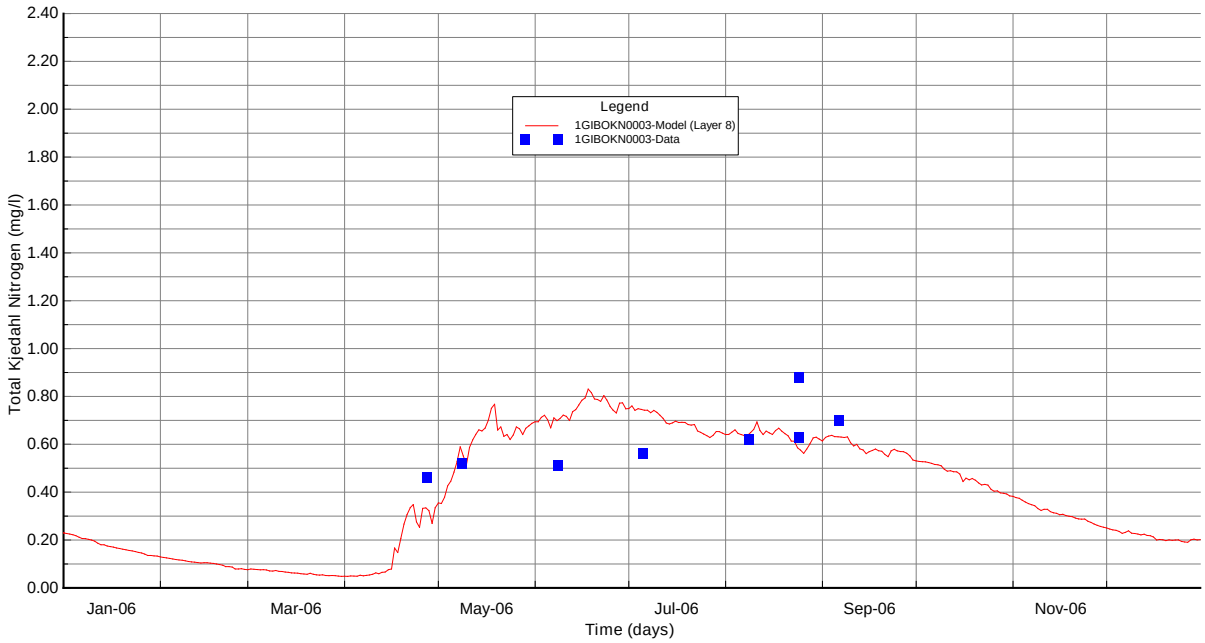

Figure B-87 Surface Layer TKN Validation Plots at Station 1GIBOKN0003

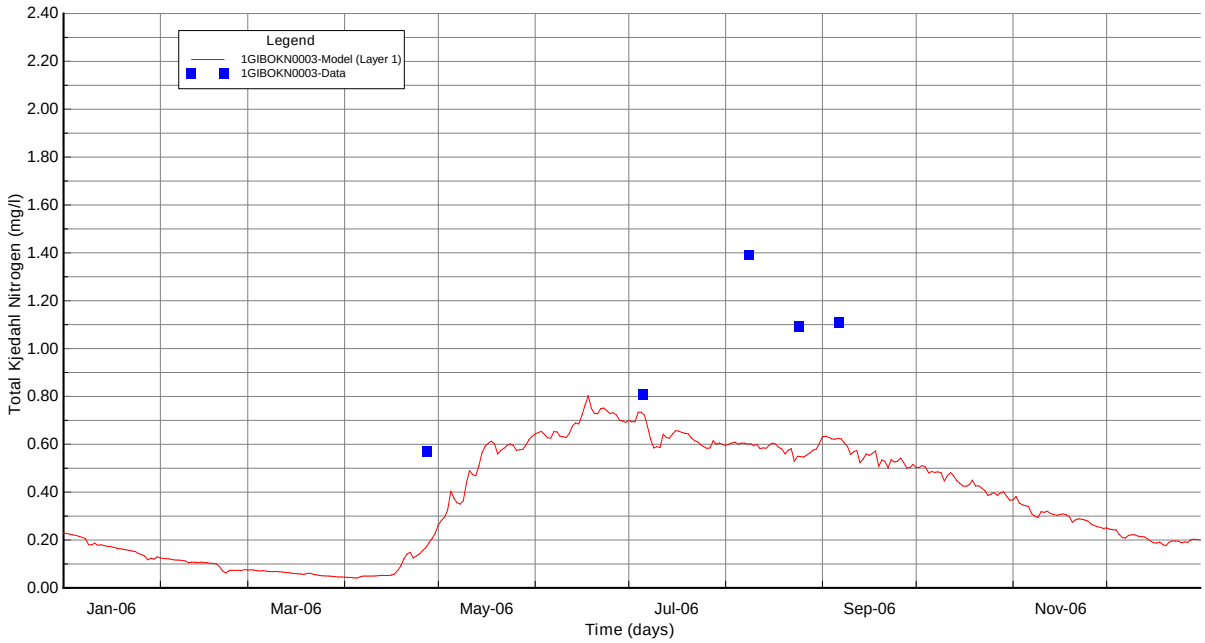

Figure B-88 Bottom Layer TKN Validation Plots at Station 1GIBOKN0003

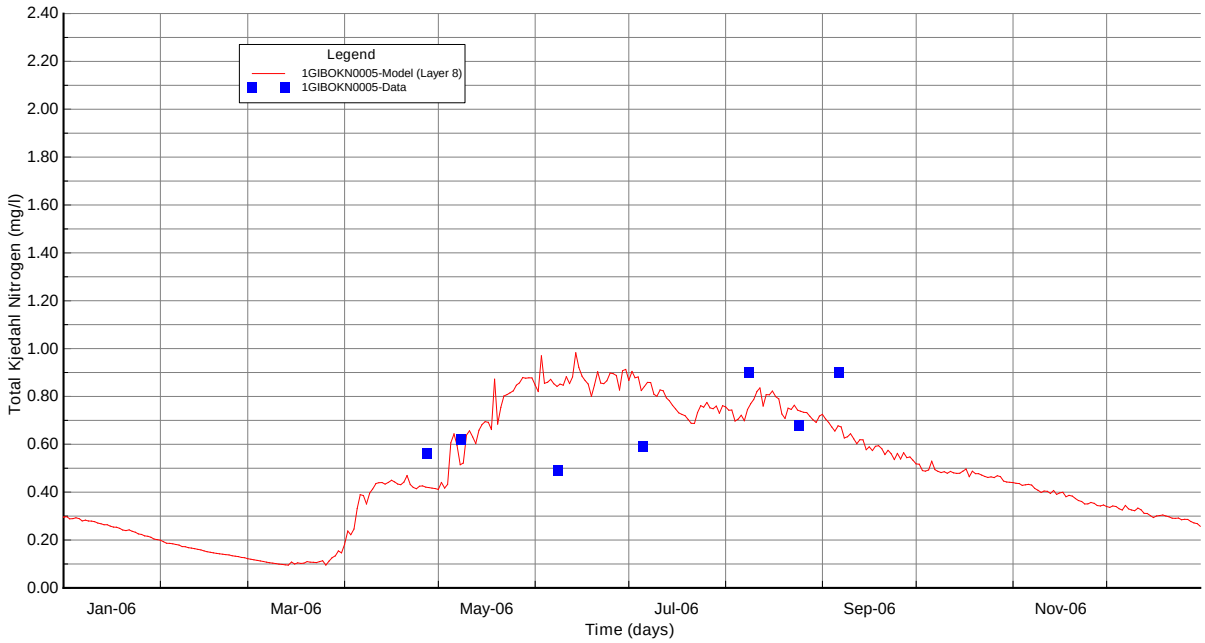

Figure B-89 Surface Layer TKN Validation Plots at Station 1GIBOKN0005

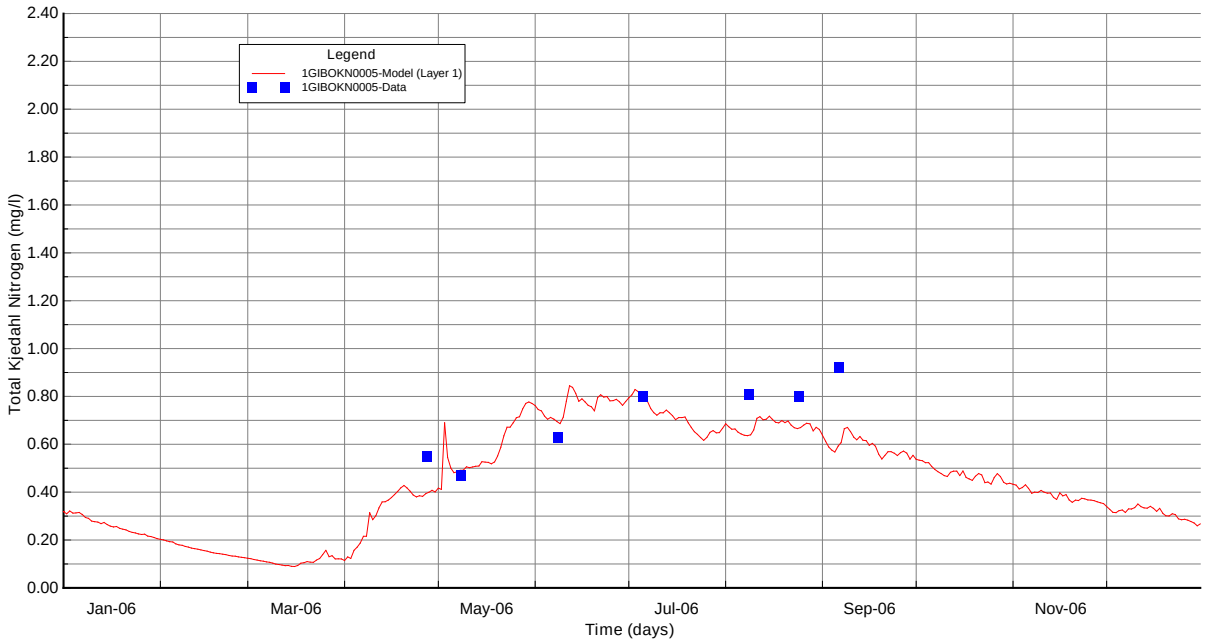

Figure B-90 Bottom Layer TKN Validation Plots at Station 1GIBOKN0005

B-7.9 Phosphorus Calibration and Validation

Total phosphate (TPO4) and total phosphorus (TP) model results are presented for comparison to the observed data for the surface layer (k=8) and bottom layer (k=1). The TPO4 calibration and validation plots at 1GIBOKN0003 and 1GIBOKN0005 are given in Figure B-91 through Figure B-98. The TP calibration and validation plots at 1GIBOKN0003 and 1GIBOKN0005 are given in Figure B- 99 through Figure B-106. As can be seen in the model-data plots, the model results are in reasonable agreement with measured TPO4 and TP for both calibration and validation periods.

The summary statistics of the TPO4 and TP are given in Table B-21 and Table B-22. In most of the cases, the model results for TPO4 and TP are within or close to the defined model performance target of $\pm 50\%$ for nutrients. The complete calibration and validation time series plots for all monitoring stations are given in APPENDIX C through APPENDIX D.

The calculated RMS errors of TPO4 ranged from 0.022 mg/L at the bottom layer of station 1GIBOKN0004 to 0.076 mg/L at the bottom layer of station 1GIBOKN0003 (Table B-21). The calculated relative RMS errors of TPO4 ranged from 15.29% at the surface layer of station 1GIBOKN0006 to 63.69% at the bottom layer of station 1GIBOKN0004 (Table B-21).

The calculated RMS errors of TP ranged from 0.021 mg/L at the surface layer of station 1GIBOKN0003 to 0.091 mg/L at the bottom layer of station 1GIBOKN0003 (Table B-22). The calculated relative RMS errors of TP ranged from 22.56% at the surface layer of station 1GIBOKN0006 to 104.11% at the surface layer of station 1GIBOKN0004 (Table B-22).

Table B-21 Summary Statistics of TPO4 (mg/l)

Station ID	Layer	Starting	Ending	# Pairs	RMS (mg/l)	Rel RMS (%)	Data Average (mg/l)	Model Average (mg/l)
1GIBOKN0003	Layer 8	3/24/2005 10:20	9/6/2006 9:50	17	0.024	26.14	0.034	0.022
1GIBOKN0003	Layer 1	3/24/2005 10:20	8/24/2006 9:30	12	0.076	42.35	0.104	0.064
1GIBOKN0004	Layer 8	3/24/2005 10:50	9/6/2006 10:21	17	0.027	37.98	0.023	0.009
1GIBOKN0004	Layer 1	3/24/2005 10:50	9/21/2005 12:40	9	0.022	63.69	0.017	0.025
1GIBOKN0005	Layer 8	3/24/2005 12:50	9/6/2006 9:10	16	0.037	30.21	0.033	0.013
1GIBOKN0005	Layer 1	3/24/2005 12:50	9/6/2006 9:10	16	0.025	32.46	0.044	0.047
1GIBOKN0006	Layer 8	3/24/2005 9:25	9/6/2006 8:40	17	0.026	15.29	0.06	0.051

Table B-22 Summary Statistics of TP (mg/l)

Station ID	Layer	Starting	Ending	# Pairs	RMS (mg/l)	Rel RMS (%)	Data Average (mg/l)	Model Average (mg/l)
1GIBOKN0003	Layer 8	3/24/2005 10:20	9/6/2006 9:50	17	0.021	30.70	0.084	0.067
1GIBOKN0003	Layer 1	3/24/2005 10:20	9/6/2006 9:50	13	0.091	31.63	0.157	0.099
1GIBOKN0004	Layer 8	3/24/2005 10:50	9/6/2006 10:21	17	0.040	104.11	0.074	0.04
1GIBOKN0004	Layer 1	3/24/2005 10:50	9/21/2005 12:40	9	0.037	71.99	0.082	0.053
1GIBOKN0005	Layer 8	3/24/2005 12:50	9/6/2006 9:10	16	0.045	56.54	0.096	0.057
1GIBOKN0005	Layer 1	3/24/2005 12:50	9/6/2006 9:10	16	0.029	36.28	0.112	0.093
1GIBOKN0006	Layer 8	3/24/2005 9:25	9/6/2006 8:40	17	0.028	22.56	0.133	0.13

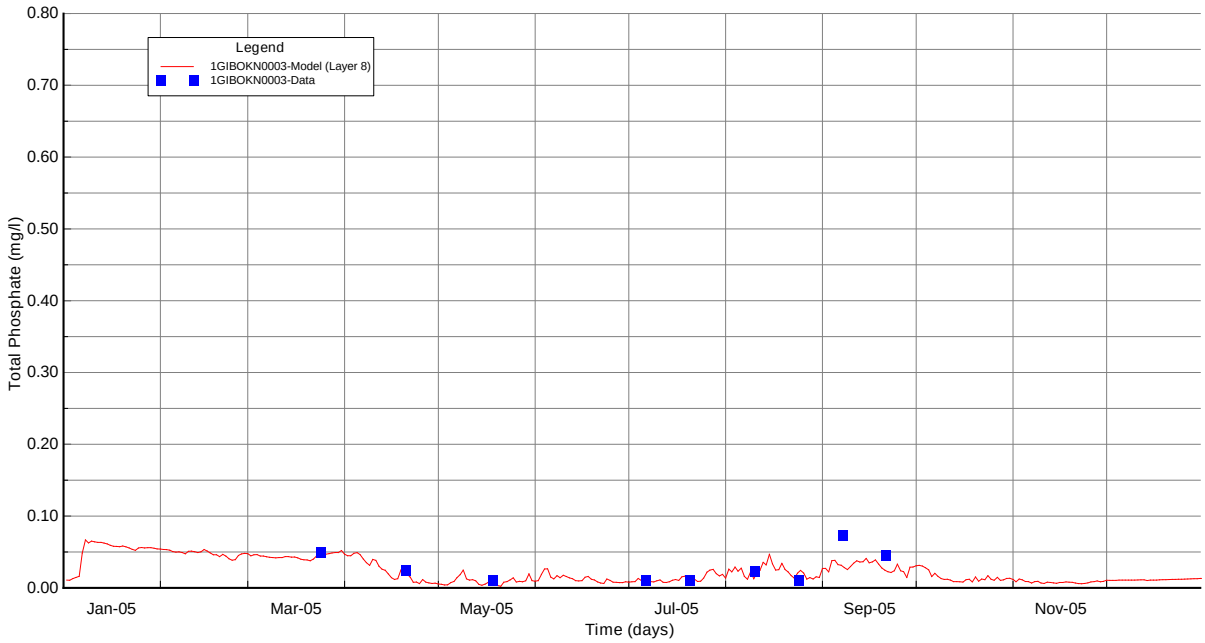

Figure B-91 Surface Layer TPO4 Calibration Plots at Station 1GIBOKN0003

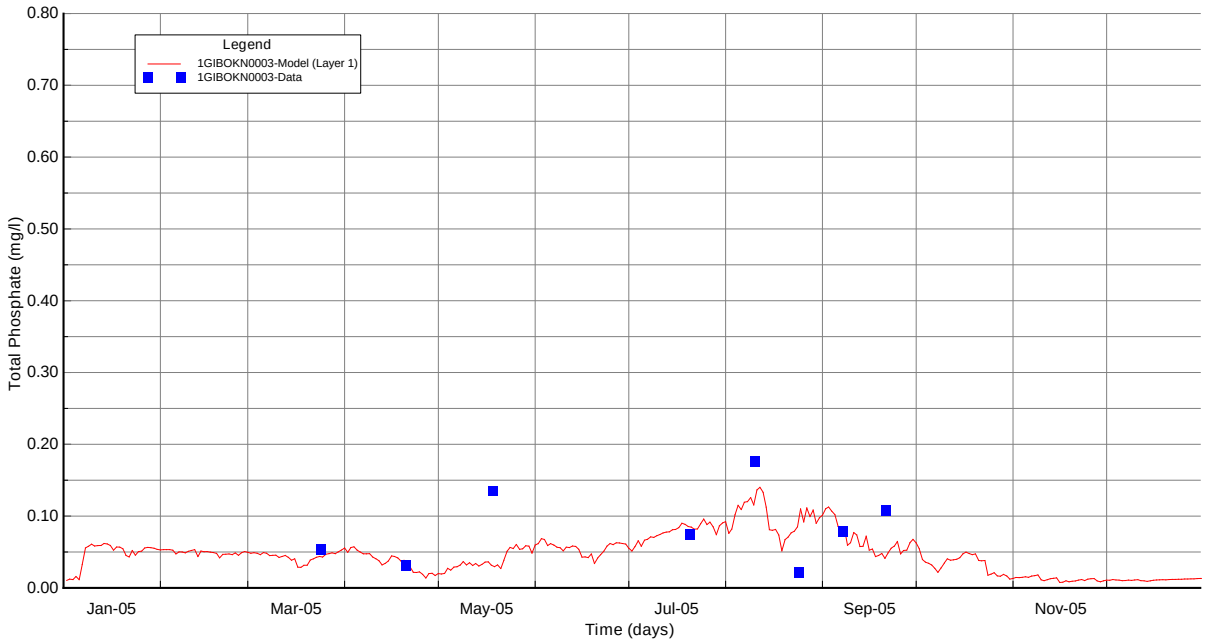

Figure B-92 Bottom Layer TPO4 Calibration Plots at Station 1GIBOKN0003

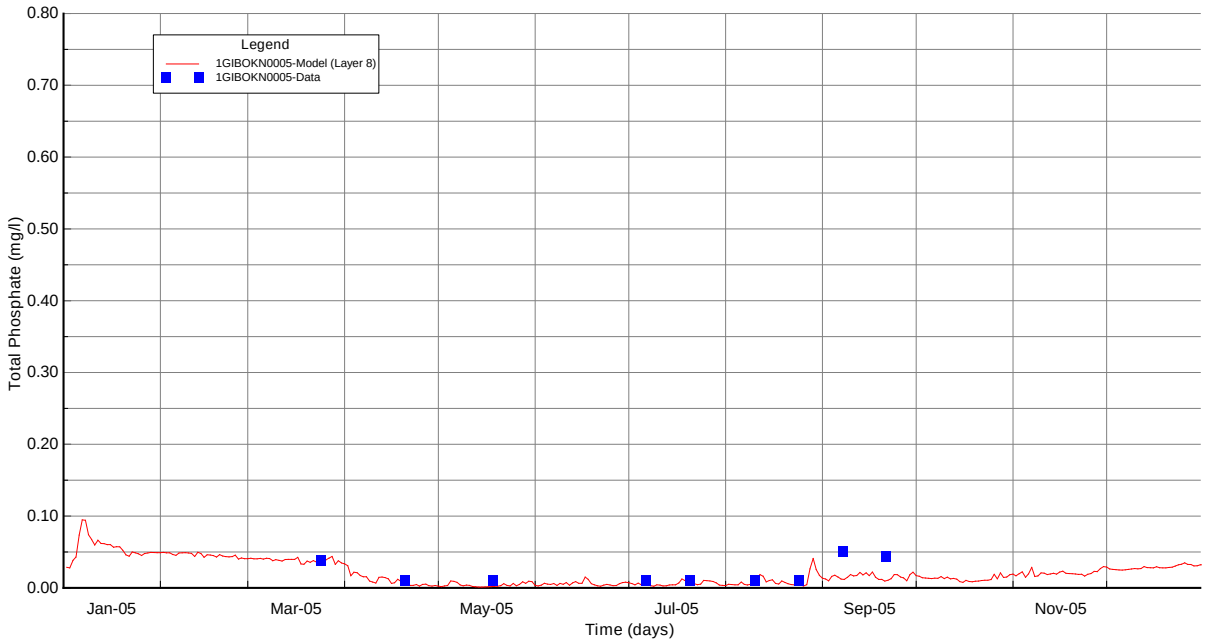

Figure B-93 Surface Layer TPO4 Calibration Plots at Station 1GIBOKN0005

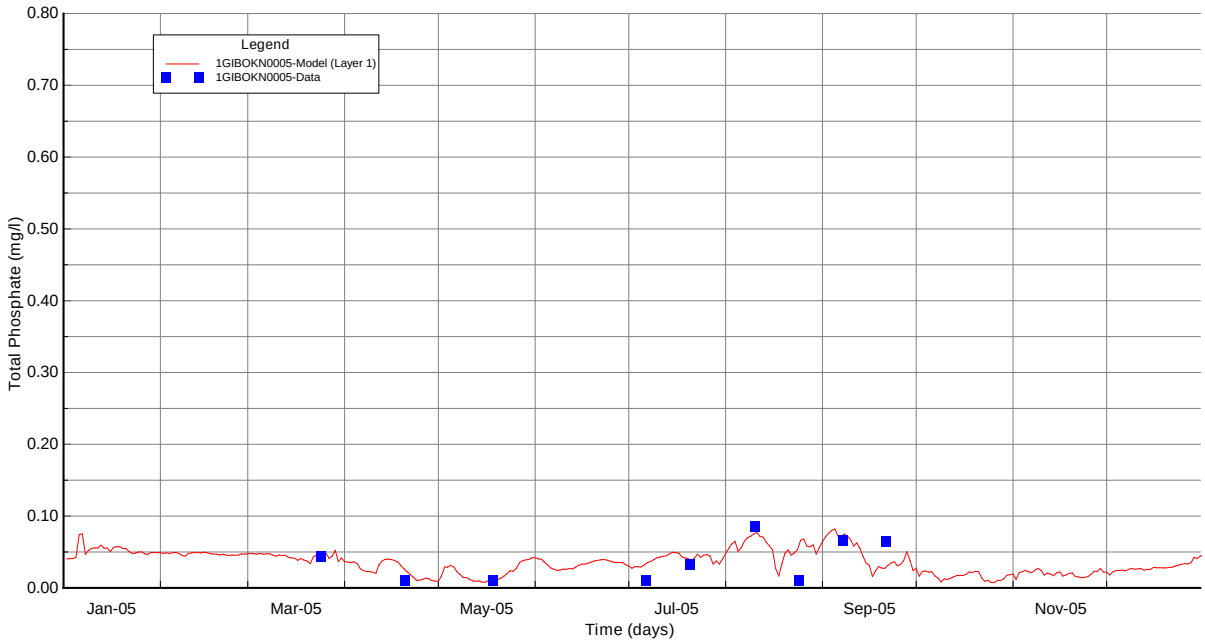

Figure B-94 Bottom Layer TPO4 Calibration Plots at Station 1GIBOKN0005

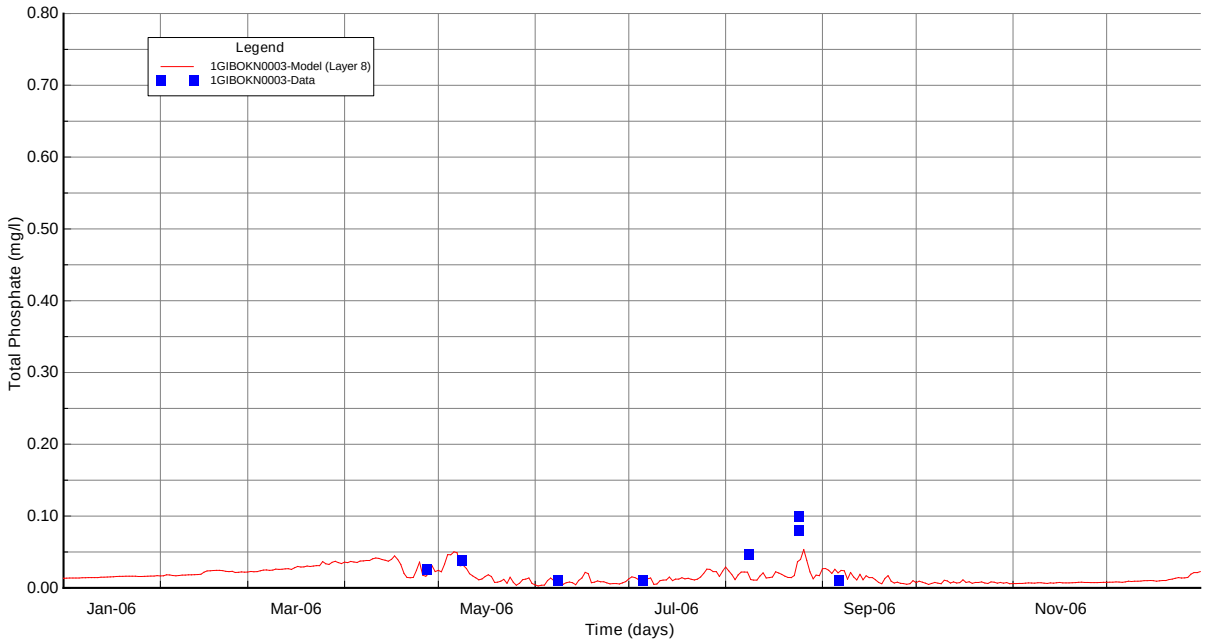

Figure B-95 Surface Layer TPO4 Validation Plots at Station 1GIBOKN0003

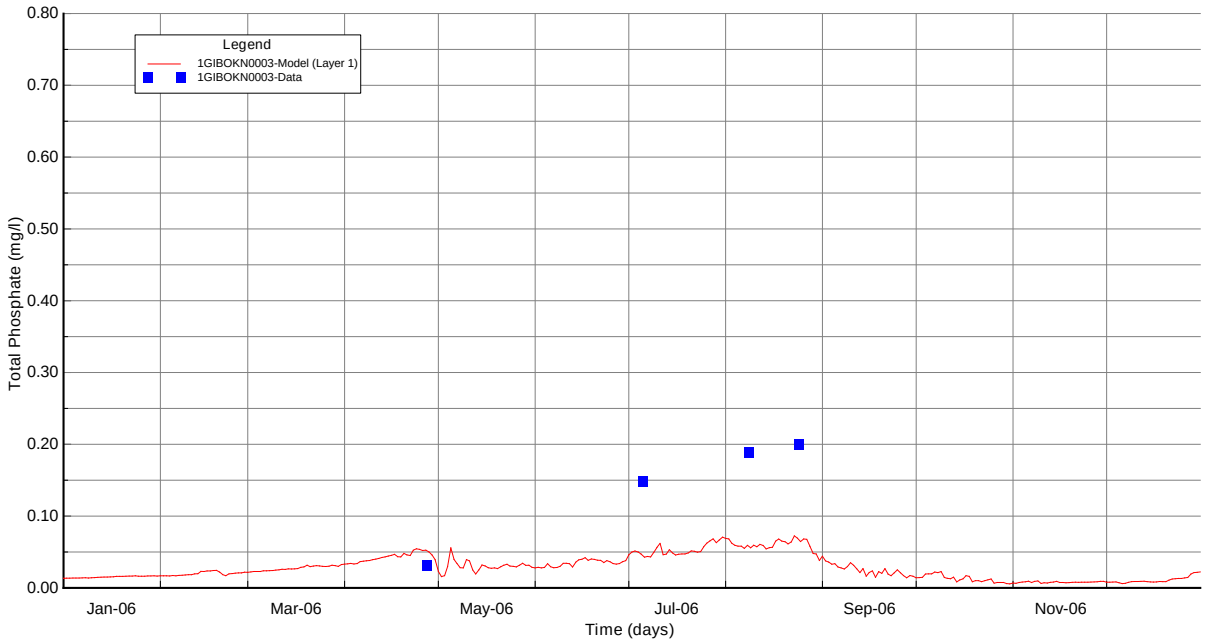

Figure B-96 Bottom Layer TPO4 Validation Plots at Station 1GIBOKN0003

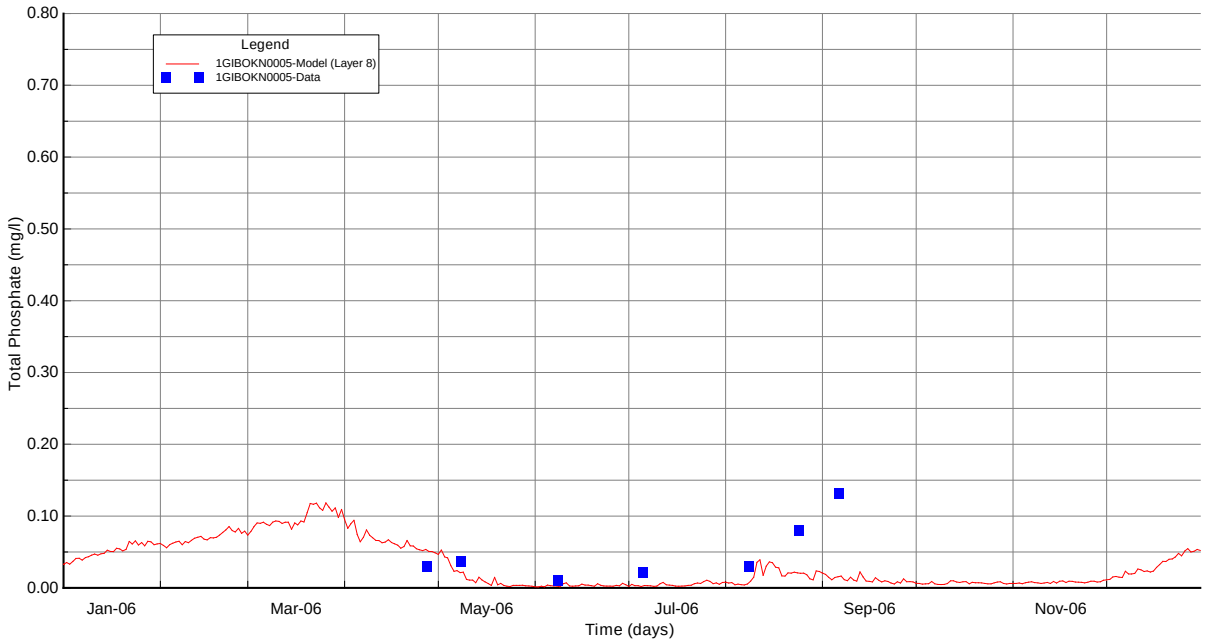

Figure B-97 Surface Layer TPO4 Validation Plots at Station 1GIBOKN0005

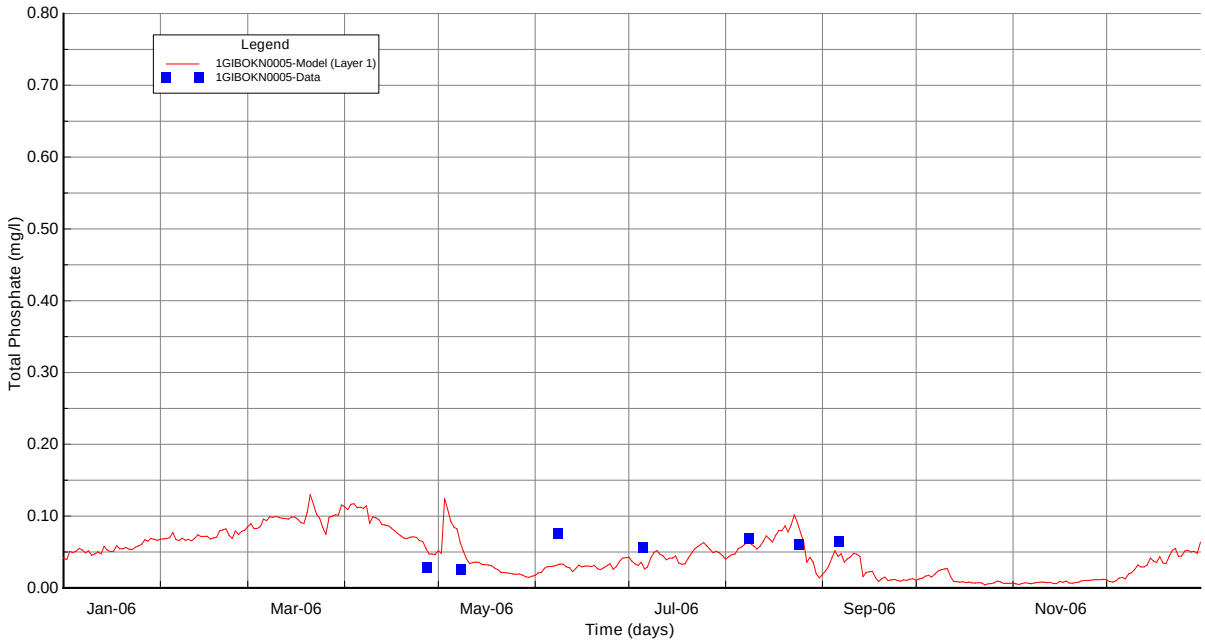

Figure B-98 Bottom Layer TPO4 Validation Plots at Station 1GIBOKN0005

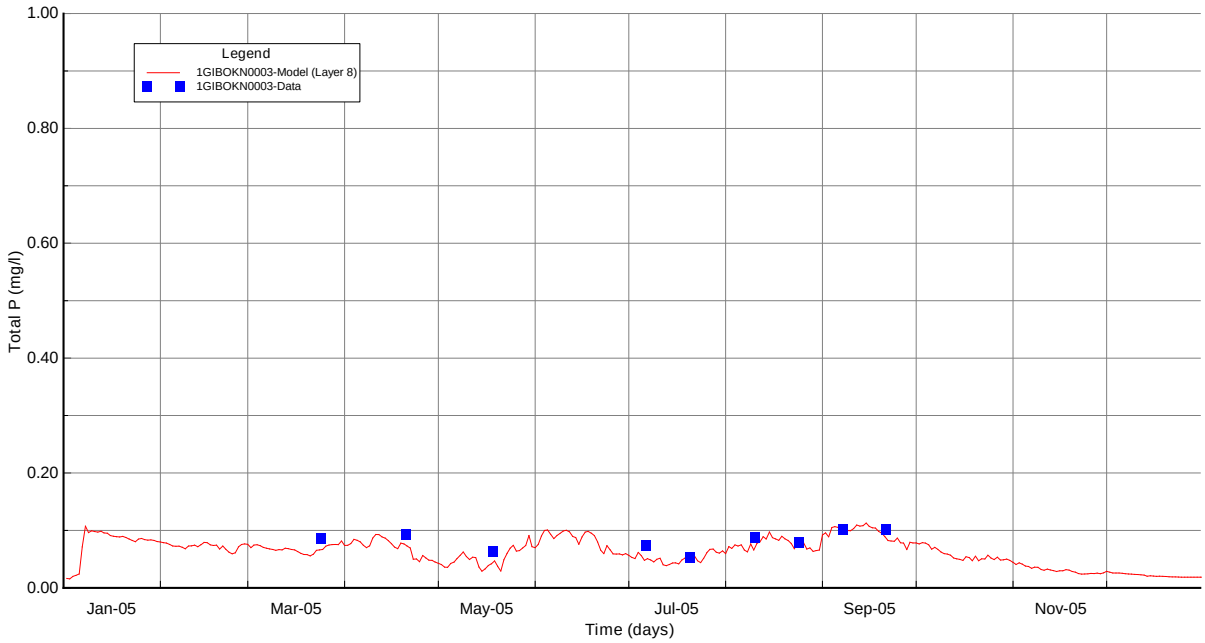

Figure B-99 Surface Layer TP Calibration Plots at Station 1GIBOKN0003

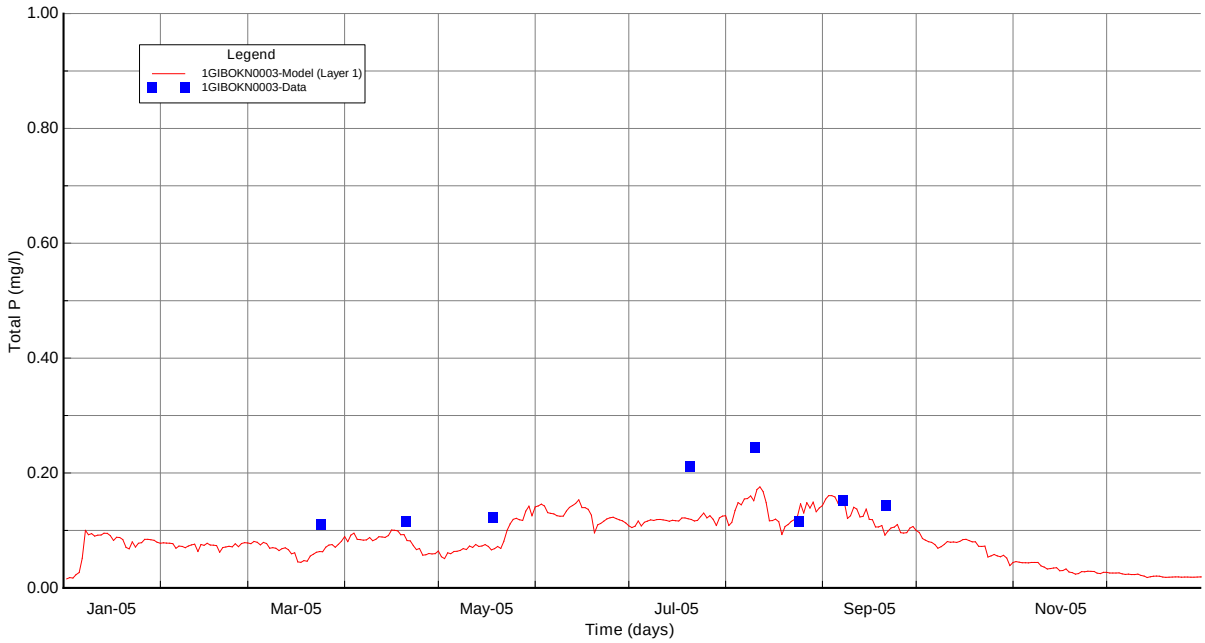

Figure B-100 Bottom Layer TP Calibration Plots at Station 1GIBOKN0003

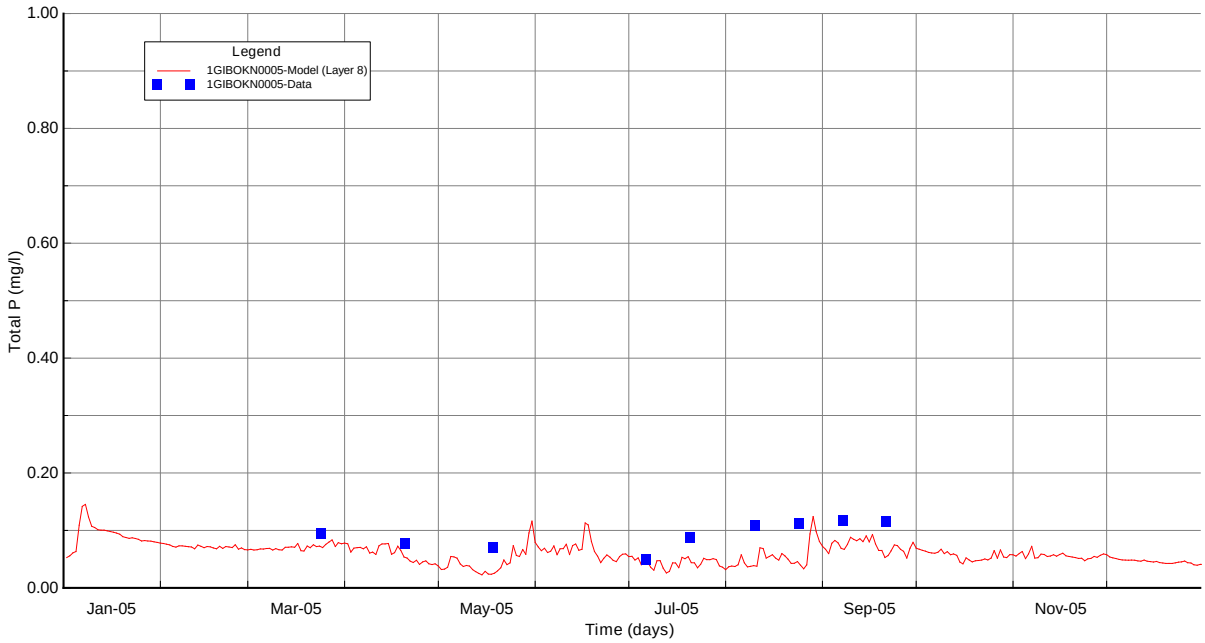

Figure B-101 Surface Layer TP Calibration Plots at Station 1GIBOKN0005

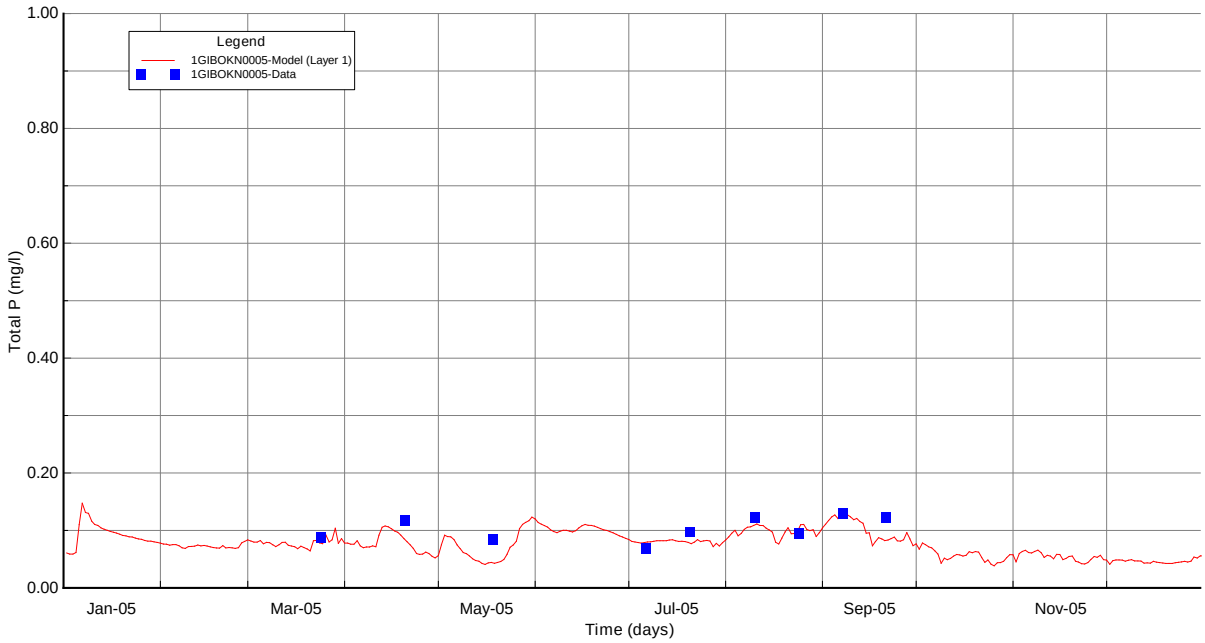

Figure B-102 Bottom Layer TP Calibration Plots at Station 1GIBOKN0005

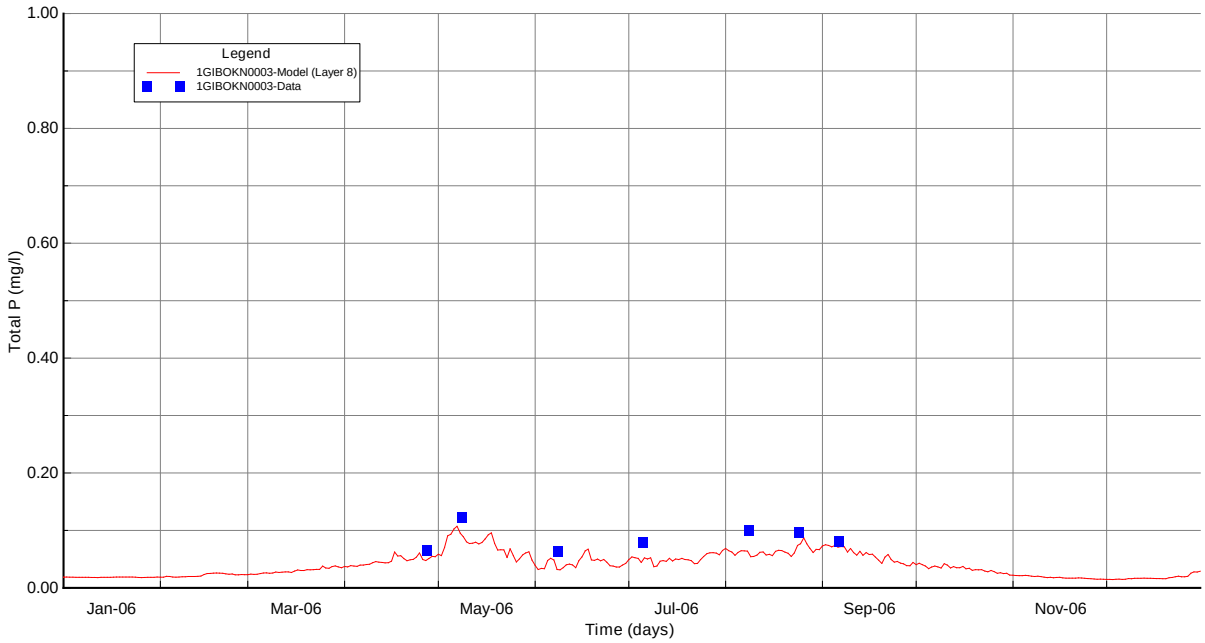

Figure B-103 Surface Layer TP Validation Plots at Station 1GIBOKN0003

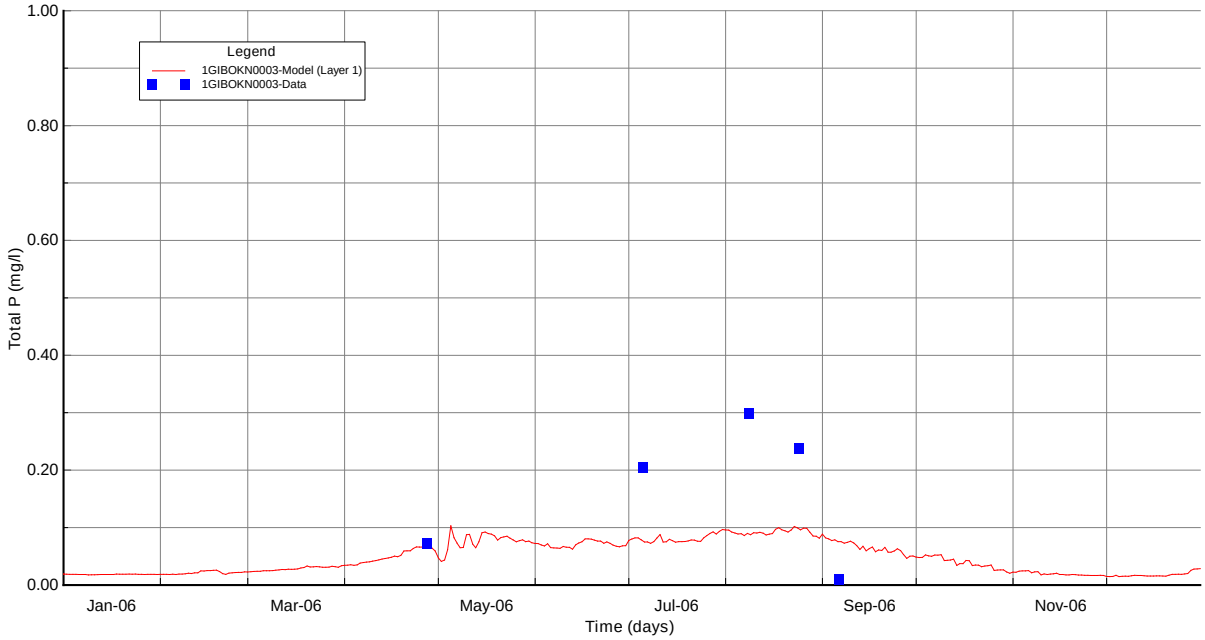

Figure B-104 Bottom Layer TP Validation Plots at Station 1GIBOKN0003

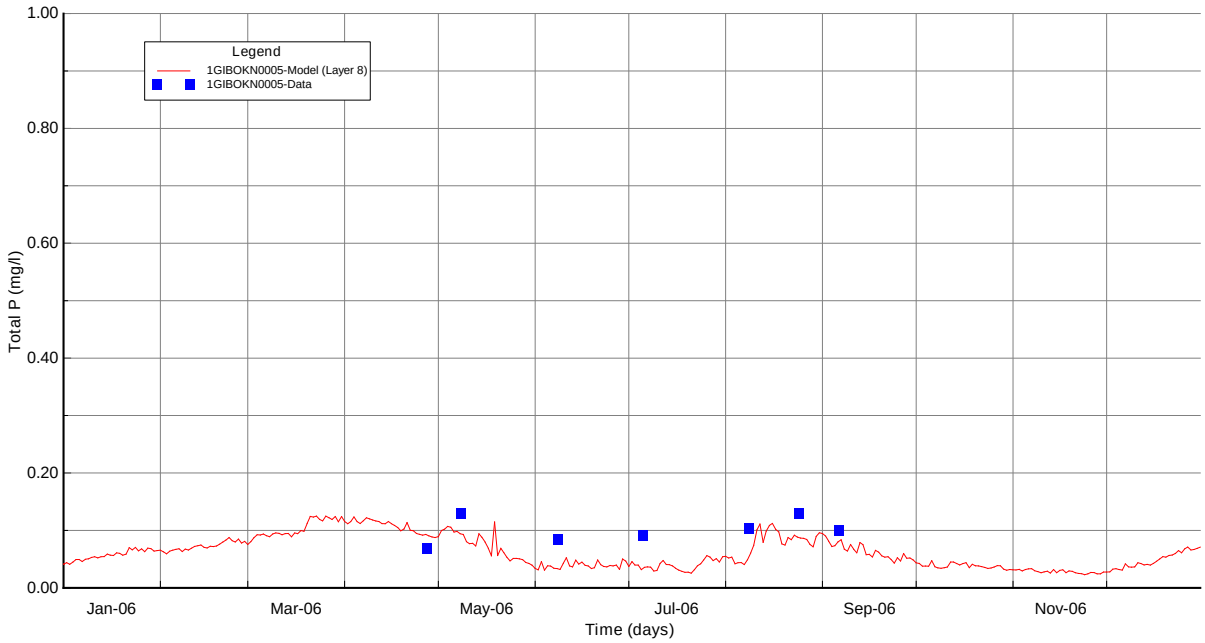

Figure B-105 Surface Layer TP Validation Plots at Station 1GIBOKN0005

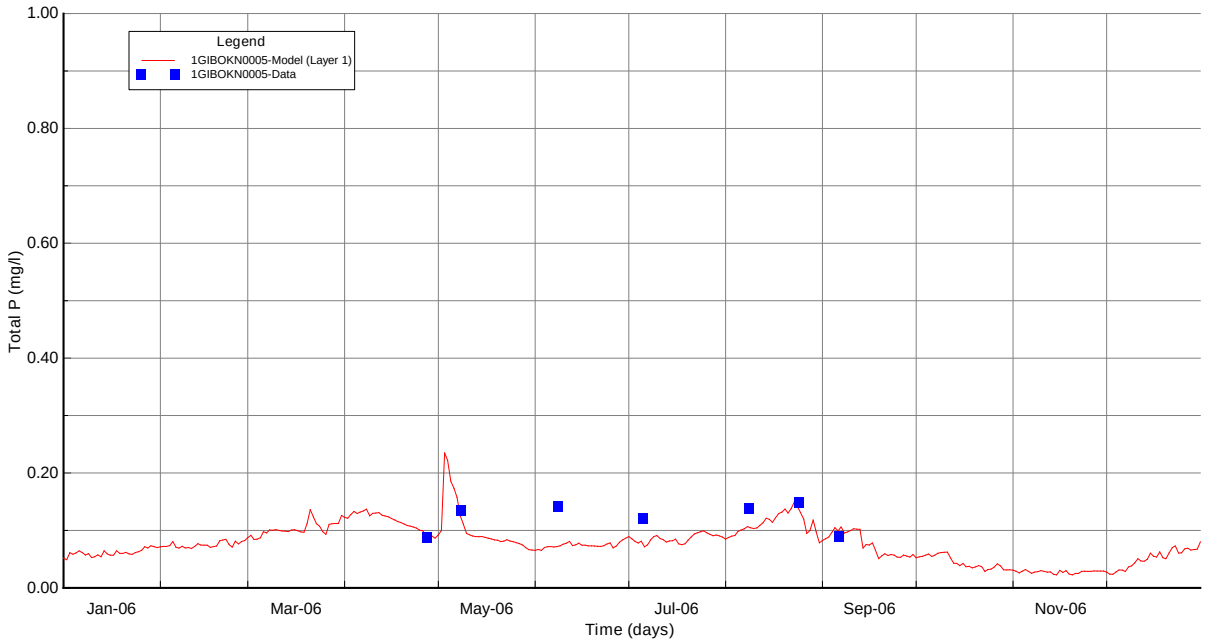

Figure B-106 Bottom Layer TP Validation Plots at Station 1GIBOKN0005

B-7.10 SOD and Sediment Flux

The oxygen demand from the sediment bed is an important sink for the dissolved oxygen level in lakes and the bottom oxygen dependent phosphate release across the sediment-water interface is an important source for the phosphate in the water column, which in turn, fuels algae growth in the surface

layer. Descriptions of the mechanisms related to sediment oxygen demand and nutrient fluxes across the sediment water interface can be found in Mortimer (1941,1942); Di Toro (2001); Nowlin et al. (2005); and Hupfer and Lewandowski (2008).

In the absence of site-specific measurements of sediment oxygen demand and phosphate release from the sediment bed under anoxic conditions in Fort Gibson Lake, the model results for benthic phosphate flux and SOD shown in Figure B-107 through Figure B-110 are compared to observed datasets available from Lake Wister (Haggard and Scott, 2011); Lake Frances (Haggard and Soerens, 2006); Eucha Lake (Haggard et al., 2005); Beaver Lake in Arkansas (Sen et al., 2007; Hamdan et al., 2010), Acton Lake in Ohio (Nowlin et al., 2005) and a set of 17 lakes and reservoirs in the Central Plains (Dzialowski and Carter, 2011) to support calibration of the sediment flux model for Fort Gibson Lake.

Model results were extracted for each station and processed to compile summary statistics to present box-whisker plots for benthic phosphate fluxes and SOD simulated during stratified conditions from May 15 through October 1 shown in Figures B-111 and B-112. Stratified conditions correspond to the period of anoxia so that model results can be compared to measurements of phosphate release made under anoxic conditions. The box-whisker plots show the summary statistics computed from the model results. Minimum and maximum values are shown as "outlier" data points plotted outside the tails of the box (* symbol). The lower and upper tails of the box show the 10^{th} and 90^{th} percentile values. The lower and upper horizontal lines of the box show the 25^{th} and 75^{th} percentile with the 50^{th} percentile shown as the line through the box. The mean value is shown as a data point within the box.

As expected, the highest phosphate release rates and SOD simulated under stratified conditions occurred in the lacustrine area (1GIBOKN0003 and 1GIBOKN0305). The mean phosphate release rates are 0.02 and 0.025 g/m^2-day at 1GIBOKN0003 and 1GIBOKN0305, respectively. The mean phosphate release rate at 1GIBOKN0386, located close to the riverine area, is -0.001 g/m^2-day, which means the water column contributes phosphate to the sediment bed. The model results are seen to be close to the range of anoxic phosphate fluxes (2.6-18.5 mg P/m^2-day) measured in eutrophic reservoirs in the Central Plains states as shown in Figure B-113 (see Dzialowski and Carter, 2011). Excluding station 1GIBOKN 0386, which is too close to the riverine area, the mean SOD ranged from 0.82 to 6.21 g/m^2-day, which are consistent with the reported SOD measurements in Central Plains states shown in Table B-23.

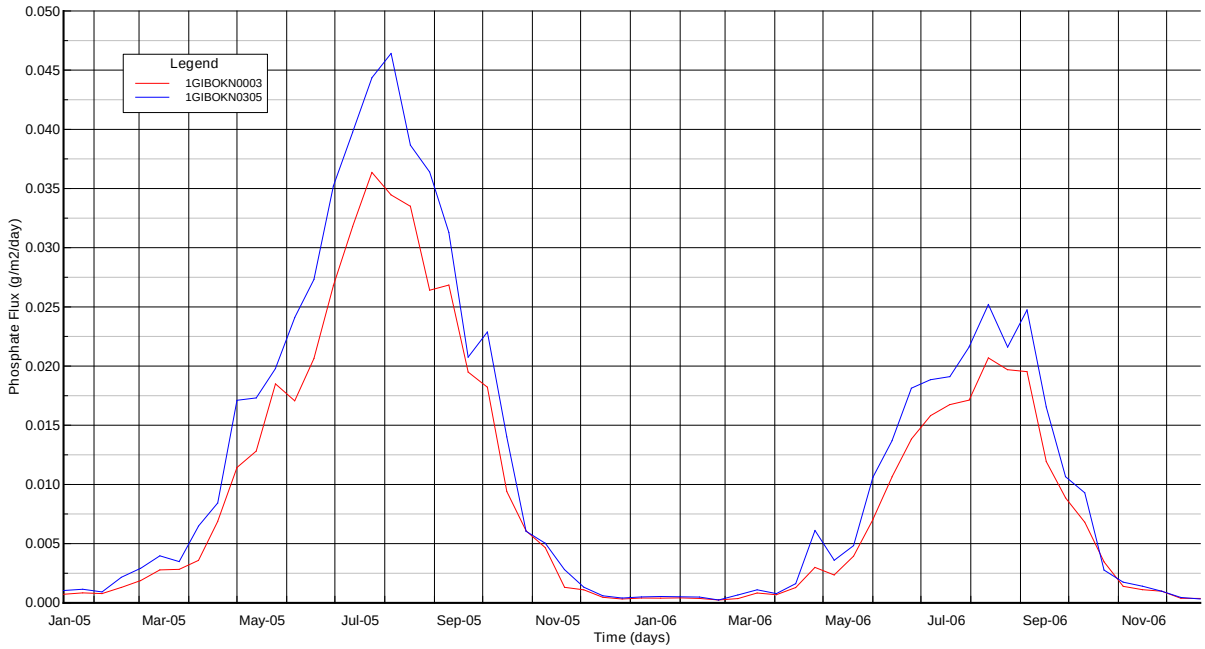

Figure B-107 – Sediment Flux of Phosphate (PO4) (as g/m2-day) Calibration Results at 1GIBOKN0003 and 1GIBOKN0305

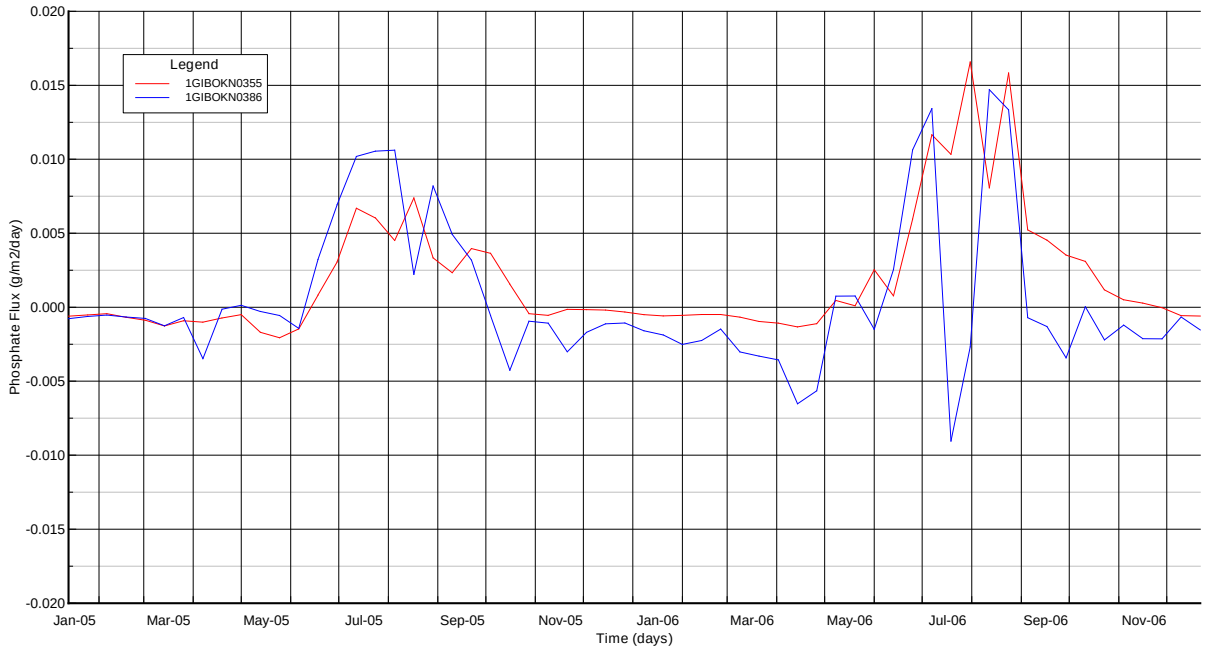

Figure B-108 – Sediment Flux of Phosphate (PO4) (as g/m2-day) Calibration Results at 1GIBOKN0355 and 1GIBOKN0386

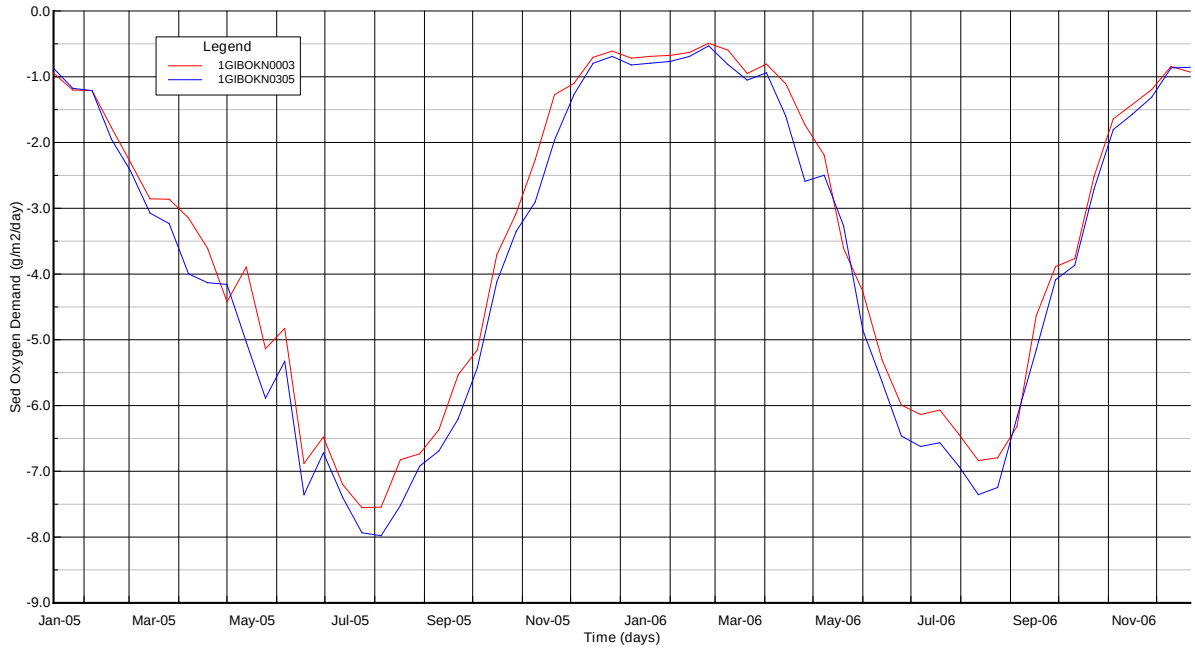

Figure B-109 SOD (as g/m^2-day) Calibration Results at 1GIBOKN0003 and 1GIBOKN0305

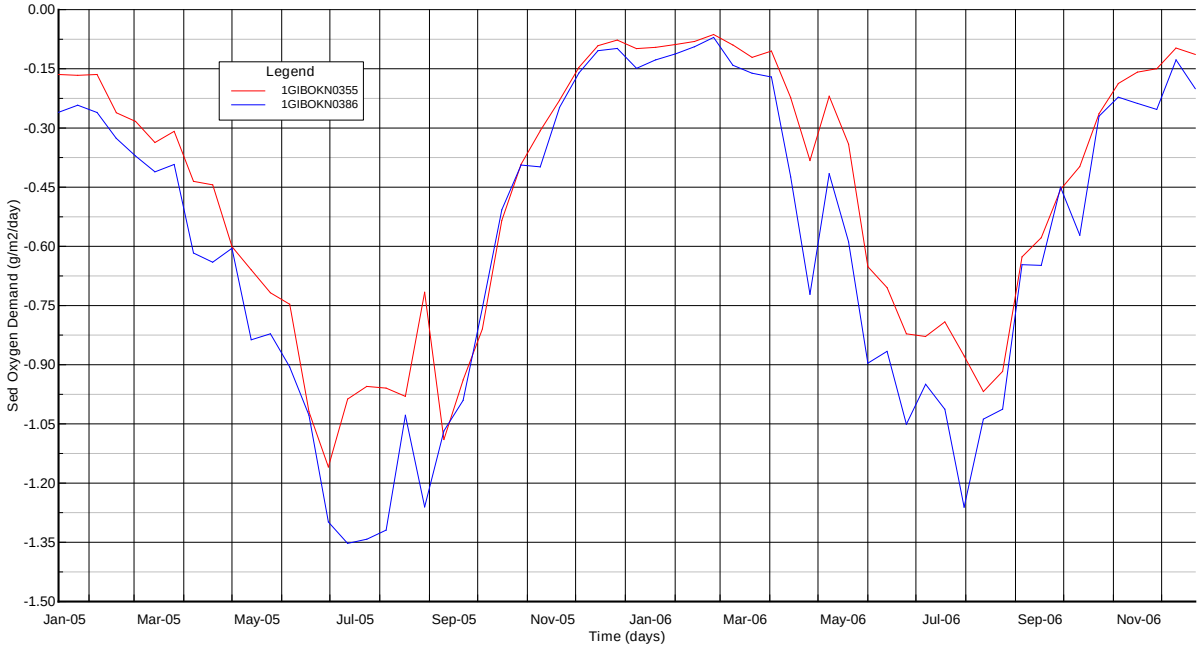

Figure B-110 SOD (as g/m2-day) Calibration Results at 1GIBOKN0355 and 1GIBOKN0386

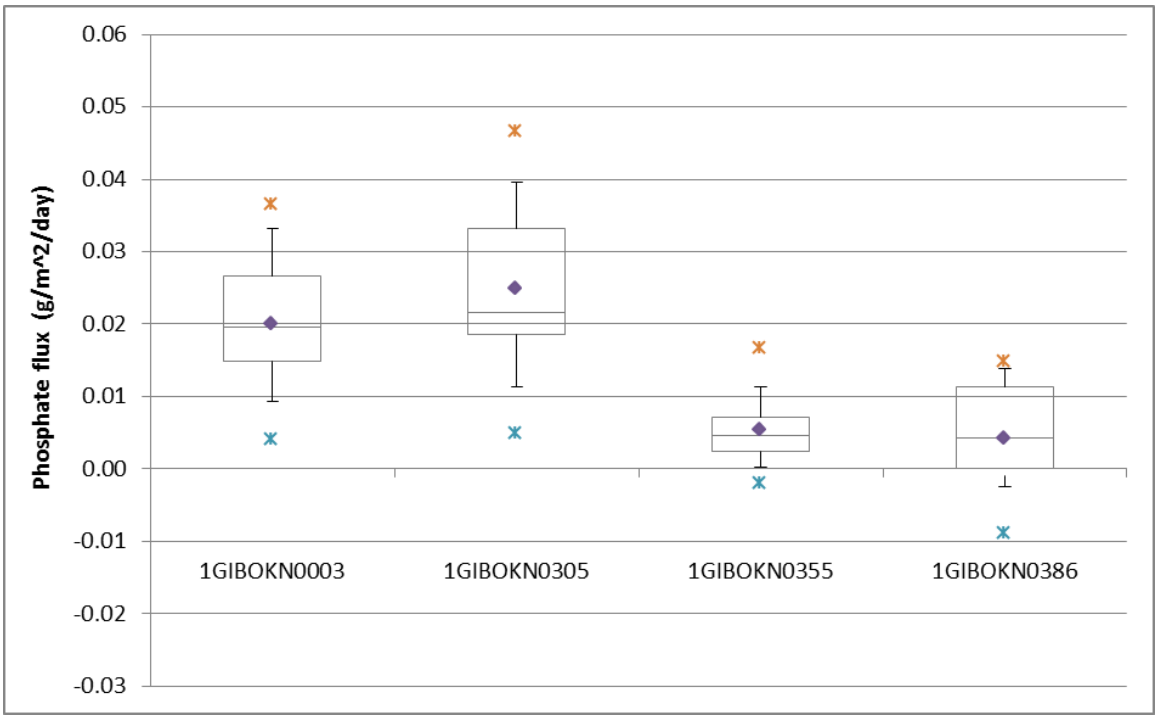

Figure B-111 – Sediment Flux of Phosphate (PO4) (as g/m2-day) Model Calibration Results in Fort Gibson Lake (May 15-October 1). Line within the box represents the median; data point within the box marks mean; edges of the box represent the 25th and 75th percentiles; error bars represent the 10th and 90th percentiles; data points outside the box represent the minimum and maximum values.

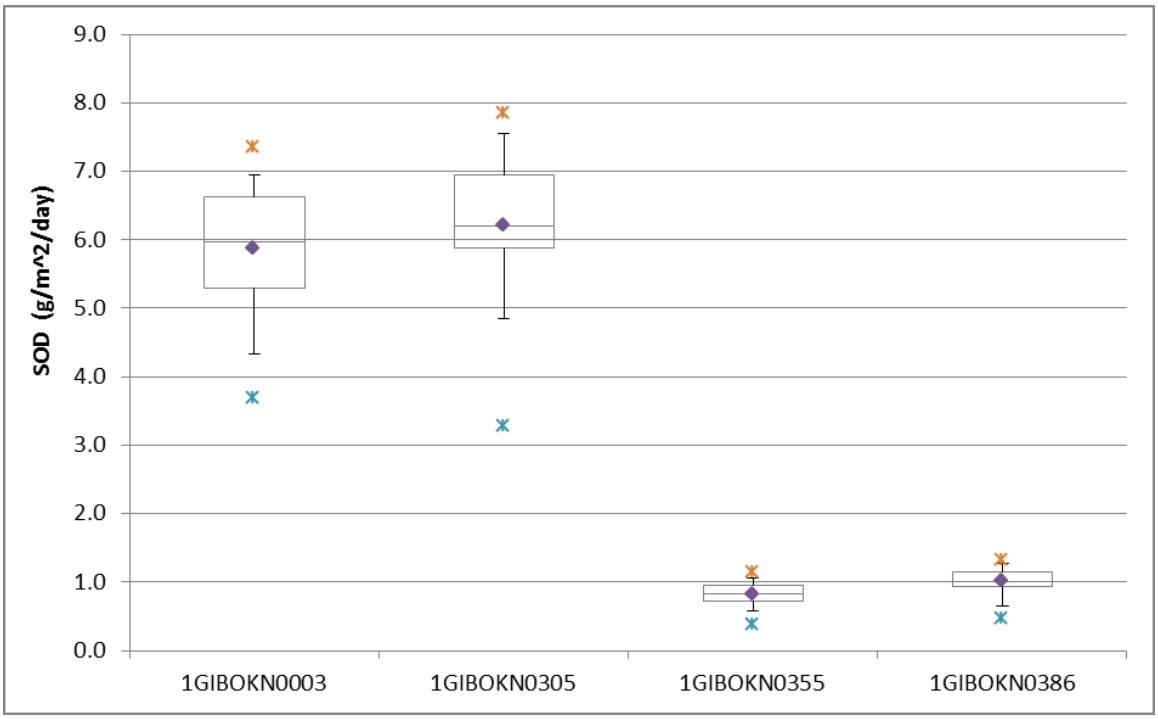

Figure B-112 SOD (as g/m2-day) Model Calibration Results in Fort Gibson Lake (May 15-Oct 1)
Line within the box represents the median; data point within the box marks mean; edges of the box represent the 25th and 75th percentiles; error bars represent the 10th and 90th percentiles; data points outside the box represent the minimum and maximum values.

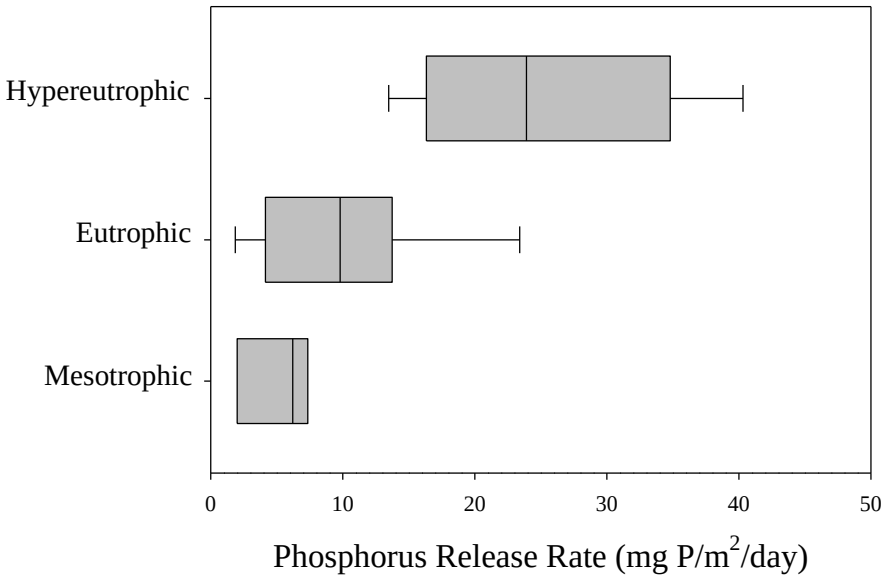

Figure B-113 – Comparisons of anoxic release rates of phosphorus (as mg/m2-day) from mesotrophic (n=3), eutrophic (n=9), and hypereutrophic (n=5) reservoirs in the Central Plains. Line within the box represents the median; edges of the box represent the 25th and 75th percentiles; error bars represent the 10th and 90th percentiles (Dzialowski and Carter, 2011).

Table B-23 Comparison of Measured Sediment Flux Rates for Oxygen and Phosphate in Central Plains.

Reservoir		Site		Aerobic	Anoxic	Reference
Name		Description	SOD	P-Flux	P-Flux	
			g/m^2-d	mgP/m^2-d	mgP/m^2-d	
Beaver Lake	AR	Riverine Zone		0.13	0.85	Sen et al. (2007)
		Transition Zone		0.15	1.77	
		Lacustrine Zone		0.04	< 0.01	
Lake Eucha	OK	Riverine Zone		1.14	4.7	Haggard et al. (2005)
		Transition Zone		1.01	2.46	
		Transition Zone		0.95	6.05	
Lake Frances	AR	Headwaters		0.37	14.53	Haggard & Soerens (2006)
	OK					
Wister Lake	OK	Site 1 (deep channel, dam)	0.54	0.75	1.52	Haggard & Scott (2011)
		Site 2(deep cove)	0.54	1.13	3.3	
		Site 3 (shallow, headwaters)	0.24	0.94	-0.23	
Acton Lake	OH	Dam site (summer mean)		n/a	9.2	Nowlin et al. (2005)
Central Plains	KS,MO	Mesotrophic (10%-90%ile)			(1.72-7.43)	Dzialowski & Carter, (2011)
	KS,IA	Eutrophic (10%-90%ile)			(2.64-18.5)	
	KS,NE	Hypereutrophic(10%-90%ile)			(15.0-37.4)	
Broken Bow	OK	Oligotrophic	1.49			Veenstra & Nolen (1991)
Texoma	TX,OK	Eutrophic	1.69			
Birch	OK	Eutrophic	3.2			
Pine Creek	OK	Mesotrophic	3.39			
Pat Mayse	TX	Eutrophic	4.08			

B-8 SUMMARY, CONCLUSIONS AND RECOMMENDATIONS

B-8.1 Summary

Fort Gibson Lake, owned and operated by the USACE Tulsa District, is a 19,900-acre reservoir lake that was constructed in 1953. Fort Gibson Lake, like many reservoirs in the Central Plains, is seasonally characterized by thermal stratification and hypolimnetic anoxia. Summer anoxic conditions, in turn, are associated with internal nutrient loading from the benthic release of phosphate and ammonia into the water column that is triggered, in part, by low hypolimnetic dissolved oxygen conditions. In the 2009 OWRB BUMP report on the lakes of Oklahoma, Fort Gibson Lake is identified as impaired for beneficial uses related to (a) Fish & Wildlife Propagation (FWP) because of low dissolved oxygen and (b) Aesthetic (AES) uses because of its status as a Nutrient Limited Watershed (NLW).

To provide a sound technical basis for TMDL determinations and a water quality management plan for Fort Gibson Lake, two EPA-supported public domain models have been selected to describe hydrology, runoff and pollutant loading from the Neosho River watershed with HSPF and hydrodynamics, sediment transport and water quality in Fort Gibson Lake with EFDC. The EFDC model incorporates internal coupling of organic matter production and deposition from the water column to the sediment bed with decomposition processes in the sediment bed that, in turn, produce benthic fluxes of nutrients and dissolved oxygen across the sediment-water interface.

The Fort Gibson Lake EFDC model was calibrated to USACE Tulsa District observations at seven station locations collected in the year 2005 and validated to observations collected in the year 2006. Model results were compared to observations of lake stage level, water temperature, total suspended solids (TSS), dissolved oxygen, chlorophyll-a, Trophic State Index (TSI), nitrogen, phosphorus, and organic carbon. The calibration and validation results are seen to be in reasonable, agreement with the observed data.

B-8.2 Conclusions

The EFDC hydrodynamic and water quality model of Fort Gibson Lake was calibrated and validated to data available to describe lake water quality conditions from January 2005 through December 2006. Lake model results, in general, were in good agreement with observations and either met, or were very close to, model performance targets established for lake stage, water temperature, dissolved oxygen, TSS, nutrients, and chlorophyll-a.

The calibrated and validated water quality model for Fort Gibson Lake accounts for the cause-effect interactions of watershed loading, nutrient cycling, algal production, organic matter deposition, sediment decay, and sediment-water fluxes of nutrients and oxygen. The linked watershed-lake model provides ODEQ with a technically credible framework to (a) describe the water quality response within the lake to existing watershed loading; (b) describe the potential response of in-lake water quality to alternative watershed load reduction scenarios; (c) evaluate the effectiveness of point source and nonpoint source load reduction scenarios on compliance with Oklahoma water quality standards; and (d) develop a TMDL and a watershed-based water quality management plan for Fort Gibson Lake.

B-8.3 Recommendations

Based on the findings of this study, the following recommendations for potential data collection efforts and future efforts to support water quality management planning for Fort Gibson Lake are submitted for consideration by DEQ:

- Increase the frequency of water quality monitoring of the key water quality parameters at the USACE and OWRB monitoring sites in Fort Gibson Lake. USACE and OWRB could coordinate scheduling of sampling programs so that the frequency of combined data availability could increase without the burden associated with an increase in sampling effort for either agency;
- Initiate surveys coordinated with the routine lake monitoring program to collect measurements of (a) sediment bed solids, organic carbon, organic nitrogen and organic phosphorus content and porewater nutrients; and (b) benthic release rates for ammonia, nitrate, and phosphate and sediment oxygen demand. The collected sediment bed chemistry data can be used to refine the developed EFDC lake model by setting up a reasonable initial condition of the sediment bed. The monitored sediment flux data sets can be used for comparison to the sediment flux modeling results.
- Install streamflow gages on Clear Creek and initiate a routine monitoring program to begin to develop a database to characterize streamflow and water quality loading from the Neosho River watershed into the lake to further calibrate and validate the watershed HSPF model.

B-9 REFERENCES

Anderson, K.A. and J.A. Downing. 2006. Dry and Wet Atmospheric Deposition of Nitrogen, Phosphorus and Silicon in an Agricultural Region. Water, Air, and Soil Pollution, 176:351-374.

Arhonditsis, G.B. and M.T. Brett. 2005. Eutrophication model for Lake Washington (USA) Part I. Model description and sensitivity analysis. Ecol. Model. 187:140-178.

Blumberg, A.F., L.A. Khan and J. St. John .1999. Three-dimensional hydrodynamic model of New York Harbor Region. *Jour. Hydr. Engineering Div., Proc. ASCE, 125(8):799-816, August.*

Carlson, R.E. 1977. A trophic state index for lakes*. Limnol. Oceanogr*. 22:361-369.

Cerco, C.F. and T.M. Cole. 1995. User's Guide to the CE-QUAL-ICM Three-Dimensional Eutrophication Model: Release 1.0. Prepared for U.S. Army Waterways Experiment Station, Vicksburg, MS. Technical Report 95-15.

Cerco, C.F., B.H. Johnson and H.V. Wang. 2002. Tributary refinements to the Chesapeake Bay Model. US Army Corps of Engineers, Engineer Research and Development Center, ERDC TR-02-4, Vicksburg, MS.

Craig, P.M.. 2012. *User's Manual for EFDC_Explorer7: Pre/Post-Processor for the Environmental Fluid Dynamics Code (Rev 00)*, Dynamic Solutions, LLC, Knoxville, TN.

Delft Hydraulics 2007. *Generation and manipulation of curvilinear grids for FLOW and WAVE*. Delft, The Netherlands, October.

DEQ 2008. *Water Quality in Oklahoma 2008 Integrated Report.* Appendix C: 303 (d) List of Impaired Waters. Oklahoma Department of Environmental Quality, Oklahoma City, OK, 376 pp.

Di Toro, D.M. 2001. *Sediment Flux Modeling*. Wiley Interscience, New York, NY.

Donigian, Jr., A.S. 2000. *HSPF Training Workshop Handbook and CD*. Lecture #19. Calibration and Verification Issues, Slide #L19-22. EPA Headquarters, Washington Information Center, 10-14 January 2000. Presented and prepared for U.S. EPA Office of Water, Office of Science & Technology, Washington, DC.

Dynamic Solutions, LLC. 2012. 3-Dimensional Hydrodynamic EFDC Model of Lake Thunderbird, Oklahoma Model Setup and Calibration, Tasks 1A, 1B(b) and 1B(c). Technical report prepared by Dynamic Solutions, Knoxville, TN for Oklahoma Dept. Environmental Quality, Water Quality Division, Oklahoma City, OK.

Dzialowski, A.R. and L. Carter .2011. Predicting internal nutrient release rates from Central Plains reservoirs for use in TMDL development. Final Report, Project Number: X7 97703801, Dept. Zoology, Oklahoma State University, Stillwater, OK, Submitted to U.S. Environmental Protection Agency, Region 7, TMDL Program, Water Quality Management Branch, Kansas City, KS.

Haggard, B.E. and T.S. Soerens. 2006. Sediment phosphorus release at a small impoundment on the Illinois River, Arkansas and Oklahoma, USA. Ecol. Eng'r. 28:280-287.

Haggard, B.E., D.R. Smith and K.R. Brye. 2007. Variations in stream water and sediment phosphorus among select Ozark catchments. J. Environ. Qual. 36(6):1725-1734.

Haggard, B.E., P.A. Moore and P.B. DeLaune. 2005. Phosphorus flux from bottom sediments in Lake Eucha, Oklahoma. J. Environ. Qual. 34:724-728.

Haggard, B.E. and J.T. Scott .2011. Phosphorus release rates from bottom sediments at Lake Wister, Oklahoma,Summer, 2010. Arkansas Water Resources Center-University of Arkansas, Tech. Pub. Number MSC 364-Year 2011.

Hamdan, T., T. Scott, D. Wolf and B.E. Haggard 2010. Sediment phosphorus flux in Beaver Lake in Northwest Arkansas. Discovery, Student Journal of Dale Bumpers College of Agricultural, Food and Life Sciences, University of Arkansas, Fayetteville, AR, Volume 11, Fall 2010, pp. 3-12.

Hamrick, J.M. 1992. *A Three-Dimensional Environmental Fluid Dynamics Computer Code: Theoretical and Computational Aspects*. Special Report No. 317 in Applied Marine Science and Ocean Engineering, Virginia Institute of Marine Science, Gloucester Point, VA. 64pp.

Hamrick, J.M. 1996. *User's Manual for the Environmental Fluid Dynamics Computer Code*. Special Report No. 331 in Applied Marine Science and Ocean Engineering, Virginia Institute of Marine Science, Gloucester Point, VA.

Hamrick, J.M. 2007. The Environmental Fluid Dynamics Code Theory and Computation Volume 3: Water Quality Module. Technical report prepared by Tetra Tech, Inc., Fairfax, VA.

Hyder, S. and A. Bari. 2011. Characterization and study of correlations among major pollution parameters in textile wastewater. Mehran University Research Journal of Engineering and Technology, 30(4): 577-582.

Hupfer, M. and J. Lewandowski. 2008. Oxygen controls the phosphorus release from lake sediments-along-lasting paradigm in limnology. Internat. Rev. Hydrobiol. 93:415-432.

Ji, Z-G. 2008. *Hydrodynamics and Water Quality Modeling Rivers, Lakes and Estuaries*. Wiley Interscience, John Wiley & Sons, Inc., Hoboken, NJ, 676 pp.

Metcalf & Eddy .1991. Wastewater Engineering, Treatment, Disposal and Reuse, 3rd Edition. Irwin/ McGraw Hill, 1334 pp.

Mortimer, C.H. 1941. The exchange of dissolved substances between mud and water in lakes. J. Ecology 29:280-329.

Mortimer, C.H. 1942. The exchange of dissolved substances between mud and water in lakes. J. Ecology 30:147-201.

Nowlin, W.H., J.L. Evarts and M.J. Vanni 2005 Release rates and potential fates of nitrogen and phosphorus from sediments in a eutrophic reservoir. *Freshwater Biology*, 50, 301-322.

OWRB. 2009. Lake Fort Gibson Water Quality 2008. Oklahoma Water Resources Board, Oklahoma City, OK.

OWRB. 2010. Lake Fort Gibson Water Quality 2009. Oklahoma Water Resources Board, Oklahoma City, OK.

OWRB. 2008. *2007-2008 Oklahoma's Lakes Report. Beneficial Use Monitoring Program*. Oklahoma Water Resources Board, Oklahoma City, OK. www.owrb.ok.gov/quality/monitoring/bump/pdf_bump/CurrentLakesReport.pdf

Park, R, A.Y. Kuo, J. Shen and J. Hamrick.2000. *A Three-Dimensional Hydrodynamic-Eutrophication Model (HEM-3D): Description of Water Quality and Sediment Process Submodels.* Special Report 327 in Applied Marine Science and Ocean Engineering, School of Marine Science, Virginia Institute of Marine Science, the College of William and Mary, Gloucester Point, Virginia.

Rozzi, A, F. Malpei, L. Bonomo and R. Bianchi .1999. Textile wastewater reuse in northern Italy (COMO) , Water Science and Technology, Vol 39 No 5 pp 121–128, IWA Publishing

Sen, S., B.E. Haggard, I. Chaubey, K.R. Brye, T.A. Costello and M.D. Matlock. 2007. Sediment phosphorus release at Beaver Reservoir, northwest Arkansas, USA, 2002-2003: a preliminary investigation. Water, Air & Soil Pollution 179:67-77.

Stoddard, A., J. B. Harcum, J.R. Pagenkopf, J. Simpson and R.K. Bastian .2002. *Municipal wastewater treatment: evaluating improvements in national water quality.* John Wiley & Sons, Inc., New York, NY.

Veenstra, J.N. and S. L. Nolen. 1991. *In-situ* sediment oxygen demand in five southwestern U.S. lakes. Water Research, 25(3):351-354.

Wells, S.A., V.I. Wells, and C.J. Berger. 2008. Water Quality and Hydrodynamic Modeling of Tenkiller Reservoir. Expert report prepared for State of Oklahoma in Case No. 05-CU329-GKF-SAJ State of Oklahoma v. Tyson Foods, et al. (in the United States District Court for the Northern District of Oklahoma).